4. PERFORMANCE ANALYSES

The total system performance analyses of the postclosure period for the potential Yucca Mountain repository are presented in this section. The previous sections have detailed both the approach to the analyses and the subsystem components used in the analyses. Appendix E summarizes the primary source information to the TSPA-SR. This TSPA was conducted according to the guidance from proposed 10 CFR Part 63 (64 FR 8640 [101680]), and 40 CFR 197 and the guidance and criteria specified in proposed 10 CFR Part 963 (64 FR 67054 [124754]) of the Site Suitability Guidelines.

The nominal performance evaluation is presented in Section 4.1 and includes a systematic analysis of the contribution of each component to the total system dose. The nominal performance case analyses evaluate the total repository system in the absence of low-probability disruptive events.

Section 4.2 provides a discussion of the disruptive performance analyses. The igneous disruption scenario described in this section covers both the effect of direct release of radionuclides due to an igneous intrusion through the repository leading to an eruption and the effect of indirect release of radionuclides due to igneous intrusion damaging a number of waste packages at the repository level. Although the igneous disruptive scenario is a very low probability event, it is analyzed within the TSPA to show its potential consequence.

As is required by the proposed 40 CFR Part 197 (64 FR 46976 [105065]) and the proposed 10 CFR Part 963 (64 FR 67054 [124754]), Section 4.3 provides an evaluation of the combined nominal and disruptive event scenarios to show overall performance.

Section 4.4 presents the stylized scenario as required by the proposed 10 CFR Part 963 (64 FR 67054 [124754]) to evaluate an assumed human intrusion occurrence. The general parameters for the analysis are defined by the regulation, but additional models and assumptions are required to evaluate the scenario. The alternative scenarios considered by the U.S. Environmental Protection Agency in proposed 40 CFR Part 197 (64 FR 46976 [105065]) were not analyzed.

Section 4.5 provides coverage of some of the major potentially disruptive events that have not been included in either the nominal or disruptive events because they were screened out as being either inconsequential or of extremely low probability. Among the events discussed qualitatively in this section are the criticality scenario and the scenario of a rapid increase of groundwater to inundate the repository.

Section 4.6 closes this section with a discussion and analysis of a couple design alternatives. The two cases considered were 1) the reference design with backfill, and 2) the low thermal load design. The discussion in this section focuses on the analyses conducted using the alternative designs and comparing them with the no-backfill reference design.

Appendix G lists the simulations that have been conducted for the Total System Performance Assessment-Site Recommendation (TSPA-SR). For each model case, the appendix provides the run number and run name by which the case is referred to, the basic scenario used, and a description of the run. The appendix also lists the figures illustrating the model case results,

which can be found in this report, and finally the Data Tracking Number (DTN) through which the model data can be accessed in the Technical Data Management System's Model Warehouse. The documentation of the base case model is found in *Total System Performance Assessment (TSPA) Model for Site Recommendation* (CRWMS M&O 2000 [148384]).

4.1 TOTAL SYSTEM PERFORMANCE FOR THE NOMINAL SCENARIO

The nominal scenario consists of all relevant FEPs that are expected to occur over the thousands to tens of thousands of years following the construction of the potential repository and emplacement of the waste packages. The nominal scenario is distinguished from the potentially disruptive scenario described in Section 4.2, which includes events and processes (specifically, those related to igneous activity) that have low probability of occurrence over the periods of interest.

Total system performance assessments (TSPAs) are by nature uncertain projections of the possible behavior of the potential repository system. These projections reflect the relevant processes affecting the containment and isolation of radioactive wastes from the biosphere. Uncertainty is explicitly included in the models and the resulting analyses in the form of probability distributions that encompass a range of possibilities. In the results presented, uncertainty in the possible performance is evaluated through the use of these probabilistic analyses.

The nominal scenario consists of models and parameters of the processes described in Section 3, in particular:

- Groundwater flow in the UZ, including infiltration processes at the ground surface, water seepage into drifts, and the effects of climate changes
- The effects of the temporal and spatial evolution of the physical and chemical environments on the engineered barriers (notably the drip shields and waste packages)
- The degradation of the engineered barriers within this range of possible physical and chemical environments
- The physical and chemical environments within the waste packages once the primary containment has been degraded to the point that through-going cracks penetrate the waste package
- The alteration of the waste form within the waste package, whether it is CSNF, DSNF, HLW, or another waste form, such as immobilized plutonium or naval SNF
- The release of dissolved or colloidal radionuclides through the degraded engineered barriers to the host rock
- The transport of dissolved or colloidal radionuclides through the UZ to the water table

- The transport of dissolved or colloidal radionuclides through the SZ to the point where the water is extracted for irrigation or household use, assumed to be 20 km (12 miles) downgradient from the potential repository

- The transport of radionuclides in the biosphere through a range of possible biological pathways to the point where they are either ingested or inhaled by people.

Models of all the above processes are integrated into the TSPA model. The submodels and some of their linkages are illustrated in Figures 4.1-1 to 4.1-4. The TSPA model is used to predict how the integrated and interdependent processes evolve over time and space, following the emplacement of the waste packages and drip shields and the ultimate closure of the potential repository.

Each of the component models included in the TSPA model directly incorporates the uncertainty in the understanding of the underlying processes, or bounds that uncertainty appropriately by selecting parameters that maximize the potential consequences of the model from an overall performance perspective (i.e., that maximize the expected dose to a human receptor). Because the component models include conservative assumptions as a method of dealing with uncertainties, the TSPA results are biased toward higher doses. The extent of that bias cannot be quantified without additional information. The uncertainties in the models are discussed in Section 3 and in the PMRs and AMRs.

In Section 4.1.1, the TSPA results for annual dose to the receptor over a 100,000-year period are presented. (See Section 3.9.1 for an explanation of the receptor, and Section 3.9.2.4 for an explanation of the method used for calculating dose TEDE.) In Section 4.1.2, a number of subsystem results are presented for the same time period, in order to provide a greater understanding of the way the system works as it degrades over time. In Section 4.1.3, the TSPA results are extended to a 1-million-year period, which includes the time when the annual dose reaches its highest values. In Section 4.1.4, TSPA results are shown for simulations with different numbers of realizations, in order to confirm that the base case includes enough realizations that the results are stable. Lastly, in Section 4.1.5, the nominal base-case results are presented for comparison with groundwater-protection requirements.

4.1.1 Overall Results for One Hundred Thousand Years

Figure 4.1-5 presents the TSPA results for the nominal scenario. The time period of regulatory interest specified in the three applicable DOE, NRC, and EPA regulations is 10,000 years after the closure of the potential repository (see Section 1.3.1.4), and the figure shows that the calculated doses are zero throughout this period. The simulations were continued out to 100,000 years to evaluate the behavior of the system after the containment of the engineered barriers is significantly degraded and to show that doses remain below the proposed limits well past 10,000 years. The 100,000-year period is not necessarily the "period of geologic stability" required to be addressed in EIS by the proposed EPA standard. Note that results for a 1-million-year period are discussed in Section 4.1.3.

The upper graph in Figure 4.1-5 shows 300 simulated dose histories along with some statistical measures of the dose distribution. The figure illustrates the temporal evolution of dose to the

receptor and the uncertainty associated with that dose projection. The mean curve is generated by averaging the 300 dose values at each time step, and the percentile curves are generated by determining the location of the given percentile at each time step (for example, the median curve is generated by determining the dose that has half of the calculated doses above it and half below it at each time step). The figure illustrates that there is a considerable amount of variability in the projections of dose, but no dose occurs for any of the 300 realizations for the nominal scenario until approximately 10,000 years after closure. The differences in results for different realizations are caused by the differences in their input parameters. It is shown in Section 5.1 that the variance in dose results seen in Figure 4.1-5 is largely related to uncertainties in waste package degradation processes. At 45,000 years after closure, nearly 50 percent of the predicted doses are essentially zero, over 90 percent of the doses are less than 1 mrem/yr, and the mean dose is approximately 0.25 mrem/yr. At 100,000 years, the mean dose is approximately 70 mrem/yr, the median dose (50 percent probability) is about 10 mrem/yr, and there is about a 20 percent probability of the predicted dose being less than 1 mrem/yr.

The total dose illustrated in Figure 4.1-5 is the sum of the doses attributed to each radionuclide in the groundwater at the point of use. Figures 4.1-5 to 4.1-7 illustrate the contribution of individual radionuclides to the total dose. The lower graph in Figure 4.1-5 shows the mean dose histories for the most important radionuclides and Figure 4.1-6 shows pie charts for the mean contribution of radionuclides to the total dose at four times. These figures indicate that, initially, the dominant dose contributors are the more mobile radionuclides, ^{99}Tc and ^{129}I. As time progresses, less-mobile radionuclides, which have lower solubility and slower transport through the UZ and SZ, become the dominant dose contributors. After about 60,000 years, the dose is dominated by ^{237}Np and colloidally-transported ^{239}Pu. For completeness, Figure 4.1-7 shows the mean dose histories for the rest of the radionuclides that were tracked in the TSPA simulation. These radionuclides make very small contributions to the total dose.

4.1.2 Subsystem Results for One Hundred Thousand Years

The preceding figures describe the total system results in terms of the total annual dose to the receptor. However, it is also important to understand the causal relationships that determine these results. This section describes the evolution of the potential repository as it relates to the performance of the overall system, including the degradation of the primary containment barrier (i.e., the waste package) and the subsequent release rates of radionuclides across different barriers.

Some of the discussion to follow refers to the environmental groups that are used in calculating waste form degradation and transport out of the EBS. As discussed in Section 3.3.2, the division into environmental groups is based on infiltration during the glacial-transition climate (0 to 3 mm/yr [0 to 0.1 in./yr], 3 to 10 mm/yr [0.1 to 0.4 in./yr], 10 to 20 mm/yr [0.4 to 0.8 in./yr], 20 to 60 mm/yr [0.8 to 2.4 in./yr], or 60+ mm/yr [2.4+ in./yr]), waste type (CSNF or co-disposal waste, which refers to waste packages that have both HLW glass waste and DSNF), and seepage state (seepage at all times, some of the time, or none of the time). There is a total of 30 environmental groups, resulting from five infiltration bins, times two waste types, times three seepage states. The division of waste packages into those 30 groups is given in Table 4.1-1. Shown are the averages over all 300 realizations; note that the number of packages in each group changes from realization to realization. There is effectively little or no difference between the

groups with seepage some of the time and seepage all of the time. The packages that have seepage only some of the time typically do not seep during the early dry period (i.e., during the present-day climate), but then seep all the time later on during the wetter glacial-transition climate. Thus, during the glacial-transition climate, when waste packages start failing, waste packages with seepage some of the time or seepage all of the time generally all have seepage. It can be seen from the table that only about 13 percent of the waste packages are subjected to seepage, on average. In the model, the other 87 percent are in locations where the local percolation flux is below the local seepage threshold.

Table 4.1-1. Average Division of Waste Packages into Environmental Groups

Waste Type	Seepage State	0–3 mm/yr	3–10 mm/yr	10–20 mm/yr	20–60 mm/yr	60+ mm/yr
Commercial Spent Nuclear Fuel	No Seepage	759	928	1338	2876	653
	Seepage Some of the Time	70	101	180	405	93
	Seepage All of the Time	0	1.8	8.2	98	75
Co-Disposal Waste	No Seepage	394	480	693	1487	341
	Seepage Some of the Time	33	51	89	205	44
	Seepage All of the Time	0	0.66	4.5	50	38

NOTE: 25.4 mm = 1 in.
The TSPA model has an additional 274 CSNF waste packages with stainless-steel cladding that are not included in the table. See text for explanation.

In addition to the waste packages listed in the table, the TSPA model has 274 CSNF waste packages with stainless-steel cladding. These 274 packages are placed in a separate environmental group because they are treated differently from the packages with Zircaloy cladding (the stainless-steel cladding is assumed to be perforated when the waste package fails; see Section 3.5.4.2). Because the number of packages with stainless-steel cladding is small, they are all placed together in a single environmental group, rather than creating numerous additional groups for them. The environmental conditions for the group with stainless-steel cladding were taken from the infiltration bin with the greatest number of waste packages for each infiltration case. Thus, environmental conditions from the 0 to 3 mm/yr (0 to 0.1 in./yr) infiltration bin were used for low-infiltration realizations (17 percent of the realizations), and environmental conditions from the 20 to 60 mm/yr (0.8 to 2.4 in./yr) infiltration bin were used for medium- and high-infiltration realizations (83 percent of the realizations). (For the number of waste packages in each infiltration bin, see Figure 3.3-3 and CRWMS M&O 2000 [152204], Table 5). A seepage state was needed for the stainless-steel-cladding group as well, so environmental conditions for seepage all of the time were specified. For low-infiltration realizations, there were no seepage results available for seepage all of the time in the 0 to 3 mm/yr (0 to 0.1 in./yr) infiltration bin, so the TSPA model defaulted to no seepage for those packages.

When the numbers of packages in Table 4.1-1 are added up, and the 274 CSNF waste packages with stainless-steel cladding are included, a total of 7,860 CSNF packages and 3,910 co-disposal packages is obtained, as specified in Section 3.5.1.1. Note that the proportions of waste

packages in the five infiltration bins are a reflection of the spatial variability of infiltration (see Figures 3.3-3 and 3.2-8). The proportions of waste packages in the three seepage states are a reflection of the spatial variability of seepage (see Section 3.2.4.3). The large fraction of waste packages with no seepage is caused, in part, by the inclusion in the model of flow focusing, which reduces the number of waste packages that have seepage but increases the flow rate of water onto the packages that have seepage (see Section 3.2.4.3).

Water is key to performance of the potential repository system. Without water to mobilize radionuclides and provide transport pathways, the only doses that would occur would be very small doses from the few radionuclides that can be transported in gaseous form. Conceptually, the first barrier protecting the waste from water is the portion of the UZ overlying the potential repository. Surface effects such as runoff and evapotranspiration limit the amount of water that percolates to depth (Section 3.2.2), and the emplacement-drift openings have a capillary-barrier effect that diverts much of the water flow around the drifts rather than into them (Section 3.2.4). The reduction of water flow at the surface is illustrated in Table 4.1-2, which lists the ratio of mean infiltration flux to mean precipitation flux, over the area of the potential repository, for each infiltration case and climate state. The table shows that only a small fraction of the precipitation is converted to infiltration that can percolate through the mountain and potentially contact waste. Because of the stochastic nature of the seepage abstraction, it is difficult to make a similar illustration for the reduction of the amount of flow into the drifts, but Table 4.1-1 serves as an illustration of the spatial distribution of seepage into drifts. As noted previously, only about 13 percent of the waste packages are subjected to seepage, on average. However, because of flow focusing and threshold effects, the fraction of water flow entering drifts is not necessarily the same as the fraction of waste packages with seepage.

Table 4.1-2. Ratio of Infiltration to Precipitation for the Infiltration Cases

Infiltration	Present-Day Climate	Monsoon Climate	Glacial-Transition Climate
Low infiltration	0.2%	2.4%	1.1%
Medium infiltration	2.4%	4.0%	6.1%
High infiltration	4.2%	4.8%	8.5%

Source: USGS 2000 [123650], Tables 6-10, 6-14, 6-19

Before liquid water can contact the waste package, the titanium drip shield must be breached. Figure 4.1-8 shows how the drip shields fail over time in the TSPA model. The mean cumulative-failure history (i.e., the average of the failure histories for the 300 realizations) is shown, as well as the median, 5th-percentile, and 95th-percentile failure histories. The meaning of the 5th-percentile curve is that in 5 percent of the TSPA realizations that number or fewer drip shields have failed; the other percentile curves are analogous (note that median is the same as 50th-percentile). The figure shows that drip shields do not start failing until approximately 20,000 years after emplacement. Most of the drip shields have failed by about 40,000 years, though in a small fraction of realizations most of the drip shields last for more than 100,000 years.

Figure 4.1-9 shows how the waste packages fail over time in the TSPA model. The mean failure curve rises from one waste package at about 15,000 years to about 50 percent of the waste packages by 100,000 years. However, there is a great deal of spread about the mean failure curve. At the 5-percent probability level, no waste packages fail for over 90,000 years and less than 1 percent fail by 100,000 years, whereas at the 95-percent probability level, 50 percent of the waste packages fail before 50,000 years and nearly all of them fail by 100,000 years. The "waves" visible in the curves in Figure 4.1-9 result from the time discretization of the waste-package failure model (see Section 3.4). While the waste packages are generally much longer-lived that the drip shields (compare Figures 4.1-8 and 4.1-9), the first waste-package failures occur before the first drip-shield failures. This occurrence underscores the fact that the waste-package failure model is independent of dripping conditions, and therefore has little or no dependence on the presence of the drip shield (see Section 3.4).

Once the outer, corrosion-resistant barrier (Alloy-22) of a waste package has degraded, moisture can enter the package. The TSPA model conservatively neglects any containment potentially provided by the inner, less corrosion-resistant barrier of the waste package (stainless steel). In addition, no credit is taken for the pour canisters that encapsulate the HLW glass. However, corrosion-resistant Zircaloy cladding provides additional protection to about 99 percent of the CSNF. The progression of initial cladding failure is illustrated in Figure 4.1-10, which shows the mean fraction of cladding failed over time for the 20 to 60 mm/yr (0.8 to 2.4 in./yr) infiltration bin. Cladding failure only applies to the CSNF waste type. Approximately 8 percent of the cladding fails at early times when temperatures are high, mostly by creep rupture. Failure after that is caused primarily by localized corrosion, which only occurs in the presence of seepage (see Section 3.5.4.2). Note that the cladding is protected from seepage as long as either drip shield or waste package is intact; thus, the number of fuel rods with perforated cladding starts rising after about 40,000 years—after most drip shields have failed and large numbers of waste packages have started failing. For perspective, Table 4.1-1 shows that, in the TSPA model, most waste packages are in locations that have no seepage; the "never dripping" curve in Figure 4.1-10 accounts for 85 percent of the waste packages in the 20 to 60 mm/yr (0.8 to 2.4 in./yr) infiltration bin. Thus, the additional cladding failures in the "always dripping" and "sometimes dripping" groups represent only a small increase in failed cladding overall within 100,000 years.

Having examined the failure history of the primary engineered barriers, next the movement of radionuclides through the system will be presented. Figure 4.1-11 shows the release rates of three important radionuclides as they pass some of the key engineered and natural barriers. Rate of release of radioactivity from the waste form, from the waste packages, from the EBS (i.e., from the emplacement drifts), from the UZ, and from the SZ (to the biosphere) are presented.

Figure 4.1-11a shows mean release histories for ^{99}Tc, which is a very mobile radionuclide. It is highly soluble and has little or no retardation due to sorption during transport. In the TSPA model, ^{99}Tc has no sorption at all in most hydrogeologic units. Only a small amount of sorption occurs in the part of the SZ path that is through alluvium. The behavior of ^{129}I is the same as that of ^{99}Tc; it also is highly soluble and has a small amount of sorption only in the alluvium. Releases of ^{99}Tc start as soon as the first waste package failures occur, just after 10,000 years. At late times, after about 60,000 years, a quasi-steady state is achieved, in which the release rates are the same throughout the system (the rate at which ^{99}Tc reaches the biosphere is the same as

the rate at which it is released from the waste form). The jumps in the waste form release rate (for example at approximately 20,000 years) occur at times when there is an increase in the rate of waste package failures (see Figure 4.1-9). The separation between the waste form and waste package curves indicates a residence time within the waste packages on the order of 10,000 years. It is seen that the waste packages are important in limiting releases of radionuclides even after they are breached. In contrast, the EBS curve overlays the waste package curve, indicating little residence time in the invert below the waste packages. Some residence time in the UZ can be seen, but there is apparently little additional residence time in the SZ. The long residence time for ^{99}Tc in the waste packages occurs because the waste packages have very small openings (cracks) when they first fail (see Figure 4.1-12). In the model, transport through the EBS is primarily diffusive for ^{99}Tc (see Figure 4.1-13a), and diffusion is quite slow when only small cracks are present. As the area available for diffusion increases, the residence time in the waste packages decreases, as shown by the convergence of the waste form curve with the other curves in Figure 4.1-11a. See Section 3.6 for details of the TSPA model for radionuclide transport within the EBS.

It is worth noting here that the EBS flow and transport abstractions include a number of conservatisms (see Section 3.6.3). Those conservatisms tend to overestimate radionuclide releases from the EBS, and therefore tend to overestimate the annual dose to the receptor 20 km (12 miles) away. Conservatisms are acceptable in TSPA simulations, but it should be kept in mind that they can affect conclusions regarding the relative importance of various release mechanisms. For example, diffusive releases from the EBS are overestimated because the diffusion time within the waste package is neglected, a continuous pathway for diffusion from the waste package to the invert is assumed always to be present after waste-package failure, and the diffusion coefficient in the invert is a conservative estimate (Section 3.6.3). The result that diffusive releases of ^{99}Tc are much greater than advective releases (and the results, discussed below, that diffusive releases of some other radionuclides are greater than or approximately equal to their advective releases) could be caused by these conservatisms, and therefore might not be realistic.

Figure 4.1-11b shows mean release histories for ^{237}Np, which is a moderately mobile radionuclide. It is more soluble than most species, though much less soluble than ^{99}Tc. It is weakly sorbing during transport. Releases of ^{237}Np from the waste form start as soon as the first waste package failures occur, but there is a lag of a few thousand years before releases reach the biosphere. The peaks in some of the curves (especially the waste package and EBS curves) result from failure of individual waste packages, or small groups of packages that fail at approximately the same time. The gap between the waste form and waste package curves is even larger than it is for ^{99}Tc, indicating an even longer residence time within the waste packages after being released from the waste form. Once again, the EBS curve overlays the waste package curve, indicating little residence time in the invert below the waste packages. Unlike the case for ^{99}Tc, the gap between the UZ and SZ curves is larger than the gap between the EBS and UZ curves, indicating a greater residence time in the SZ than the UZ. The greater residence time occurs because there is more sorption of neptunium in the SZ (especially in the alluvium) than in the UZ; however, the residence time in the SZ is very small compared to that in the waste packages. The greater residence time in the waste packages is a result of the lower solubility of neptunium as compared to technetium. The concentration of ^{237}Np cannot rise as high, which means that the concentration gradient cannot be as large, and therefore diffusive releases cannot

be as large. Lower concentration reduces advective releases as well, since advective releases are proportional to source concentration. Figure 4.1-13b shows the split between diffusive and advective releases from the EBS for ^{237}Np. Unlike for ^{99}Tc, diffusive and advective releases are approximately equal for ^{237}Np after about 40,000 years. Before about 20,000 years releases are purely diffusive because the drip shields are all still intact (see Figure 4.1-8).

Advective releases are small compared to diffusive releases until about 40,000 years, when the first patch openings in the waste packages occur. Prior to that time, the waste package openings are small cracks (Figure 4.1-12), which prevent most water from entering the waste packages. In the TSPA model, the amount of seepage entering the drift above a waste package is reduced at the drip shield according to the fraction of the drip shield area that is open. The water flow is further reduced at the waste package according to the fraction of the waste package area that is open. The model for flow of water within the drifts is discussed in Section 3.6.2.1. The reduction of seepage at the drip shield and waste package is illustrated in Figure 4.1-14, which shows the mean amount of seepage into drifts for a waste package that has seepage, along with the mean amount of flow through the drip shield and into the waste package. CSNF packages with seepage some of the time in the 20 to 60 mm/yr (0.8 to 2.4 in./yr) infiltration bin were chosen for the illustration because that is the largest group with seepage (see Table 4.1-1). The sharp rise in water entering the waste package at approximately 40,000 years (Figure 4.1-14) explains the sharp rise in advective releases from the EBS at the same time (Figure 4.1-13b).

Figures 4.1-11c and 4.1-11d show mean release histories for ^{239}Pu. It is less soluble than ^{237}Np. When transporting as a solute it is highly sorbing, so ^{239}Pu can only transport significantly if facilitated by colloids (the same is true for all highly sorbing species, including americium and other isotopes of plutonium). Two types of colloid-facilitated transport are modeled: reversible (Figure 4.1-11c) and irreversible (Figure 4.1-11d). "Reversible" refers to radionuclides attached to colloids by reversible sorption interactions, while "irreversible" refers to radionuclides that are permanently attached to colloids (the radionuclides are actually part of the structure of the colloids). More information on modeling of colloidal transport in the EBS, the UZ, and the SZ can be found in Sections 3.6, 3.7, and 3.8, respectively.

Figure 4.1-11c shows that releases of ^{239}Pu from the waste form start as soon as the first waste package failures occur, but there is a lag of several thousand years before releases of ^{239}Pu reversibly attached to colloids reach the biosphere. The very large gap between the waste form and waste package curves indicates a long residence time of reversible colloids within the waste packages after being released from the waste form. The reason for the long residence in the waste package is the same as discussed for ^{237}Np, and the residence time is even longer for ^{239}Pu because the solubility limit for plutonium is lower than that for neptunium. The EBS curve overlays the waste package curve after about 30,000 years, once again indicating little residence time in the invert below the waste packages. A significant residence time in the UZ is indicated by the gap between the EBS and UZ curves, and several thousand years in the SZ as well. The EBS curve is anomalous before 30,000 years, in that releases from the EBS are higher than releases from the waste package. This occurrence results from ingrowth of ^{239}Pu from ^{243}Am, which is released from the waste packages in greater quantities than ^{239}Pu at early times, and then decays and is released from the EBS as ^{239}Pu.

Figure 4.1-11d shows mean release histories for ^{239}Pu irreversibly attached to colloids. Comparison to Figure 4.1-11c shows that releases of irreversible colloids are much lower than releases of reversible colloids in the TSPA model. The EBS and UZ curves both overlay the waste package curve, indicating a short residence time for irreversible colloids in the EBS and the UZ. There is a small gap between the UZ and SZ curves, indicating some residence time in the SZ, but only a few thousand years. The longer residence in the SZ results from inclusion of a retardation factor for irreversible colloids in the SZ transport model (see Section 3.8.2.4), whereas such retardation is neglected in UZ and EBS transport. A very long residence time in the waste packages is indicated. This long residence time results because there is very little diffusive release of colloids, (because the diffusion coefficients of colloids are much lower than the diffusion coefficients of the dissolved species; see Section 3.6.2.2) so significant releases do not occur until the water flow into waste packages becomes significant, at about 40,000 years (see Figure 4.1-14).

Mean diffusive and advective releases from the EBS for reversible and irreversible ^{239}Pu are shown in Figures 4.1-13c and 4.1-13d, respectively. Figure 4.1-13d shows that diffusive releases of irreversible colloids are very low, as just discussed. In contrast, Figure 4.1-13c shows that there are significant diffusive releases of reversible colloids from the EBS. The reason for this is that the reversible component also includes ^{239}Pu that transports as a solute. Because of its high sorption, normally solute transport of ^{239}Pu is negligible, but sorption of all species was conservatively neglected for EBS transport, thus allowing significant releases from the EBS of dissolved ^{239}Pu. This dissolved ^{239}Pu then continues its transport through the UZ and SZ reversibly attached to colloids. Figures 4.1-13c and 4.1-13d also show that there is a small amount of advective release of the reversible component from the EBS prior to 40,000 years, whereas advective releases of the irreversible component do not begin until after 40,000 years. The earlier advective releases of reversible ^{239}Pu can also be attributed to transport of solute within the EBS.

Figure 4.1-15 shows releases from the EBS split into the mean releases from CSNF (top) and from co-disposal waste (bottom). Even though co-disposal waste accounts for only approximately 10 percent of the total waste mass, the releases of ^{99}Tc and ^{239}Pu from co-disposal waste and CSNF are comparable. The CSNF releases are relatively low because of the additional cladding barrier that the CSNF has (see Figure 4.1-10). An exception is ^{237}Np, which has co-disposal releases much lower than CSNF releases. This difference results from higher pH in the co-disposal packages, which lowers the in-package solubility of neptunium significantly (see Section 3.5.5.1). Technetium and plutonium solubilities are not sensitive to pH, so they are not affected in the same way. Another difference between CSNF and co-disposal waste is that the irreversible colloids come only from the latter. They are essentially tiny pieces of HLW glass that break off as the glass waste is degrading.

In the TSPA model, EBS releases are transferred to the UZ transport model separately for the five infiltration bins so that the releases in wetter repository regions are correlated with transport through wetter parts of the UZ (see Section 3.7.2). The mean EBS releases for the five infiltration bins are shown in Figure 4.1-16 for ^{99}Tc (top) and ^{237}Np (bottom). The differences in the two figures are a further illustration of the fact that ^{99}Tc releases are dominated by diffusion, whereas ^{237}Np releases have a significant advective component. In Figure 4.1-16, for ^{99}Tc, the curves are ordered simply by the number of waste packages in each bin. From Table 4.1-1 it can

be seen that the 20 to 60 mm/yr (0.8 to 2.4 in./yr) bin has the greatest number of waste packages, with over twice as many packages as the next largest bin. The next largest bin is the 10 to 20 mm/yr (0.4 to 0.8 in./yr) bin, then 3 to 10 mm/yr (0.1 to 0.4 in./yr), 0 to 3 mm/yr (0 to 0.1 in./yr), and lastly 60+ mm/yr (2.4+ in./yr). The releases are closely proportional to the number of waste packages, because the diffusive releases are similar for all waste packages. In particular, the diffusive releases have little if any dependence on the local UZ flow. In contrast, in the bottom graph of Figure 4.1-16, for ^{237}Np, the order of the curves reflects the amount of water flow: The 20 to 60 mm/yr (0.8 to 2.4 in./yr) bin is still highest since it has so many waste packages, but the 60+ mm/yr (2.4+ in./yr) bin is second highest even though it has the smallest number of waste packages. The 10 to 20 mm/yr (0.4 to 0.8 in./yr) bin is next, then 3 to 10 mm/yr (0.1 to 0.4 in./yr), and lastly 0 to 3 mm/yr (0 to 0.1 in./yr).

Radionuclides reaching the water table are separated into four regions for input to the SZ transport model (see Section 3.8.2.2). The mean UZ releases for the four regions are shown in Figure 4.1-17 for ^{99}Tc (top) and ^{239}Pu (bottom). The curves in the top graph of Figure 4.1-17, for ^{99}Tc, match the general picture of UZ transport described in Sections 3.2.3.4 and 3.7.4. In this picture, there is significant lateral flow and transport to the east (down-dip) and then down in the northern part of the potential repository because of the presence of perched water below the potential repository, whereas in the southern part of the potential repository flow and transport are more nearly vertical, with much less lateral movement. As shown in Figure 3.8-14, Regions 1 and 3 are directly below the potential repository, with Region 1 in the north and Region 3 in the south; Regions 2 and 4 are to the east of the potential repository area (Region 2 in the north and Region 4 in the south), where laterally diverted radionuclides would reach the water table. In the top graph of Figure 4.1-17, the highest UZ releases are in Regions 3 and 2, representing transport directly down to the water table below the southern part of the potential repository and laterally to the east and down in the northern part of the potential repository. UZ releases from Regions 1 and 4, representing transport directly down through the perched water in the northern part of the potential repository and laterally to the east and down in the southern part of the potential repository, are lower, confirming that those pathways are less important in the model.

The bottom graph of Figure 4.1-17, for ^{239}Pu, is included because of some interesting differences. Compared to the curves for ^{99}Tc, the ^{239}Pu releases in the southern part of the potential repository are relatively lower (that is, curves 3 and 4 for ^{239}Pu are lower relative to curves 1 and 2 than they are for ^{99}Tc). The lower (or slower) ^{239}Pu releases in the south are a result of the greater occurrence of flow and transport through the porous rock matrix in the south, which is a result of the greater occurrence of vitric Calico Hills nonwelded tuff in the south. Plutonium is highly sorbing on the rock matrix, whereas sorption on fracture faces is neglected in the TSPA model. The ^{239}Pu transport is primarily via reversible sorption on colloids, and when the transport is through a highly sorbing porous medium some of the radionuclides sorb to the porous matrix instead of the colloids, which causes an effective retardation of the transport.

Figure 4.1-18 shows the mean releases of ^{99}Tc from the SZ for the four source regions (the same four regions discussed above). Shown are the release rates at 20 km (12 miles) distance, where the radionuclides are assumed to be pumped up a well and used for farming and household activities. Releases from the four regions are added together to obtain the total release rate, which is then divided by the groundwater-usage volume and multiplied by BDCF for each

radionuclide to calculate the dose to the receptor (see Section 3.9.2.4). The final dose curve for ^{99}Tc is shown in Figure 4.1-5. Comparison of Figure 4.1-18 (SZ releases) with the top graph of Figure 4.1-17 (UZ releases) shows no significant difference between them, thus indicating no significant difference in the SZ transport of radionuclides that start in the different source regions. Though not shown, transport of ^{237}Np and ^{239}Pu also shows no significant dependence on the source location.

4.1.3 Results for One Million Years

The bulk of the analyses presented in this and other sections of this document have the objective of evaluating the ability of the Yucca Mountain site and its related natural barriers and the engineered barriers associated with the Site Recommendation design to meet performance objectives specified in the applicable environmental standard set by the U.S. EPA in the proposed 40 CFR Part 197 (64 FR 46976 [105065]) and the licensing criteria specified in the U.S. NRC's proposed 10 CFR Part 63 (64 FR 8640 [101680]). Both of these regulations at present require performance assessments to extend through the compliance period of 10,000 years. The analyses conducted to evaluate the ability of the site to meet these standards during the compliance period have been extended to longer time periods, specifically to 100,000 years, in order to assure that no dramatic degradation of the performance occurs after the 10,000-year compliance period. Additional analyses of peak dose to 1,000,000 years have also been conducted.

Both the compliance period models and analyses and the extension of these models and analyses to 100,000 years have used the principal of bounding the uncertainties in order to assure that the projected dose would be an overestimation of the range of possible performance. Extending the analyses significantly beyond the 10,000-year compliance period, especially when using the models and analyses purposely designed to be bounding, raises questions about the interpretation of the results. As noted by EPA in their evaluation of the potential for compliance periods of greater than 10,000 years: "as the compliance period is extended to such lengths, uncertainty increases and the resulting projected doses are increasingly meaningless from a policy perspective" (40 CFR Part 197 [64 FR 46976 [105065], p. 46994]).

In addition to the lack of policy meaning for such long term projections, EPA has noted that there is no policy basis for determining "the level of proof or confidence necessary to determine compliance based upon projections of hundreds-of-thousands of years into the future" (40 CFR Part 197 [64 FR 46976 [105065], p. 46995]). In addition, the EPA notes that although the "far future can be bounded, a large and cumulative amount of uncertainty is associated with those numerical projections." (40 CFR Part 197 [64 FR 46976 [105065], p. 46995]).

In the evaluations of potential compliance with the above regulatory requirements, overall conservative (i.e., pessimistic) calculations of the potential impacts of this system to estimate the potential risks of the repository for 10,000 years were used. Much effort has gone into providing an appropriately defensible technical basis for the 10,000-year compliance period analyses recognizing the uncertainty in these projections. To gain insight into the 10,000-year performance results, calculations have been carried out to 100,000 years. These were calculations expressly done to gain insight into the robustness of the regulatory

compliance-period case, however. It is not a good indicator of expected performance to take conservative calculations for 10,000 years and project them significantly beyond their basis.

Much of the 10,000-year calculational structure and basis properly supports a longer term calculation, but there are some features and processes that are not important to 10,000-year performance that can therefore be bounded or even neglected. However, these same features or processes become important in the longer time frames if the goal is to project a reasonable expectation of performance for the longer term. Some purposely neglected or bounded features and processes that become potentially important to performance only after the time period of regulatory concern would act to increase potential risk, others to decrease potential risk. In order to provide a reasonable expectation of a peak dose beyond 10,000 years, however, all potentially important processes must be appropriately included.

With these qualifiers in mind, three separate total system analyses of peak dose have been performed out to 1,000,000 years. In the first case, the models developed for the 10,000-year compliance period have simply been extrapolated out to the peak dose. The result of utilizing this conservative assumption is illustrated in Figure 4.1-19a. The key radionuclides affecting the dose assessment are illustrated in Figure 4.1-19b. In examining these results, several observations are possible, including:

- The peak mean dose is about 490 mrem/yr and occurs at about 270,000 years
- The dominant radionuclide contributing to the peak dose is ^{237}Np, with lesser contributions provided by colloids of thorium, radium, and plutonium
- The distribution of peak dose indicated by the range of results for the different realizations spans several orders of magnitude. This range is significantly less than the range of possible dose projections at earlier times because the uncertainty in the performance of some key aspects of the engineered and natural barriers decreases with time. In particular, after about 100,000 years, all of the waste packages and drip shields have been sufficiently degraded to allow the waste contained in these packages to be available for mobilization and transport.

In the second case, an alternative representation for the solubility of actinide elements (e.g., neptunium, plutonium, and americium, in particular) was utilized that employed the observation that these radioisotopes are commonly entrapped in secondary uranium phases when waste fuel alters. These secondary phases induce a significantly lower solubility of these key radionuclides as discussed in Section 3.5.5.3. Employing these expected solubilities for the expected dose projection results in significantly lower doses as illustrated in Figure 4.1-20. The key radionuclides contributing to these dose estimates are indicated on the bottom plot in Figure 4.1-20. The following observations assist in explaining the differences between the two analyses:

- The peak mean dose decreases from 490 mrem/yr to about 30 mrem/yr at 1,000,000 years.

- The dominant radionuclides contributing to the peak dose are the more soluble radionuclides such as ^{99}Tc and the colloidally transported species of ^{239}Pu and ^{242}Pu. The dose attributed to ^{237}Np is reduced by several orders of magnitude from the previous case, reflecting the significantly reduced soluble fraction when long-term secondary phases are included in the analysis.

In the third case, the long-term climate was adjusted to account for the expectation that glacial climate periods are likely to recur several times during the 1,000,000-year simulation period. As described in Section 3.2.5, these glacial climate periods have the effect of increasing the net infiltration (due to increased precipitation and reduced temperature) which in turn causes an increase in percolation flux and seepage at the repository horizon. In addition, the glacial climates have the effect of raising the water table and increasing the advective flux in the saturated zone. The result of utilizing the modified long-term climate in conjunction with the expected reduction in the long term solubilities due to the formation of secondary phases is illustrated in Figure 4.1-21. The following observations assist in explaining the effects of these changes on the projected mean peak dose:

- The peak mean dose is about 120 mrem/yr at about 700,000 years.

- The timing of the mean peak dose is dependent on the timing and magnitude of the change in the net infiltration rate. This correlation is primarily driven by the fact that increased infiltration yields an increase in seepage, which in turn yields an increase in the advective release of solubility-limited and colloidally transported radionuclides from the engineered barrier system.

- The "spikiness" of the mean dose response when the post-10,000-year climate changes are implemented is a result of the relative abruptness in the timing of the climate change and the rapid propagation of the induced changes through the system as well as the relatively short duration of the full-glacial climate states. The full-glacial climate states have durations on the order of 10,000 years, and once the climate returns to intermediate conditions, the infiltration and seepage return to the base-case conditions, including the base-case release and dose projections.

In summary, the peak of the expected dose curve is a function of the degree of conservatism incorporated in the models and analyses used to produce the peak dose estimate. Because the base-case models used in the development of the nominal performance projections were designed to be reasonably conservative to maximize their defensibility during the 10,000-year compliance period, they are less appropriate for projections of the peak dose. More appropriate representations would include considerations of the long-term (post-10,000-year) climate states and the long term effects of secondary phases. Although these alternative representations are less appropriate for the compliance period analyses, they are more suitable for the peak dose assessments.

In any assessment of the peak dose, the cautions provided by EPA should be considered in the interpretation of the results, namely "extremely long-term calculations are useful only as indicators, rather than accurate predictors, of the long-term performance of the Yucca Mountain disposal system" (40 CFR Part 197 [64 FR 46976 [105065], p. 46996]).

4.1.4 Precision of Probabilistic Results

The number of realizations to use in a Monte Carlo simulation is a significant issue in terms of reliable analyses and proper allocation of computing resources. All probabilistic results presented thus far were based on 300 realizations for developing estimates of the mean annual dose and its corresponding uncertainty. In this section, it is shown that 300 realizations are adequate to calculate mean annual doses reliably. To this end, the TSPA model was re-run using 500 realizations, and the results compared to those obtained for the base-case simulation with 300 realizations.

Figure 4.1-22 shows a comparison of the statistics of the dose history for the two cases. Results of a simulation with 100 realizations are also included in the comparison. The 100-realization mean dose history is used for comparison with a number of sensitivity cases in Sections 5.2 and 5.3. Figure 4.1-22 indicates very good agreement over the 100,000-year time period for the mean, median, 5th percentile, and 95th percentile dose histories. These results verify that various measures of uncertainty in the projected dose, quantifying the central tendency as well as the overall spread, are essentially equivalent for the 500- and 300-realization simulations. Even the 100-realization simulation appears robust enough to predict the mean of the annual-dose distribution through time. However, a sample size of 100 is less reliable for estimating the tails of the annual-dose distribution or the dependency of the uncertain annual-dose distribution on the uncertain distributions of the various input parameters (see Section 5.1). Thus, the 300-realization sample size is considered to be an appropriate compromise for analysis of the base case, although the 100-realization sample is considered to be adequate for comparing the trends in predictions of mean annual dose for the various sensitivity cases in Sections 5.2 and 5.3.

4.1.5 Groundwater Protection

An analysis of groundwater protection was conducted in accordance with the EPA's proposed 40 CFR 197.35 (64 FR 46976 [105065]). The proposed rule is based on meeting three maximum levels. The first is that the maximum concentration of ^{226}Ra and ^{228}Ra shall not exceed 5 pCi/L in a representative volume of groundwater at the point of compliance, considering both natural sources and releases from the potential repository. The second limit is that the gross alpha activity (excluding radon and uranium) shall not exceed 15 pCi/L in the representative volume of groundwater at the point of compliance, again from both natural sources and releases from the potential repository. The third limit is that beta- and photon-emitting radionuclides released from the potential repository shall not cause a dose in excess of 4 mrem/yr to the whole body or any organ of a human receptor.

The proposed rule specifies that the representative volume of groundwater would be withdrawn annually from an aquifer containing less than 10,000 mg/L of total dissolved solids, be centered on the highest concentration in the plume of contamination at the point of compliance, and contain 1,285 acre-ft (1,591,000 m^3) of water. For the analysis presented here, the point of compliance is taken to be 20 km (12 miles) from the potential repository, near the intersection of U.S. Route 95 and Nevada State Route 373 (alternative 2 for proposed 40 CFR 197.37 [64 FR 46976 [105065]). There is a Nevada Department of Transportation well near that highway intersection, and water from that well has been measured to have 385 mg/L of total dissolved

solids (DTN: GS971000012847.004 [149980]), satisfying the first part of the definition of the representative volume. In this analysis, all radionuclides that reach a distance of 20 km (12 miles) from the potential repository in any given annual period are contained in 1,285 acre-ft of water to determine the concentration. Taking all radionuclides in this manner produces the highest estimate of concentration that is possible for the specified volume of water. The exact location or dimensions for the representative volume could be different in each Monte Carlo realization with this method. The proposed rule also specifies a time period of compliance of 10,000 years. There are no releases from the potential repository in 10,000 years, but results are presented for 100,000 years to show that they remain below the proposed limits well past 10,000 years.

To address the proposed rule, the existing background concentrations of ^{226}Ra, ^{228}Ra, and radionuclides contributing to gross alpha activity (excluding radon and uranium) must be known. Gross alpha activity (excluding radon and uranium) was measured at the Nevada Department of Transportation well and reported as 0.4 ± 0.7 pCi/L (CRWMS M&O 1999 [150420], Section 3.2.1). The same reference reports measurements at other wells and springs in the vicinity of Yucca Mountain and Amargosa Valley ranging from –0.2 ± 0.5 to 2.7 ± 3.0 pCi/L. Concentrations of ^{226}Ra and ^{228}Ra were not reported in that reference because the gross alpha activity was below 5 pCi/L. However, another source reports ^{226}Ra concentration of 0.04 pCi/L and ^{228}Ra concentrations as less than 1 pCi/L at the Nevada Department of Transportation well (DTN: GS971000012847.004 [149980]). The measurement errors are not reported in that reference. Measurements in the same reference at other wells and springs in the vicinity of Yucca Mountain and Amargosa Valley range from 0.03 to 0.5 pCi/L for ^{226}Ra and from less than 1 to 1.1 pCi/L for ^{228}Ra.

Figure 4.1-23 shows the calculated activity concentration of ^{226}Ra and ^{228}Ra, not including the background concentration. These isotopes have short half-lives and are created by ingrowth from other (parent) radionuclides released from the potential repository. Their transport is not modeled explicitly, but rather by assuming secular equilibrium with their parents, and thus these concentrations could be overestimates of the actual values. The sum of the two radium concentrations is shown in Figure 4.1-24, and is virtually identical to the concentration history of ^{226}Ra. Note that the concentrations of both isotopes are zero over 10,000 years, and are significantly less than the 5-pCi/L limit over 100,000 years. The highest concentration shown is approximately 0.06 pCi/L. Given this result, the activity concentration of ^{226}Ra and ^{228}Ra with background included is still less than 5 pCi/L over the whole 100,000-year period. From above, the background concentration of ^{226}Ra plus ^{228}Ra is less than 1.04 pCi/L at the point of compliance. Adding the releases from the repository brings the total up to 1.1 pCi/L at most, within 100,000 years.

In addition to the summed ^{226}Ra and ^{228}Ra activity, Figure 4.1-24 shows the calculated gross alpha activity (excluding radon and uranium) over 100,000 years, not including the background activity. Radionuclides included in this calculation are ^{210}Pb, ^{226}Ra, ^{228}Ra, ^{227}Ac, ^{229}Th, ^{230}Th, ^{231}Pa, ^{237}Np, ^{238}Pu, ^{239}Pu, ^{240}Pu, ^{242}Pu, ^{241}Am, and ^{243}Am. The activity concentrations of these radionuclides are zero over 10,000 years. The highest concentration shown is approximately 14 pCi/L at 100,000 years. If the background gross alpha activity of 0.4 ± 0.7 pCi/L at the point of compliance is added to the calculated gross alpha activity, the sum approaches the limit of 15 pCi/L at 100,000 years. However, the limit only applies for 10,000 years.

Figure 4.1-25 shows the contribution of radionuclides to the calculated gross alpha activity. The major contributors are ^{237}Np and ^{239}Pu. It is expected that ^{237}Np will continue to be the major contributor over later times, because its half-life is 2.1 million years, while ^{239}Pu should decrease in significance over later times because its half-life is 24,000 years. Radionuclides whose abundance is mainly controlled by ingrowth, e.g., the $^{230}Th/^{226}Ra/^{210}Pb$ group and ^{229}Th, show increasing activity at 100,000 years. Two groupings of radionuclides are covered by the same line type in the legend: the $^{230}Th/^{226}Ra/^{210}Pb$ group and the $^{231}Pa/^{227}Ac$ group. These are radionuclides whose transport is modeled by assuming secular equilibrium, and therefore they have the same activity.

Figure 4.1-26 shows the concentrations of the three beta- and photon-emitting radionuclides that are important to TSPA-SR and the proposed EPA rule: ^{14}C, ^{99}Tc, and ^{129}I. For ^{14}C, the critical organ is fat and the concentration in drinking water that can cause a 4 mrem/yr dose is 2000 pCi/L. For ^{99}Tc, the critical organ is the gastrointestinal tract and the concentration in drinking water that can cause a 4 mrem/yr dose is 900 pCi/L. For ^{129}I, the critical organ is the thyroid and the concentration in drinking water that can cause a 4 mrem/yr dose is 1 pCi/L. (These concentrations are based on 2 L/day drinking-water intake and are taken from U.S. Environmental Protection Agency 1976 [151667], Table IV-2A.) As there are no radionuclides with the same critical organ among these three, and none involve the total body, the concentrations in Figure 4.1-26 can be compared directly with the given concentrations. First note that the concentrations for all three radionuclides are zero for 10,000 years. The maximum concentration of ^{14}C occurs at about 24,000 years and is approximately 0.07 pCi/L. The concentration decreases after 24,000 years because of the relatively short ^{14}C half-life of 5,700 years. The maximum concentration of ^{99}Tc occurs at 100,000 years and is approximately 640 pCi/L. The maximum concentration of ^{129}I occurs at 100,000 years and is approximately 1.7 pCi/L; the concentration of ^{129}I exceeds 1 pCi/L at about 65,000 years.

The dose to a critical organ from a radionuclide can be estimated by multiplying the calculated concentration of the radionuclide in groundwater by the ratio of 4 mrem/yr over the respective concentration that would cause a 4-mrem/yr dose.. For example, the dose to fat from ^{14}C can be estimated by multiplying the groundwater concentration of ^{14}C (in pCi/L) by 4 mrem/yr and dividing by 2000 pCi/L. Figure 4.1-27 shows the doses caused by ^{14}C, ^{99}Tc, and ^{129}I to their respective critical organs when estimated in this manner. Again, there is no dose in the first 10,000-yr period. At 100,000 years, a dose of approximately 3 mrem/yr to the gastrointestinal tract is estimated from ^{99}Tc, a dose of approximately 7 mrem/yr to the thyroid is estimated from ^{129}I, and a relatively insignificant dose to fat is estimated from ^{14}C.

Again, remember that many of the component TSPA models include conservative assumptions as a method of dealing with uncertainties, and as a result the TSPA results are biased toward higher doses.

4.2 TOTAL SYSTEM PERFORMANCE FOR THE DISRUPTIVE SCENARIO CLASS

As described in Section 3.10, igneous activity has been identified as the primary disruptive event that has a potential to affect long-term performance of the potential repository. The FEPs relevant to igneous activity that have been retained following the screening process (see Section 3.10.2.1) have been included in the TSPA-SR through two separate models for igneous

disruption: a model for volcanic eruptions that intersect drifts and bring waste to the surface, and a model for igneous intrusions that damage waste packages and expose radionuclides for groundwater to transport. The TSPA-SR models and parameter values used to analyze radionuclide releases and possible doses to the exposed individual are described in detail in Section 3.10. Proposed regulatory requirements (see Section 1.3) require evaluations of disruptive scenarios for 10,000 years following repository closure. To provide additional confidence in the adequacy of the 10,000-year analysis, results of the TSPA-SR analysis are described in this section for igneous disruptions during the first 50,000 years after repository closure. Unlike the results for the nominal performance scenario class, described in Section 4.1, analyses of igneous disruption have not been extended to 100,000 years because of the additional computational burden imposed by the need to evaluate events at different times. Results shown in this section are suitable, however, for evaluating system-level performance during the period when expected annual dose is dominated by igneous disruption.

4.2.1 Incorporating Event Probability in the Total System Performance Assessment-Site Recommendation

The approach taken in the TSPA-SR to calculating doses resulting from igneous disruption of the repository is consistent with the probabilistic methodology described in NRC guidance (see NRC 2000 [149372], Section 4.4), where the NRC describes the method for weighting consequences of individual scenarios by their probability before summing the scenario consequences to determine the overall expected annual dose. (See also Section 3.4 of Reamer [1999 [119693]] for a discussion of the NRC's implementation of this approach for igneous activity.) Scenario consequences are multiplied (weighted) by the probability of the occurrence to yield an appropriate estimate of the overall risk posed by low-probability events. As described in Section 3.10.1, the probability of intrusive igneous disruption is extremely low (the mean annual probability is 1.6×10^{-8}), and the annual probability of more than one igneous disruption occurring during the period of repository performance is far less. The TSPA-SR therefore considers only a single igneous disruption of the repository during the next 50,000 years, occurring with a mean 50,000-year probability of approximately 8×10^{-3} (corresponding to a 10,000-year probability of approximately 1.6×10^{-4}). The year in which the igneous disruption might occur is uncertain, and the TSPA-SR calculates consequences for disruptions at many different times, and weights the consequences by the probability that the disruption could have occurred in the time interval represented by that simulation.

4.2.1.1 Incorporating Eruptive Event Probability

For the eruptive scenario, the TSPA-SR examines the consequences of eruptions occurring in each 31.25-year time interval during the 50,000-year period and weights the consequences of each eruption by a probability equal to 31.25 times the annual probability of an eruption that intersects the repository. This probability is sampled from the distribution characterizing uncertainty in the probability of igneous intrusion (i.e., a mean annual probability of 1.6×10^{-8}), multiplied by a factor of 0.36 to account for the fraction of intrusive events for which the associated eruption does not intersect the drifts, and then multiplied by 31.25 to yield a 31.25-year eruption probability. (For example, the mean 31.25-year eruption probability is 1.8×10^{-7}). Because eruptions are considered in each 31.25-year interval, each 50,000-year realization of the TSPA-SR GoldSim model thus includes consequences of 1,600 eruptions,

weighted appropriately so that the mean probability of a single eruptive event in 50,000 years is 8×10^{-3} times 0.36, or 2.88×10^{-3}. The average dose resulting from an eruptive event for a single realization is determined by calculating doses resulting from igneous events in each 31.25-year period, multiplying by the sampled probability, and adding the doses from each eruptive event.

Computationally, the analysis takes advantage of the simplifying assumption that, although the physical properties of an eruption and the response of the repository are uncertain, this uncertainty is not dependent on the time at which the event occurs. Volcanic eruptions 100 years after closure are assumed to have the same properties as volcanoes 50,000 years after closure. Because waste packages that are intersected by an eruptive conduit are assumed to be sufficiently damaged that they provide no further protection for the waste (see Section 3.10.2.2.2) regardless of the time of the event, effects of the eruption on the repository are also assumed to be constant through time. These assumptions allow the GoldSim code (Golder Associates 2000 [151202]) to use ASHPLUME results (CRWMS M&O 2000 [151349]) for a single volcano occurring at the beginning of the 50,000-year simulation to represent the behavior of similar volcanoes occurring in each 31.25-year interval. Total radionuclide mass concentrations at the receptor point are calculated by ASHPLUME (CRWMS M&O 2000 [151349]) for the first eruptive event, and are then allocated to individual radionuclides according to their relative abundance in the inventory before being used to calculate doses. Doses from eruptions occurring at later times are calculated using the same initial radionuclide concentrations, adjusted to account for radioactive decay and ingrowth.

Uncertainty is included in the analysis of eruptive consequences by completing multiple realizations using different sampled values for input parameters that characterize uncertainty in understanding the system. As described in Section 3.10, these uncertainties include parameters that describe event probability, eruptive processes, the response of the repository, and the biosphere. For the TSPA-SR, results are calculated assuming wind blows to the south in all realizations. This assumption is unrealistic, but provides a conservative bound to uncertainty regarding wind direction and compensates for uncertainty regarding the possibility that contaminated ash deposited by winds blowing in directions other than south might later reach exposed individuals.

4.2.1.2 Incorporating Intrusive Event Probability

The potential repository's response to igneous intrusion cannot be assumed to be constant through time (for example, climate change and the thermal evolution of the system result in different groundwater flux at different times), and consequences of intrusions at different times must be analyzed separately using complete 50,000-year simulations of the full groundwater transport model. This poses a heavy computational burden, and makes it impractical to simulate multiple intrusive events at each time interval, as is done for the eruptive releases. For computational efficiency, igneous intrusions are simulated using a simpler approach in which the time of intrusion is sampled randomly from the 50,000-year period, and the probability associated with each simulation is the full 50,000-year probability, with a mean value of 8×10^{-3}. Although this approach results in statistically sparser analysis of uncertainty than the approach taken for the eruptive scenario, it yields the correct overall probability of igneous intrusion during the period of interest. The approach incorporates both uncertainty in the intrusive event's

probability (by sampling from the distribution of annual probabilities) and uncertainty in the system's response to disruption (by sampling uncertain parameters describing damage to the repository and subsequent radionuclide transport).

4.2.2 TSPA-SR Results for the Igneous Disruption Scenario Class

The TSPA-SR results include 5,000 realizations, each of which represents a different set of input parameters. The probability-weighted doses from both eruptive and intrusive events calculated as described in the preceding sections are added together to give the total probability-weighted dose from igneous disruption. Results of each realization are presented as a 50,000-year probability-weighted dose history that includes 1,600 eruptions occurring at 31.25 year-intervals and a single igneous intrusion occurring at a random time.

Figure 4.2-1 shows a range of probability-weighted dose histories representing possible doses to an exposed individual following disruption of the potential Yucca Mountain repository by igneous activity. Results do not include doses that might result from the nominal performance of the repository, in the absence of igneous activity. These doses are discussed in Section 4.1. Rather than showing the full set of 5,000 realizations included in the analysis, which would result in a display too dense to interpret, the figure shows 500 individual curves (in gray) that represent every tenth realization from the total of 5,000 that were completed. These curves display probability-weighted annual dose rates calculated using different sets of sampled values for uncertain input parameters in the model. The range of results shown by these individual curves displays the uncertainty in the calculated dose history resulting from uncertainty in model parameter values. Four additional curves, shown in color, provide summary information about the distribution of results from the full set of 5,000 realizations. The mean curve, shown in red, is the average probability-weighted annual dose rate and is the performance measure appropriate for comparison to the limit specified in the proposed regulation (see Section 1.3.1.4). The percentile curves, shown for the 95th, 50th (i.e., median), and 5th percentile, show an annual dose rate that is greater than 95 percent (or 50 or 5 percent) of the calculated values at that time. The mean curve lies above the 95th percentile curve throughout the interval between approximately 3000 and 8000 years because the mean is dominated by the relatively small fraction of the total number of realizations that contribute to a high groundwater dose rate at early times. The number of realizations contributing to this pathway increases through time as the cumulative probability of an intrusion having occurs increases, causing the 95th percentile curve to climb above the mean at later times. Figure 4.2-2 shows the mean probability-weighted dose histories for the individual radionuclides that contributed to the total igneous dose rates shown in Figure 4.2-1. These individual radionuclide doses are discussed in more detail in the following paragraphs, in the context of the discussion of the mean total igneous dose history.

For approximately the first 2,000 years, the dose history is a smooth curve dominated by the effects of a volcanic eruption. As shown in Figure 4.2-2, the probability-weighed mean dose during this period reaches a peak of approximately 0.004 mrem/yr roughly 300 years after repository closure, and then drops off due to radioactive decay of the relatively shorter-lived radionuclides that contribute to doses from the ashfall exposure pathway. As shown in Figure 4.2-2, the major contributors to the eruptive dose are ^{241}Am and ^{240}Pu, ^{239}Pu, and ^{238}Pu. ^{90}Sr is a significant contributor at extremely early times, but drops off rapidly because of radioactive decay. Inhalation of resuspended particulates in the ash layer is the primary exposure

pathway during this period, and the smooth decline of the mean dose curve from approximately 300 to 2,000 years results from decay of ^{241}Am, which has a half-life of 432 years.

From approximately 2,000 years after closure onward, the mean igneous dose is dominated by groundwater releases from packages damaged by igneous intrusion. The irregular shape of the curve from this point forward is in part a result of the complex groundwater transport processes, and in part also reflects the occurrence of intrusive events at random times, rather than the prescribed intervals used for the extrusive simulations. Close examination of Figure 4.2-1 shows that individual realizations display distinct peaks occurring at times that are controlled by the sampled time of intrusion and the time required for radionuclide transport through the geologic system. The intrusive event may occur at any time, and the first appearance of groundwater doses in the mean curve at approximately 2,000 years reflects retardation during transport, rather than the absence of intrusions at earlier times. The observation that some of the 500 individual curves continue to be dominated by the smooth eruptive doses for essentially all of the 50,000-year period indicates either that for those realizations the sampled time of intrusion was relatively late or that, in some cases, retardation of radionuclides during transport in the geologic system was effective for a relatively long period of time.

The overall probability-weighted mean igneous dose rate reaches a peak during the first 10,000 years of approximately 0.08 mrem/yr, occurring at 10,000 years. At later times, the calculated mean igneous dose rate is higher, increasing slowly to approach 0.2 mrem/yr at the end of the 50,000-year period. This peak mean igneous dose is dominated entirely by the groundwater releases following igneous intrusion. As shown on Figure 4.2-2, ^{239}Pu and ^{237}Np are the primary contributors to the peak mean dose.

Figures 4.2-3 and 4.2-4 provide an alternative display of the relative contributions of individual radionuclides to the total probability-weighted igneous dose rate at 1,000 and 10,000 years following repository closure. At 1,000 years after closure (Figure 4.2-3), the igneous dose rate is dominated completely by the eruptive releases, and ^{241}Am contributes more than half of the total. ^{241}Am and ^{240}Pu together account for more than three-quarters of the total, and essentially all of the dose comes from ^{241}Am, ^{240}Pu, ^{239}Pu, ^{243}Am, ^{99}Tc, and ^{129}I combined. This is consistent with the dominance of the inhalation exposure pathway for the eruptive scenario and only a minor contribution from the groundwater pathway. At 10,000 years after closure (Figure 4.2-4), the igneous dose rate is dominated by groundwater releases, and the dose is dominated by ^{239}Pu, ^{237}Np, and ^{240}Pu. Additional contributions come from ^{99}Tc and ^{129}I. These results are consistent with the dominance of the groundwater pathway, and are similar to results for nominal performance at later times (see Section 4.1) because of the long half-lives of the major contributors. Contributions from ^{99}Tc and ^{129}I, which dominate the earliest releases in the nominal scenario (Figure 4.1.6), are relatively smaller in the igneous disruption scenario because the assumptions regarding drip shield and waste package performance (see Section 3.10.2) reduces the relative importance of the diffusive transport pathway.

4.2.3 Sensitivity of the TSPA-SR Results for the Igneous Disruption Scenario to Sample Size

Because of the approach taken to sampling on the time of intrusive events, the mean probability-weighted dose for igneous disruption is potentially sensitive to the number of realizations

included in the analysis. For smaller sample sizes, individual realizations, as shown in Figure 4.2-1, have a potential to skew the mean upward or downward if, for example, combinations of parameter values that result in a high dose rate combine with early event times and high event probabilities or late event times and low event probabilities, respectively. Increasing the sample size provides a greater density of sampling on both event time and parameter stability, and provides a stable mean appropriate for comparison to the proposed regulatory limits.

Figure 4.2-5 shows a comparison of probability-weighted mean annual dose rates for igneous disruption calculated using three different sample sizes. The dose rate during the first 2000 years, when the curve is dominated by the eruptive releases, is essentially unchanged because of the very large number of eruptions included in the calculation (see Section 4.2.1.1). At later times, however, the curves differ due to the relative density of sampling on the time of the intrusive event. The blue curve, which is the case discussed in Section 4.2.2 and shown in Figure 4.2-1, uses 5,000 realizations to calculate performance for 50,000 years. This case has the highest density of sampling on the time of the event, and is the case used in Section 4.3 to construct the overall expected annual dose. The black curve in Figure 4.2-5 is calculated using 1,000 realizations for 100,000 years. The irregular shape of the curve in the first 20,000 years indicates that the sample size is too small, and that too few realizations are contributing to the determination of the mean during this interval. At later times, however, the probability that an intrusive event has already occurred increases, more realizations contribute to the mean, and the curve becomes smoother. The convergence of the 50,000 and 100,000 year cases between 30,000 and 40,000 years indicates that the sample size for the 100,000-year simulation is adequate at later times. The observation that the peak mean annual probability-weighted dose remains essentially constant after 50,000 years in the 100,000-year case provides a high degree of confidence that the overall expected annual dose rate, as described in Section 4.3, can be appropriately presented using results from the 50,000-year case.

The intermediate curve in Figure 4.2-5, shown in red, uses 1000 realizations to simulate the probability-weighted mean annual dose rate from igneous disruption during the first 20,000 years. This curve represents a smaller density of sampling on the time of the event than the 50,000-year case, but provides reasonable coverage during the period of primary interest. The near convergence of this curve with the two other curves as it approaches 20,000 years provides further confidence that it provides a reasonable estimate of performance. Because of the relative efficiency of this calculation and because of its emphasis on the period of greatest interest for igneous disruption, the 20,000-year case is used as a base case for comparison purposes in the sensitivity analyses reported in Section 5.2.9.

4.3 TOTAL SYSTEM PERFORMANCE FOR THE COMBINED SCENARIOS

As specified (see Section 1.3.3.2) in proposed 10 CFR 63.113(c) (64 FR 8640 [101680]), the TSPA for a compliance demonstration must consider all FEPs that have not been excluded through a systematic screening process (see Section 2.1). Specifically, the expected annual dose used for comparison with the dose limit in proposed 10 CFR 63.113(b) (64 FR 8640 [101680]) must be estimated "considering the probability of the occurrence of the events and the uncertainty, or variability, in parameter values used to describe the behavior of the geologic repository" (proposed 10 CFR 63.2 [64 FR 8640 [101680]). Thus, the expected annual dose

includes all significant nominal and disruptive FEPs (i.e., both the likely behavior of the disposal system and the consequences of unlikely events), and the nominal and disruptive dose results must be combined to obtain the overall dose results specified in the proposed regulations.

In the TSPA&I issue resolution status report (NRC 2000 [149372], Section 4.4.1), the NRC provides guidance on the method of combining the expected annual doses for nominal and disruptive scenarios. The dose for each scenario is weighted by the scenario probability, so the summed expected annual dose includes both consequence and probability and therefore represents the expected risk for the repository (NRC 2000 [149372], Section 4.4.1). Consistent with the requirements of proposed 10 CFR 63.113(c) (64 FR 8640 [101680]), the expected annual dose histories do not include the human intrusion scenario. Results for the inadvertent human intrusion scenario are evaluated separately through a TSPA for a stylized human intrusion scenario, designed in accordance with NRC proposed requirements and guidance (Section 4.4).

4.3.1 Method for Combining Scenarios

As described in Sections 4.1 and 4.2, Monte Carlo simulations have been performed for the nominal and igneous-disruption scenarios. Within a scenario, uncertainty in input parameters and the future behavior of the system are addressed by computing many realizations, each of which has a different set of input parameters. As discussed in Sections 4.1.4 and 4.2.3, the base case includes 300 realizations of the nominal scenario and 5000 realizations of the igneous-disruption scenario. The large number of realizations needed for the igneous-disruption scenario is primarily driven by the need to have a fine-enough sampling on the time of the intrusive event (Section 4.2.3).

A straightforward method of combining the dose results for the nominal and disruptive scenarios (CRWMS M&O 2000 [147323], Section 4.4) is illustrated in Figure 4.3-1. In this method, first a conditional mean dose history is calculated for each scenario by averaging the dose values at each time step. Then, a weighted-mean dose history for each scenario is generated by multiplying the conditional mean dose by the scenario probability at each time step. Lastly, the final expected annual dose history is calculated by adding the two weighted-mean doses at each time step. This method is easily extended to any number of scenarios, but the illustration shows only two because those are the only scenarios that survived the scenario screening process (Section 2.1.1.1).

The method actually used for the TSPA-SR is slightly different (Figure 4.3-2). As discussed in Section 4.2, the igneous disruption simulations do not include nominal waste package failure processes; all releases are caused by igneous intrusion, directly or indirectly. Thus, the igneous disruption scenario differs slightly from the usual definition, in which all nominal processes are included in addition to the disruptive processes. It is important to note that for the regulatory period of 10,000 years there are no nominal waste package failures, so for that period, the igneous disruption scenario can be said to include all nominal processes. However, by 100,000 years many waste packages have failed by nominal processes (see Figure 4.1-9), and the igneous disruption results are significantly affected by the absence of nominal waste package failures.

Nominal processes are fully incorporated into the final expected annual dose by weighting the nominal scenario by 1 rather than by its actual probability, which is slightly less than 1. To explain further, let the probability of an igneous intrusion be p_i. Then the probability of no intrusion, which is to say the probability of only nominal processes, is $1 - p_i$. At a particular time, denote the nominal annual dose by D_n and the disruptive annual dose (not including nominal failures) by D_i. Because it is assumed that nominal models can be used in simulating the igneous disruption scenario (Section 3.10), the annual dose for an igneous disruption, including all nominal processes, is approximated by $D_n + D_i$. This approximation is an equality if there is no overlap between the waste packages that fail because of nominal processes and the waste packages that fail because of the igneous event. The approximation is conservative if there is an overlap because, in that case, releases from one or more waste packages are being counted twice. The probability-weighted total annual dose is then approximated by $D_t = (1 - p_i)D_n + p_i(D_n + D_i) = D_n + p_iD_i$. This equality shows that if the nominal scenario is weighted by 1 and the igneous disruption scenario without nominal failures is weighted by the disruption probability, then the correct expected annual dose will be calculated (Figure 4.3-2).

Another difference between the method illustrated in Figure 4.3-1 and the method used for this TSPA (shown in Figure 4.3-2) is that the conditional mean dose history for the igneous disruption scenario is never calculated. The probability weighting is applied individually to each realization, and each realization has a different probability weight, as discussed in Section 3.10. This variant of the method is applied because the probability of an igneous intrusion is considered to be uncertain and is sampled from a probability distribution. The net effect is still to weight each dose history by its appropriate probability to obtain the proper expected annual dose.

4.3.2 Results for Combined Performance

Results for the nominal scenario are discussed in Section 4.1, with the dose histories and some statistical measures (mean, median, 5th percentile, and 95th percentile) given in Figure 4.1-5. Results for the igneous disruption scenario (with nominal waste package failures excluded) are discussed in Section 4.2, with the dose histories and statistical measures given in Figure 4.2-1. For both the nominal and disruptive scenarios, the results given previously already have the proper weighting. The nominal doses shown in Figure 4.1-5 are conditional, so they have the full probabilistic weighting of 1. The igneous doses shown in Figure 4.2-1 are already weighted by the probability of an igneous event. Thus, the combined dose for the total system is obtained simply by adding them. Because the nominal and disruptive Monte Carlo simulations do not use the same values for parameters that are common to both (because of their different numbers of realizations), the individual realizations can not be added. However, the correct mean annual dose is obtained by adding together the two scenario mean curves, as discussed above. The combined mean dose curve, along with the mean curves for the two individual scenarios for comparison, are shown in Figure 4.3-3. The combined mean curve in Figure 4.3-3 corresponds to the expected annual dose, which is the performance measure of proposed 10 CFR 63.113(b) (64 FR 8640 [101680]).

At early times (before about 40,000 years), igneous disruption doses dominate the scenario combination. In particular, the combined dose is given by igneous disruption alone during the 10,000-year regulatory period, because there are no nominal waste package failures that early.

However, during later times (after about 40,000 years), the combined dose is dominated by the nominal dose because of the large number of nominal waste package failures. The base-case igneous disruption scenario was simulated for only 50,000 years. However, by 50,000 years the sum is dominated by the nominal scenario, so the combined mean curve is continued out to 100,000 years by neglecting the contribution from igneous intrusion after 50,000 years.

The detail regarding radionuclide contributions to dose and intermediate subsystem results contained in Sections 4.1 and 4.2 will not be duplicated here. The radionuclide and subsystem results described in Section 4.2 apply as well to the combined system at early times, and the radionuclide and subsystem results described in Section 4.1 apply as well to the combined system at later times.

4.4 INTRUSION HUMAN PERFORMANCE RESULTS

Proposed 10 CFR Part 963 (64 FR 67054 [124754], Sections VI.B(g), VI.B(h), 963.16, and 963.17) includes a requirement for the DOE to conduct a separate performance assessment to evaluate the consequences of human intrusion (see Section 1.3.1.4). The separate human intrusion performance assessment must be evaluated in terms of compliance with the same radiation protection standard considered for the combined nominal and disruptive performance assessment described in Section 4.3 (Figure 4.4-1).

Proposed 10 CFR Part 963 (64 FR 67054 [124754], Section 963.16[a][2]) states that the human intrusion evaluation should be "consistent with applicable NRC regulations regarding a stylized human intrusion case." The applicable NRC regulations are contained in proposed 10 CFR Part 63 (64 FR 8640 [101680], Sections XI, 63.102, and 63.113). Proposed 10 CFR Part 963 (64 FR 67054 [124754], Section II.K.1) also states that "it is anticipated that NRC would conform its proposed licensing regulation at 10 CFR Part 63 (64 FR 8640 [101680]) to the final EPA radiation protection standards, as necessary and appropriate." The EPA radiation protection standards are contained in proposed 40 CFR Part 197 (64 FR 46976 [105065], Sections III.C, III.E, 197.25, and 197.26). As discussed in Section 1.3 (see Table 1.3-3), the proposed NRC regulation and the proposed EPA standard are not identical for human intrusion, although they must be consistent when finally promulgated. Therefore, it is necessary to consider aspects of human intrusion contained in both the NRC regulation and the EPA standard that might logically be incorporated when they are finally promulgated.

The details of the stylized human intrusion scenario, based on the NRC regulations, are described in Section 4.4.1. Aspects of human intrusion contained in the proposed EPA radiation protection standards that differ from the proposed NRC regulations are also discussed. The results of the human intrusion performance assessment and comparison with the radiation protection standards are presented in Section 4.4.2.

4.4.1 Technical Bases for Human Intrusion Analyses

4.4.1.1 Regulatory Basis for Human Intrusion

The flow of information wheel for the stylized human intrusion scenario is shown in (Figure 4.4-2). It is based on the current TSPA-SR conceptualization of the human intrusion assumptions that are outlined in both the proposed NRC regulation and EPA standard. These

assumptions, and resolution of any differences, are summarized in Table 4.4-1 (also see Table 1.3-3).

Table 4.4-1. Human Intrusion Scenario Regulatory Assumptions

NRC Base Assumptions (from Proposed 10 CFR Part 63 [64 FR 8640 [101680])	EPA Additional and/or Conflicting Assumptions (from Proposed 40 CFR Part 197 [64 FR 46976 [105065])	Conceptualization for TSPA-SR
Assumed intrusion is a drilling event.	Assumed intrusion is acute and inadvertent.	Inadvertent drilling event.
Drilling result is a single, nearly vertical borehole that penetrates a waste package and extends down to the SZ.	Borehole penetrates a degraded waste package.	Single vertical borehole from surface through a single waste package to the SZ.
Intrusion occurs 100 years after closure.	Intrusion time should take into account the earliest time after disposal that a waste package could degrade sufficiently that current drilling techniques could lead to waste package penetration without recognition by the drillers.	Intrusion occurs at 100 years (a 10,000 year intrusion time is examined in a sensitivity simulation).
Borehole properties (diameter, drilling fluids) are based on current practices for resource exploration.	Borehole results from exploratory drilling for groundwater.	Borehole diameter consistent with an exploration groundwater well.
Borehole is not adequately sealed to prevent infiltrating water.	Natural degradation processes gradually modify the borehole, the result is no more severe than the creation of a groundwater flow path from the crest of Yucca Mountain through the potential repository and to the water table.	Infiltration and transport through the borehole assumes a degraded, uncased borehole, with properties similar to a fault pathway.
Hazards to the drillers or to the public from material brought to the surface by the assumed intrusion should not be considered.	Only consider releases through the borehole to the SZ; consider releases occur gradually through air and water pathways, not suddenly as with direct removal.	Groundwater is only pathway considered.
A separate consequence analysis is required, identical to the performance assessment, except for the occurrence of the specified human intrusion scenario.	Unlikely natural processes and events are not included, but analysis could include disturbances by other processes or events that are likely to occur.	Intrusion borehole is applied to nominal case; effects of volcanism are not included.
Peak dose is not to exceed 25 mrem/yr. in the first 10,000 years.	Peak dose is not to exceed 15 mrem/yr. in the first 10,000 years.	Does not affect simulations.

A key difference noted in Table 4.4-1 between the NRC and EPA regulations is the time of intrusion. In proposed 10 CFR 63.113 (d) (64 FR 8640 [101680]), the NRC assumes the intrusion to occur 100 years after permanent closure (Figure 4.4-3 (a)). The EPA states in proposed 40 CFR 197.26 (g) (64 FR 46976 [105065]) that the intrusion occurs at a time determined by the NRC, but also states in proposed 40 CFR 197.25 and 197.26 (g) (64 FR 46976 [105065]) that the NRC should take into account the earliest time after disposal that a waste package could degrade sufficiently that current drilling techniques could lead to waste package penetration without recognition by the drillers (Figure 4.4-3 (b)). The EPA (64 FR 46976 [105065], Section III.E) further points out that a waste package would likely be recognizable to a driller for "at least thousands of years" and that if the intrusion could not occur until after

10,000 years that the results would not be part of the licensing process but would be included in the Yucca Mountain EIS instead.

For TSPA-SR, human intrusion was assumed to occur at 100 years after closure into a relatively intact waste package. This early intrusion time was selected because it was considered to be conservative and because it was difficult to defensibly quantify a later intrusion time consistent with EPA guidance. A later intrusion time (10,000 years), approximating the EPA guidance, was examined in a sensitivity analysis (see Section 4.4.2).

The construction of the human intrusion conceptual model for TSPA-SR, based on the regulatory guidance summarized in this section, is described in Section 4.4.1.2. The implementation and integration of the human intrusion model in TSPA-SR is described in Section 4.4.1.3.

4.4.1.2 Features, Events, Processes, and Conceptual Model for Human Intrusion

A comprehensive set of FEPs relevant to the human intrusion scenario were evaluated (see Appendix B). The FEPs directly relevant to the human intrusion event are listed in Table B-9 (all FEPs with a FEP number beginning with 1.4). In general, the human intrusion FEPs were screened in or out of the TSPA-SR based on the regulatory guidance summarized in Table 4.4-1. For excluded (screened out) FEPs, the basis for exclusion is summarized in Appendix B. Those FEPs that are included (screened in) in the human intrusion conceptual model (as listed in Table B-9) along with the regulatory guidance in Table 4.4-1, form the basis for the TSPA-SR human intrusion conceptual model (Figure 4.4-4).

The TSPA-SR human intrusion scenario conceptual model includes five key components (Figure 4.4-5):

- Infiltration of water down the borehole and into the penetrated waste package
- Mobilization and release of radionuclides from the penetrated waste package
- Transport of radionuclides down the borehole to the water table
- Transport of radionuclides through the SZ
- Biosphere exposure pathways and dose calculation at the receptor location.

The implementation and integration of these five key components of human intrusion into the TSPA-SR model are described in Section 4.4.1.3.

4.4.1.3 Implementation and Integration of Human Intrusion within Total System Performance Assessment

As identified in Table 4.4-1, the human intrusion scenario is identical to the nominal scenario, except for the intrusion borehole. Therefore, the TSPA-SR model for human intrusion derives from the TSPA-SR nominal scenario model. The human intrusion borehole is assumed to be drilled from the ground surface (at a random location within the footprint of the potential repository), through the drip shield and a single waste package (top and bottom), to the water table. The borehole is assumed to have the diameter of a standard rock bit used for water well drilling.

Three of the key human intrusion components identified in Section 4.4.1.2—infiltration down the borehole, waste mobilization and release, and borehole transport—are associated with the intrusion borehole. In the TSPA-SR human intrusion model, infiltration down the borehole and borehole transport replace the performance contribution provided by the UZ in the nominal scenario. Implementation of waste mobilization and release in the human intrusion model differs slightly from the nominal model because the failure mode (drilling breach rather than corrosion) and number of packages failed (one rather than many) are different. All of the waste within the penetrated waste package is assumed to have cladding perforations from the action of the drillbit.

Implementation of the other two key human intrusion components—SZ transport and biosphere—is consistent with the nominal model. Wherever possible, nominal model components and input data for climate, SZ transport, and biosphere processes were used.

The TSPA-SR human intrusion model was used to simulate a 100,000-year period using climatic and hydrogeologic conditions consistent with the nominal scenario. Consistent with the regulatory definition of a TSPA (64 FR 67054 [124754], Section 963.2), the human intrusion model was run probabilistically.

The five key components of human intrusion described in Section 4.4.1.2 are based on FEPs screening and regulatory guidance. However, to fully define the human intrusion scenario for implementation within TSPA-SR, a number of additional technical assumptions, not addressed in the regulations, were required. The technical assumptions are summarized in Table 4.4-2. Key technical assumptions are shown schematically in Figure 4.4-6.

Table 4.4-2. Human Intrusion Scenario Technical Assumptions

Issue	Key Component Affected	TSPA-SR Implementation
Borehole diameter	Infiltration Borehole Transport	Typical water well borehole has a diameter of 20.3 cm (8 in.).
Infiltration into borehole	Infiltration	Assumed infiltration rate distribution is based on modeled infiltration in the Yucca Mountain region for the glacial transition climate. Values at the high end of the distribution inherently include the possibility of surface water collection basin focusing.
Seepage into penetrated waste package	Infiltration Waste Mobilization	Volumetric flux is equivalent to infiltration rate times borehole area. Volume of drilling fluid is ignored.
Type of waste package penetrated	Waste Mobilization	Sampled from CSNF and co-disposed waste packages. Co-disposed packages contain both DSNF and HLW glass.
Thermal and geochemical conditions in waste package	Waste Mobilization	Assume temperature and in-package chemistry as calculated in nominal scenario. This assumes Well J-13 water and ignores any chemical effects of the drilling fluid.
Waste form degradation	Waste Mobilization	Waste in penetrated package is assumed to have perforated cladding from drilling disturbance.
Solubilization of radionuclides in water	Waste Mobilization	Infiltrating water can mix with waste in entire waste package. Solubility is based on temperature and in-package chemistry as in nominal scenario.

Table 4.4-2. Human Intrusion Scenario Technical Assumptions (Continued)

Issue	Key Component Affected	TSPA-SR Implementation
Borehole flow and transport properties	Infiltration Borehole Transport	Volumetric flux consistent with seepage into the waste package. Transport properties consistent with a UZ fault pathway.
Borehole location	Infiltration SZ Transport	Random over the footprint of the potential repository. Uncertainty in location is captured in infiltration rate and location that radionuclides enter the SZ.
Borehole length	Borehole Transport	Borehole length from the potential repository to SZ conservatively assumes water level consistent with glacial transition climate.
SZ	SZ Transport	Assume SZ flow and transport properties identical to nominal scenario.
Biosphere processes	Biosphere	Assume exposure pathways and receptor characteristics identical to nominal scenario.

The implementation and integration of the five key components and the associated technical assumptions in the TSPA-SR human intrusion model are described in more detail in the following five subsections. The model implementation is shown schematically in Figure 4.4-7. A more detailed description of specific input parameters and their values is presented in the TSPA-SR Model (CRWMS M&O 2000 [148384], Section 6.3.9.3).

4.4.1.3.1 Infiltration Down Borehole

The inputs, outputs, and technical assumptions associated with the infiltration of water down the borehole and into the penetrated waste package are summarized in Figure 4.4-8. The volume of water flowing down the intrusion borehole and into the waste package was based on infiltration rather than precipitation. It was deemed unrealistic to assume that all precipitation would flow directly down a degraded borehole. Instead, infiltrating water was assumed to flow preferentially down the degraded borehole, bypassing the UZ. The infiltration rate was sampled from a distribution based on the modeled infiltration calculated for the glacial transition climate (CRWMS M&O 2000 [145774], Section 3.5.2). Infiltration rates at the upper end of the distribution account for the possibility of enhanced infiltration if the borehole is located in an area where it might capture significant runoff (e.g., a wash or other surface water collection basin). The volumetric flux of water down the borehole is based on the infiltration rate entering a 20.3-cm-diameter borehole. The calculated volumetric flux down the borehole from surface infiltration was assumed to flow directly into the penetrated waste package, with no gain or loss from the surrounding UZ.

In the TSPA-SR, the infiltration down the borehole was not explicitly modeled, rather the borehole infiltration flux was assumed to flow directly into the penetrated waste package. The effect of a higher infiltration flux (with the flux fixed at the 95th percentile value) was examined in a sensitivity simulation (see Section 5.2.10).

4.4.1.3.2 Waste Mobilization and Release

The inputs, outputs, and technical assumptions associated with the mobilization and release of radionuclides from the penetrated waste package are summarized in Figure 4.4-9. The volumetric flux of water from infiltration (described in Section 4.4.1.3.1) was assumed to flow directly into the penetrated waste package, with no resistance from the drip shield or waste package. The penetrated waste package was represented by a mixing cell in which the entire volume of waste from the waste package was available for degradation. The waste package type was sampled based on the relative number of CSNF and co-disposed waste packages present in the inventory. Under the current thermal loading, the penetrated waste package would be thermally hot at 100 years to the extent that liquid water entering the waste package would be converted to vapor. Therefore, a conservative bias is incorporated into the human intrusion scenario by assuming that liquid water flows through the penetrated waste package and dissolves radionuclides at 100 years.

Waste mobilization and release processes are not specified in regulations. It was assumed that all waste in the penetrated package had cladding perforated by drillbit damage, enhancing mobilization. However, no waste was assumed to be transported directly to the SZ (e.g., as cuttings on the drillbit or by falling to the bottom of the borehole before it degrades) or to the surface. The radionuclides in the waste were assumed to be mobilized by advection (mixing with and dissolution in the infiltrating water) and diffusion. Radionuclide solubilities were based on nominal scenario in-package temperature and chemistry. This assumes Well J-13 water, which inherently ignores the chemical effects of the drilling fluid.

As described in Section 3.5.1.1, the human intrusion analysis used the radionuclides from the nominal scenario along with two additional radionuclides: ^{90}Sr and ^{137}Cs. The additional radionuclides were screened out of the nominal scenario based on short half-lives and/or high sorption in the UZ. With a human intrusion at 100 years that bypasses the UZ, they were potentially important to the human intrusion scenario. The human intrusion analyses include transport of both dissolved species and colloidal particles. This suite of radionuclides adequately encompasses doses that could result from both dissolved and colloidal transport of radionuclides.

All of the mobilized radionuclides were assumed to be released through the bottom breach in the waste package for advective transport down the borehole to the SZ.

4.4.1.3.3 Borehole Transport

The inputs, outputs, and technical assumptions associated with the transport of radionuclides down the borehole to the water table (i.e., to the SZ) are summarized in Figure 4.4-10. The radionuclide mass (both dissolved and colloidal) released from the waste package (described in Section 4.4.1.3.2) was assumed to be transported down the human intrusion borehole to the water table. At the water table, the radionuclide mass was transported by processes appropriate for the SZ (see Section 4.4.1.3.4). As described in Table 4.4-1, the borehole transport pathway was assumed to be a degraded, uncased borehole, with properties similar to a fault pathway in the UZ.

The implementation of the borehole transport pathway below the potential repository in TSPA-SR is a one-dimensional "pipe" pathway. The pipe pathway requires borehole cross-sectional area, volumetric flux, porosity, fluid saturation, and dispersivity. The volumetric flux was assumed to be the same as in the borehole above the waste package. The pipe transport included sorption (based on devitrified unit properties), but did not include matrix diffusion.

The borehole length from the potential repository to the SZ of 190 m (623 feet) conservatively assumed a water level consistent with the glacial transition climate. The distance from the potential repository to the water table is greater for the present day and monsoon climates.

4.4.1.3.4 Saturated Zone Transport

The transport of radionuclides through the SZ in the TSPA-SR human intrusion model was identical to the nominal model, with two exceptions. First, two additional radionuclides (^{90}Sr and ^{137}Cs) were added. Second, the radionuclide source region for the SZ was sampled between regions 1 and 3; regions 2 and 4 were never used (CRWMS M&O 2000 [139440], Figure 2).

Because the intrusion borehole could be located anywhere within the footprint of the potential repository, the radionuclides transported down the borehole could enter the SZ at any point below the footprint with equal probability. Sampling between regions 1 and 3 (the two SZ source regions that underlie the footprint) accounts for the randomness in the location of the intrusion borehole.

4.4.1.3.5 Biosphere Processes

The biosphere exposure pathways and dose calculation at the receptor location in the TSPA-SR human intrusion model were identical to the nominal model, except that additional BDCFs were required to account for the two additional radionuclides.

4.4.2 Results and Interpretation of Human Intrusion Analyses

The regulations require a separate performance assessment to evaluate the consequences of human intrusion. The separate human intrusion performance assessment was evaluated in terms of compliance with the same radiation protection standard considered for the combined nominal and disruptive performance assessment.

As with the combined nominal and disruptive scenario, the human intrusion scenario was run probabilistically. Uncertainty is explicitly included in the models and input parameters in the form of discrete probability distributions. Uncertainty in the possible performance was evaluated through the use of these probabilistic analyses. Although the expected (or mean) human intrusion performance of potential repository system can be determined from the range of probabilistic outcomes, the entire range of possible outcomes was examined.

Figure 4.4-11 shows the TSPA results for the base case human intrusion scenario with an intrusion at 100 years after closure. As with the combined nominal and disruptive performance assessment, the time period of regulatory interest is 10,000 years after the closure of the potential repository. This figure illustrates the human intrusion dose that is projected to occur out to

100,000 years to provide a level of confidence that there are no unexpected changes in dose beyond the regulatory period of performance.

Figure 4.4-11 shows 300 simulated dose histories along with some statistical measures of the dose distribution. The mean curve is generated by averaging the 300 dose values at each time step, and the percentile curves are generated by determining the location of the given percentile at each time step (for example, the median curve is generated by determining the dose which has half of the calculated doses above it and half below it at each time step). There is a considerable amount of variability in the projections of human intrusion dose, and there are non-zero doses within the first 10,000 years. However, no dose for any of the 300 realizations exceeds 0.5 mrem/yr over the first 10,000 years. The peak mean human intrusion dose during the first 10,000 years after potential repository closure is approximately 0.008 mrem/yr., occurring at approximately 1,000 years. Over the entire 100,000 years, the peak mean dose is also approximately 0.008 mrem/yr. and the peak median dose (50 percent probability) is about 0.00007 mrem/yr. The mean dose rate is significantly larger than the median dose rate because the mean is dominated by a few realizations with high dose rate histories, while the median represents the mid-point results from all 300 realizations.

Figure 4.4-12 shows the TSPA results for the human intrusion scenario with an intrusion at 10,000 years after closure. This simulation examines the effect of an intrusion at a hypothetical time more consistent with the EPA regulation (see Table 4.4-1). Figure 4.4-12 shows a comparison of the mean human intrusion dose curve from an intrusion at 10,000 years with the mean dose curve from the base case intrusion at 100 years. For the intrusion at 10,000 years, there were no doses prior to 10,000 years and the peak mean dose over 100,000 years is less than for the base case intrusion at 100 years. At 100,000 years, the mean dose is nearly identical to the mean dose from the base case.

The analyses compared in Figure 4.4-12 were performed using probabilistic TSPA simulations with 100 realizations. One hundred realizations were used rather than the 300 used for the base-case simulation because 100 realizations are sufficient to see the relative effects when comparison is made to the base case.

4.5 TREATMENT OF POTENTIALLY DISRUPTIVE EVENTS IN THE TOTAL SYSTEM PERFORMANCE ASSESSMENT

The following sections describe the TSPA-SR treatment of specific potentially disruptive events identified in the Repository Safety Strategy Rev. 3 (CRWMS M&O 2000 [139593], Section 2.3) and Rev. 4 (CRWMS M&O 2000 [148713], Section 5.3) as being of special concern. These potentially disruptive events fall into two categories:

- Those leading to extreme environments or conditions that could affect any one of the principal factors that determine postclosure performance
- Those directly disrupting important potential repository system barriers, including
  - Inadvertent human intrusion
  - Rise of the water table

- Seismic activity
- Igneous activity
- Waste-generated disruptions (radiolysis, pyrophoricity, nuclear criticality)
- Early failure of engineered barriers
- Drift collapse.

As described in Section 2.1.1.1, the TSPA-SR has defined disruptive events (as distinguished from potentially disruptive events) to be those events that have a probability less than one and that have not been excluded by the FEPs screening process. This definition was chosen to be consistent with the FEP screening process, and is somewhat inconsistent with other usages that define events as disruptive prior to the evaluation of their impact on overall performance. For example, the *Disruptive Events Process Model Report* (CRWMS M&O 2000 [141733]) addresses only those FEPs related to igneous activity, tectonic activity, and seismicity, and includes consideration of FEPs that are screened out of the TSPA on the basis of low probability (e.g., faulting) or low consequence (e.g., long-term tectonic changes), as well as FEPs that are included in the nominal scenario class (seismically-induced cladding failure) and the disruptive scenario class (igneous activity). Proposed 10 CFR Part 963.117 (64 FR 67054 [124754]) specifies consideration of four disruptive events: volcanism, seismic events, nuclear criticality, and inadvertent human intrusion. Each of these four events is treated differently in the TSPA-SR: volcanism, seismicity, and criticality have been examined through the FEPs process, and only volcanism has been retained for analysis in a separate disruptive scenario. Human intrusion has been treated through a separate performance assessment analysis (Section 4.4), consistent with proposed regulatory requirements. Other potentially disruptive events have been evaluated in detail through the FEPs screening process (see Section 2.1 and Appendix B) and have been excluded from the TSPA-SR on the basis of the probability or consequence criteria defined by the applicable proposed regulations. The YMP FEP database (CRWMS M&O 2000 [150806], Appendix D) provides detailed documentation of the screening of all potentially disruptive events, including many not listed above. The treatment of the potentially disruptive events listed above is discussed in the following sections.

4.5.1 Extreme Conditions Affecting Principal Factors

As described in the Repository Safety Strategy Rev. 3 (CRWMS M&O 2000 [139593], Section 2.3.1), extreme conditions affecting any one of the principal factors may include, for example, potentially high local flow conditions or extreme water chemistries that could affect waste package performance. In general, extreme environmental conditions that are within the range of reasonable and realistic possibilities for the future have been included in the models and parameter distributions used to characterize the nominal performance of the potential repository, as described in Section 3. The probabilistic approach used in the TSPA-SR uncertainty analysis (Section 2.2.4) ensures that effects of these extreme conditions are included in the analysis. Sensitivity analysis techniques (Section 2.2.5) allow recognition of the impact of extreme parameter values on overall performance. Results of the TSPA-SR uncertainty analysis are described in Section 5.1. In some cases, additional sensitivity analyses have been performed using specified parameter values, rather than distributions, to provide insight into the importance of parameters representing processes of interest. These sensitivity analyses are described in Section 5.2.

4.5.2 Barrier Disruption Due to Inadvertent Human Intrusion

Because future human activity cannot be predicted, the possibility of inadvertent intrusion into the potential repository in the future cannot be precluded. The NRC and the EPA have each recognized this possibility, and they have proposed requiring that the DOE assess potential repository performance following a stylized drilling intrusion, such as might occur during exploration for water or other natural resources. An analysis of the consequences of human intrusion, as prescribed in the proposed NRC and EPA regulations, is presented in Section 4.4. In addition, studies have been conducted regarding the potential for future exploration at the site. Extensive review of the potential for occurrences of natural resources at Yucca Mountain has concluded that no currently economic resources occur at the site, nor are any likely to be found in the future (DOE 1998 [100548], Section 2.2.7.3). Regardless of the specification to consider human intrusion by drilling, the probability of future drilling for natural resources at Yucca Mountain is extremely low.

4.5.3 Barrier Disruption Due to Water Table Rise

Various mechanisms have been proposed that could cause changes in the elevation of the water table, including climate change, seismic pumping, changes in regional stress, and hydrothermal effects associated with igneous activity. Water table changes due to climate change have been included in the nominal scenario through changes in the SZ groundwater flow model (Section 3.8). Other causes of water table rises have been evaluated through the FEPs screening process and have been shown to be of sufficiently low consequence or probability to have been excluded from the TSPA analysis (see Appendix B and CRWMS M&O 2000 [150806], Appendix D).

4.5.4 Barrier Disruption Due to Seismic Activity

Seismic events of uncertain magnitude are likely to occur at Yucca Mountain in the future, and seismicity is therefore more appropriately thought of as an expected, or nominal, process rather than as a disruptive event. Various consequences of seismic activity and faulting have been considered in detail for the TSPA-SR, including direct damage to drifts due to fault displacement; effects of fault displacement on groundwater flow; damage to drip shields, waste packages, and the waste itself from vibratory ground motion; and damage to drifts and engineered barriers from rock falls induced by ground motion. Damage to fuel rod cladding due to seismic ground motion is explicitly included in the TSPA-SR, as described in Section 3.5.4. All other consequences of ground motion have been excluded from the TSPA-SR on the basis of low consequence or low probability (see Appendix B and CRWMS M&O 2000 [150806], Appendix D).

4.5.5 Barrier Disruption Due to Igneous Activity

Igneous activity has been included in the TSPA-SR explicitly in the disruptive scenario class. Section 3.10 describes the TSPA models for the probability and consequence of igneous activity at the site, and Section 4.2 describes the results of the TSPA-SR analysis of igneous activity. As described in Section 3.10.2, not all FEPs potentially relevant to igneous activity have been included in the model. Instead, the model focuses on analyzing two igneous disruption

scenarios: (1) the direct release of waste during an eruption and the subsequent atmospheric transport in an ash plume and (2) the release and subsequent groundwater transport of radionuclides from packages that are damaged by intrusion. Other potentially relevant events and processes, including those associated with the effects of intrusions that do not intersect the potential repository, have been evaluated and excluded from the TSPA on the basis of low consequence or probability (see Appendix B and CRWMS M&O 2000 [150806], Appendix D).

4.5.6 Barrier Disruption Due to Waste-Generated Changes

Waste-generated changes include FEPs related to repository-generated thermal effects on fluid flow and chemistry and FEPs related to waste-specific processes such as radiolysis, pyrophoricity, and nuclear criticality. Most waste-generated changes are included in the uncertainty analysis of nominal performance through models and parameters that characterize thermal, hydrologic, and chemical effects. Radiolysis and pyrophoricity have been evaluated and have been excluded from the TSPA-SR on the basis of low consequence or low probability (see Appendix B and CRWMS M&O 2000 [150806], Appendix D).

Nuclear criticality was evaluated in *Disposal Criticality Analysis Methodology Topical Report* (YMP 1998 [104441]). Criticality in the waste and the engineered barrier system (EBS) has been excluded from the TSPA-SR on the basis of low probability of occurrence during the first 10,000 years of performance. As described in *Probability of Criticality Before 10,000 Years* (CRWMS M&O 2000 [149939]), the probability of a nuclear criticality event at Yucca Mountain has been examined under conditions of nominal performance, potential damage due to seismicity, and igneous disruption. The probability of criticality in the waste package, near-field, and far-field has been shown to be below one chance in 10,000 in the first 10,000 years following repository closure for nominal performance for all waste types. This conclusion is based on the low probability of waste package failure during the first 10,000 years (waste package failure is a necessary condition for all configurations that could lead to criticality), and includes consideration of potential seismic effects. For the igneous disruption scenario, the probability of criticality in commercial spent nuclear fuel (CSNF) both within partially damaged packages and in fuel/magma mixtures that might occur following complete damage of packages are also shown to be below one chance in 10,000 in 10,000 years. The screening decision is preliminary because calculations are incomplete for criticality of DSNF in magma following igneous disruption, and for criticality events of all waste types outside the package following igneous disruption, in both the near-field and far-field.

4.5.7 Early Failure of Engineered Barriers

Waste packages and drip shields have a potential to fail earlier than might be predicted simply as a result of corrosion processes for a variety of reasons, including manufacturing defects, damage during shipment, improper placement, or other factors that escape detection during the operational period. As discussed in Section 3.4, manufacturing defects in the waste packages are included in the modeling of waste package performance for the nominal scenario, and are shown to have little effect on failure due to corrosion. Manufacturing defects in the drip shield are excluded from the TSPA-SR due to the low probability that significant defects will remain following construction of the drip shield components. Defects associated with errors in waste package and drip shield emplacement (and other operational activities) have been excluded from

the TSPA on the basis of low probability that they will escape detection during operational phase inspections (CRWMS M&O 2000 [147359]).

4.5.8 Barrier Disruption Due to Drift Collapse

Degradation of the ground support system and subsequent rockfall are probably more appropriately thought of as part of the nominal evolution of the potential repository (and any underground mined facility), rather than as disruptive events. The timing and magnitude of rockfall are uncertain, but the eventual occurrence of some rockfall and drift degradation is highly likely. Analyses of the joint orientation and spacing in the underground support system define the range of block sizes expected; analyses of the response of waste packages and drip shields to this range of rockfalls indicates that rockfalls will not significantly affect performance of the engineered barriers, with or without backfill. Rockfall and drift collapse have, therefore, been screened out of the TSPA-SR analysis on the basis of low consequence (see Appendix B and CRWMS M&O 2000 [150806], Appendix D).

4.6 ALTERNATIVE REPOSITORY DESIGN ANALYSES

The SR reference repository design is presented in Section 1.7. One of the aspects of the reference design is the concept that no backfill will be emplaced over the drip shields. The analyses presented in this section include comparisons between the reference design and the two following alternative design cases: (i) the reference design with backfill (partially filling the drift over the drip shield) and (ii) a low thermal load design. These comparisons evaluate the effect of each alternative design case on waste package temperature profiles, waste package failure, and overall performance of the potential repository. Note that the backfill design alternative causes an increase in internal waste package temperatures above design goals, making it unacceptable as a reference design.

4.6.1 Reference Design with Backfill

The backfill alternative (CRWMS M&O 2000 [151014]) is intended to provide some protection of the drip shield from rockfall and to reduce the amount of liquid water in contact with the drip shield and waste package, which is an important factor impacting waste package lifetimes. Backfill may cause a reduction in relative humidity for longer periods after waste emplacement, thus causing further delay in the initiation of corrosion. Backfill also may be considered to control the chemistry of the system, thus controlling waste package corrosion, waste form dissolution, EBS transport, and to some extent geologic transport.

The design for covering the drip shields with backfill is shown in Figure 4.6-1. This design was incorporated into the thermal hydrologic model, the drip shield degradation model, and the waste package degradation model to determine the effect on waste package and, ultimately, repository system performance. The backfill was assumed to have the thermal properties of crushed tuff, to be dry at emplacement, and to be introduced 50 years after waste emplacement. The initial moisture in the backfill may cause early corrosion, but this effect is expected to be small as temperatures in the potential repository quickly rise to drive off the moisture in the backfill. The primary effect on the system is an increase in temperature at the time of backfilling and a corresponding delay in the relative humidity increase as the potential repository cools. While the

effect of moisture control is an important potential benefit of backfill, no change in seepage contacting the waste package as a result of backfilling was included in the modeling. The full evaluation of the effects of backfill on system performance have not been completed because the effects of backfill on seepage have not been quantified and included in the analysis. However, it is expected that the seepage implemented in this model is conservative because the seepage is all expected to contact the waste package and not be redirected around the waste package due to backfill. For the model assumptions included herein, there is little difference in total system performance between backfill and no-backfill cases.

The thermal hydrologic results comparing the case with the reference design (no backfill in the emplacement drift) and a backfilled emplacement drift are illustrated in Figure 4.6-2. The large temperature increase at 50 years corresponds to the emplacement time of the backfill. Dramatic increases of temperature in waste package, drip shield, and invert are observed from the no-backfill to the backfill cases. Average peak temperature of the waste package increases from 160 to 280°C. The higher temperature of the backfill case is maintained up to 2,000 years. The top of the drip shield demonstrates a pattern of temperature increase similar to the waste package. The sharp increase of temperature was expected because the backfill should localize heat near the waste package. For an emplacement drift without backfill, the dominant mode of heat transfer is radiation, which is an efficient mode of heat transfer between the waste package surface and the drift wall. For a backfilled drift the dominant mode of heat transfer is no longer thermal radiation, the resistance to heat transfer from the waste package surface to the drift wall is greatly increased; therefore, the waste package temperature increases. Accompanying the increase in surface temperature is a corresponding decrease in relative humidity in the drift. These results are presented in Figure 4.6-3.

The initial waste package failure curves are shown in Figure 4.6-4 for the no-backfill case and the backfill case. The curves show that there is not a significant difference in the two cases as they are currently modeled. This leads to the conclusion that the overall dose comparison between the two cases will not show a significant difference either.

The effects of backfill in the drift wall are minimal in the thermal hydrologic sensitivity analysis. The temperature only increases 16°C of averaged peak temperature, and a small amount of relative humidity decrease is noted regarding with the increase of temperature. However, because the backfill decreases the heat transfer to the drift wall, which creates large thermal gradients within the drift, the predicted drift wall temperatures tend to be hotter due to scaling difficulties between the mountain scale and drift scale models. Even considering the scale effects, the effects of backfill for the drift wall are still insignificant for the performance of the potential repository (see Figure 4.6-5).

In conclusion, the backfill design localizes the heat near the waste package and decreases relative humidity for a considerable time which could delay waste package degradation. However, the effects of backfill are diminished even at the drift wall because the temperature and the relative humidity changes at that location are insignificant.

The effect of backfill on seepage is uncertain, and additional testing is being conducted to better understand these effects. As noted, the backfill is assumed in these analyses not to alter the

seepage onto the waste package. Some of the potential effects of backfill on seepage are as follows:

- Diversion of the seepage around the waste package
- Reduction of seepage reaching waste package because of evaporation of incoming water that is at a low flow rate
- Concentration of salts in the backfill from seepage water
- Promotion of water condensation at the contacts between the backfill and the waste package surface
- The backfill is not expected to restore the preconstruction UZ flow conditions. These effects have not been fully evaluated for their impact on overall system performance.

The backfill potentially has an impact on the conditions in the disruptive event or volcanism scenario. The backfill may tend to clog or slow the intrusion of the magma into the drift, thus preventing damage to as many waste packages as may be damaged if the magma flows unimpeded down a drift. The difference in the dose as modeled in the disruptive scenario is shown in Figure 4.6-6. The relatively small difference in performance between the backfill case and the no-backfill case is mainly derived from the assumption that only a small surface area of the waste package is disturbed in the zone 2 waste packages.

4.6.2 Low Temperature Operating Mode

The SR reference repository design includes a 50-year ventilated preclosure period, a lineal loading of 1.45kW/m, and a constant drift to drift spacing of 81 meters. The reference design would allow boiling to occur several meters into the host rock surrounding the emplacement drifts for tens to hundreds of years after closure, depending on the relative location of the drift (i.e., edge versus center of the potential repository). Alternatively, compensation for some key uncertainties may be achieved by operating the repository differently. Keeping temperatures below the boiling point of water may reduce uncertainties associated with assessing the thermal response of the host geology and its impact on the performance of the repository. Keeping temperatures below 85°C (185°F) and/or relative humidity below 50 percent may reduce the susceptibility of waste packages, and other components of the engineered barrier system, to corrosion.

Several design variables have a significant impact on the temperature and/or relative humidity in the repository. These variables include: (1) the thermal output of the waste packages, (2) the linear power density at which emplacement drifts are loaded, (3) the distance between emplacement drifts, and (4) the duration and rate at which drifts are ventilated after being loaded. Other parameters (e.g., the thermal properties of the mountain and the infiltration flux) also impact the temperature and humidity of the repository. These latter parameters, however, cannot readily be altered by the design of the repository.

In this section, a low temperature operating mode that includes 0.90 kW/m (a change in the linear power density at which emplacement drifts are loaded) and a 100 year ventilated preclosure period (a change in the ventilation duration) is compared to the reference design. This alternate design would not produce boiling in the host rock and would keep waste package temperatures below boiling as well. Note that is just one example of a possible lower temperature operating mode. The variables described above can be combined in many ways to achieve a lower temperature operating mode depending on what thermal goals and design constraints must be satisfied.

The thermal hydrologic results used to represent the low thermal load design in this TSPA comparison are described in *Thermal Hydrology EBS Design Sensitivity Analysis* (CRWMS M&O 2000 [152201]). To facilitate the comparison between the reference and low thermal load designs, the following key assumptions were made in the analysis:

1. It is assumed that the line-loaded, two-dimensional, drift-scale, thermal-hydrologic submodel, L4C4, that was extracted from the Multiscale Thermal-hydrologic Model (CRWMS M&O 2000 [152201]) is representative of an average location in the potential repository footprint. This assumption is based on the selected submodel's physical location relative to the geometric center of the potential repository footprint (Easting: 170,500m, Northing: 233,800m).

2. Spatial variability in potential repository thermal-hydrologic variables does not have a significant effect on EBS performance. Therefore, thermal-hydrologic output variables from the line-loaded thermal-hydrologic submodel L4C4 can be applied throughout the potential repository.

3. The reduction of power output from 1.45 kW/m to 0.90 kW/m is accomplished by increasing the waste package to waste package spacing. This increase in waste package spacing is accounted for in the two-dimensional model by applying a scaling factor to the original reference design model's thermal power curve. A scaling factor of 0.621 (0.90/1.45 = 0.621) was used (CRWMS M&O 2000 [152201]).

4. The reduction in lineal power output is assumed to be accomplished by increasing waste package to waste package spacing in the emplacement drifts. As a result the potential repository footprint should also increase accordingly. In the analyses presented here, it is assumed that effects of an increased footprint on potential repository performance are not important and can be neglected.

5. The effects and uncertainties associated with coupled thermal-hydrologic-chemical-mechanical processes, such as dissolution/precipitation of minerals and thermally induced fracturing in the host rock, may decrease in magnitude as the potential repository thermal loading decreases. These potential decreases in effects and uncertainties are neglected in the present comparison between the reference design case and the low thermal load case.

The thermal hydrologic results comparing the low thermal load case with the reference design are illustrated in Figures 4.6-7 and 4.6-8. The waste package surface temperature comparisons in

Figure 4.6-7 show that surface temperatures in the low thermal load case reach a much lower peak temperature as expected. As discussed previously in Section 4.6.1, an increase in waste package surface temperature is accompanied by a corresponding decrease in relative humidity around the waste package. As shown in Figure 4.6-8, this decrease in relative humidity does not occur in the low thermal load case since surface temperatures do not rise significantly.

The initial waste package failure curves are shown in Figure 4.6-9 for the reference design case and the low thermal load case. These curves show that there is not a significant difference in the two cases as they are currently modeled. This result illustrates the insensitivity of the SR waste package corrosion and degradation model to thermal hydrologic conditions around the waste package. Furthermore, since waste package failure does not occur until after 10,000 years when both cases exhibit similar thermal hydrologic conditions, the overall dose comparison between the two cases will not show a significant difference either. This result is shown in Figure 4.6-10.

In conclusion, although this low temperature operating mode reduces waste package surface temperatures and increases the relative humidity around waste packages these effects do not significantly impact waste package performance. In addition, since waste package failure does not occur until after 10,000 years, the thermal hydrologic conditions for both cases are similar during the period when radionuclides are mobilized. As a result, doses for both cases show very little difference. It should be emphasized that these results are based on the simplifying assumptions such as the effects of coupled thermal-hydrologic-chemical-mechanical processes on potential repository performance in both cases may be accounted for by using the same models and input data. Given the assumptions, the example demonstrates that lower temperature operating modes may perform in a manner comparable to high temperature operating modes. Other combinations of: (1) the thermal output of the waste packages, (2) the linear power density at which emplacement drifts are loaded, (3) the distance between emplacement drifts, and (4) the duration and rate at which drifts are ventilated after being loaded may be evaluated to optimize the system depending on design goals and any operating constraints that may be imposed. Model refinements may provide insight into the potential for reducing uncertainties that are not currently available based on the simplifying assumptions that were used in this particular analysis.

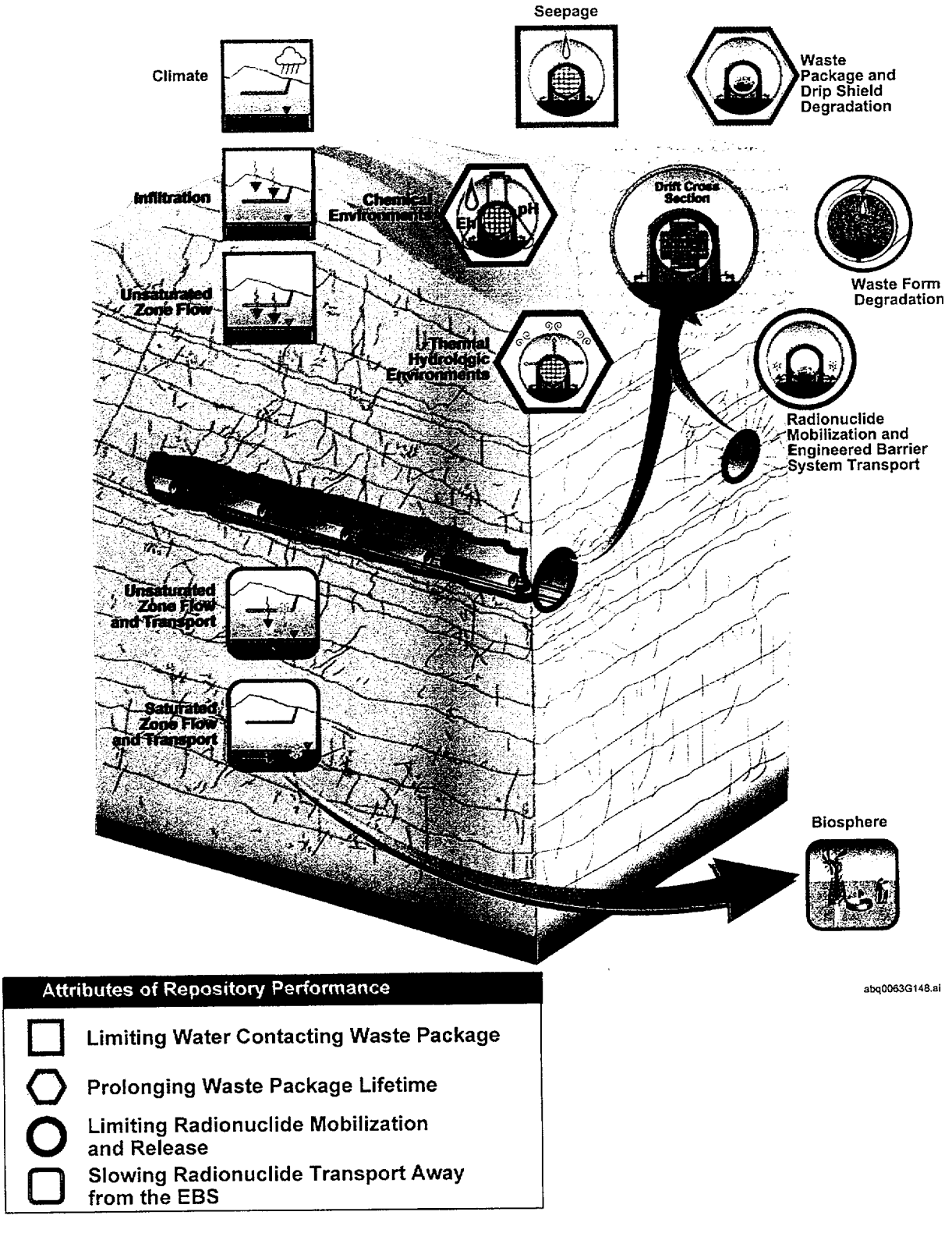

abq0063G148

Figure 4.1-1. Illustration Showing the Important Total System Performance Assessment Submodels for the Nominal Scenario

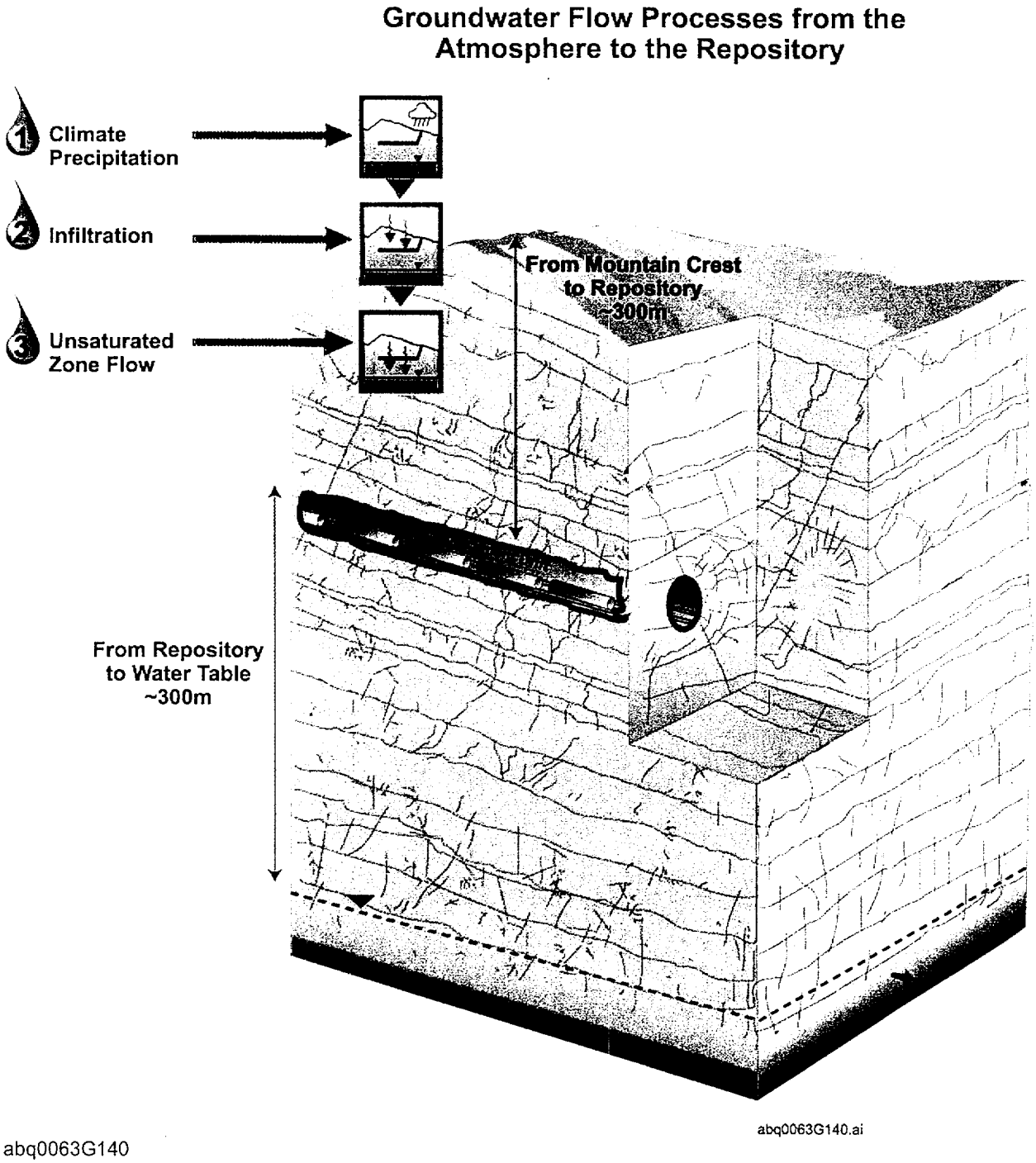

abq0063G140

Figure 4.1-2. Total System Performance Assessment Submodels for Groundwater Flow above the Potential Repository

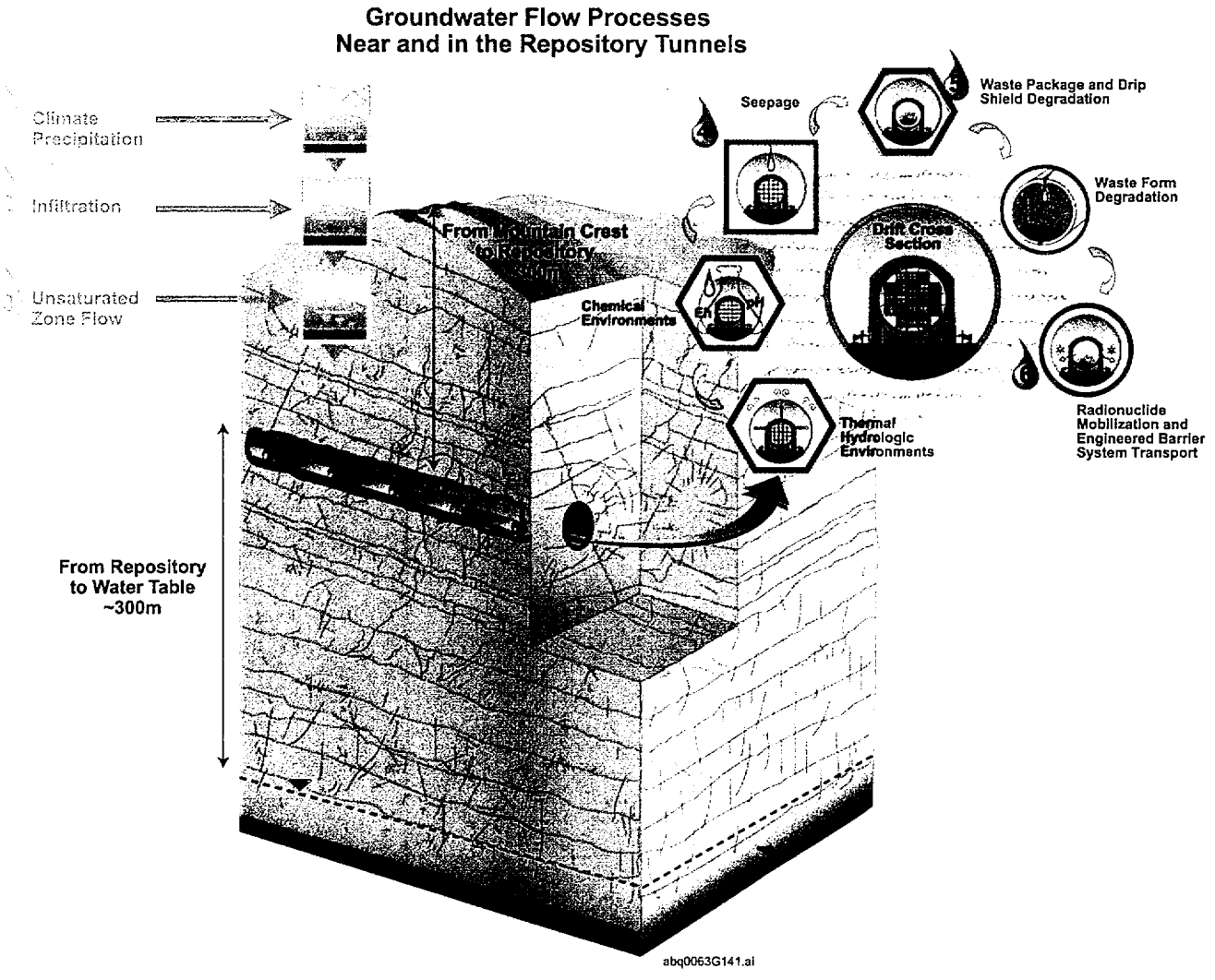

abq0063G141

Figure 4.1-3. Total System Performance Assessment Submodels for Flow and Transport near and in the Potential Repository Tunnels

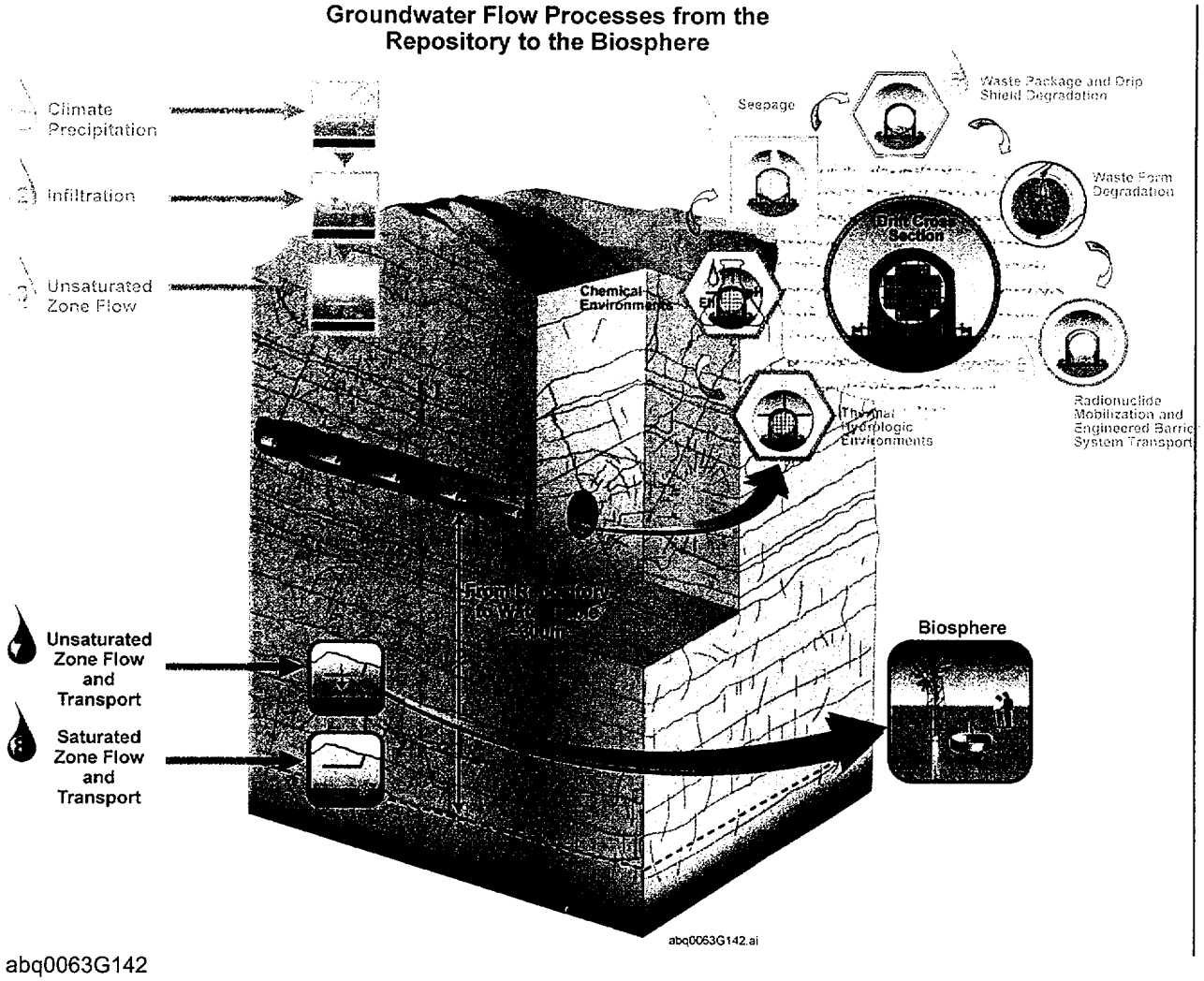

abq0063G142

Figure 4.1-4. Total System Performance Assessment Submodels for Flow and Transport from the Potential Repository to the Biosphere

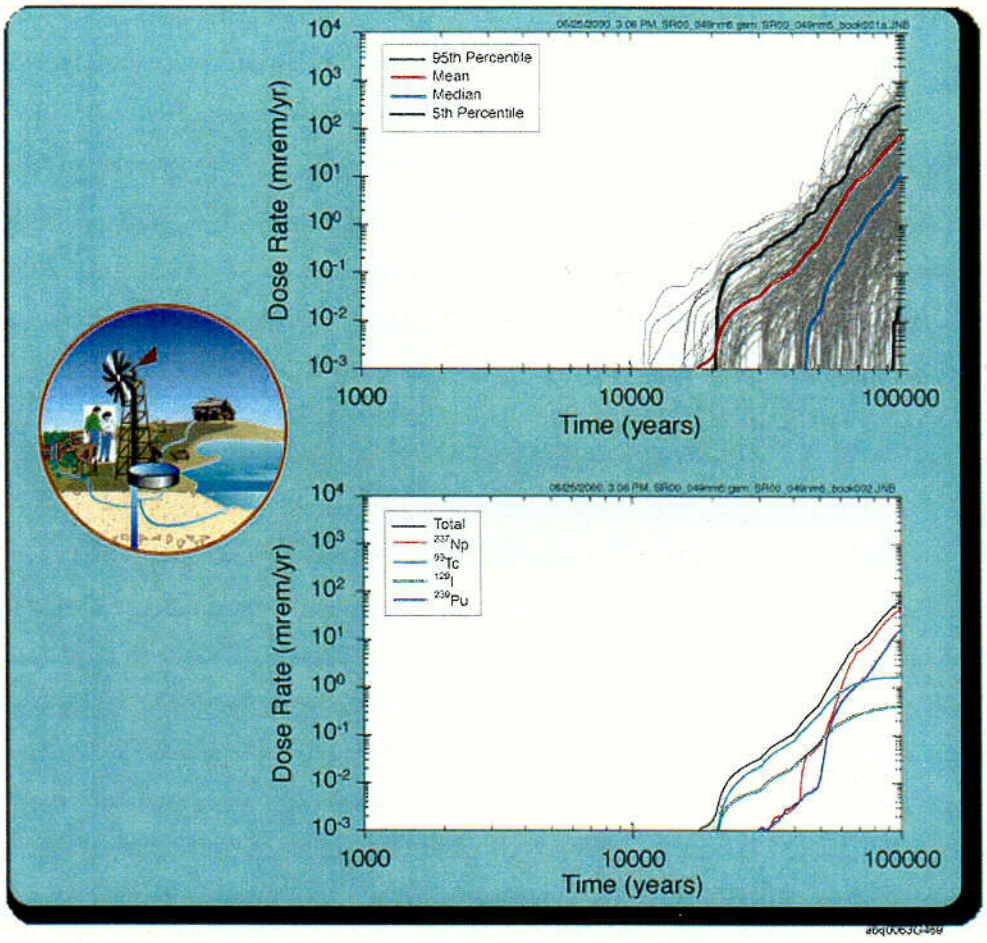

abq0063G469

Figure 4.1-5. Simulated Annual Dose Histories for the Nominal Scenario

C-1

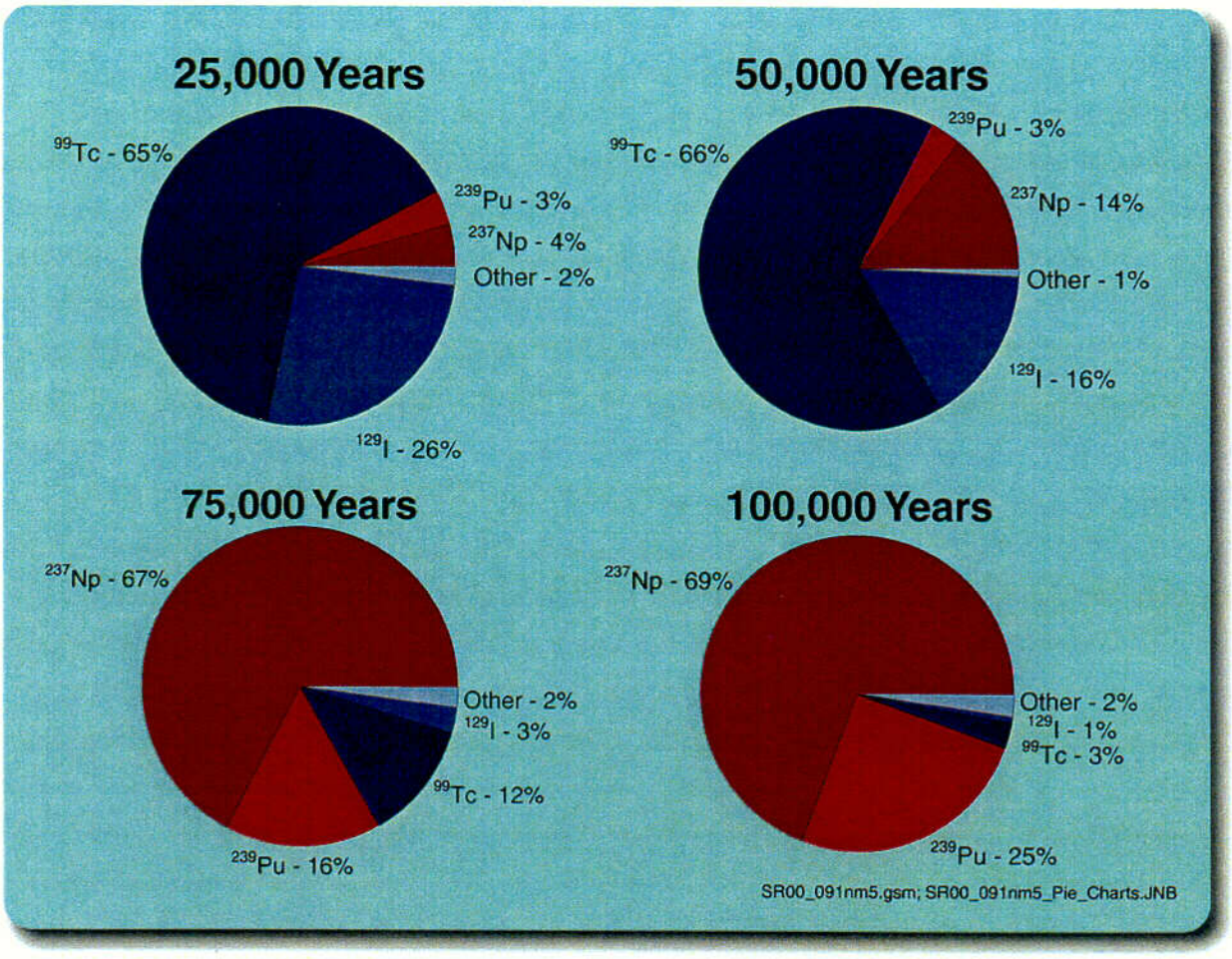

abq0063G497

Figure 4.1-6. Contribution of Radionuclides to the Mean Annual Dose at Four Times

L-2

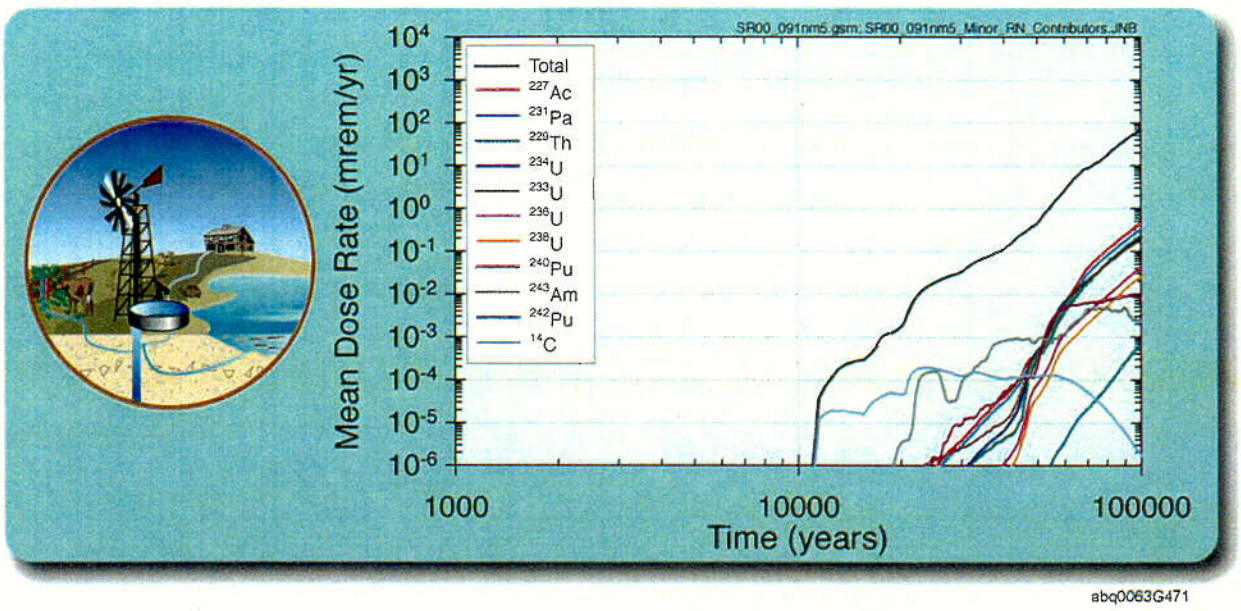

abq0063G471

Figure 4.1-7. Mean Annual Dose Histories for Less-Important Radionuclides

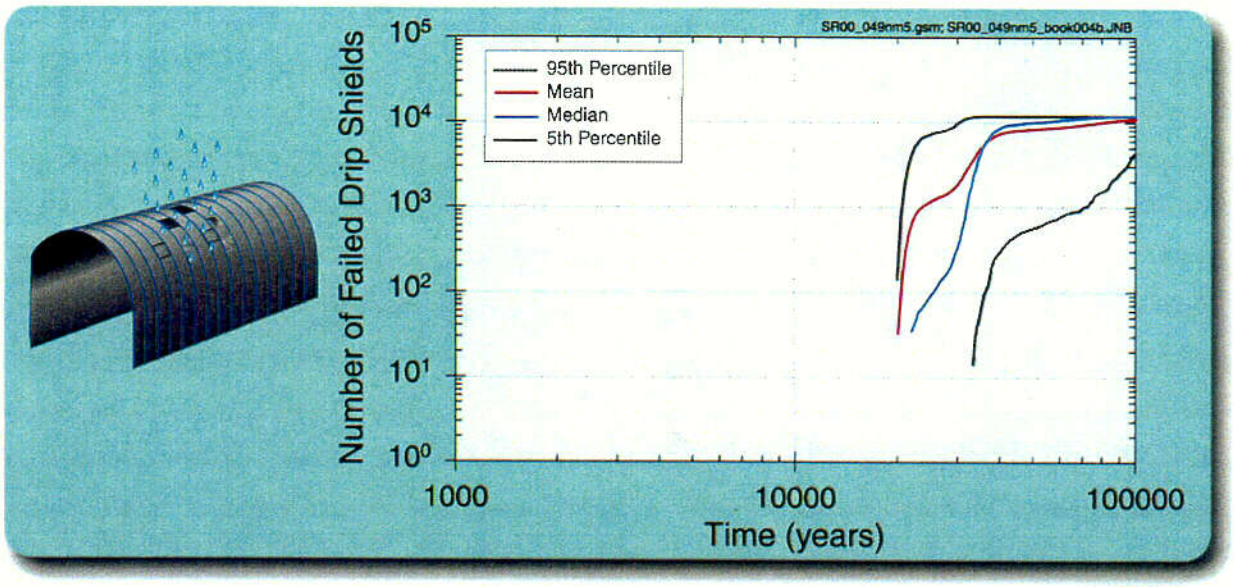

abq0063G473

Figure 4.1-8. Number of Failed Drip Shields over Time

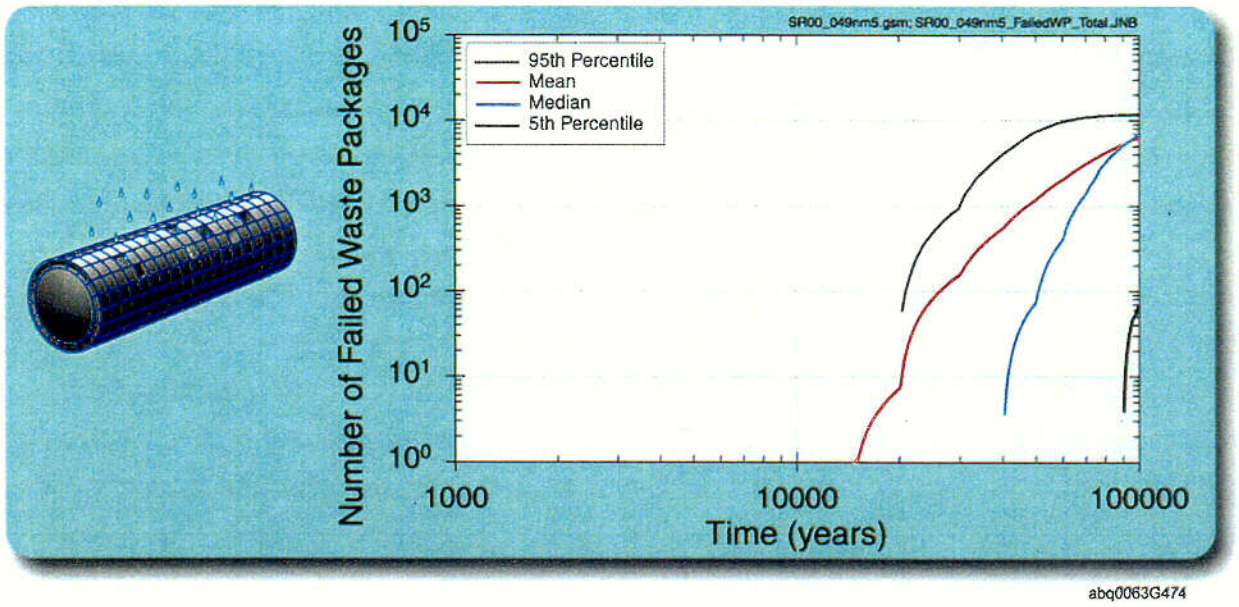

abq0063G474

Figure 4.1-9. Number of Failed Waste Packages over Time

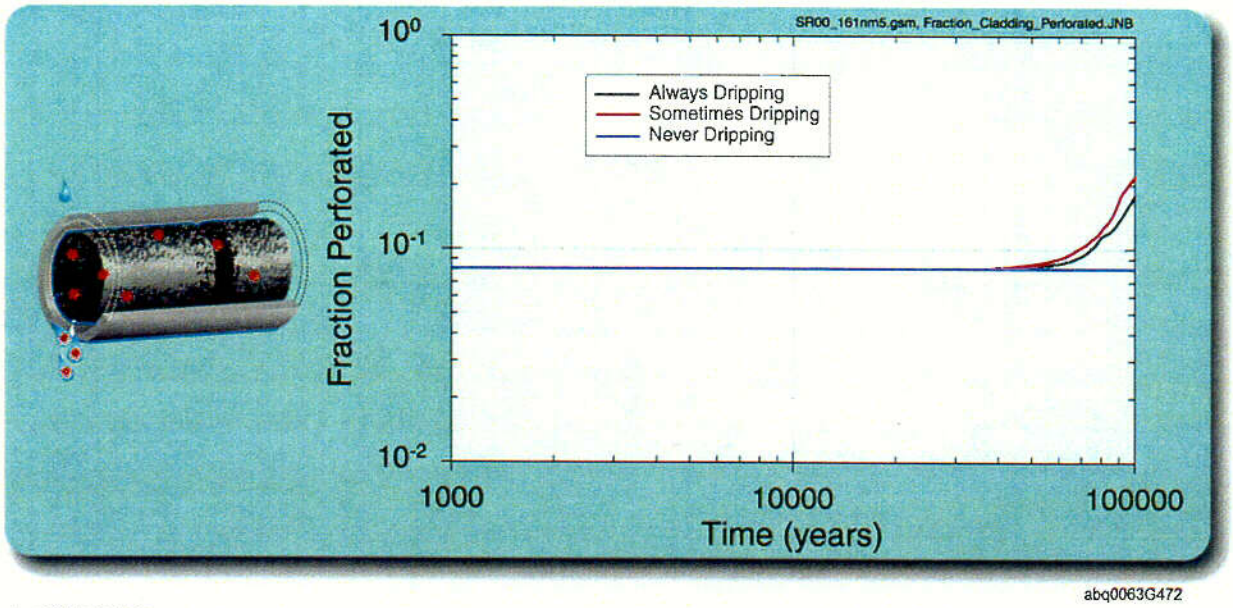

abq0063G472

Figure 4.1-10. Fraction of Failed Cladding over Time

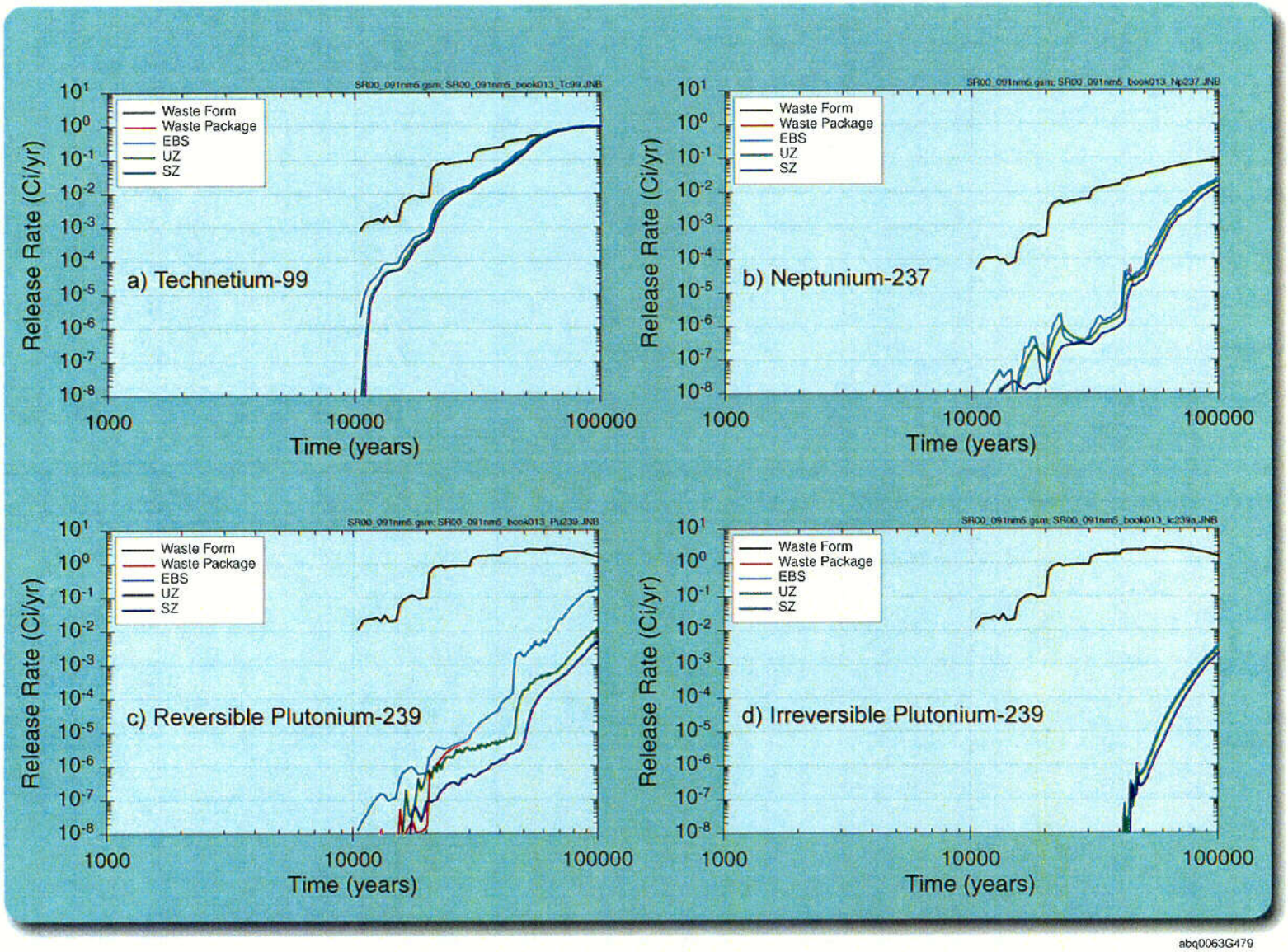

abq0063G479

Figure 4.1-11. Mean Radionuclide Release Rate from Five Locations

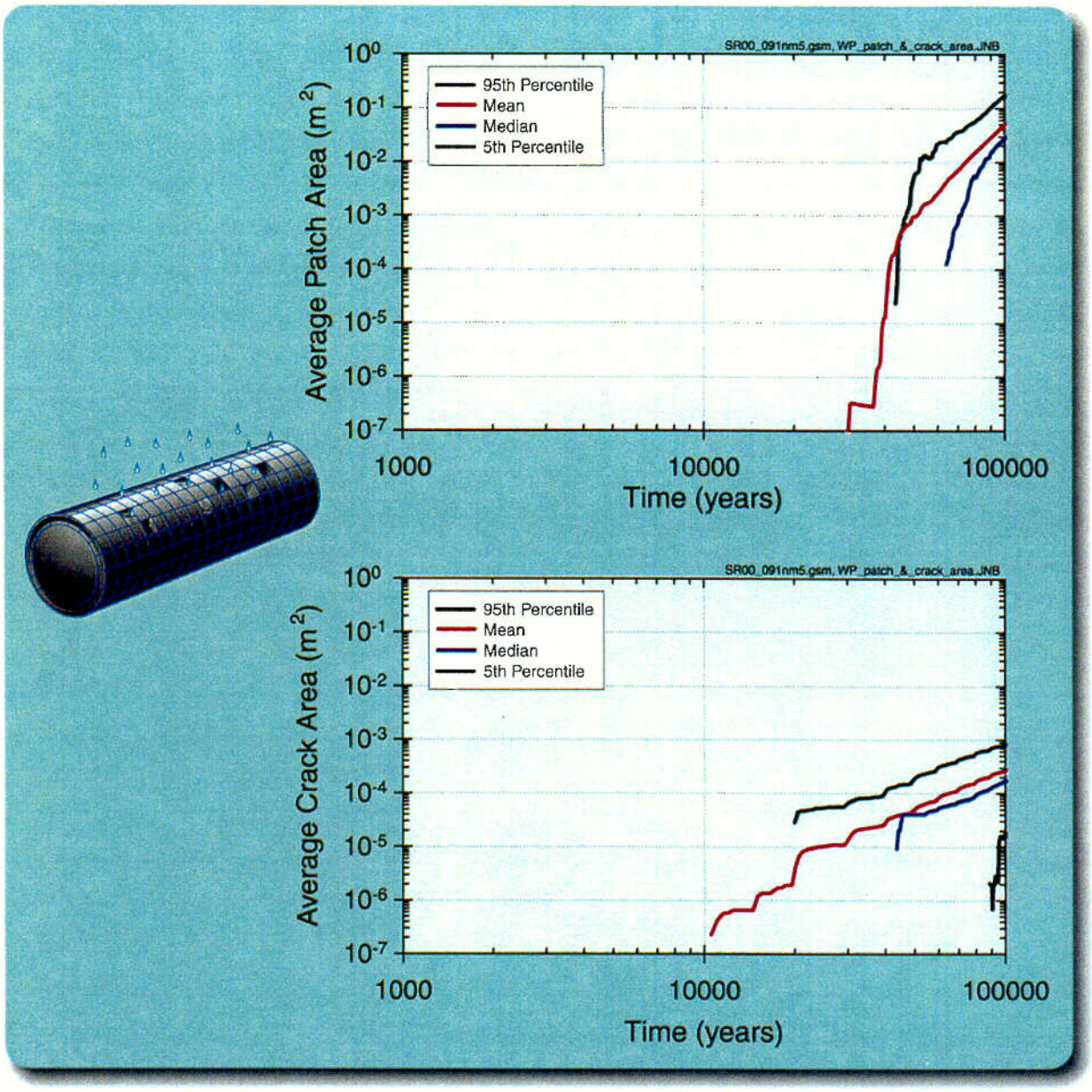

abq0063G475

Figure 4.1-12. Waste Package Opening Area over Time

L-8

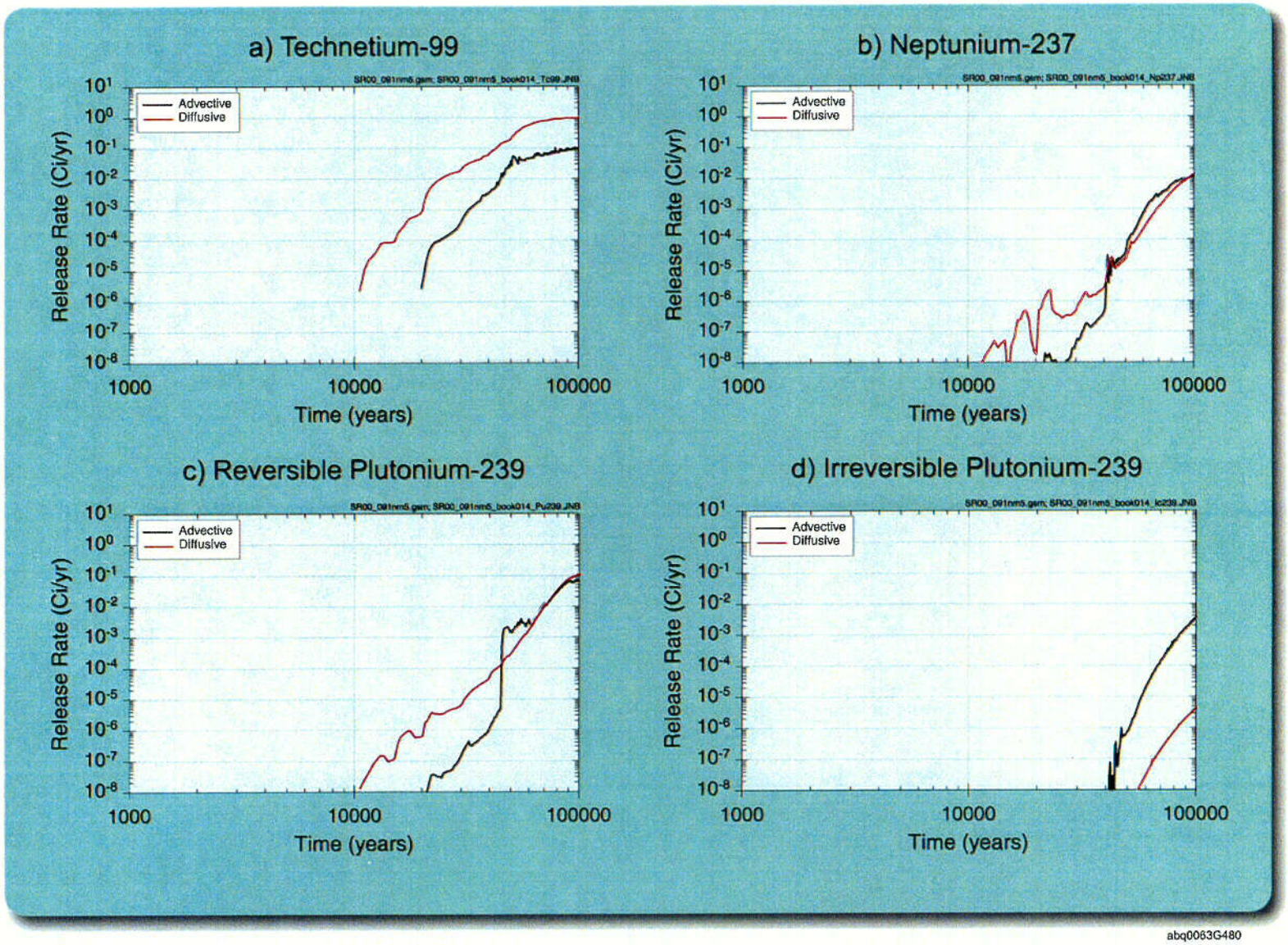

abq0063G480

Figure 4.1-13. Mean Diffusive and Advective Releases from the Engineered Barrier System

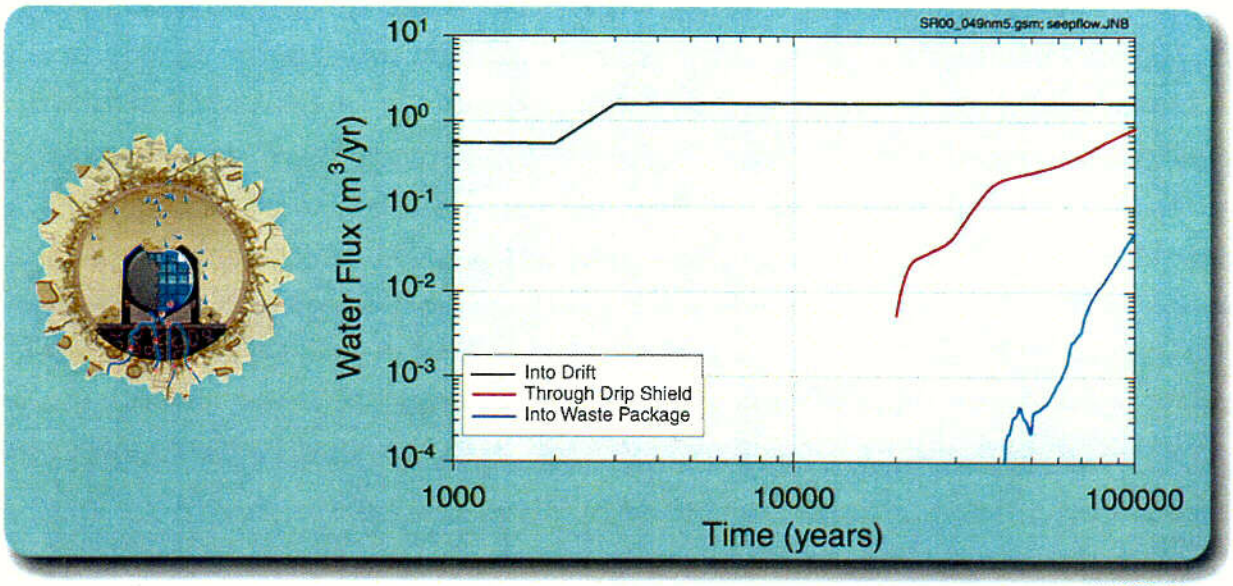

abq0063G476

Figure 4.1-14. Mean Water Flow Rates for Sometimes-Seeping Locations in the 20 to 60 mm/yr Infiltration Bin

L-10

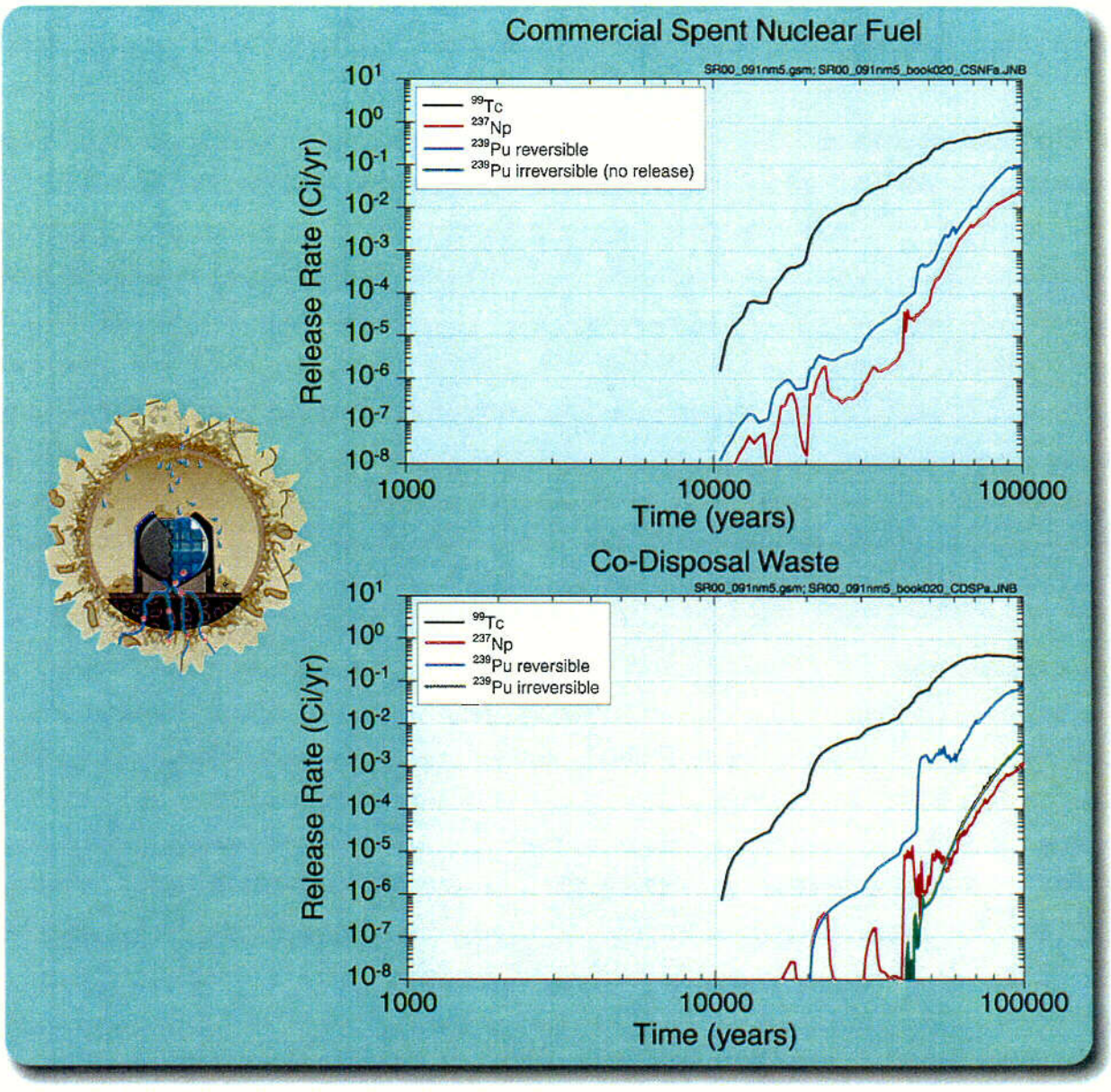

abq0063G481

Figure 4.1-15. Mean Release Rates from the Engineered Barrier System for Two Waste Types

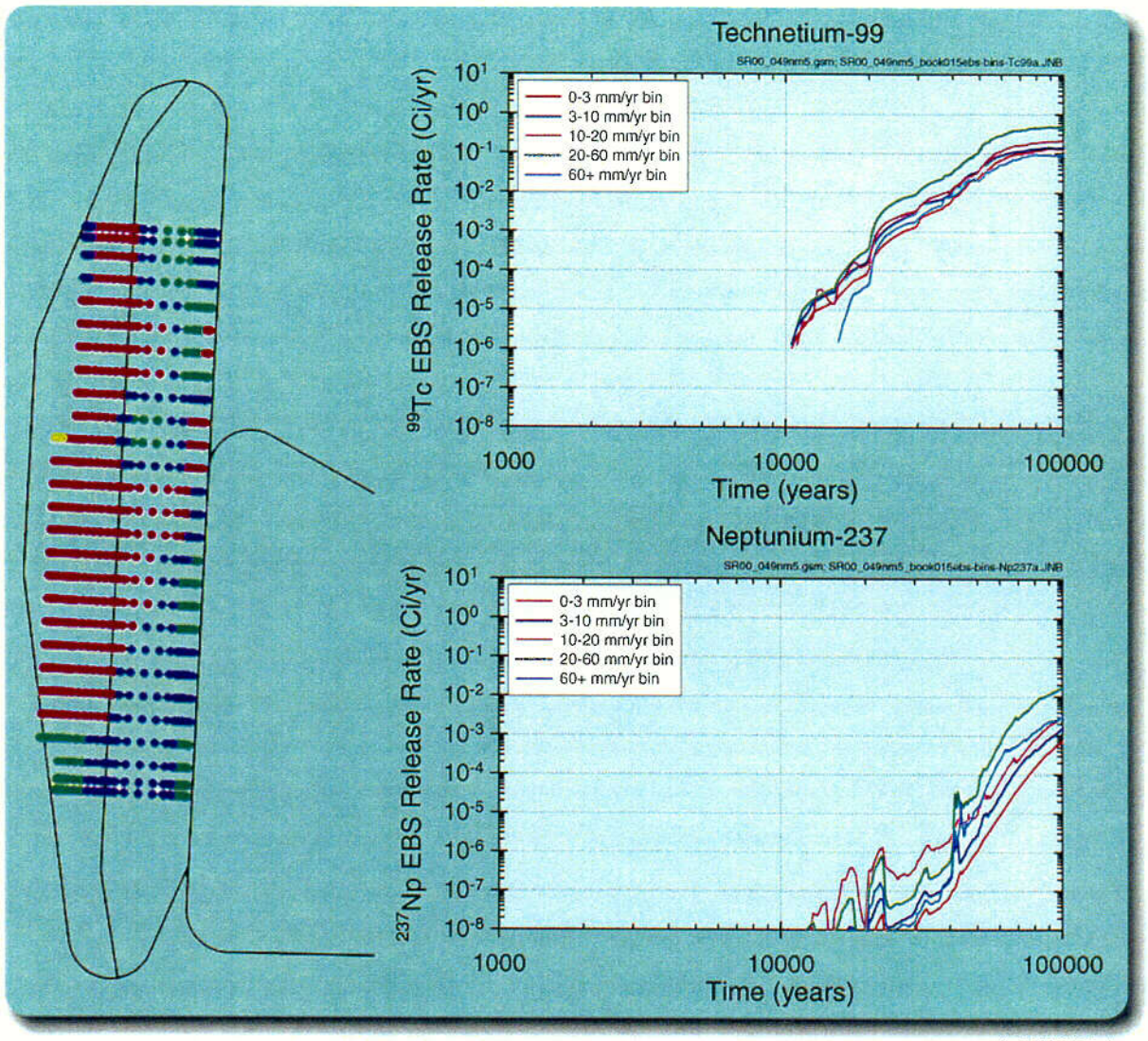

abq0063G483

Figure 4.1-16. Mean Engineered Barrier System Releases from the Five Infiltration Bins

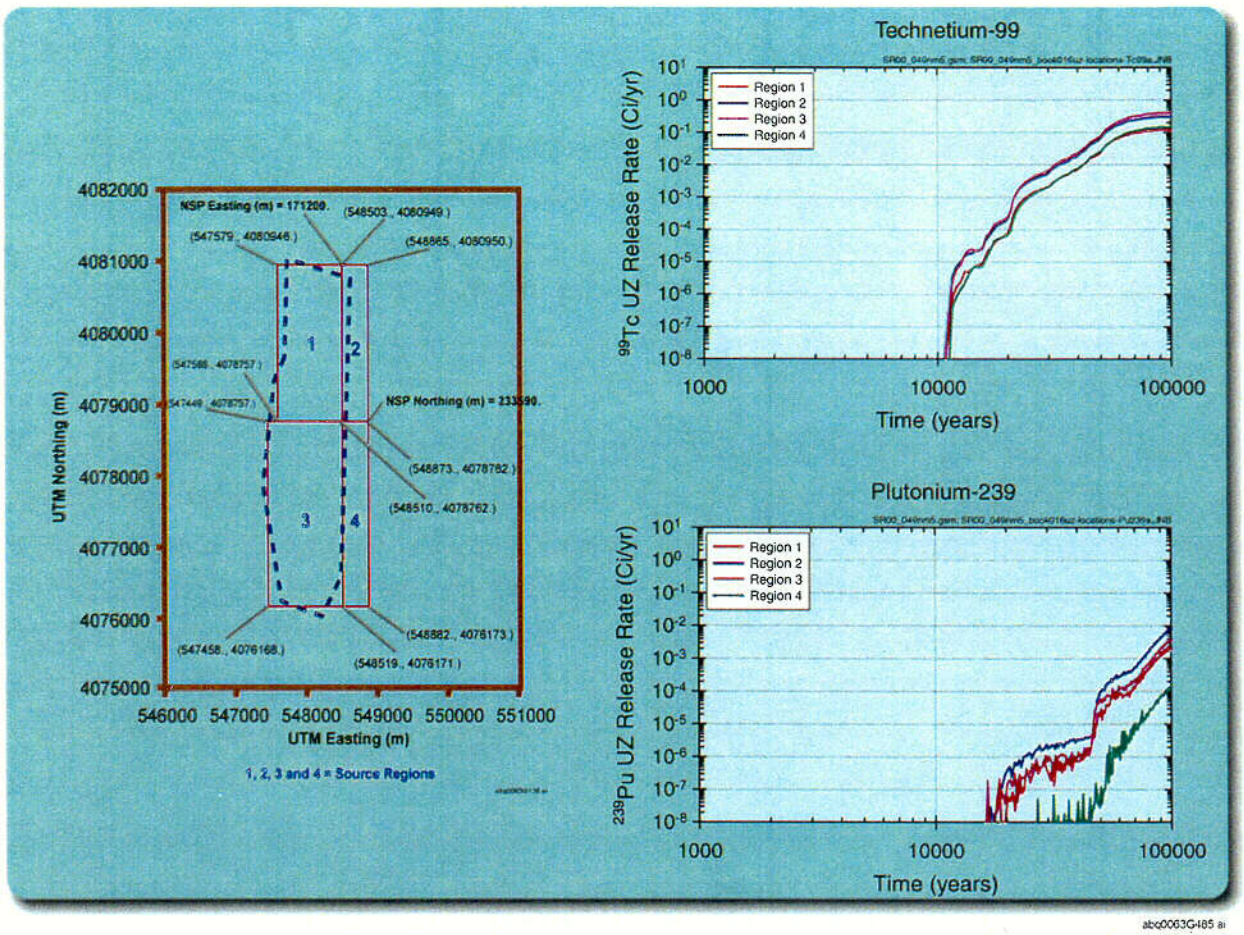

abq0063G485

Figure 4.1-17. Mean Unsaturated Zone Releases from Four Regions

L-13

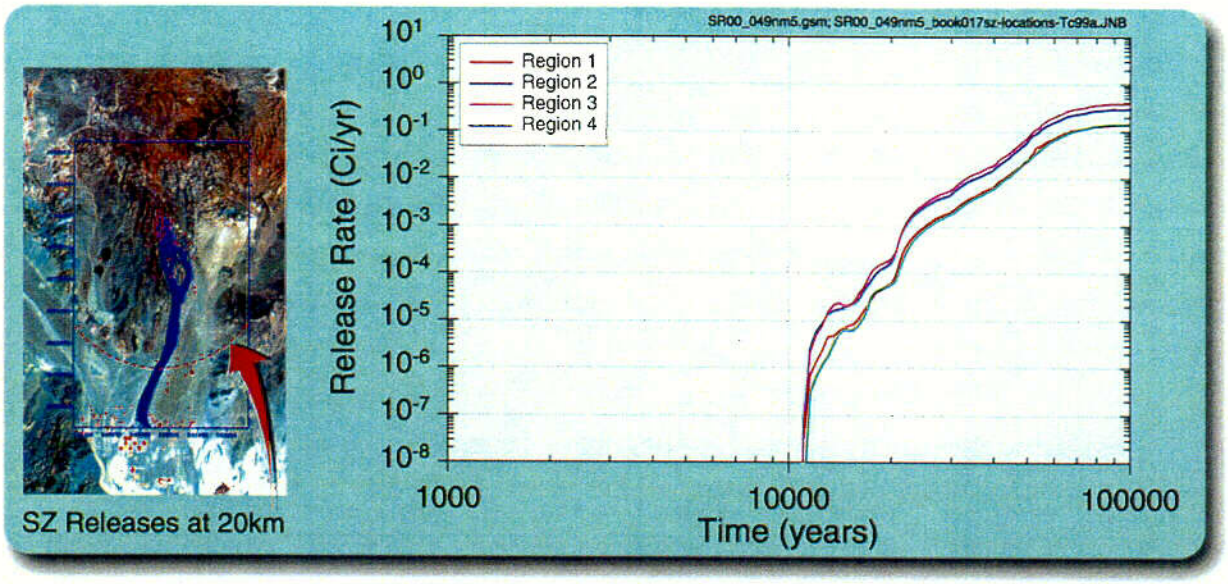

abq0063G478

NOTE: SZ graphic is same as Figure 3.8-12

Figure 4.1-18. Mean Saturated Zone Releases of ^{99}Tc for Four Source Regions

C-14

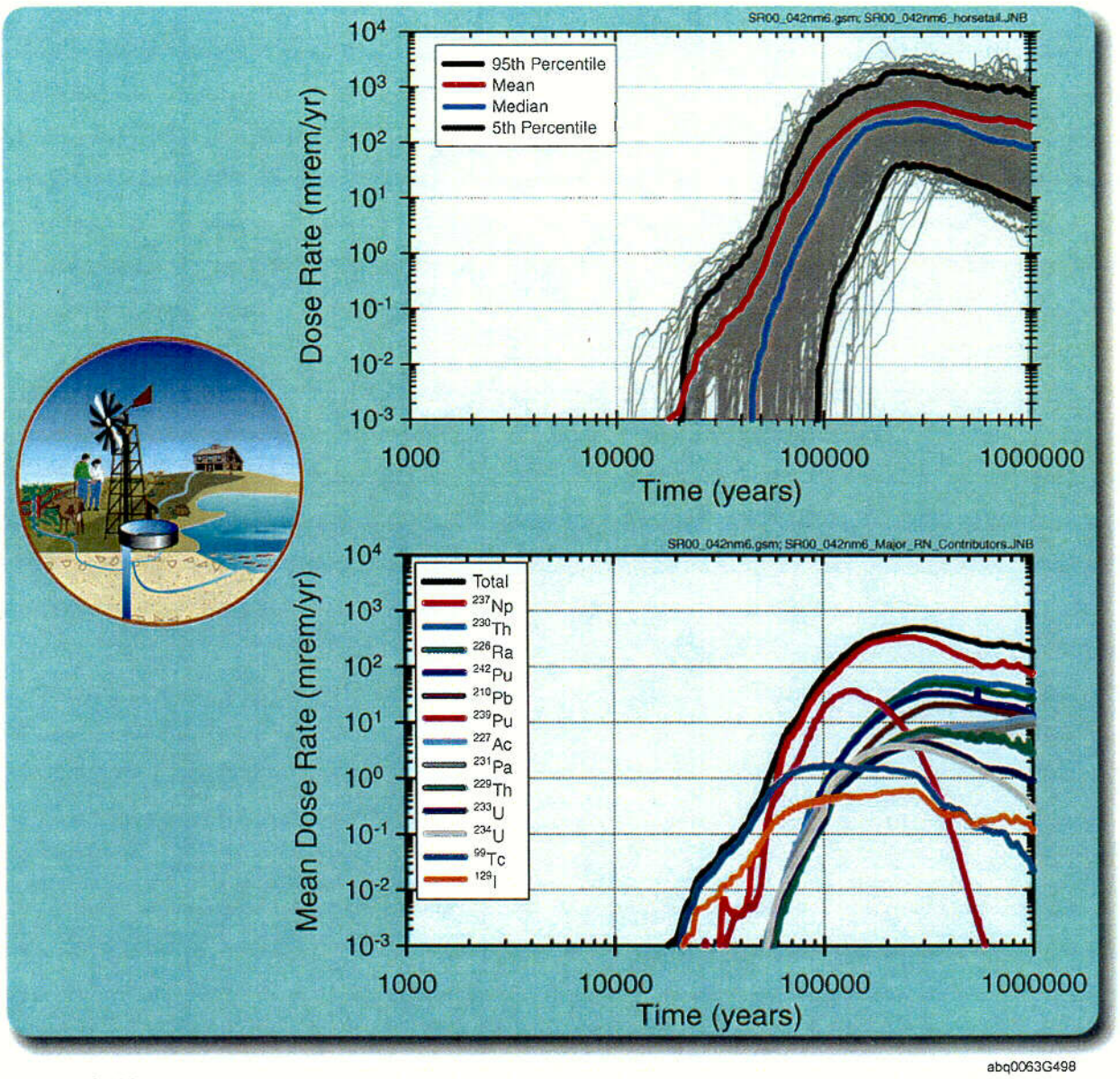

abq0063G498

NOTE: Upper plot presents the full distribution of multiple realizations and key statistical representations of this distribution and the lower plot presents the key radionuclides associated with the mean dose rate derived from the multiple realizations.

Figure 4.1-19a. Simulated Annual Dose Histories for the Nominal Scenario over 1,000,000 Years Using the Base Case Models

c-15

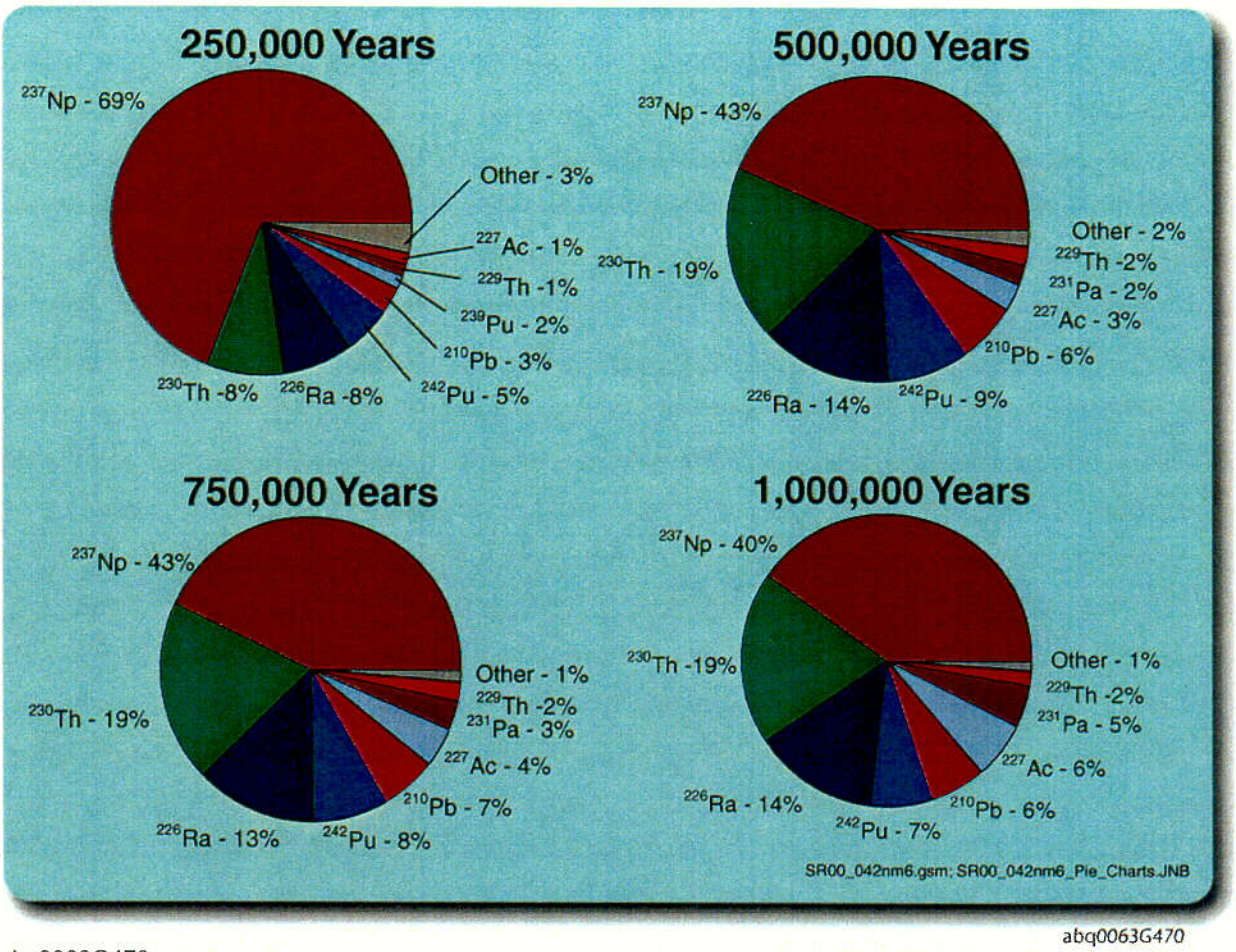

abq0063G470

Figure 4.1-19b. Key Radionuclides Affecting Mean Annual Dose for the Nominal Scenario over 1,000,000 Years Using the Base Case Models

C-10

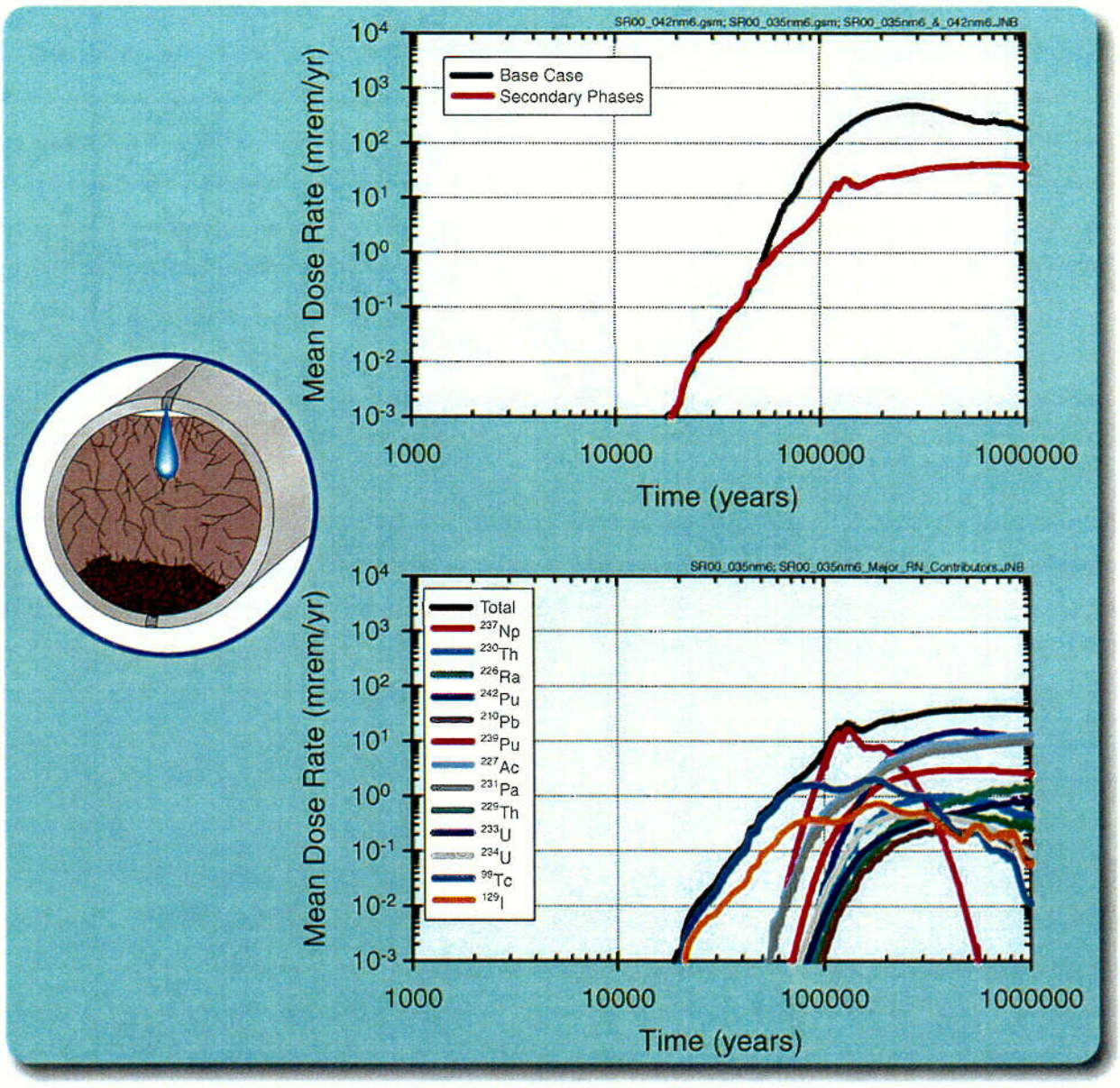

abq0063G663

NOTE: Upper plot presents the full distribution of multiple realizations and key statistical representations of this distribution and the lower plot presents the key radionuclides associated with the mean dose rate derived from the multiple realizations.

Figure 4.1-20. Simulated Annual Dose Histories for the Nominal Scenario over 1,000,000 Years Using the Long-Term Secondary Phase Solubility Model

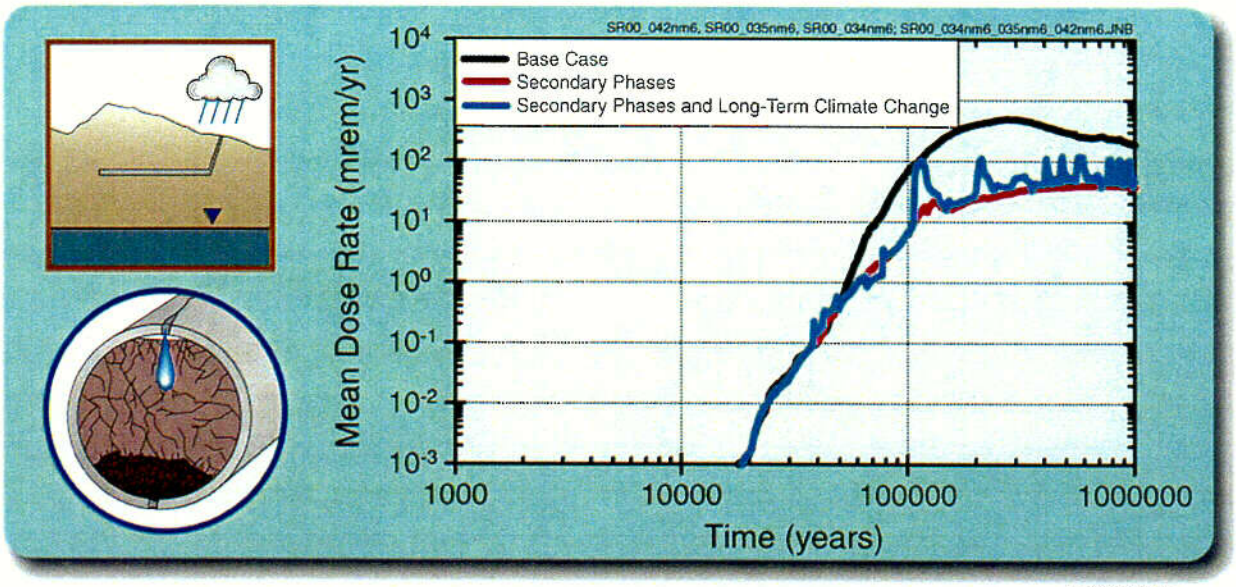

abq0063G499

Figure 4.1-21. Simulated Mean Annual Dose for the Nominal Scenario over 1,000,000 Years Using the Long-Term Secondary Phase Solubility Model and the Post-10,000 Year Climate Model

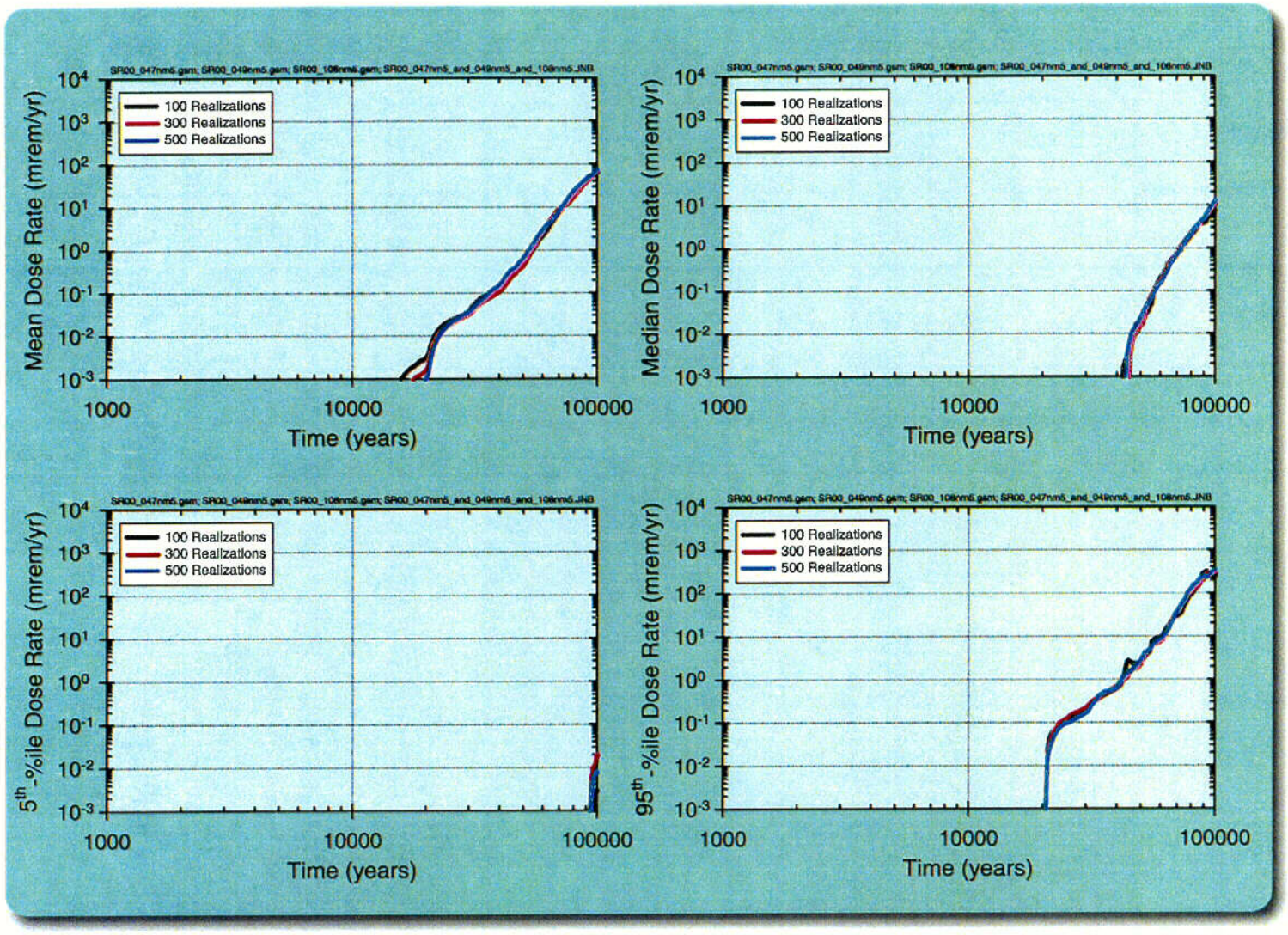

abq0063G626

Figure 4.1-22. Comparison of Annual Dose Results for Different Numbers of Realizations

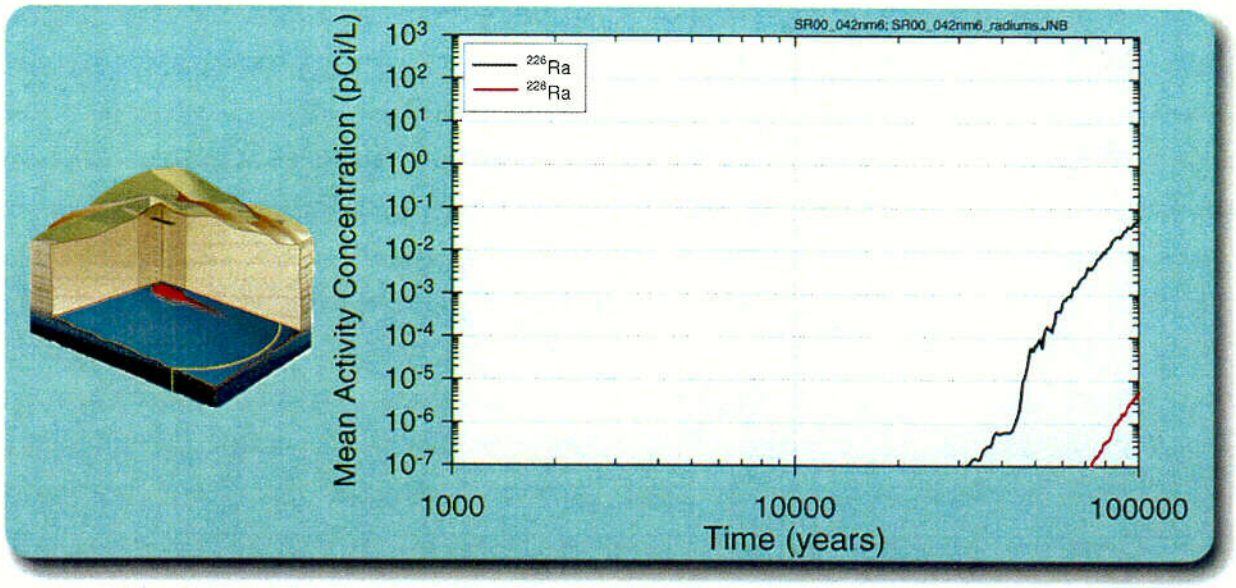

abq0063G631

Figure 4.1-23. Mean Time History of Radium Activity in Groundwater (Excluding Background)

C-20

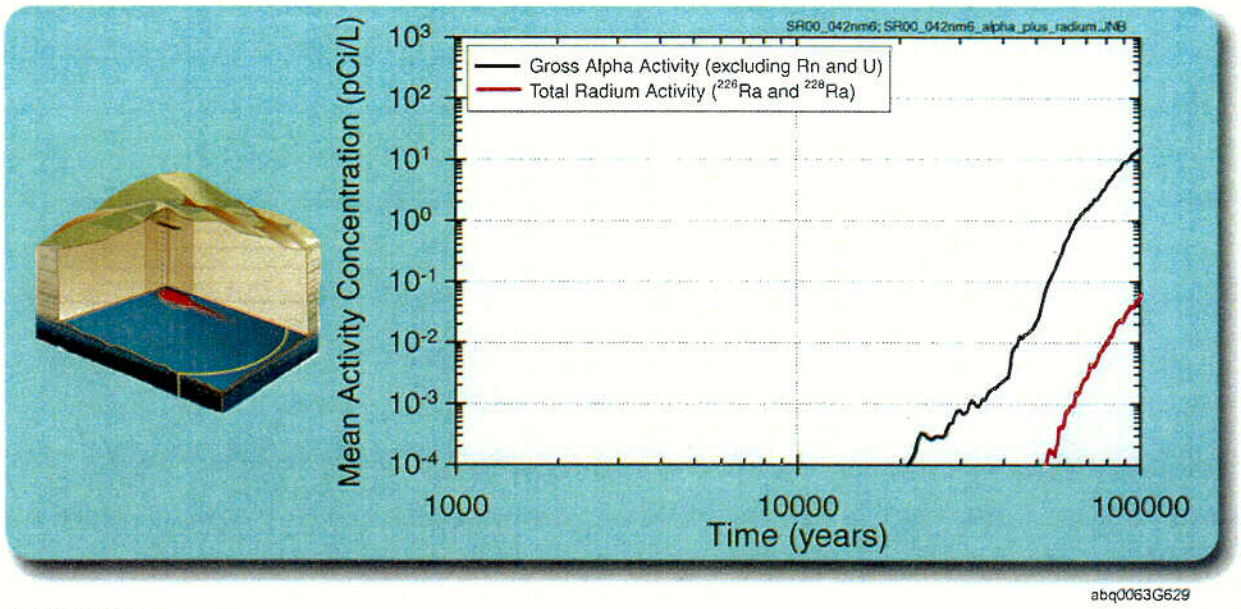

abq0063G629

Figure 4.1-24. Mean Time History of Radium and Gross Alpha Activity in Groundwater (Excluding Background)

C-21

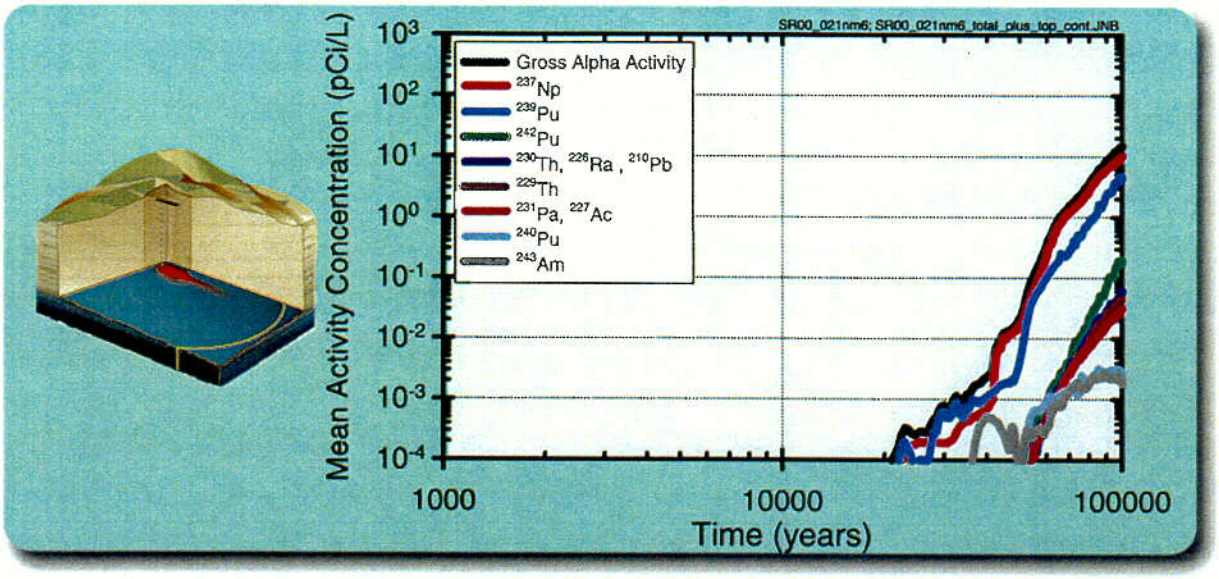

abq0063G628

Figure 4.1-25. Contribution of Radionuclides to the Mean Gross Alpha Activity (Excluding Background)

L-22

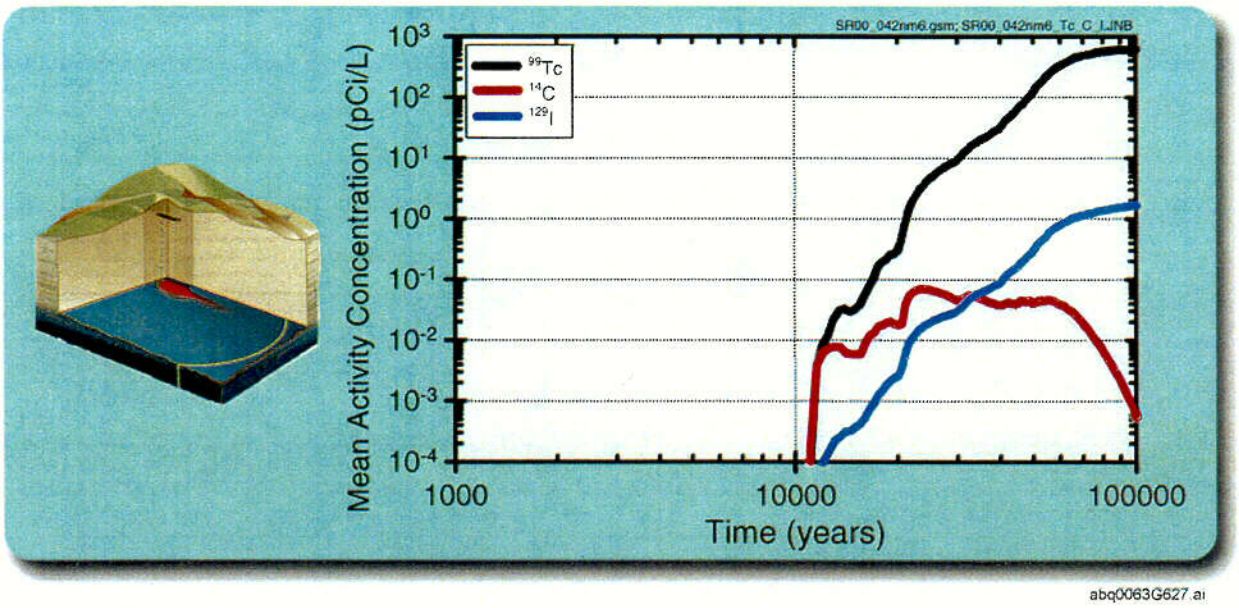

abq0063G627

Figure 4.1-26. Mean Time History of Activity for Beta and Photon Emitters in Groundwater (Excluding Background)

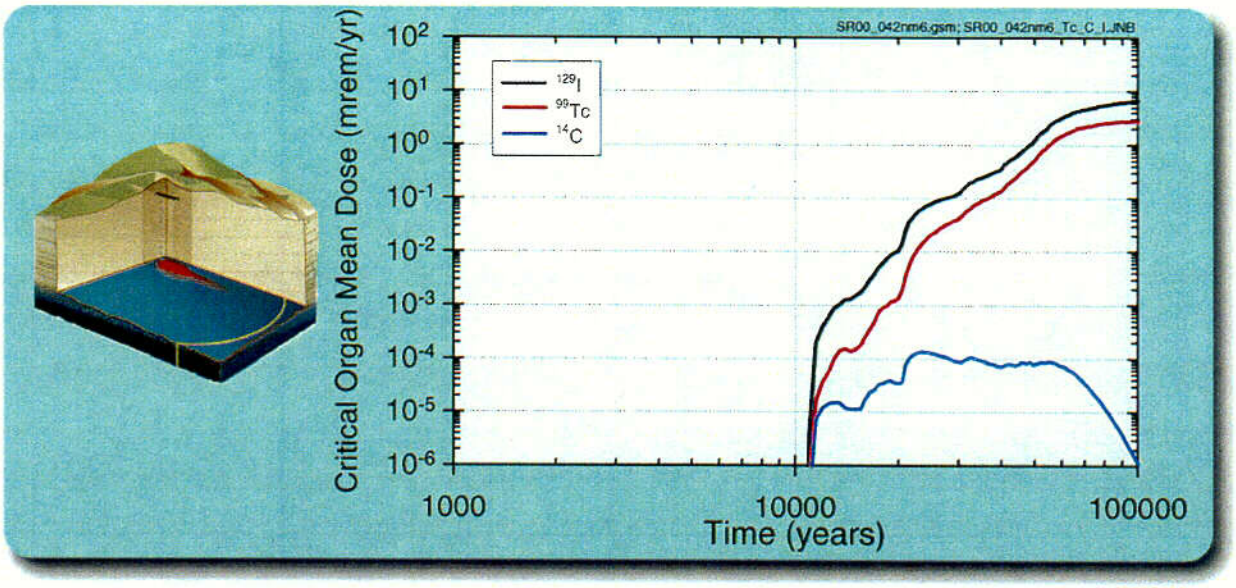

abq0063G630

Figure 4.1-27. Mean Time History of Dose to Critical Organ for Beta and Photon Emitters in Groundwater (Excluding Background)

C-24

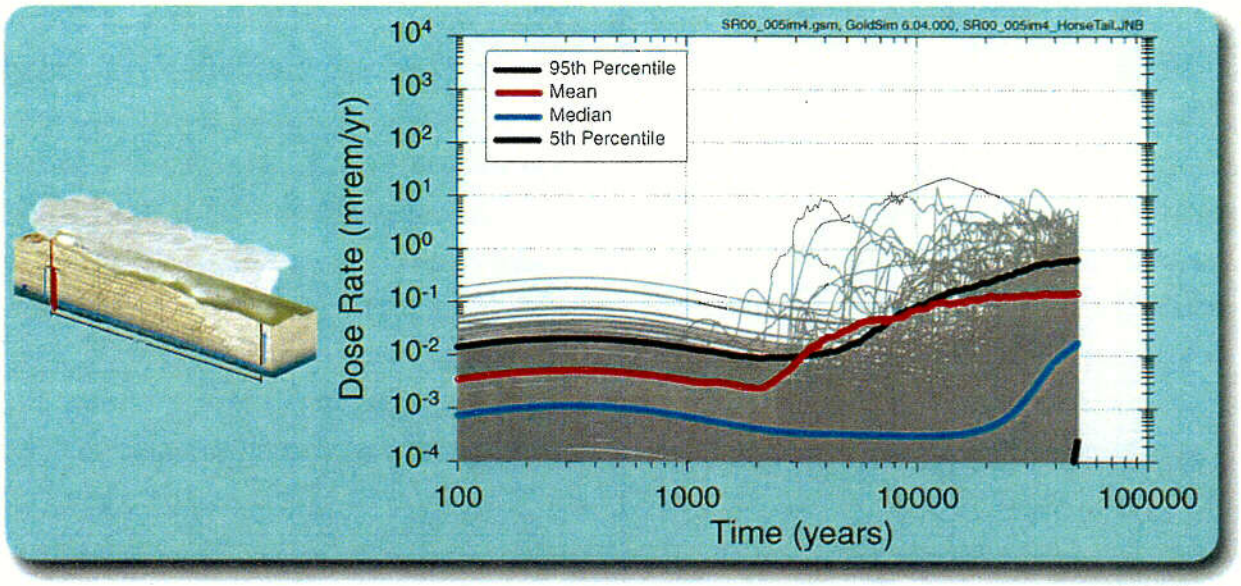

abq0063G531

NOTE: Including both eruptive and intrusive releases from the repository.
Simulation was only for 50,000 year time period. See text for discussion.

Figure 4.2-1. Total Probability-Weighted Annual Dose Rate from Igneous Disruption

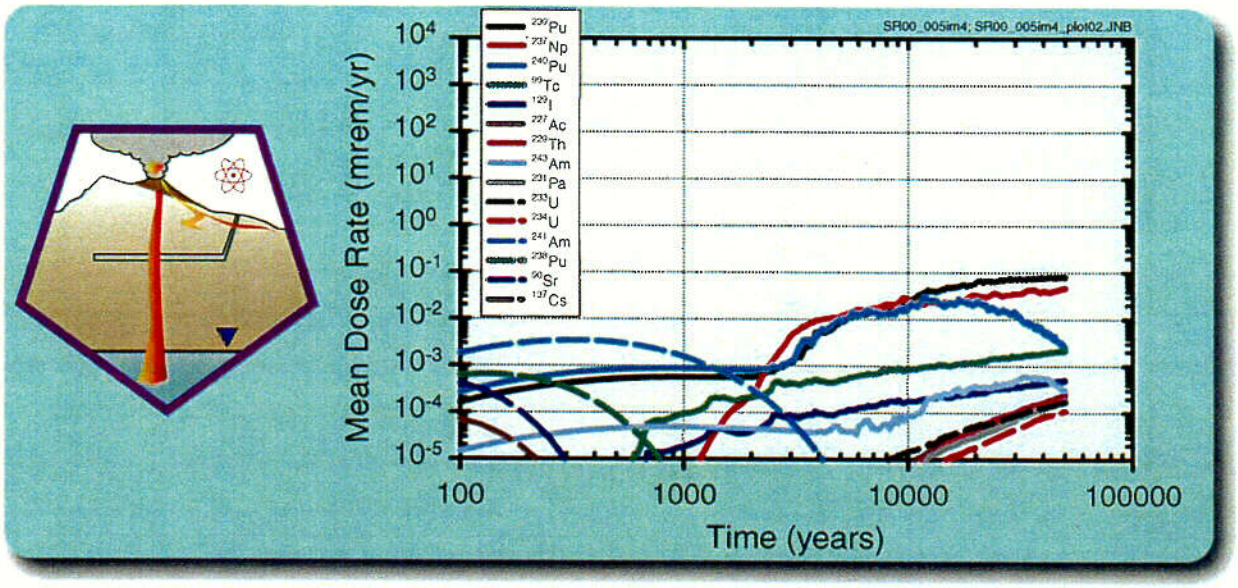

abq0063G530

NOTE: Igneous disruption shown in Figure 4.2-1.

Figure 4.2-2. Probability-weighted Annual Dose Rate from Individual Radionuclides Contributing to the Total Probability-weighted Annual Dose Rate from Igneous Disruption

C-26

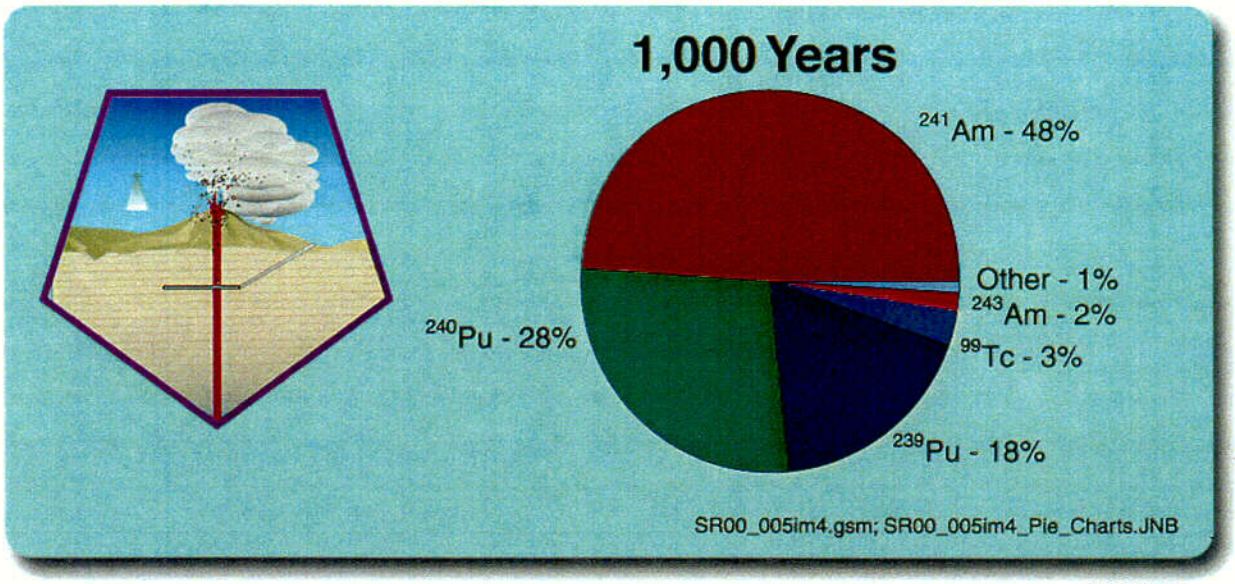

abq0063G532

Figure 4.2-3. Relative Contributions of Individual Radionuclides to the Total Probability-Weighted Igneous Dose Rate at 1,000 Years after Potential Repository Closure

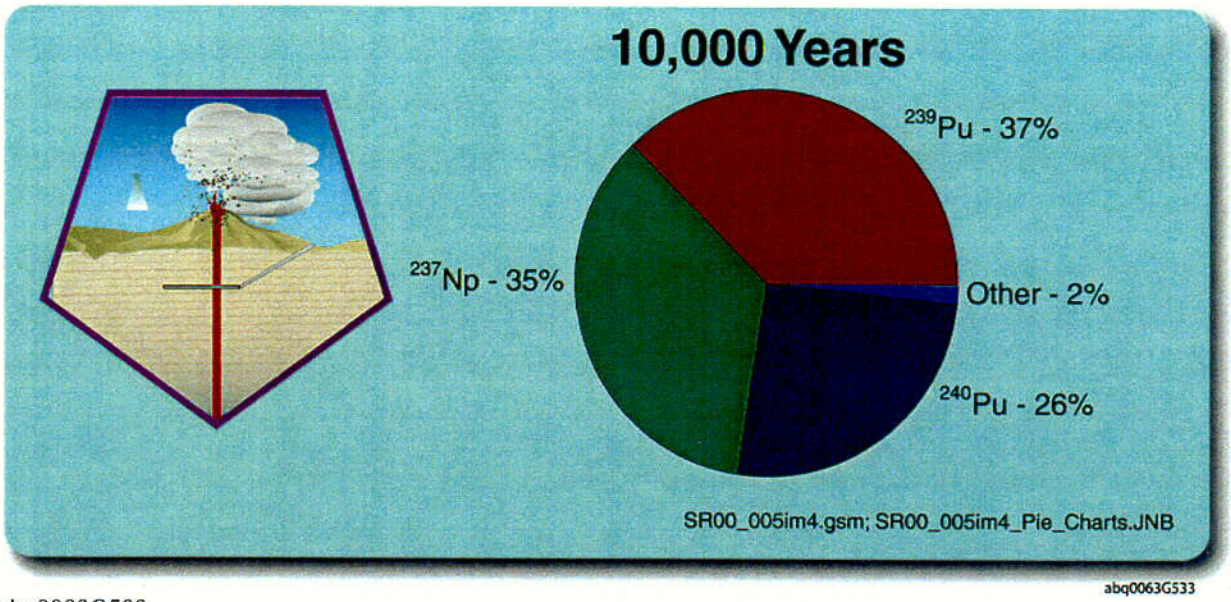

abq0063G533

Figure 4.2-4. Relative Contributions of Individual Radionuclides to the Total Probability-Weighted Igneous Dose Rate at 10,000 Years after Potential Repository Closure

L-28

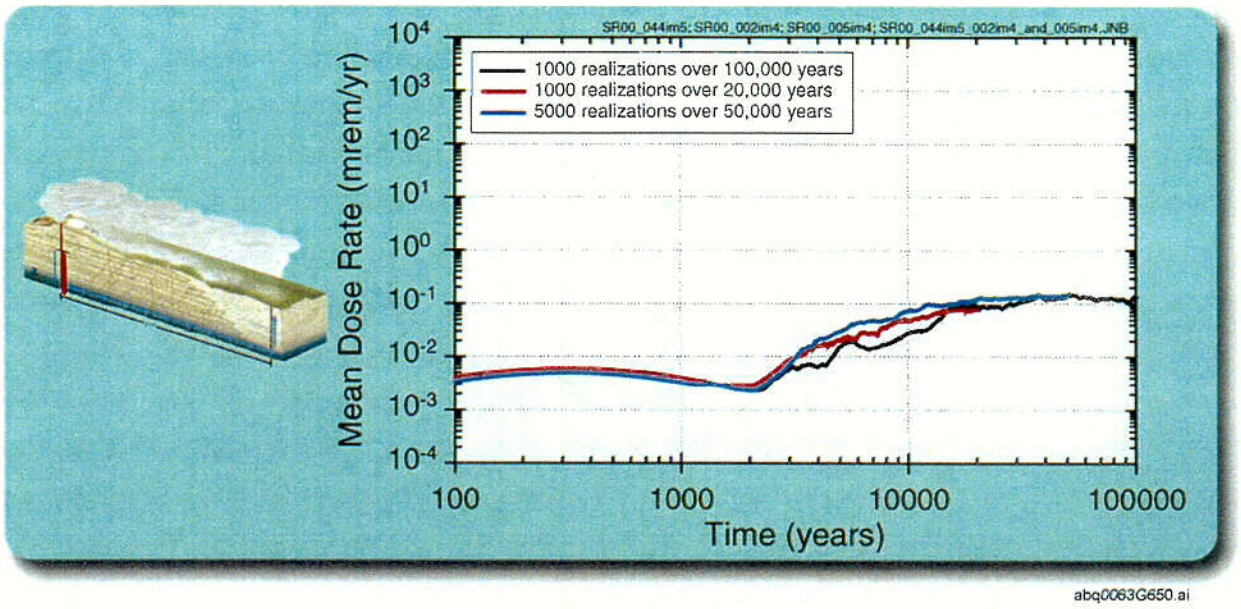

abq0063G650

Figure 4.2-5. Comparison of Three Analyses Showing Sensitivity of the Probability-Weighted Mean Annual Dose Rate Following Igneous Disruption to the Number of Realizations and Duration of the Simulation

L-29

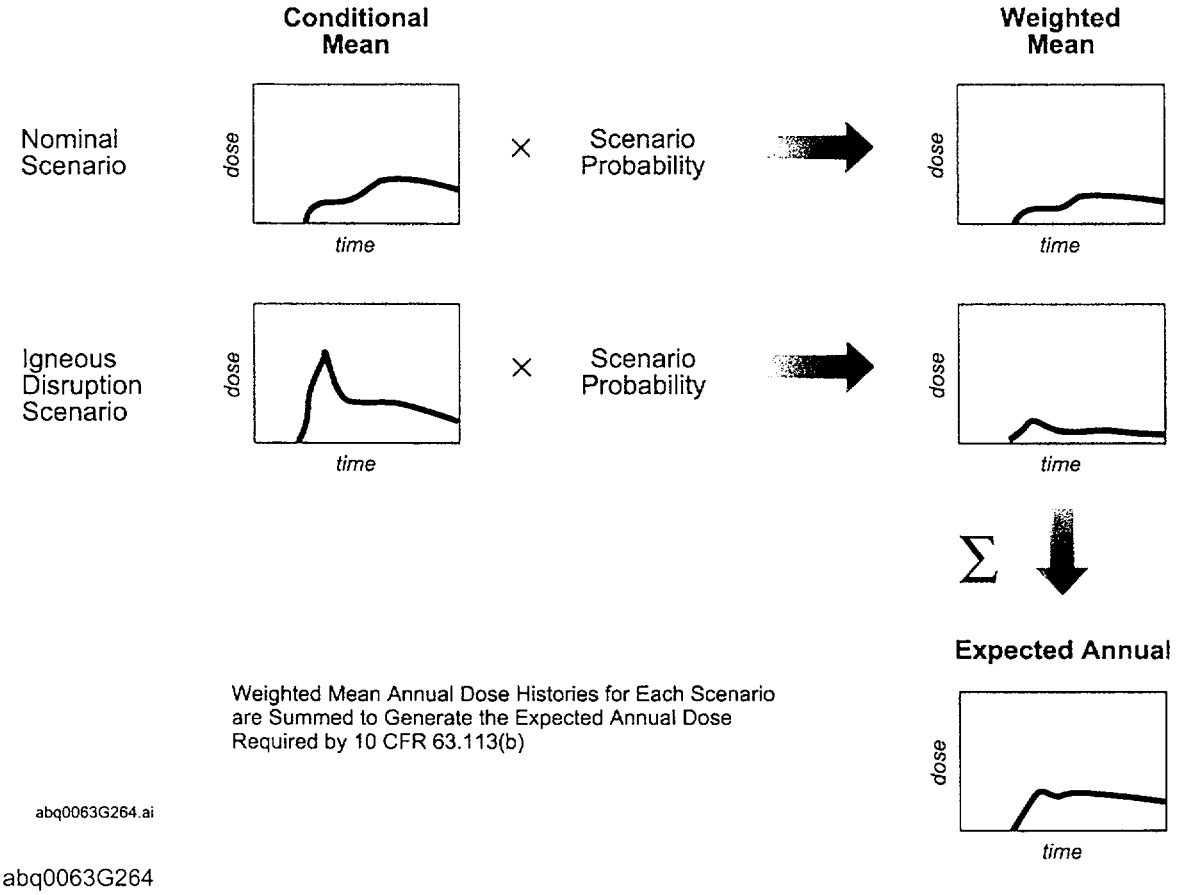

abq0063G264

Source: Adapted from CRWMS M&O 2000 [147323], Figure 4.4-3

Figure 4.3-1. A Possible Method for Combining Scenarios

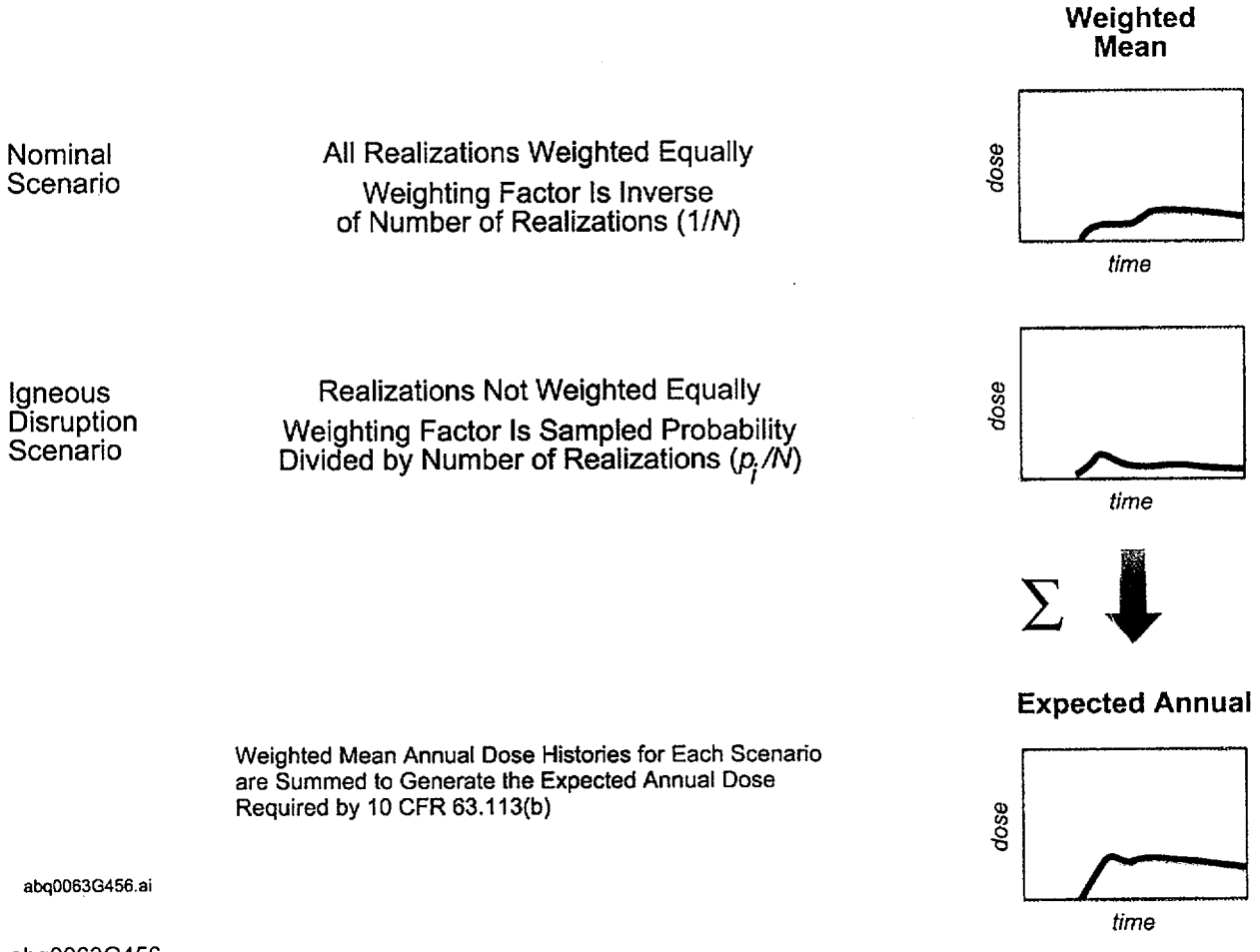

abq0063G456

NOTE: Igneous Disruption Scenario Does Not Include Nominal Waste Package Failures

Figure 4.3-2. Method for Combining Scenarios Used in this Total System Performance Assessment

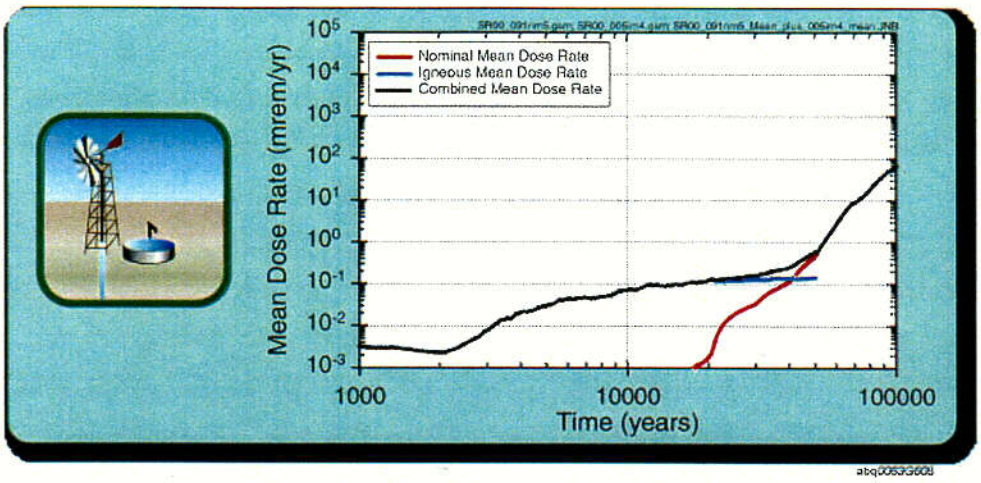

abq0063G608

Figure 4.3-3. Time Histories of Mean Annual Dose for Combined Nominal Plus Disruptive Results

C-30

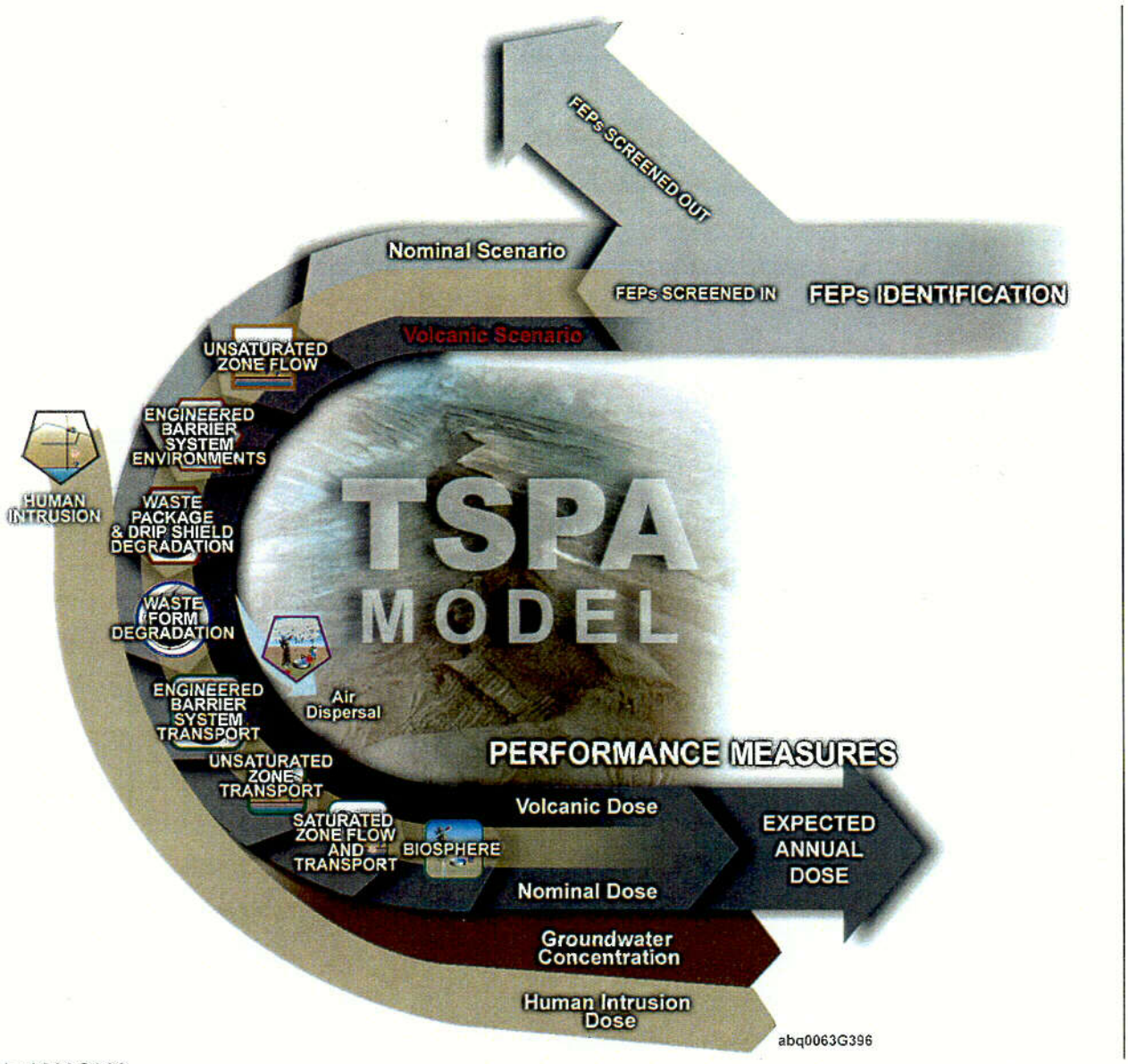

abq0063G396

Figure 4.4-1. Relationship of the Separate Human Intrusion Performance Assessment to Total System Performance Assessment-Site Recommendation

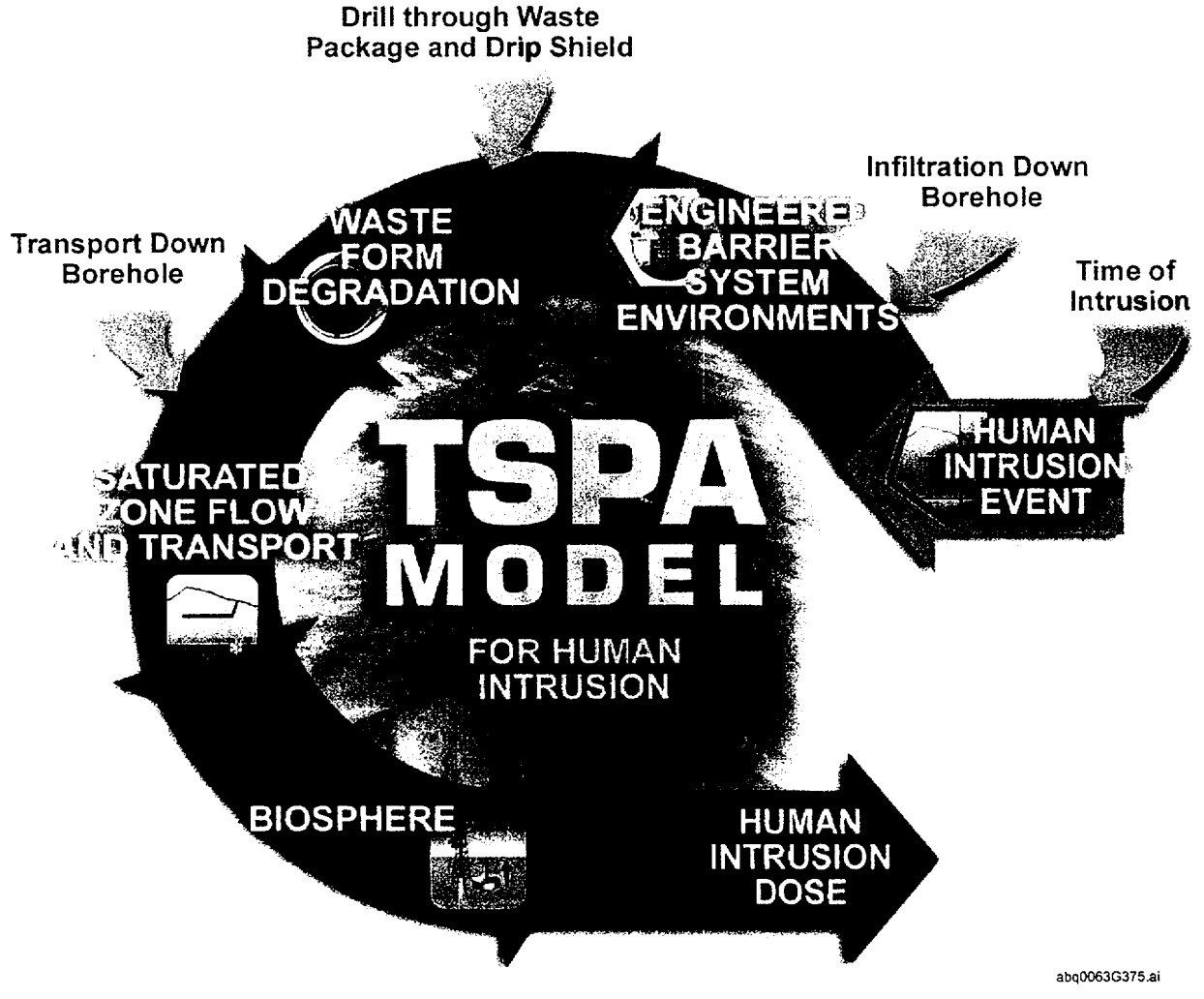

abq0063G375

Figure 4.4-2. The Human Intrusion Scenario in Total System Performance Assessment-Site Recommendation

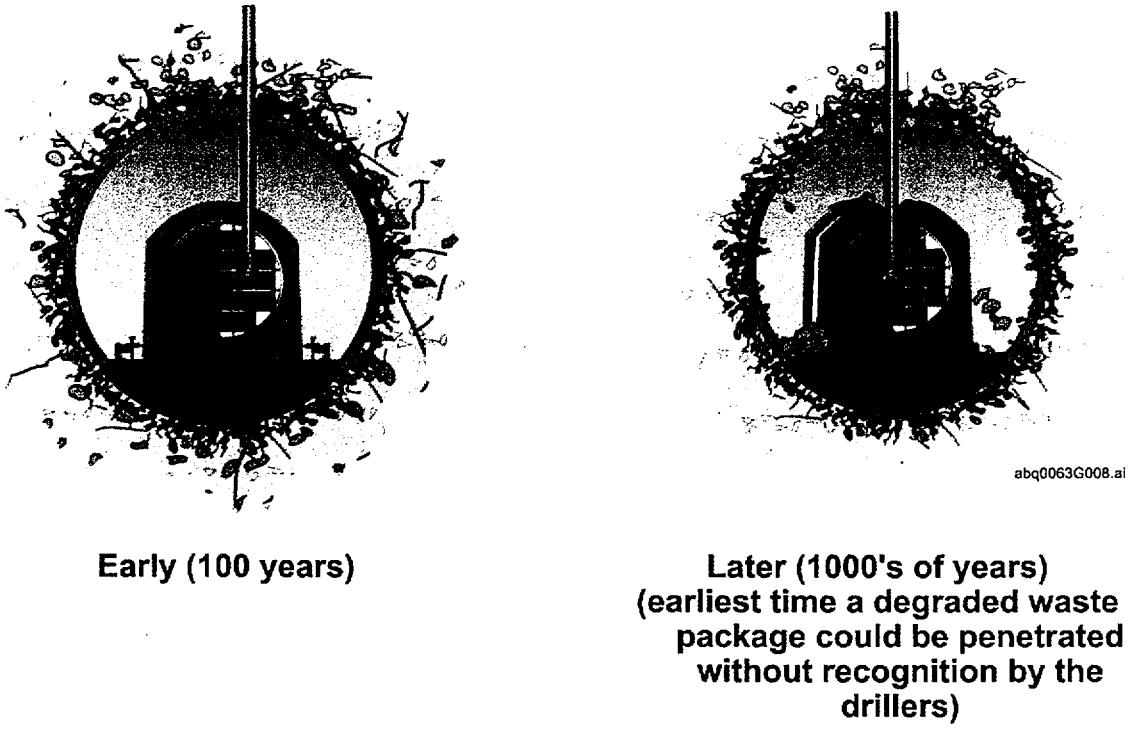

abq0063G008

Figure 4.4-3. Schematic Illustration of Intrusion Time as Specified in (a) NRC Regulations, and (b) EPA Regulations

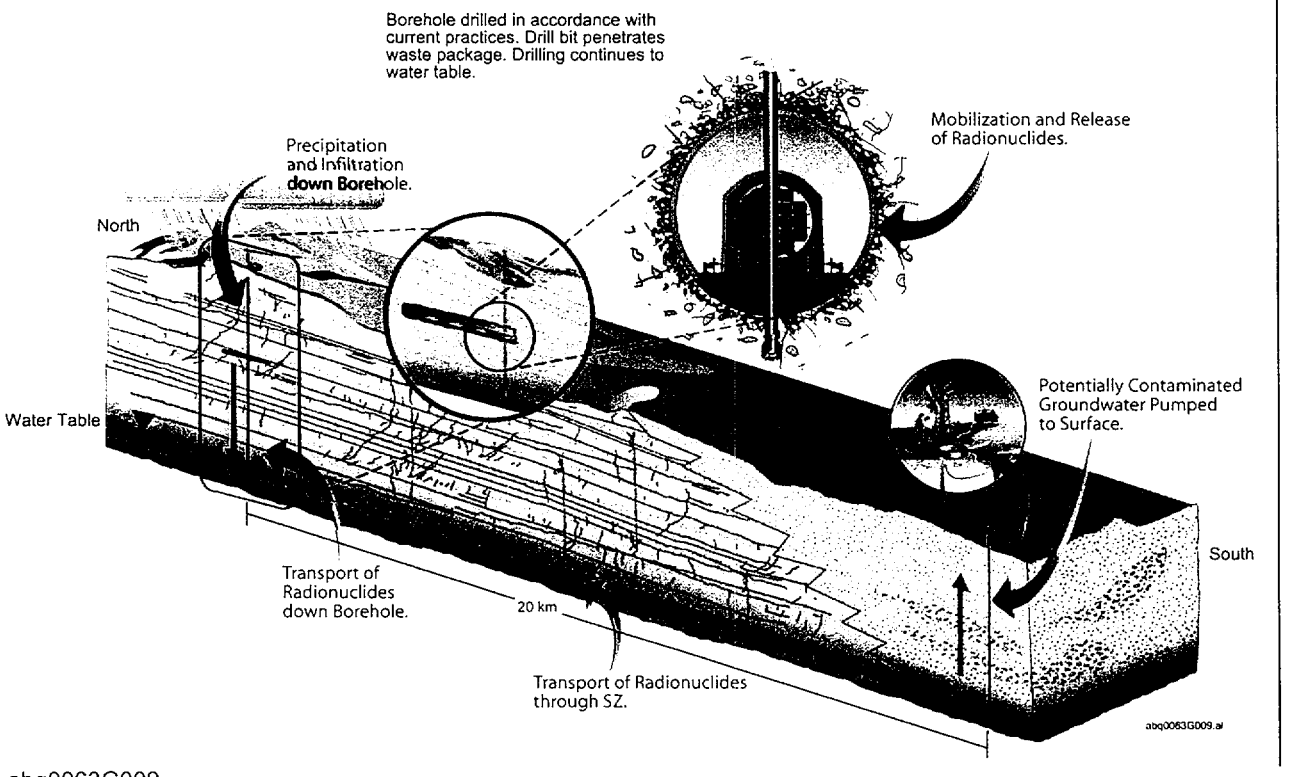

abq0063G009

Figure 4.4-4. Conceptualization of Human Intrusion for Total System Performance Assessment-Site Recommendation

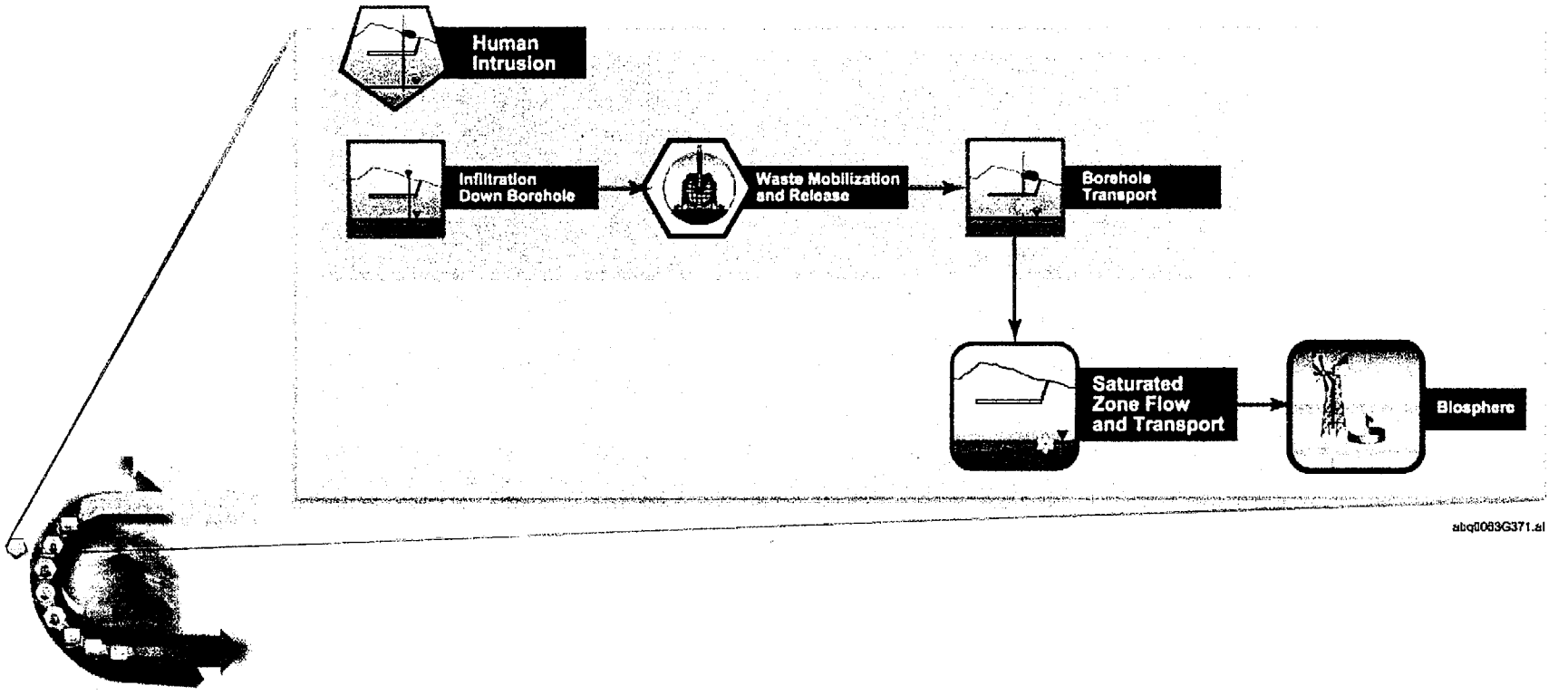

abq0063G371

NOTE: Index figure in lower left is same as Figure 2.1-5

Figure 4.4-5. Key Components of Human Intrusion for Total System Performance Assessment-Site Recommendation

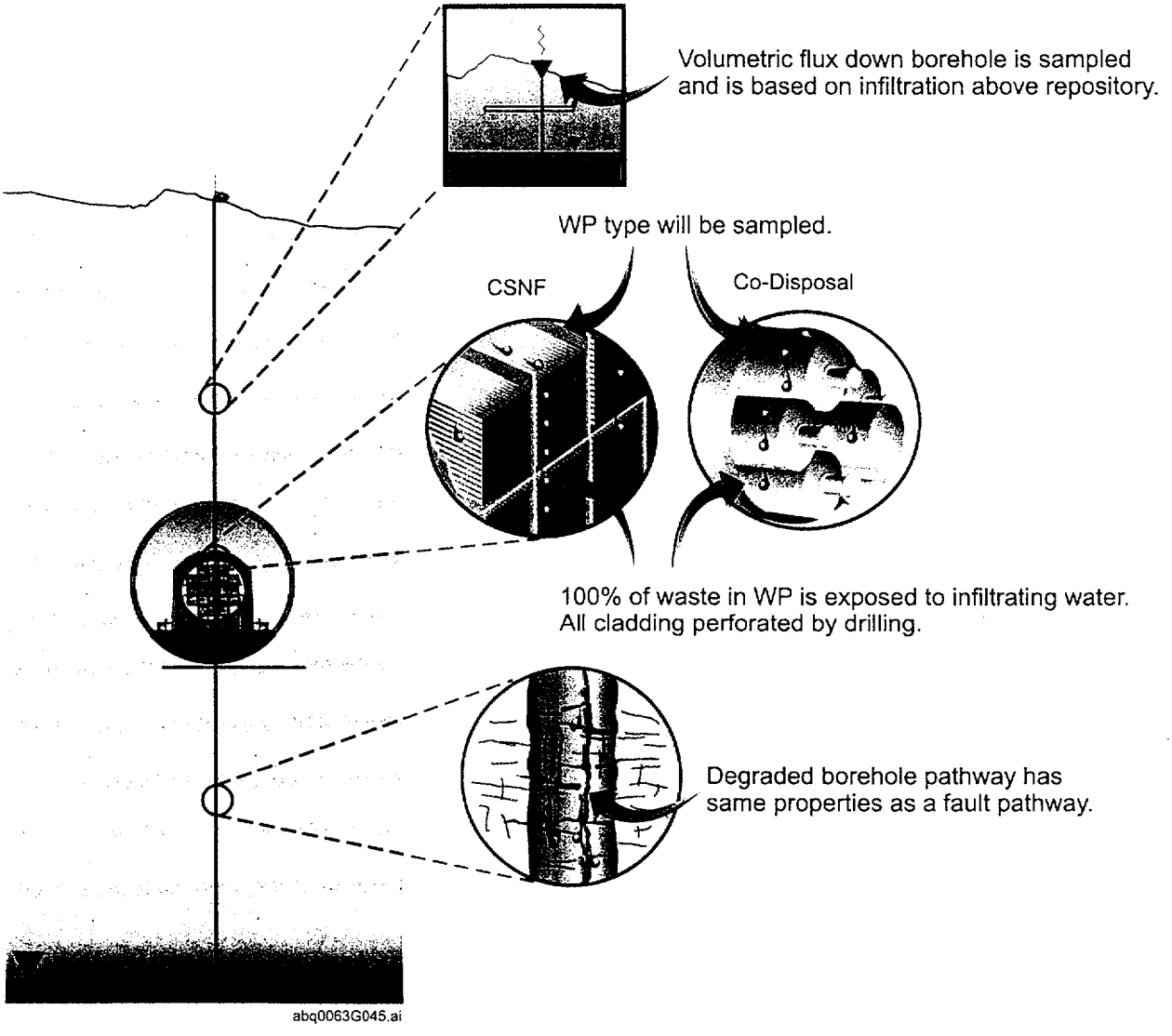

abq0063G045

Figure 4.4-6. Key Technical Assumptions for Human Intrusion in Total System Performance Assessment-Site Recommendation

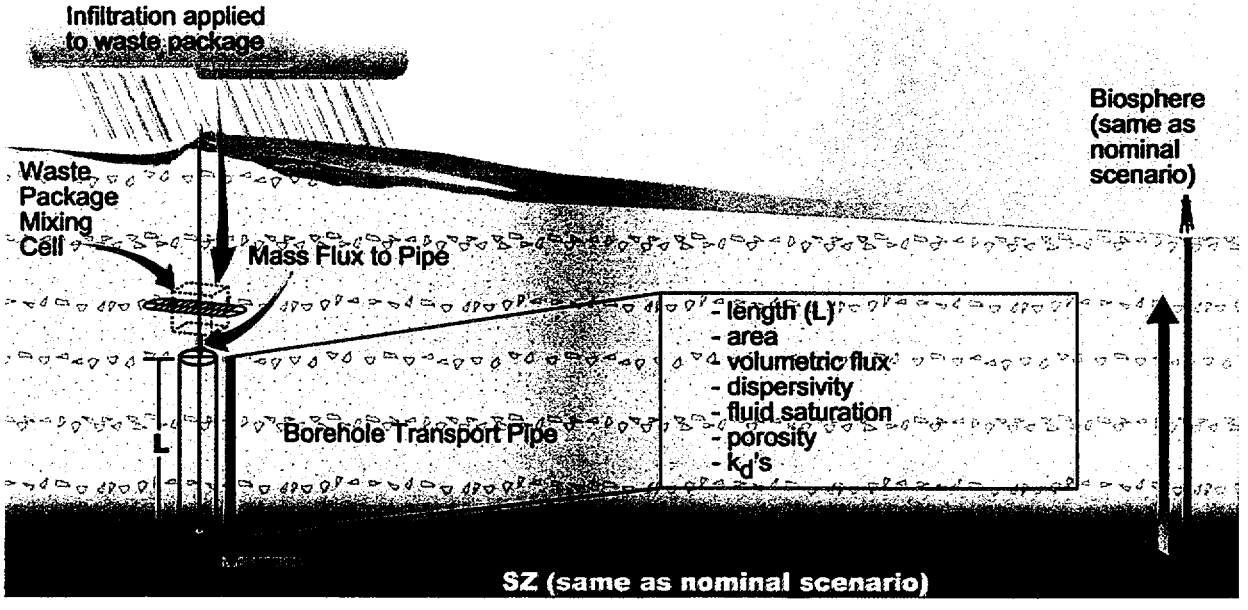

abq0063G073

Figure 4.4-7. Implementation of Human Intrusion in Total System Performance Assessment-Site Recommendation

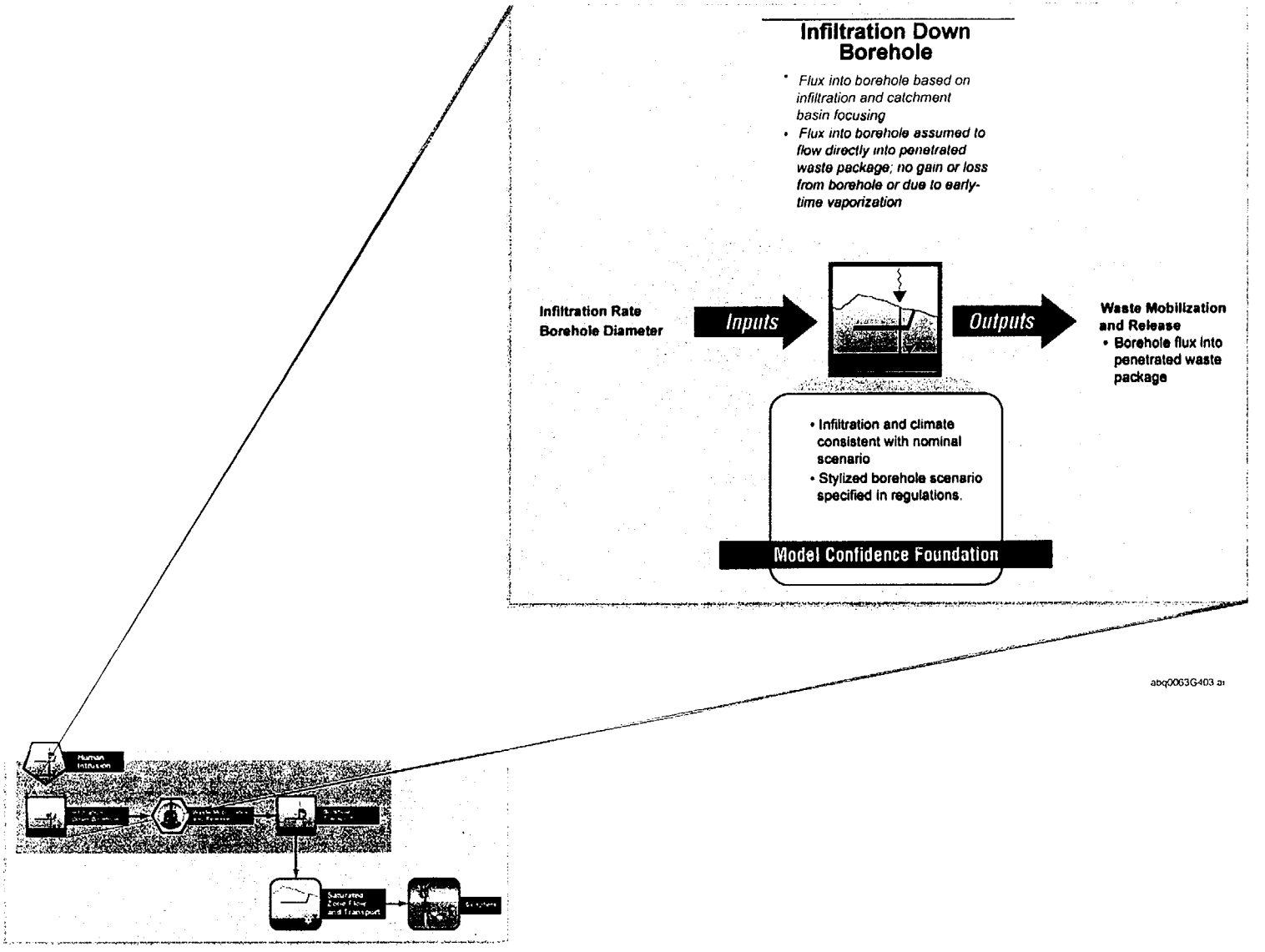

abq0063G403

NOTE: Index figure in lower left is same as Figure 4.4-5

Figure 4.4-8. Coupling of the Infiltration down Borehole Component to other Human Intrusion Components

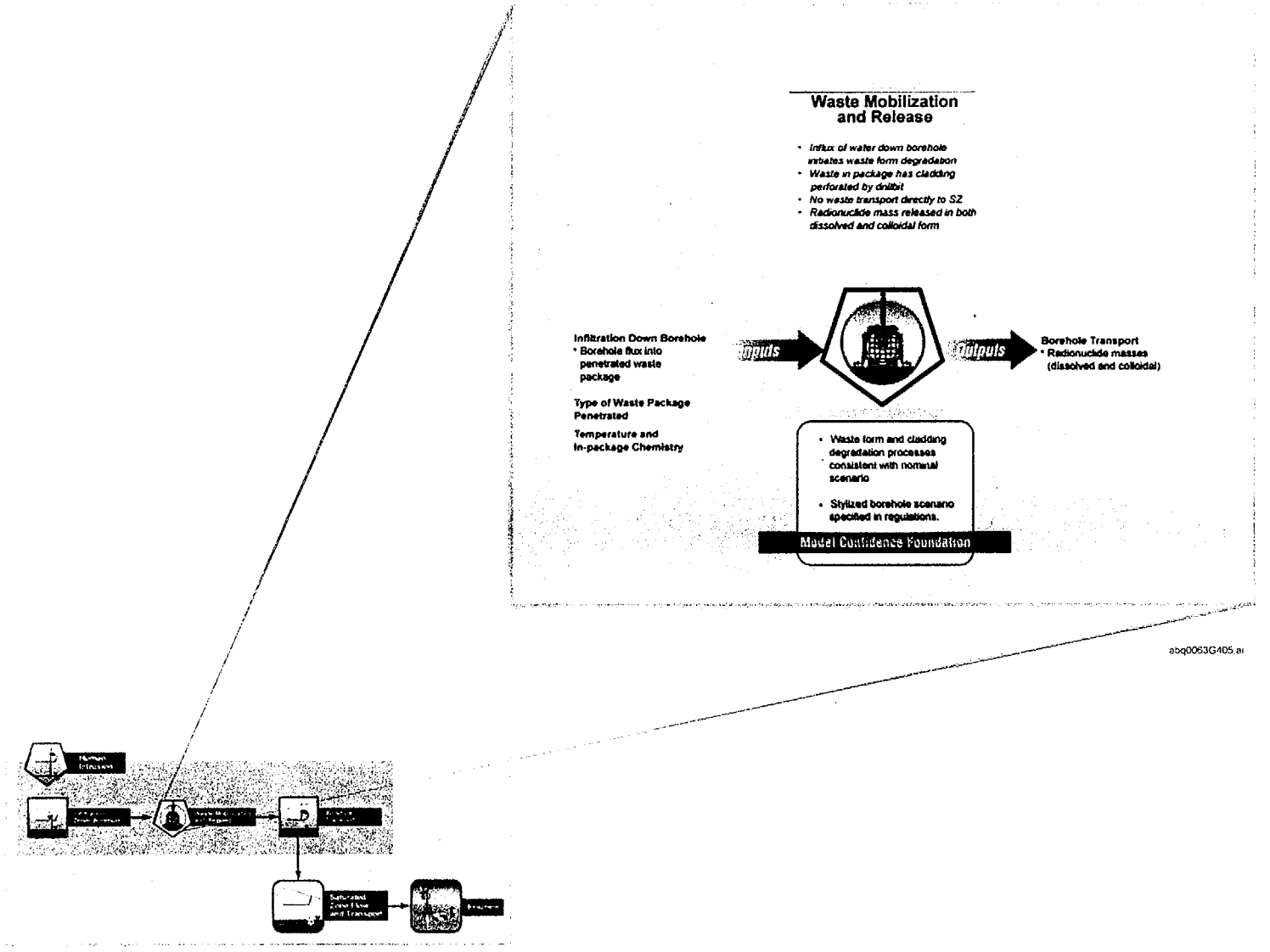

abq0063G405

NOTE: Index figure in lower left is same as Figure 4.4-5

Figure 4.4-9. Coupling of the Waste Mobilization and Release Component to other Human Intrusion Components

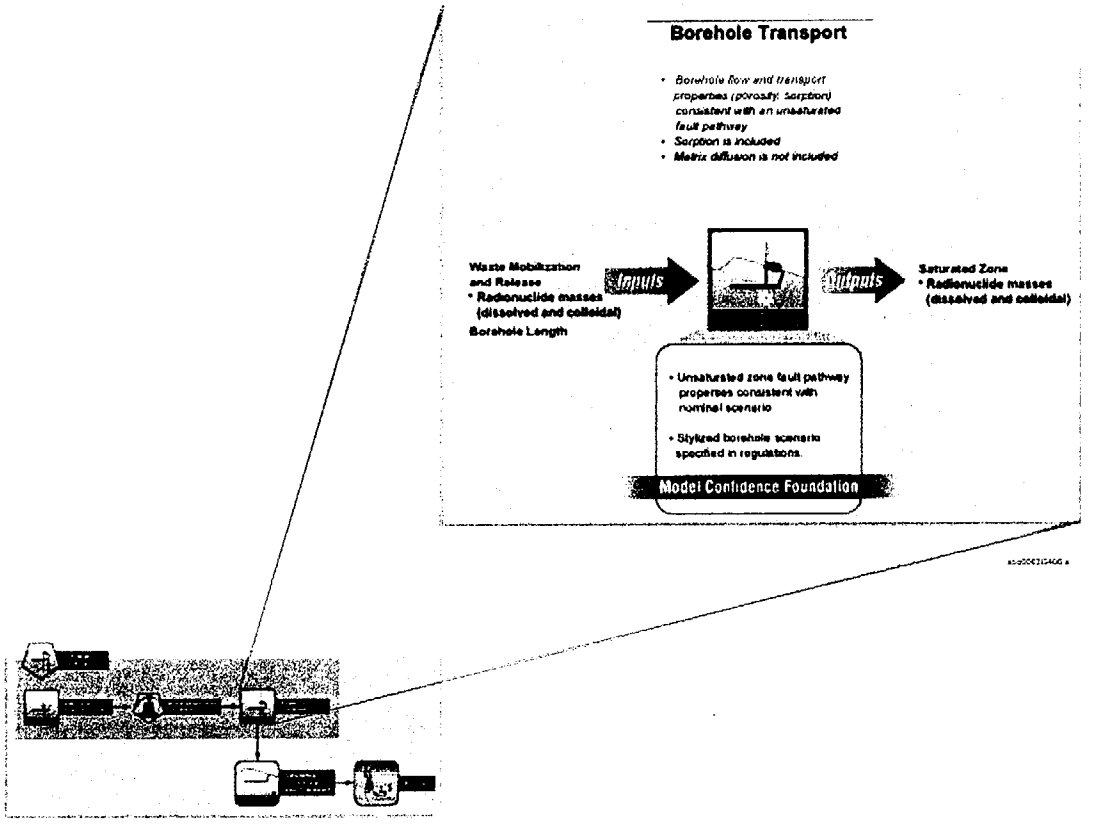

abq0063G406

NOTE: Index figure in lower left is same as Figure 4.4-5

Figure 4.4-10. Coupling of the Borehole Transport Component to other Human Intrusion Components

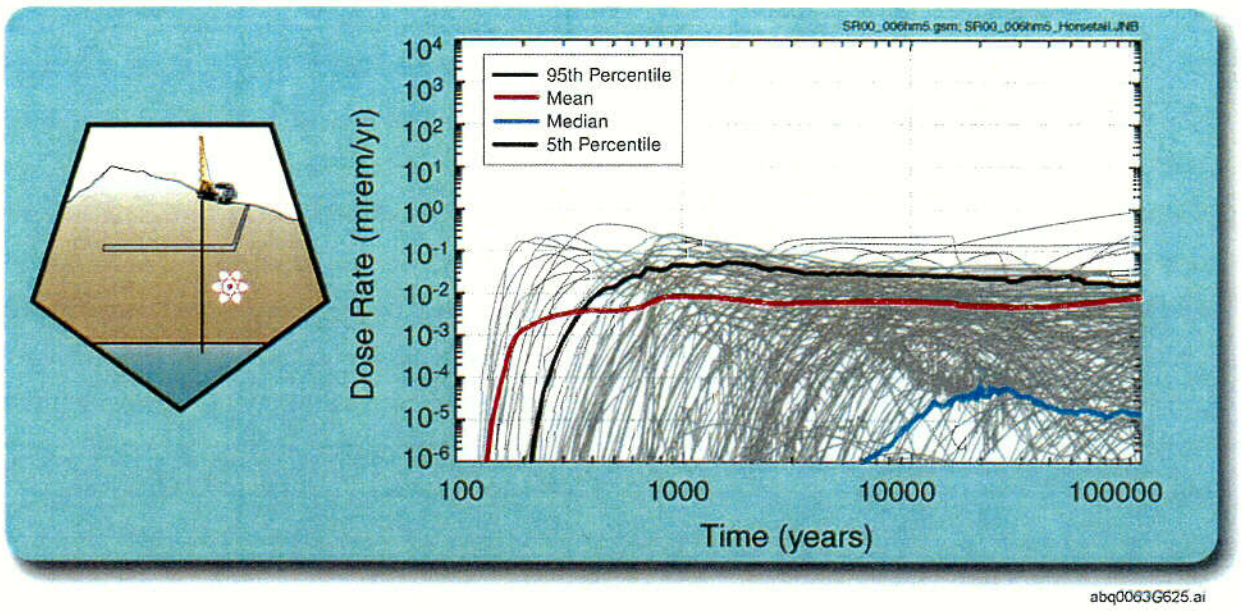

abq0063G625

NOTE: The results from each of the 300 realizations are shown along with the mean, median, 95th, and 5th percentile curves

Figure 4.4-11. Simulated Dose Rate Histories for the Human Intrusion Scenario

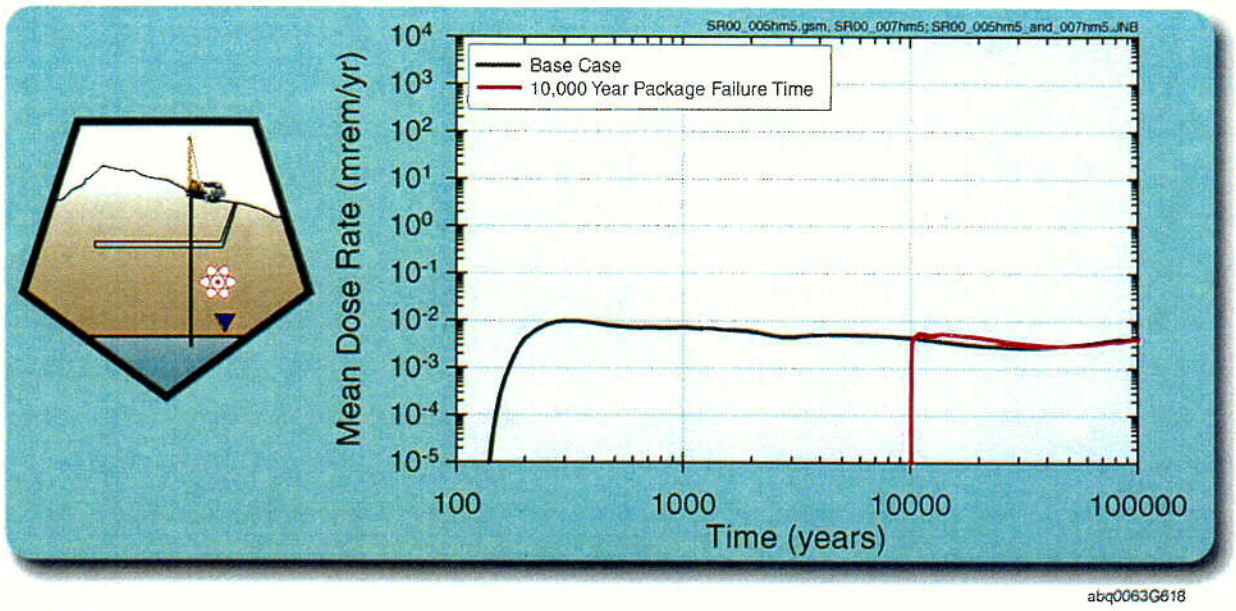

abq0063G618

Figure 4.4-12. Comparison of Total Mean Dose Histories for Human Intrusion Scenarios with Intrusions at 100 Years and 10,000 Years after Potential Repository Closure

L-33

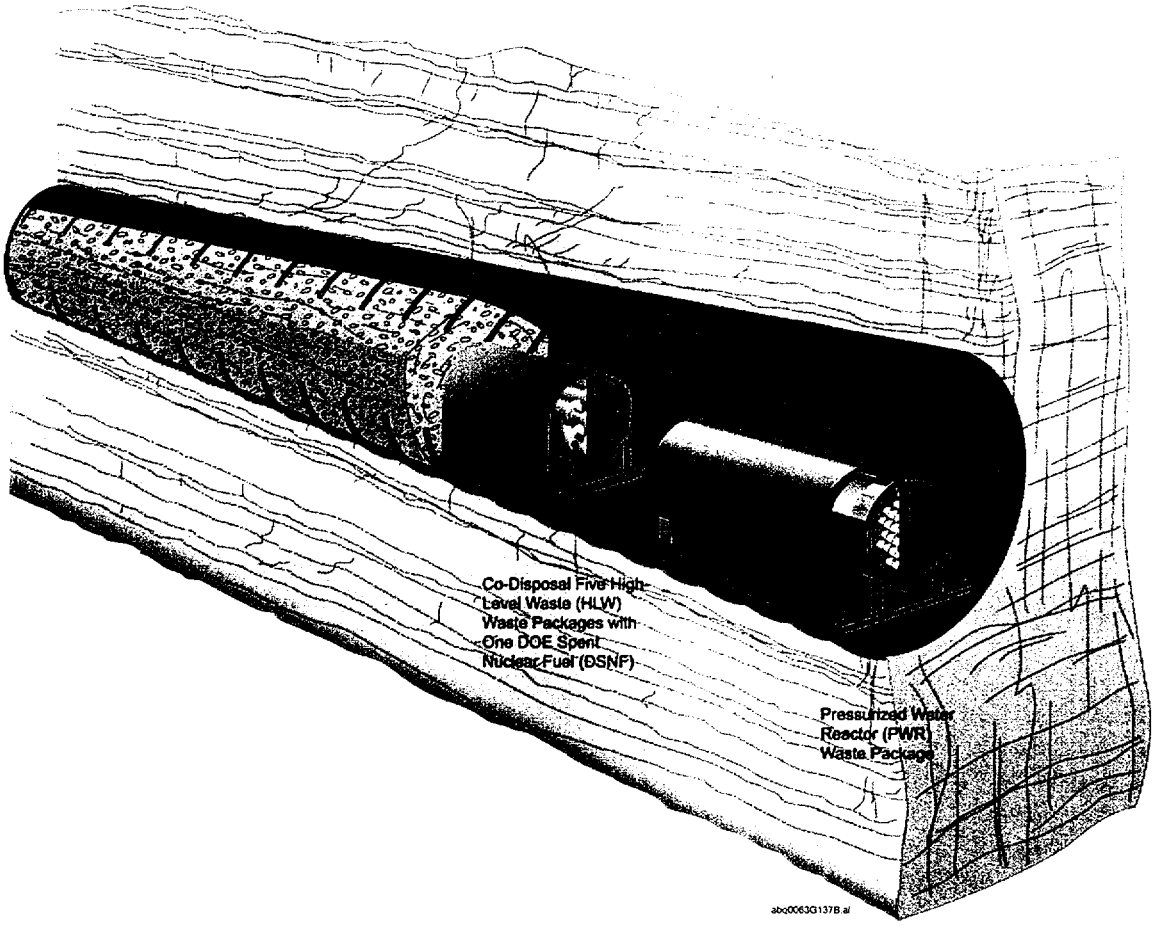

abq0063G137B

Figure 4.6-1. EBS Design with Backfill

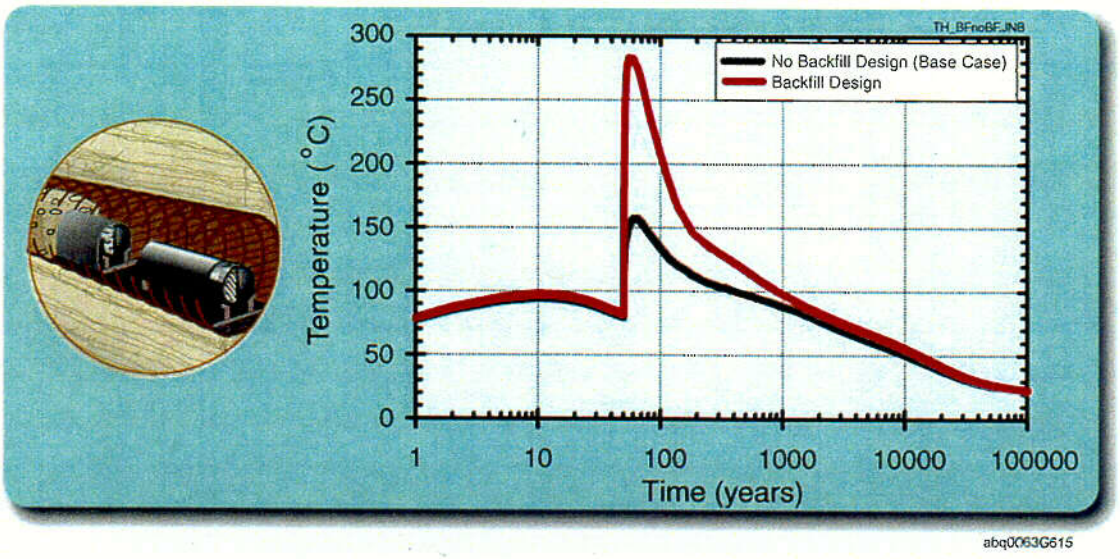

abq0063G615

Figure 4.6-2. Comparison of Waste Package Temperature for no Backfill and Backfill Cases (Nominal Scenario)

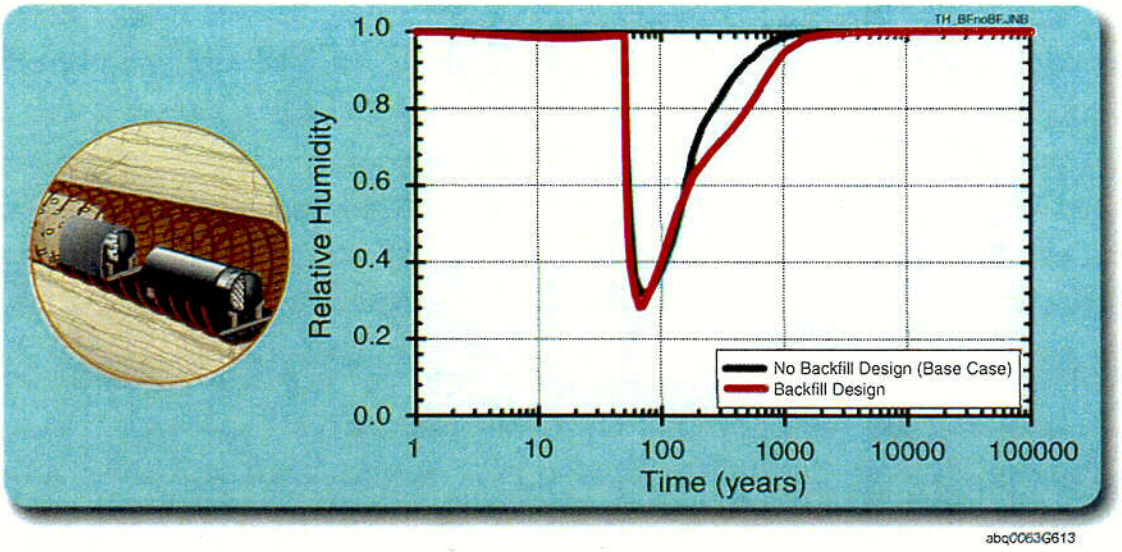

abq0063G613

Figure 4.6-3. Comparison of Relative Humidity for no Backfill and Backfill Cases (Nominal Scenario)

C-35

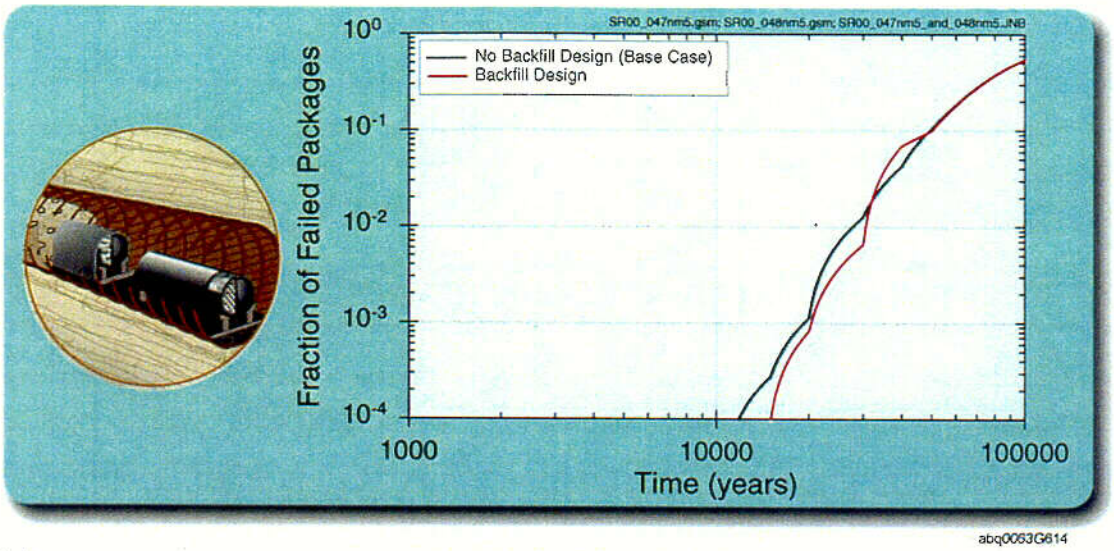

abq0063G614

Figure 4.6-4. Comparison of Initial Waste Package Failure for no Backfill and Backfill Cases (Nominal Scenario)

C-36

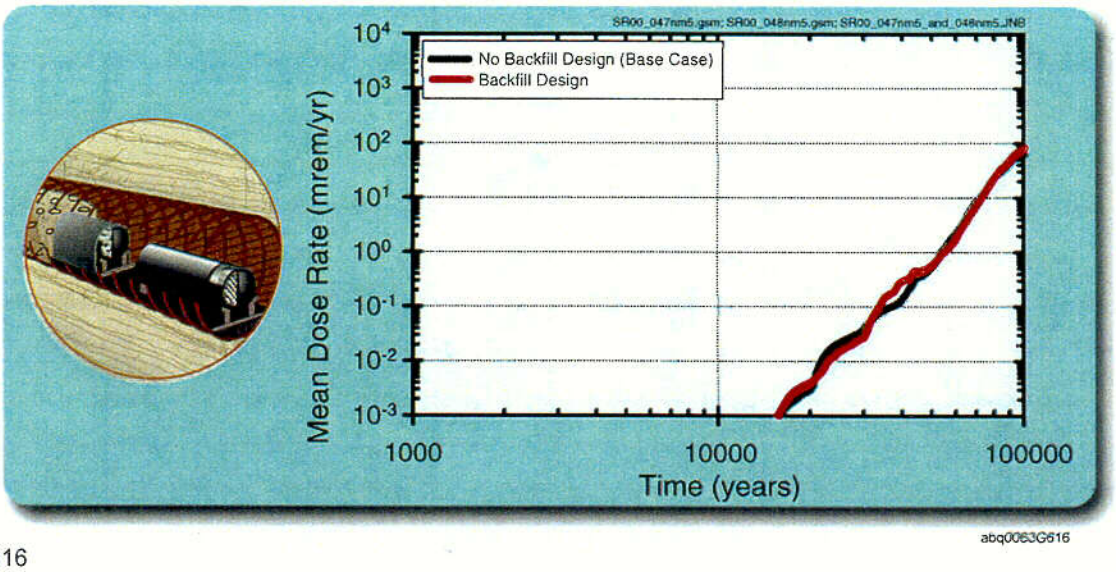

abq0063G616

Figure 4.6-5. Comparison of Dose for no Backfill and Backfill Cases (Nominal Scenario)

C-37

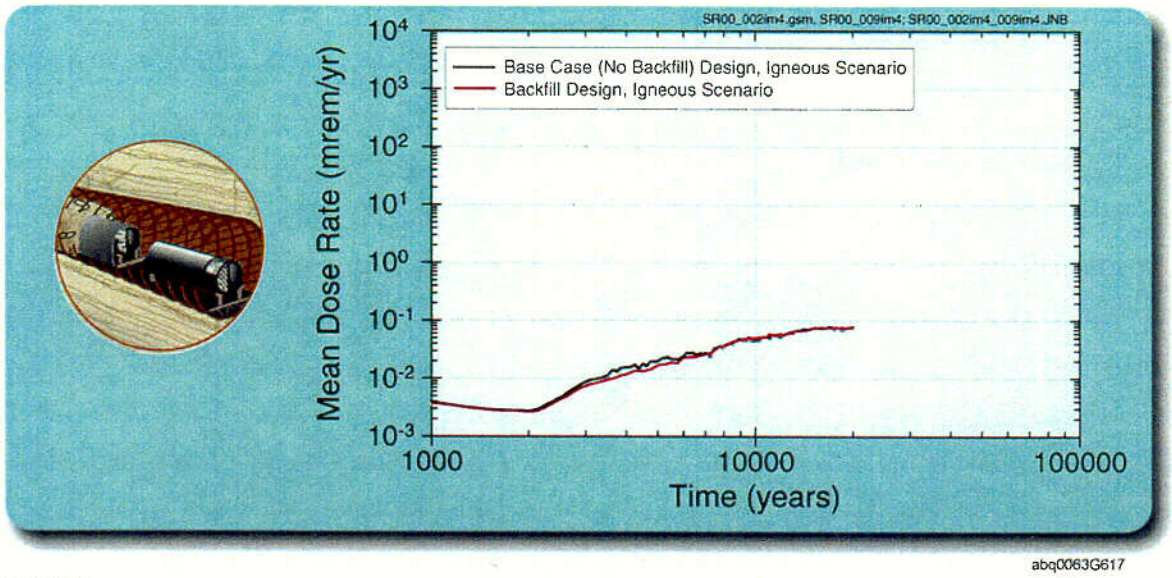

abq0063G617

Figure 4.6-6. Comparison of Dose for no Backfill and Backfill Cases (Igneous Scenario)

C-38

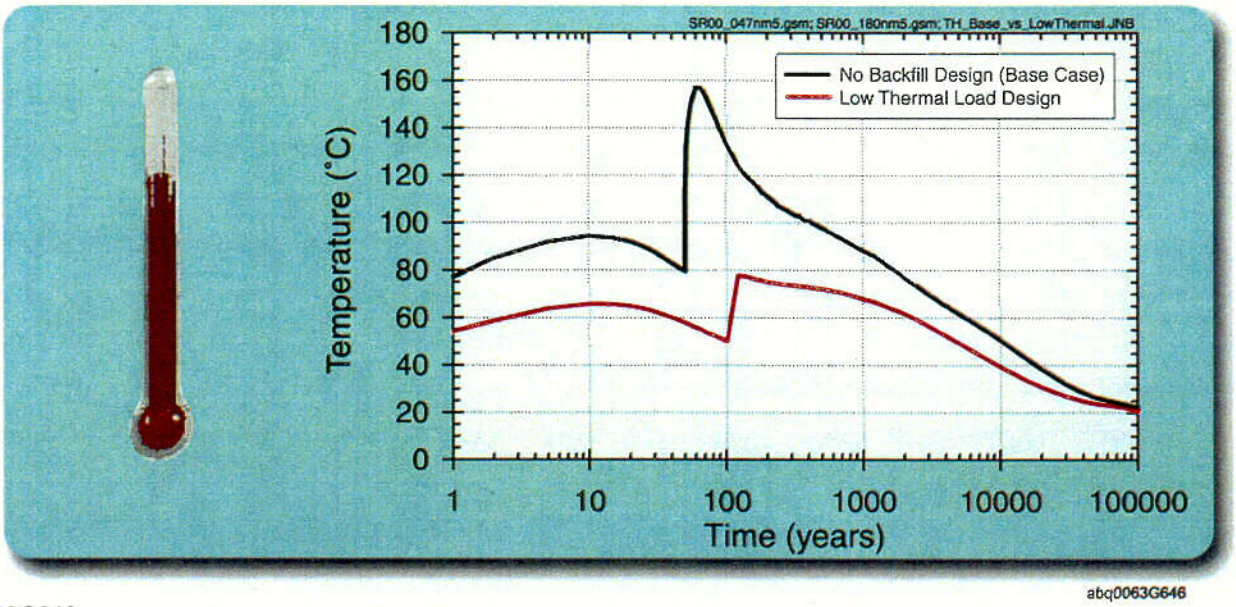

abq0063G646

Figure 4.6-7. Comparison of Waste Package Temperature for no Backfill and Low Thermal Load Design (Nominal Scenario)

C-39

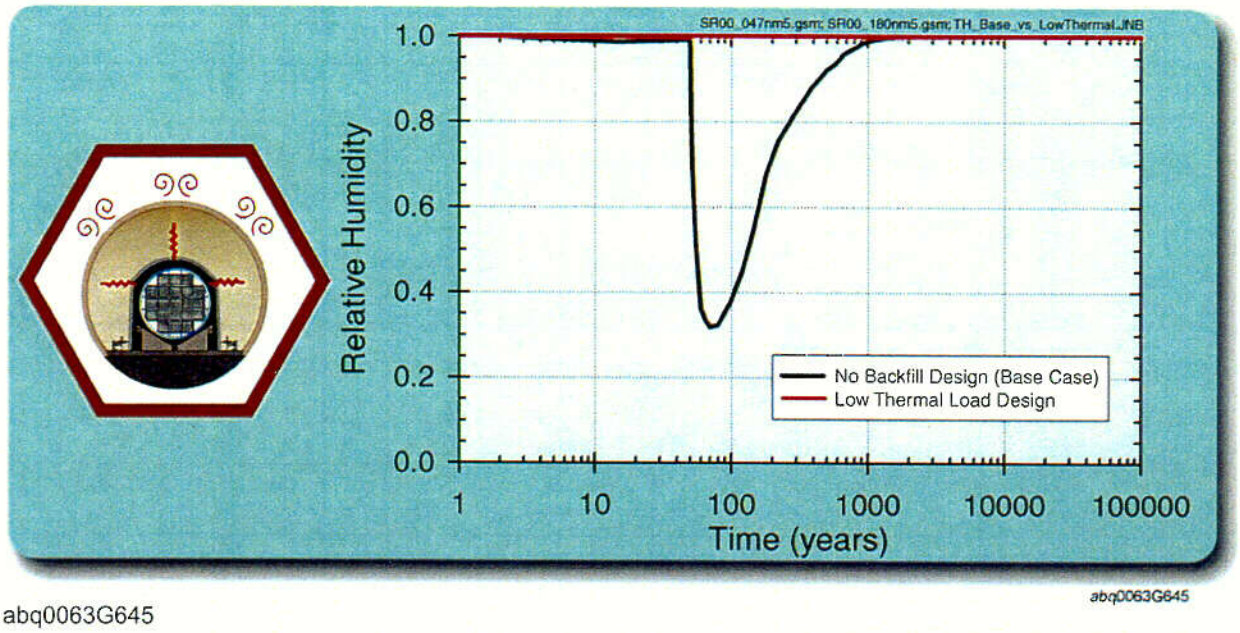

abq0063G645

Figure 4.6-8. Comparison of Relative Humidity for no Backfill and Low Thermal Load Cases (Nominal Scenario)

C-40

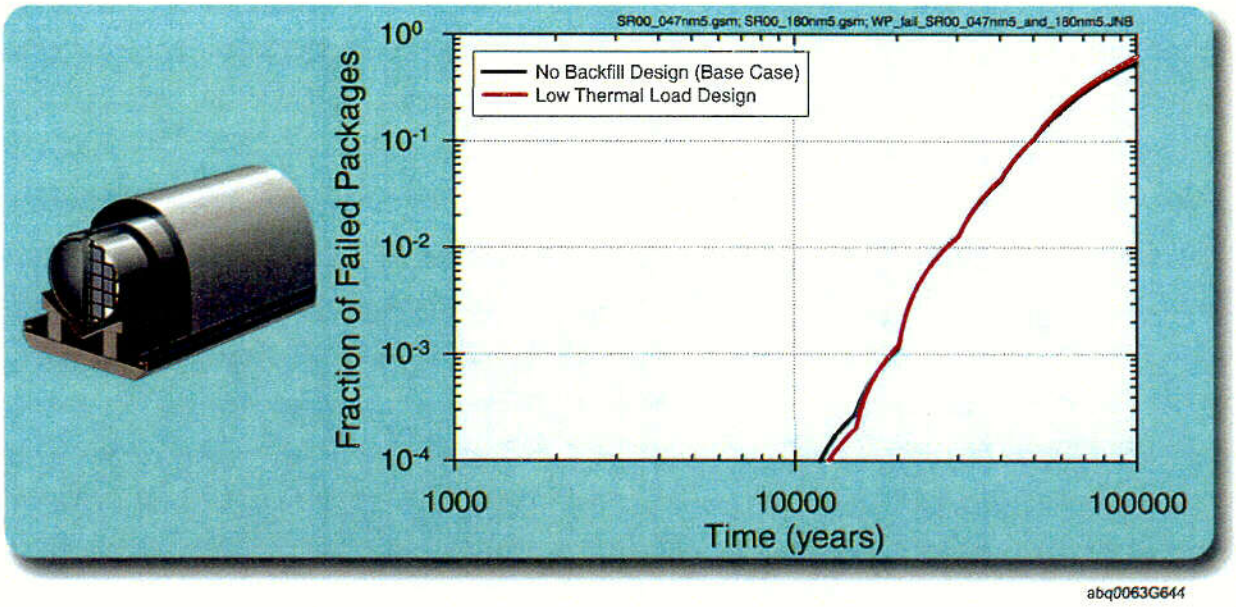

abq0063G644

Figure 4.6-9. Comparison of Initial Waste Package Failure for no Backfill and Low Thermal Load Design Case (Nominal Scenario)

C-41

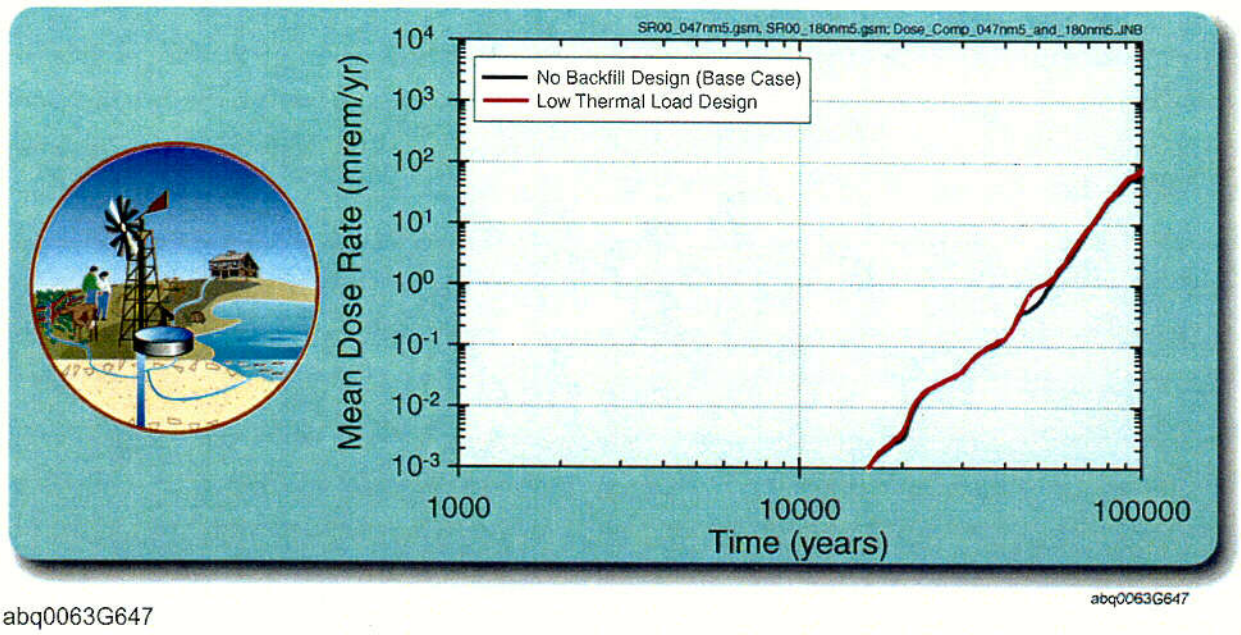

abq0063G647

Figure 4.6-10. Comparison of Dose for no Backfill and Low Thermal Load Design Cases (Nominal Scenario)

C-42

5. SENSITIVITY ANALYSES

The uncertainty in and sensitivity of the total system performance analyses of the postclosure period for the potential Yucca Mountain repository are presented in this section. The previous section provided a detailed evaluation of the nominal scenario, the igneous scenario, and the result of combining these scenarios, as well as the stylized human intrusion scenario and analyses of alternative designs. This section provides three fundamental sections that allow a greater look at the uncertainty in those results, as well as sensitivity analyses to evaluate which parameters or features of the potential repository system are most important in explaining the overall performance.

Section 5.1 provides an evaluation of the stochastic variables that are most significant in determining the output of the TSPA-SR model. This "uncertainty importance analysis" is obtained by utilizing various statistical methods to identify the most important contributors to the spread in the overall model results, and to identify contributors to the extreme, or outlier, outcomes in the model results. These analyses are presented for both total system and intermediate performance results for the nominal and igneous scenarios. As identified in the discussion on design impacts, the temperature is not a key contributor to the dominant failure mode for the waste package. Thus, temperature doesn't appear as a main contributor to potential repository performance here, and is not discussed in detail in subsequent sections 5.2 and 5.3.

Section 5.2 builds on the results of Section 5.1 and describes the results of additional TSPA-SR model simulations that are intended to demonstrate the effect of individual parameters or assumptions on the model results. For these analyses, various parameters were assigned fixed values (rather than allowed to vary within the assigned uncertainty range), or alternative modeling assumptions were made, and multiple realizations were conducted of these modified inputs. These analyses are often called "one-off" sensitivity analyses, due to the nature of changing a single parameter at a time. These analyses were conducted to evaluate sensitivity of many of the components of the nominal and igneous scenario models.

An additional type of sensitivity analysis is presented in Section 5.3. These robustness analyses were intended to help evaluate the performance of the potential repository system when the various natural and engineered barriers (to release and transport of radionuclides) are assumed to be degraded, either individually or in combination. These analyses were only conducted using the nominal scenario as the basis. These analyses were conducted for the many barriers within the geologic repository system. The degradation characteristics did not increase or decrease the range of uncertainty in the nominal case. It just evaluated the extremes of the parameter or model range already in the TSPA-SR model. These analyses were based on modifying barriers, not necessarily on evaluating parameters or models identified in Section 5.1, though the analyses often confirmed the results of Section 5.1.

5.1 UNCERTAINTY IMPORTANCE ANALYSIS

This section presents the results of analyses intended to identify those stochastic variables that have the greatest impact on the output of the TSPA-SR model. The goal is twofold: (a) use regression analysis to determine the most important contributors to the spread in probabilistic model results, and (b) use classification tree analysis to identify those variables controlling

extreme outcomes in the full suite of probabilistic results. Details of these techniques, presented in Section 2.2.5, are summarized below for the reader's benefit.

Regression analysis–is a tool for quantifying the strength of input-output relationships in the TSPA-SR model. To this end, a stepwise linear rank regression model is fitted between total dose at a given time (or some other performance measure) and all randomly sampled input variables. Parameters are ranked on the basis of how their exclusion would degrade the explanatory power of the regression model. The importance ranking metric used for this purpose is the uncertainty importance factor, which is defined as the loss in explanatory power (R^2-loss) divided by the coefficient of determination (R^2) of the regression model. Note that the uncertainty importance factor also quantifies what proportion of the total spread (variance) in total dose explained by the regression model can be attributed to the variable of interest.

Classification tree analysis–a subset of classification and regression tree analysis, is a method for determining what variables or interactions of variables drive output into particular categories. Classification and regression tree analysis can be used to generate decision rules that determine whether a particular realization would produce "high" or "low" dose depending on the values of the most important variables. Unlike regression analysis, which is based on the total range of model outcomes, classification tree analysis focuses on extreme values of model results and tries to relate them to specific ranges of values for the important variables.

Each TSPA-SR model run, as discussed in Section 4.1, is typically based on a 300-realization sample. Thus, for any given time, there are 300 output values (e.g., dose) as well as 300 input values for each of the stochastic input variables. For the purposes of uncertainty importance analysis, these results are post-processed in three different ways. The most common approach is to consider the spread in dose at a fixed time slice, and use regression analysis to identify the primary contributors to this spread in dose. A second approach is to consider the spread in time to reach a specified dose level, and determine the key contributors to this spread also using regression analysis. The third approach is to partition the results at any given time into "high" or "low" dose categories, and then use classification tree analysis to identify the variables influencing this separation into categories. The results presented in this section will use all three of the approaches discussed above.

The results that follow are of uncertainty importance analysis for the nominal scenario results with total dose as the performance measure. This is followed by an analysis of various intermediate performance measures (e.g., EBS and SZ release for individual radionuclides, percent waste packages failing, etc.) for the nominal scenario. Finally, the igneous scenario results are analyzed with total dose as the performance measure. Note that unless otherwise indicated, these analyses reflect projected performance of the disposal system over 100,000 years.

5.1.1 Nominal Scenario, Total Dose

Section 4.1 presents a discussion of the range of dose that the average member of the critical group is likely to receive over 100,000 years for the nominal scenario. Figure 4.1-5 shows that there is a broad range in projected dose rates at any given time, with most of the realizations producing negligible dose during the first few tens of thousands of years. Regression analysis of

such data is difficult because of the limited number of non-zero dose producing realizations, as well as the large number of stochastic inputs in the model. Therefore, regression analysis was restricted to those time slices (at 10,000 year increments) for which at least 100 realizations produced dose in excess of 10^{-5} mrem/yr. For the nominal scenario, as shown in Figure 4.1-5, the first such time slice was 40,000 years. The choice of 10^{-5} mrem/yr was based on a visual examination of dose histograms at selected time slices to identify a consistent separation threshold between non-zero dose values and infinitesimal dose values. Requiring a minimum of 100 observations for carrying out the regression analysis was felt to be a reasonable choice for eliminating bias in building input-output models containing approximately 10 percent of the more than 240 stochastic inputs in the TSPA-SR model.

Regression analysis was carried out at 10,000-year increments, from 40,000 to 100,000 years. Stepwise rank regression models between total dose and a set of statistically significant input variables were built for each case, and the most important variables were identified based on the value of their uncertainty importance factor. Figure 5.1-1 shows a bar chart of these results generated for the 40,000-year data, indicating that the most important variables are the SCC outer and middle lid stress profiles and the Alloy-22 outer lid median general corrosion rate. Similar importance analyses results for 70,000 and 100,000 years are shown in Figure 5.1-2 and Figure 5.1-3, respectively. These also indicate that the waste package degradation related parameters such as the stress profiles and the median corrosion rates continue to be important over the longer time period. The natural system is beginning to affect the system response after about 70,000 years, albeit marginally, as indicated by the inclusion of SZ groundwater flux in the list of important variables.

Figure 5.1-4 shows how uncertainty importance factors change with time for the key uncertain variables. Over the first 100,000 years, the SCC outer lid stress profile is seen to be consistently the most important, followed by the median general corrosion rate of the Alloy-22 outer and middle lids. Note also the slow but steady increase in importance for SZ groundwater flux with time. Figure 5.1-5 presents a different interpretation of the same information in terms of time-averaged composite uncertainty importance ranking. The importance ranking (with the most important variable getting the highest rank) from all time slices is averaged and normalized such that a (perfect) rank of 1 indicates that the corresponding variable (e.g., SCC outer lid stress profile) is consistently the most important at all time slices.

As discussed in Section 2.5, another tool for investigating the relationship between model output and key uncertain inputs is the use of scatter plots. Figure 5.1-6 shows scatter plots at 40,000, 70,000, and 100,000 years between total dose and SCC outer lid stress profile, and total dose and Alloy-22 outer lid median general corrosion rate. In general, an increase in the value of these variables leads to a greater dose, although there is considerable scatter in the data. This suggests that no single uncertain input is overly dominant in affecting the spread of total dose in the current TSPA-SR model.

Next, we present an application of classification tree analysis to the same data sets to determine which variables control extreme outcomes. The 300 realizations of total dose, at any given time slice, are first categorized as "high" if the values are in the top 10 percentile, or "low" if the values are in the bottom 10 percentile. The classification tree analysis algorithm then determines

which variables are most capable of explaining the separation of these realizations into the appropriate categories.

Figure 5.1-7 (top) shows a decision tree summarizing the classification tree analysis in terms of the two most important variables for the 40,000-year data. In this case, much of the separation into high and low dose values can be explained on the basis of a single variable, the SCC middle lid stress profile. The second most important variable, uncertainty in agricultural water usage per farm, provides only marginal additional explanatory power, and that too, for the low dose values. Figure 5.1-7 (bottom) is a partition plot of the same data, showing where the high and low dose producing clusters actually occur in the bivariate parameter space of the two most important variables. Note that the partition plot is actually an input-input scatter plot, with the data points color coded to indicate which category they belong to, and the dividing lines indicating where the split between the categories occurs.

Note that these variables are important only in terms of explaining the decision rules (e.g., *if* variable_1 > x *and* variable_2 < y *then* dose high) leading to extreme outcomes. The variable importance ranking obtained from regression analysis provides a complementary piece of information, namely, which variables contribute the most to the overall spread in outcomes. Thus, agreement between the two sets of importance rankings should not be expected to be perfect for all cases. The partition plot essentially supplements the insight drawn from the regression analysis in that one can determine how exactly an important uncertain input is affecting the dose.

Classification tree analysis results for the 70,000-year dose data are summarized in the decision tree shown in Figure 5.1-8 (top). Here, the variables related to SCC middle and outer lid stress profiles provide the most explanatory power in the categorization problem. High values for both the stress profiles leads to high doses, and conversely, low values for both stress profiles leads to low doses. This trend is also demonstrated in the partition plot shown in Figure 5.1-8 (bottom), where high and low dose producing outcomes are separated into the top right and bottom left quadrants.

In Figure 5.1-9 (top), the categorization decision tree for the 100,000 year data is shown. As in the case of the 40,000 year data, a single variable (SCC outer lid stress profile) is adequate for explaining most of the separation between the two categories. Figure 5.1-9 (bottom) confirms the dominating influence of this variable using the partition plot.

Thus far, the probabilistic results have been analyzed in terms of the spread in total dose at any given time. A second way of examining the same data is to analyze the results in terms of the spread in the time to reach a given dose. Thus, instead of "slicing" the multi-realization dose versus time data vertically along the time axis, the data are sliced horizontally along the dose axis. The dependent variable for the regression model becomes the time to reach a given dose, while the independent variables remain the same set of stochastic inputs used earlier.

This analysis was carried out at 4 specified dose levels, 0.01 mrem/yr, 0.1 mrem/yr, 1 mrem/yr, and 10 mrem/yr. Stepwise regression was carried out using time (rather than dose) as the dependent variable, and uncertainty importance factors were calculated as before. The results indicate that the same set of waste package degradation-related parameters identified earlier

dominate the uncertainty in the output. Therefore, for reasons of brevity, Figure 5.1-10 presents only the graphs showing how uncertainty importance factor changes with the specified dose level for the key uncertain variables. Comparing Figure 5.1-10 with Figure 5.1-4 does confirm the general similarity in importance ranking irrespective of whether the contribution to spread in dose or spread in time is used as the ranking metric.

An analysis of uncertainty importance based on a 1-million-year simulation is presented (Figure 4.1-19). Dose values from each of the 300 realizations were regressed against the set of stochastic inputs at 100,000-year increments. The results, shown in Figure 5.1-11, depict the decreasing importance of the EBS parameters, and the increasing importance of the natural system, as compared to the importance rankings shown previously for the first 100,000 years in Figure 5.1-4. Note, in particular, how infiltration scenario becomes the single-most dominant variable at around 200,000 years and continues to remain so over the 1-million-year simulation period. It should be pointed out that the quantitative importance rankings for variables other than infiltration scenario are not very reliable, especially in the 400,000 to 800,000 year time frame, because the regression analyses provided relatively poor fits to these data sets.

5.1.2 Nominal Scenario, Intermediate Results

This section focuses on the projected spread in intermediate results such as the waste package failure distribution and the mass release at various "pinch points." A pinch point is a location at which mass (or energy) is being transferred from one modeling domain (or subsystem or barrier) to another. ^{237}Np and ^{99}Tc were selected for this purpose because of their widely differing sorption characteristics and also because these two radionuclides are major contributors to the total dose (Figure 4.1-6). The two pinch points chosen for tracking mass release were the boundary between the EBS and the UZ, and the boundary between the SZ and the biosphere.

Using the standard regression analysis methodology with ^{99}Tc mass release as the dependent variable, we calculated uncertainty importance factors at those time slices for which at least 100 realizations yielded a mass release greater than 10^{-5} g/yr. The uncertainty importance factor time history for the 5 most important variables are shown in Figure 5.1-12 and Figure 5.1-13 for the EBS release and the SZ release, respectively. These figures show that the SCC outer and middle lid stress profiles, and the Alloy-22 outer and middle lid median general corrosion rates, continue to be important as in the case of total dose. Note, however, that a new variable, CSNF dissolution rate uncertainty, becomes the most important variable at 100,000 years for both pinch points (UZ and SZ).

Corresponding results with ^{237}Np EBS mass release as the dependent variable are shown in Figure 5.1-14. Once again, waste package degradation related parameters dominate in the importance ranking. However, once the radionuclide enters the natural system, its sorption characteristics have a significant effect. This is reflected in the importance ranking for the mass release from the SZ (Figure 5.1-15), where neptunium K_d in the alluvium becomes one of the important variables, along with infiltration scenario and the SZ groundwater flux. Collectively, these variables control the amount of neptunium being retained within the natural system, which explains their importance with respect to the release from the SZ.

Next, an examination of the waste package failure distribution (Figure 4.1-9) can provide further insights into the workings of the TSPA-SR model. To this end, a scatter plot of total dose and fraction waste packages failed at 100,000 years is shown in Figure 5.1-16. In particular, there is a focus on those realizations where more than 80 percent of the packages have failed. The two shaded regions in the figure demarcate "high" dose outcomes (dose greater than 100 mrem/yr) from "low" dose outcomes (dose less than 15 mrem/yr). A classification and regression tree analysis of this data, as depicted in Figure 5.1-17 (top), indicates that infiltration scenario and SZ groundwater flux are the two most important parameters in explaining the categorization. The corresponding partition plot is shown in Figure 5.1-17 (bottom). The important point to note here is that even when a large percentage of the waste packages have failed, certain combinations of natural system parameters can yield dose below the 10,000-year regulatory limit even at 100,000 years. This analysis demonstrates the power of classification and regression tree analysis in "mining" the data to provide insights into cause-effect relationships that are not readily apparent from the results presented in Section 4.1, or the regression analyses presented in Section 5.1.1.

Returning to the issue of uncertainty importance as identified from regression analysis, it is useful to ask what parameters are driving system performance in addition to the waste package degradation related parameters already determined as critical uncertainties. For this purpose, a modification of the base case simulation was performed where the two SCC stress profile parameters and the two Alloy-22 median general corrosion rates (i.e., one for the middle lid and one for the outer lid) were fixed at their median values. As a result, probabilistic results for this case, presented in the top panel of Figure 5.1-18, show a considerable reduction in overall spread of total dose as compared to the reference case (Figure 4.1-5). Regression analysis results for this simulation, in terms of uncertainty importance factor as a function of time, are presented in the bottom panel of Figure 5.1-18. As expected, natural system parameters such as infiltration scenario and SZ groundwater flux emerge as key drivers of risk, with secondary contributions from a few of the waste package related parameters which were treated probabilistically. Note the consistency in importance ranking from this simulation and the classification and regression tree analysis discussed in the previous paragraph.

5.1.3 Igneous Scenario, Total Dose

Section 4.2 presents a discussion of the range of dose that the average member of the critical group is likely to receive over 100,000 years. As in the case of the nominal scenario, Figure 4.2-1 shows a broad range in projected dose rates at any given time. Unlike the nominal scenario, almost all of the realizations produced dose in excess of 10^{-5} mrem/yr. Regression analysis was carried out at time slices of 1,000, 10,000, and 100,000 years. Stepwise rank regression models between total dose and a set of statistically significant input variables were built for each case, and the most important variables were identified based on the value of uncertainty importance factor.

Figure 5.1-19 shows a bar chart of these results generated for the 1,000 -year data, indicating that the annual frequency of igneous intrusion is the most important variable, followed by wind speed. Similar importance analyses results for 10,000 years are shown in Figure 5.1-20, where the annual frequency of igneous intrusion is again the most important variable, followed by secondary contributions from time of igneous intrusion and wind speed. At 50,000 years, the

dominant variable in terms of importance is the annual frequency of igneous intrusions, with SZ groundwater flux and infiltration scenario providing only marginal explanatory power for the overall spread in total dose (Figure 5.1-21).

An application of classification tree analysis to the same data sets to determine which variables control extreme outcomes for the igneous scenario is discussed next. As with the nominal scenario analysis, the dose values at any given time slice were first categorized as "high" if the values were in the top 10 percentile, or "low" if the values were in the bottom 10 percentile. The classification tree analysis algorithm then determined which variables were most capable of explaining the separation of these realizations into the appropriate categories.

Figure 5.1-22 (top) shows a decision tree summarizing the classification tree analysis in terms of the two most important variables for the 1,000-year data. In this case, much of the separation into high and low dose values can be explained on the basis of a single variable, the annual frequency of igneous intrusion. The second most important variable, wind speed, provides only marginal additional explanatory power. Figure 5.1-22 (bottom) is a partition plot of the same data, showing where the high and low dose producing clusters actually occur in the bivariate parameter space of the two most important variables.

It should be pointed out that although the igneous scenario calculations were carried out using 5,000 realizations (see section 4.2), the uncertainty importance analyses presented here are restricted to a random subset of 1,000 samples drawn from this population of 5,000 samples because of computational limitations in the regression analysis software. However, an analysis of the rank correlation coefficient between total dose and key uncertain inputs indicated excellent agreement between values derived from 1,000 and 5,000 sample data sets. Such agreement, both in terms of absolute magnitude and relative ordering of the input-output rank correlation coefficients, provide confidence in the regression analysis results based on the subset of 1,000 sample values.

5.1.4 Significance of Uncertainty Importance Analysis Results

To recapitulate, the objective of uncertainty importance analysis is to identify which variables affect the overall spread (variance) in total dose, as well as to identify which variables affect extreme outcomes in probabilistic model results. It is important to note that uncertainty importance, as defined in this section, is a function of: (a) sensitivity of the output to the input variable of interest, and (b) uncertainty of that input variable. In general, variables with high importance ranking satisfy both of these criteria. Conversely, variables which do not show up as important per these metrics are either restricted to a small range in the probabilistic analysis, and/or are variables to which the model outcome does not have a high sensitivity. Also, variables fixed at bounding/conservative values will not be identified as important because of the same reasons.

It should be stressed that uncertainty importance analysis results (as presented here) are conditional to the current TSPA-SR model and all of its underlying assumptions. Therefore, variables identified as important in previous TSPAs may not recur as key uncertainties in the present study, because:

- The conceptual model of a process has changed, and the overall outcome is not sensitive to underlying parameters in the model.
- The data base for a given parameter has been updated with a reduced uncertainty range.
- Variables treated as stochastic in previous TSPA iterations are fixed at conservative/bounding values, thus excluding them from the regression-based uncertainty importance analysis.

As such, uncertainty importance analysis results have to be considered as only part of the answer with respect to the significance of component models and uncertain parameters. A complete evaluation of such issues can be accomplished by combining uncertainty importance analysis with one-off sensitivity analysis, robustness analysis and barrier importance analysis—the results of which are presented in the following sections.

5.2 SENSITIVITY ANALYSES

The uncertainty importance analysis discussed in Section 5.1 shows that in the nominal scenario the most important part of the system is the waste package, whereas in the igneous disruption scenario the most important factor is the probability of having an igneous event. In this context, importance means having a significant impact on the uncertainty in the final calculated dose. Thus, waste package failure (represented by several parameters from the waste package degradation model) contributes strongly to the uncertainty in the nominal-scenario dose (Figure 5.1-4), and igneous-event probability is by far the biggest contributor to the uncertainty in the igneous-scenario dose (Figure 5.1-22). At later times, after most of the waste packages have failed, the natural system becomes more important in explaining the spread in the nominal-scenario dose results (Figure 5.1-11).

To further illustrate the effects of a number of the most important parameters on the TSPA results, analyses were performed in which parameters were fixed at particular values, or alternative assumptions were made. Such analyses demonstrate the effects of individual parameters or assumptions more explicitly than the uncertainty importance analysis can. These analyses are called "one-off" sensitivity analyses because changes are made to one parameter at a time (in some cases, changes are made to more than one parameter). Results of a number of them are presented in this section. In most cases, the sensitivity to individual parameters is examined by setting a parameter to its 5th and 95th percentile values. This choice keeps most of the range that is considered defensible. The 5th and 95th percentiles are used rather than the entire range (i.e., 0th and 100th percentiles) because in some cases there is a very long tail out to extremely unlikely parameter values. The 5th and 95th percentile values are at the level that they are unlikely, but not so unlikely as to be unreasonable. A few exceptions to the 5th and 95th "rule" are to be found in Section 5.2, specifically related to solubilities (Section 5.2.4) and UZ transport parameters (Section 5.2.6).

It should be emphasized here that the following uncertainty and sensitivity analyses are conditional on the current TSPA-SR models and assumptions. Further, some of the assumptions and models are conservative and therefore the uncertainty and sensitivity analyses have to be interpreted with care. That is, by restricting the range of the uncertain probability distributions, conservatism in model components can cause that particular model to show up as unimportant in either the regression analyses of Section 5.1 or in the sensitivity analyses of Sections 5.2 and 5.3. In particular, a specific model or parameter might have a great effect on performance if it were varied, but the assumed range of variation is narrow, so it shows up as unimportant in sensitivity and importance analyses. An example of a parameter with this effect is neptunium solubility (see Section 5.2.4.2). An example of a conceptual model that might have this effect is the dual-porosity UZ transport model, which may result in faster transport than a dual continuum model.

It is rather difficult *a priori* to quantify the degree of conservatism among the different component models. For coupled models, conservatism in one model can mask the importance of another model. Also, until dose consequences are estimated (assuming they represent the most appropriate metric), it is not possible to quantify the relative conservatism in one model or parameter versus another. For example, uncertain K_ds in the SZ are conservatively underestimated and therefore they do not show up as being important. Also, uncertainty analyses based on dose rate as the metric necessarily deal only with those radionuclides that pass through the potential repository system. Those that are retained, for example the majority of the uranium, cannot influence these types of analyses. Thus, a case can be made that the relatively immobile waste form itself (comprised mostly of uranium) is the most important part of the system, rather than the waste package. Also, as the models, assumptions, and uncertainties are refined, other parts of the system, such as the SZ, may become relatively more important. Seepage is another example of where the performance (and/or conservatism) of one submodel masks variations or sensitivity of the system to performance of another submodel. Specifically, because diffusive transport from the waste form is quite high in the TSPA-SR models and because the vast majority of packages are assumed to never encounter dripping conditions, variations in the seepage model, which only affects advective radionuclide transport, will not appear as very important to the potential repository performance. Appendix F gives a list of other conservatisms in the various models.

The sensitivity analyses in this section were performed using probabilistic TSPA simulations with 100 realizations. One hundred realizations were used rather than the 300 used for the analysis of the base case in Sections 4.1, 4.2, and 5.1 because 100 realizations are sufficient to see the relative effects when comparison is made to the 100-realization base-case simulation. (See Section 4.1.4 for a comparison of the 100-realization and 300-realization base cases.)

5.2.1 Unsaturated Zone Flow

5.2.1.1 Sensitivity to Infiltration

Section 5.1 indicates the most important UZ parameter to be the amount of infiltration at the surface, which also affects the amount of seepage that enters emplacement drifts, the thermal hydrologic environment in the drifts, and the radionuclide transport time through the UZ. Infiltration starts to have a significant influence on the nominal-scenario results at about

100,000 years (see Figure 5.1-3) and is very important to the nominal-scenario dose uncertainty at times after 100,000 years (see Figure 5.1-11).

The uncertainty in infiltration results from both the uncertainty in climate (precipitation and temperature) and the uncertainty in infiltration processes at the surface of the mountain. The amount of infiltration uncertainty included in the TSPA model is shown in Table 3.2-2, which gives the repository-averaged infiltration for the three infiltration cases (low, medium, and high) and the three climates (present-day, monsoon, and glacial-transition). The TSPA results for the nominal scenario do not depend on the present-day and monsoon climates because they occur only within the first 2,000 years, and all of the waste packages last at least 10,000 years in the nominal TSPA model. Thus, it is the uncertainty in the glacial-transition infiltration that is important to the nominal-scenario results. Note from Table 3.2-2 that the glacial-transition infiltration is more uncertain on the low side than on the high side. The low infiltration is almost a factor of 10 lower than the medium infiltration, while the high infiltration is only about a factor of 2 higher than the medium infiltration.

Two one-off analyses were performed in which the infiltration was fixed at its low and high values, rather than being sampled from a distribution. The results of these analyses are shown in Figure 5.2-1, which shows the mean dose curve from the nominal-scenario base case, along with the mean dose curves from the two sensitivity cases (infiltration fixed at low and infiltration fixed at high). As expected from the infiltration values in Table 3.2-2, there is much greater effect from the low case than from the high case. The "high" curve in Figure 5.2-1 is quite close to the "base case" curve, but the "low" curve is significantly lower. The larger effect of the "low" case results both from the greater difference in infiltration and because it has a lower probability weighting (see Table 3.2-2), so the low case is sampled less often than the others in the nominal model.

5.2.1.2 Sensitivity to Seepage Flow-Focusing Factor

The seepage abstraction model includes a parameter called the flow-focusing factor that represents the potential for channeling of flow on intermediate scales (see Section 3.2.4). It is of interest to examine the impact that this parameter has on the TSPA results, to determine whether it has enough impact on the results to warrant additional study of flow focusing above drifts. As shown in Table 3.2-3, the flow-focusing factor is represented in the TSPA model as a log-uniform probability distribution, with different limits on the distribution depending on the infiltration case (lower infiltration is associated with higher values of the focusing factor).

To examine the effects of this factor, analyses were performed with the flow-focusing factor fixed at its 5th and 95th percentile values, rather than being sampled from the distributions. It is not clear *a priori* what results to expect from these analyses. As noted in Section 3.2.4.3, flow focusing generally increases the seep flow rate for the locations that have seepage, but at the same time it decreases the fraction of locations that have seepage, with the total amount of seepage higher than it would have been without focusing. So, the net effect on calculated doses depends on whether the seepage fraction (fraction of waste packages with seepage) or the seep flow rate has more impact on radionuclide releases.

The results of the analyses are shown in Figure 5.2-2a, which shows the mean dose curve from the base case along with the mean dose curves from the two sensitivity cases (flow-focusing factor fixed at 5th percentile and 95th percentile values). The figure shows that the flow-focusing factor has no significant effect on calculated doses for about the first 40,000 years. The lack of effect at earlier times occurs because very little water is able to enter waste packages until about 40,000 years (see Figure 4.1-14). After 40,000 years, the higher flow-focusing factor results in higher doses than the lower flow-focusing factor, indicating that the total quantity of water is more important to dose than the number of waste packages affected. The differences between the two sensitivity cases and the base case is not very large, though, indicating that focusing of flow above the emplacement drifts is not particularly important to the TSPA results. The mean dose for the 95th-percentile case becomes approximately equal to the mean base-case dose after about 80,000 years.

Another sensitivity analysis to unravel the effects of the flow focussing factor and the effects of seepage spatial variability is shown in Figure 5.2-2b. In this case the flow focussing factor was set equal to 1.0, implying no flow focussing. Plus, the "local" seepage fraction is set to 1.0, which means that all of the 635 locations in the T-H model have the possibility of seeps if their percolation flux is high enough (greater than about 3.5 mm/yr). This effectively eliminates the seepage fraction variability within each of the 5 seepage environments. Specifically, for the glacial transition climate the result is that seepage environments 10-20 mm/yr, 20-60 mm/yr, and >60 mm/yr all have a "global" seepage fraction of nearly 100 percent (i.e., all packages are in the always drip environment), while seepage environment 3-10 mm/yr has about 70 percent of its packages in the always drip environment, and the 0-3 mm/yr seepage environment (which corresponds only to the low infiltration scenario) has 100 percent of its packages in the no-drip environment. This particular sensitivity case is similar to the base-case seepage model in the TSPA-VA.

As a further test of the effect of seepage, the seepage uncertainty factor was set equal 0.95 and combined with the sensitivity case described in the preceding paragraph. With the local seepage fraction set equal to 1.0, the effect of this is to set the mean "local" seepage flux to its 95th percentile value and the corresponding standard deviation to the 95th percentile value. These two values are used in a beta distribution that is sampled randomly over the 635 T-H locations, so there is still some spatial variability related to flux. This result is shown as the red curve in Figure 5.2-2b.

Because of the high diffusive releases from the waste packages, neither of the above two cases has a very large effect, particularly at early times, prior to 40,000 years, when the drip shield is mostly intact and ^{99}Tc dominates the dose rate. Later, as the drip shields fail and more and more patch openings occur in the waste packages, advective transport from the packages takes on a greater role in combination with the release of solubility-limited ^{237}Np. This is apparent in both sensitivities in Figure 5.2-2b, with the case having the 95th percentile local seepage flux showing a greater effect, as expected. An even larger effect might be observed if the seepage into the packages were not reduced by the ratio of patch opening area to total surface area of the waste package.

5.2.2 Engineered Barrier System Environments

Because most parameters related to the EBS environment, such as pH, RH, and temperature, are modeled deterministically rather than stochastically, no individual parameters relating to environments have been identified as very enlightening for one-off sensitivity analyses comparable to the one-off analyses in other subsections of Section 5.2, i.e., setting individual stochastic parameters to their 5th and 95th percentiles within the various submodels. However, the influence of various combinations of EBS environmental parameters is examined in Sections 5.3.4.2 and 5.3.5. Furthermore, the effect of the alternative repository design with backfill, discussed in Section 4.6, is mainly a function of the EBS environment, in particular, the temperature and RH on the waste package surface, at the cladding surface, and in the invert. Section 4.6 also contains an analysis of an alternate low thermal design whose main impact is to change the temperature and RH of the EBS environment. Little effect was found, partly because the waste package degradation model itself is insensitive to environmental parameters, such as pH and temperature, as described in the next section.

5.2.3 Waste Package and Drip Shield Degradation

This section reports sensitivity analyses of the nominal repository performance to a number of major parameters of waste package degradation processes. The sensitivity analysis results are analyzed in terms of the mean dose rate for the average member of the critical group (see Section 4.1 for details) and the mean waste package failure profile.

As for the base-case analysis (see Section 3.4), the WAPDEG model is used for the sensitivity analyses. The conceptual model and logic flow of the base case WAPDEG model (CRWMS M&O 1998 [145618]) are described in Section 3.4. The following simulation parameters used in the sensitivity analyses are the same as those for the base-case analysis (see Section 3.4).

- Temperature, RH, and contacting solution pH histories in the presence or absence of backfill
- 400 waste package and drip shield pairs
- 20 mm thick waste package outer barrier (Alloy-22)
- 15 mm thick drip shield (titanium)
- 1000 patches per waste package
- 500 patches per drip shield.

The sensitivity analysis cases analyzed in this section are:

- Sensitivity to the residual stress state uncertainty at closure-lid welds
- Sensitivity to the SCC model parameters for closure-lid welds

- Sensitivity to the Alloy-22 mean general corrosion rate
- Sensitivity to the uncertainty and variability partitioning ratio for Alloy-22 general corrosion rate.

Because temperature and RH do not significantly affect waste package and drip shield degradation, except for the RH threshold for corrosion initiation (see Section 3.4), a representative set of temperature and RH histories were used in these sensitivity analyses. Different waste types (i.e., CSNF waste packages, HLW, etc.) could give rise to differing thermal hydrologic conditions on the drip shields and waste packages. However, as stated above, drip shield and waste package degradation are not sensitive to RH and temperature conditions; therefore, no sensitivity analysis was conducted for different waste-type waste packages. In addition, the presence of drips is required for localized corrosion of the drip shield and the waste package outer barrier. However, the initiation threshold of the materials is much higher than the conditions expected in the potential repository (i.e., the corrosion potentials of the materials in the expected repository conditions are less than the critical corrosion potential of the materials). Hence, no localized corrosion is initiated in the WAPDEG analyses (see Section 3.4). Other corrosion models (general corrosion and SCC) are not dependent on dripping conditions (i.e., drip vs. no-drip); therefore, no sensitivity analysis was conducted for the effect of differing dripping conditions on waste package degradation.[1] As in the base-case analysis, potential performance credit for the stainless steel inner layer of the waste package was not considered in the sensitivity analyses. Details of the approaches and assumptions associated with the WAPDEG analyses are described in the supporting report, WAPDEG Analysis of Waste Package and Drip Shield Degradation (CRWMS M&O 2000 [146427]).

5.2.3.1 Sensitivity to Residual Stress State Uncertainty at Closure-Lid Welds

As discussed for the base-case analysis results, initial waste package failures are by SCC at the closure lid welds. Among the SCC model parameters considered in the analysis, the uncertainty ranges of the residual stress (hoop stress) and corresponding stress intensity factor are considered the most important. Sensitivity analyses were conducted to evaluate the effect of the residual hoop stress uncertainty (and corresponding stress intensity factor uncertainty) on the potential repository performance. The mean waste package failure profiles are also included in the analyses. For the continuity of the analyses of the results, the base case SCC model and the WAPDEG implementation are summarized in the following paragraph.

Because complete stress mitigation may not be possible for the closure-lid welds, the welds may be subject to SCC. Once a SCC crack initiates, it penetrates the closure-lid thickness in a very short time (see Section 3.4). Thus, stress mitigation in the closure-lid welds is a key design element to avoid premature failures of waste packages by SCC. In the slip dissolution model, the following two conditions should be met before initiating a SCC crack propagation in a

[1] This lack of dependence on dripping is probably a conservatism assumption in the case of SCC, since aggressive dripping water chemistry is unlikely to be present at all times on all packages because of two reasons: (1) the presence of the drip shield and (2) only a small fraction of the packages are in a drift seepage environment. On the other hand, dust is presumed to deposit ubiquitously on the package surfaces and this dust is assumed to be composed of NaNO3, which is the most aggressive chemical environment for inducing corrosion.

patch: (1) the stress intensity factor (K_I) should be positive, and (2) the stress state must be greater than or equal to the threshold stress. The presence of a compressive stress zone (or layer) in the outer surface delays the initiation of SCC. However, the compressive zone is slowly removed by general corrosion. The delay time depends on the compressive zone thickness and the general corrosion rate sampled for the patch. Details of the residual stress and stress intensity factor abstraction are discussed in the supporting report, *Stress Corrosion Cracking of the Drip Shield, the Waste Package Outer Barrier and the Stainless Steel Structural Material* (CRWMS M&O 2000 [148375], Section 6.3).

In addition, all preexisting manufacturing defects in a patch, including embedded defects in the outer quarter of the thickness, are assumed to be surface breaking and oriented in the radial direction. This is a conservative assumption because many of the defects are likely to orient horizontally (i.e., in parallel to the weld line). Those cracks likely respond to the radial stress and, if SCC initiates, grow along the circumference of the closure-lid welds. The tip of all the manufacturing defects are assumed to advance at the general corrosion rate sampled for the patch. This is based on the modeling assumption that the same exposure condition that a patch experiences during a given time step is also applicable to the interior of defects in the patch. Growth of the preexisting defects at the general corrosion rate of the patch is a conservative assumption. Therefore, patches with preexisting defects would be subject to SCC earlier than other patches without defects. Details of the model implementation and assumptions are discussed in the supporting report, *WAPDEG Analysis of Waste Package and Drip Shield Degradation* (CRWMS M&O 2000 [146427], Sections 5, 6).

Figure 5.2-3 illustrates the mean predicted dose rate when the residual hoop stress state at the closure-lid welds is fixed at the 95th and 5th percentile values of the uncertainty distribution described in Section 3.4. The results are compared with the base-case results. As expected, the mean dose is significantly affected when the residual stress-state changes, which affects the SCC failure of waste packages. The effect on waste package failure is shown in Figure 5.2-4. With the hoop residual stress fixed at the 5th percentile value, there is no SCC failure of waste package, (i.e., all the waste packages fail by general corrosion). This is consistent with the base-case results that SCC is the dominant waste package degradation process and an important process for the potential repository performance. In addition, the variance in the dose decreases significantly when this parameter is fixed at a discrete value.

As discussed in Section 3.4, the estimated long lifetime of the waste packages in the base case analysis is attributed mostly to the following two factors: (1) the stress mitigation to substantial depths in the dual closure-lid welds, which delays the onset of SCC crack propagation until the compressive zone layer is corroded; and (2) the very low general-corrosion rate applied to the closure-lid welds to corrode the compressive stress zones, which renders a long delay time before initiating SCC crack propagation. Substantial uncertainties are associated with the current SCC analyses, especially the stress mitigation on the closure-lid welds. The current assumption for the radial orientation of all the manufacturing defects in the closure-lid welds is conservative, because most embedded defects are likely to be oriented such a way that would not lead to radial cracks.

5.2.3.2 Sensitivity to Alternative Uncertainty Ranges of Major SCC Model Parameters for Closure-Lid Welds

As discussed in the previous section (Section 5.2.3.1), the major parameters in the SCC analysis of the waste package closure-lid welds are: (1) stress state and stress intensity factor, (2) threshold stress for SCC crack propagation, and (3) orientation and size of manufacturing defects. All three parameters are uncertain. Sensitivity analyses were conducted to evaluate the effects of those uncertain SCC model parameters on the potential repository performance. Four cases were evaluated in the current sensitivity analyses by changing one or more of the three parameters in each case. The four cases, along with the base case, are summarized in Table 5.2-1. For each case the parameter (or parameters) changed is indicated in bold.

Table 5.2-1 Summary of the Four Cases Evaluated in the Sensitivity Analyses for Alternative Uncertainty Ranges of the SCC Model Parameters for the Waste Package Closure-Lid Welds

Case	Residual Hoop Stress State Uncertainty	Threshold Stress Uncertainty	Manufacturing Defect Orientation
Base Case	- ± 30 percent of yield strength. - Symmetrical triangular distribution with the mode equal to 0	- 20 to 30 percent of yield strength. - Uniform distribution between 20 and 30 percent	- 100 percent defects with radial orientation (radial SCC crack propagation)
Case 1	- ± 30 percent of yield strength. - Symmetrical triangular distribution with the mode equal to 0	- 10 to 40 percent of yield strength. - Uniform distribution between 10 and 40 percent	- 100 percent defects with radial orientation (radial SCC crack propagation)
Case 2	- ± 10 percent of yield strength. - Symmetrical triangular distribution with the mode equal to 0	- 20 to 30 percent of yield strength. - Uniform distribution between 20 and 30 percent	- 100 percent defects with radial orientation (radial SCC crack propagation)
Case 3	- ± 10 percent of yield strength. - Symmetrical triangular distribution with the mode equal to 0	- 10 to 40 percent of yield strength. - Uniform distribution between 10 and 40 percent	- 100 percent defects with radial orientation (radial SCC crack propagation)
Case 4	- ± 10 percent of yield strength. - Symmetrical triangular distribution with the mode equal to 0	- 10 to 40 percent of yield strength. - Uniform distribution between 10 and 40 percent	- 1 percent defects with radial orientation (radial SCC crack propagation) - 99 percent defects with horizontal orientation (no radial SCC crack propagation)

The sensitivity analysis results for the mean dose and mean waste package failure profile are shown in Figures 5.2-5 and 5.2-6, respectively. Comparison of the base case with Case 1 and Case 2 with Case 3 shows that the threshold stress has insignificant effects on the mean dose rate and mean waste package failure. Comparison of the base case with Case 2 demonstrates that the uncertainty range of the residual hoop stress state (and corresponding stress intensity factor) has significant effects on the mean dose and mean waste package failure profile. Reduction in the

residual hoop stress uncertainty range from ±30 percent to ±10 percent of the yield strength delays the first failure time of the mean waste package failure profile from about 12,000 years to about 20,000 years and shifts the failure profile curve to a substantially later time period. The mean dose rate curves are shifted accordingly (Figure 5.2-5).

Reduction in the number of manufacturing defects having a radial orientation by a factor of 100 (Case 4) significantly decreases the number of waste packages that fail by SCC (Figure 5.2-6) and delays the mean dose rate substantially (Figure 5.2-5). The initial failure time of the mean waste-package failure profile is delayed to about 32,000 years, and the mean dose rate is close to zero until about 40,000 years. For this case, most waste packages, except those that fail initially, fail by general corrosion.

These sensitivity analyses demonstrate that the uncertainty range of the residual hoop stress (and corresponding stress intensity factor) and the number (and size) of manufacturing defects having radial orientation are the two most important parameters that affect the SCC failure of waste packages and thus the potential repository performance.

5.2.3.3 Sensitivity to Uncertainty and Variability Partitioning Ratio for Alloy-22 General Corrosion Rate

This section and following section (Section 5.2.3.4) analyze the sensitivity of the potential repository (and waste package) performance to the parameters that are relevant to representing the uncertainty and variability of Alloy-22 general corrosion rate. As discussed in Section 3.4, the WAPDEG analysis yields an explicit representation of the uncertainty and variability in waste package (and drip shield) degradation. For the corrosion models and parameters for which data and analyses are available to quantify their uncertainty and variability, they were represented explicitly in the WAPDEG analysis. For other corrosion models and parameters for which uncertainty and variability are not quantifiable, the GVP technique was used to separate the variances due to uncertainty and variability from the total variance (see Section 3.4). In this technique, uncertainty is defined as the uncertainty in the mean value, and variability as the variance about that mean. In the analysis the fraction of the total variance to separate the uncertainty and variability variances was treated as an uncertain parameter and sampled randomly for each realization. The separation results in two distributions, one for the uncertainty and the other for the variability. Then the median of the variability distribution is sampled from the uncertainty variance, and the variability distribution is reconstructed around the sampled median.

In the WAPDEG analysis, variability in the waste package corrosion processes is represented by sampling the values of the individual corrosion model parameters from their variability distributions, and by populating the sampled values over the waste packages (referred to as package-to-package variability) and, if considered, the patches in a single waste package (referred to as patch-to-patch variability). Detailed discussions of the uncertainty and variability representation in the WAPDEG analysis are given in the supporting report, *WAPDEG Analysis of Waste Package and Drip Shield Degradation* (CRWMS M&O 2000 [146427], Section 6).

The general corrosion rate distribution for Alloy-22 (waste package outer barrier) that was developed from the measurement data from the Project's Long-Term Corrosion Testing Facility

is considered a mix of uncertainty and variability of the general corrosion rate. However, quantification of uncertainty and variability in the corrosion rate measurements is limited because the corrosion rates are extremely low and considered to be within the measurement noise. Because of this, it is difficult to quantify what the fraction of the total variance in the parent distribution represents the uncertainty and what fraction represents the variability. As discussed above, in the WAPDEG analysis, the fraction for the separation of the uncertainty and variability from the parent distribution is treated as an uncertain parameter.

Sensitivity analyses were conducted to evaluate the effect of the uncertainty-variability partitioning ratio by fixing the ratio at the 95th and 5th percentile values (i.e., using a 95 percent to 5 percent and a 5 percent to 95 percent uncertainty-variability partition, respectively). The first case is for the case that 95 percent of the total variance in the Alloy-22 general corrosion rate is due to uncertainty and 5 percent due to variability, and the second case is for the case that 5 percent of the total variance is due to uncertainty and 95 percent due to variability. For those two cases the median general corrosion rate for the variability distribution is sampled as an uncertain parameter as described above.

The results are shown in Figure 5.2-7 for the predicted mean dose rate profile and in Figure 5.2-8 for the mean waste package failure profile. As shown in the figures, there is no significant effect on the mean dose rate.

5.2.3.4 Sensitivity to Alloy-22 Median General Corrosion Rate

As discussed in the previous section, after separation of the variances due to uncertainty and variability from the total variance, the median of the variability distribution is sampled from the uncertainty variance, and the variability distribution is reconstructed around the sampled median. Another set of sensitivity analyses were conducted to evaluate the effect of the (sampled) median general corrosion rate of Alloy-22 on the mean dose rate and mean waste package failure profiles. The analyses were conducted by fixing the median general corrosion rate at the 95th and 5th percentile values of the uncertainty variance. In the analyses, the partitioning ratio for the uncertainty and variability separation was treated as an uncertain parameter and sampled for each realization.

The analysis results for the predicted mean dose rate and mean waste package failure profiles are shown in Figures 5.2-9 and 5.2-10, respectively. As shown in the figures, this parameter significantly affects the rate of degradation of waste packages and variability in waste package failures, and thus the predicted mean dose rate profile. Comparison of the current analysis results with the results from the previous section (sensitivity to the uncertainty-variability partitioning ratio) demonstrates that the median general corrosion rate is a more significant parameter to the potential repository performance than the partitioning ratio.

5.2.4 Waste Form Degradation and Mobilization

5.2.4.1 Sensitivity to Waste Type

The degradation rates of the CSNF waste matrix and HLW glass differ by only a factor of 2 using the conditions calculated for inside the waste package (Figures 3.5-15 and 3.5-19). Although the degradation rate of the DSNF is constant and is much greater, the mass of waste is much less. Hence, the CSNF release rate and the combined release rate of HLW glass and

DSNF waste matrix are about the same in the first 100,000 years, such that there is no sensitivity to the type of waste form or waste package on a per package basis. However, the total inventories of CSNF and co-disposed HLW and DSNF differ greatly, leading to a contribution to dose that is substantially different (Figure 5.2-11).

Furthermore, after 100,000 years, greater differences in release rates from the waste packages emerge. The inventory in the co-disposal packages is depleted, such that its release rate decreases. Additional perforation of cladding from localized cladding corrosion makes more radionuclides available from CSNF, so its release rate does not decrease, and parameters related to cladding become important (see Section 5.3.4.1).

5.2.4.2 Sensitivity to Secondary Mineral Phases

In this section we show some sensitivities outside the range of the base-case parameter distributions—in part, because neptunium solubility in the base-case model had variability but no uncertainty. It was only a function of environmental parameters, such as pH, which showed a narrow range of spatial variability across the potential repository.

The solubility limits presented in Section 3.5.5 were developed with several conservative features: 1) pure mineral phases are selected to control solubility, while in reality a radionuclide could be controlled by solid solution or co-precipitation; 2) when there are several possible solubility controlling minerals, the most soluble one is chosen, unless experiments say otherwise; and 3) sorption of radionuclides is neglected. The solubility limit models with these conservative features could overestimate the dose rate. To assess how much the calculated performance might improve by utilizing more realistic dissolved concentration models, a sensitivity calculation on element solubility is shown in this section.

The sensitivity analysis is based on high drip rate tests at Argonne National Laboratory (CRWMS M&O 2000 [153105], which are a set of experiments simulating spent fuel dissolution under potential repository conditions. As discussed in Section 3.5.5, the solubility limits based on the Argonne experiments (as interpreted for this sensitivity study) are much lower than the base-case solubilities for two key dose contributors, Np and Th (CRWMS M&O 2000 [153105]. The Argonne-based solubility for Np is more than 3 orders of magnitude lower than the base-case solubility (in CSNF packages); the Argonne-based solubility for Th is more than 7 orders of magnitude lower; the Argonne-based solubility for Am is about 2 orders of magnitude lower (in CSNF packages); the Argonne-based solubility for U is about the same (in CSNF packages); and the Argonne-based solubility for Pu is about the same.

Figure 5.2-12 shows the results of using the secondary-phase-controlled solubility limits. The reduced solubilities have their greatest impact on late time doses when solubility-limited radionuclides, such as Np, begin to control the total dose rate (see Figure 4.1-5). Figure 5.2-12a indicates an approximately one order-of-magnitude reduction in the peak of the mean total dose rate history (at 100,000 years). Figure 5.2-12b indicates that most of the reduction in the 100,000-year total dose rate compared to the base case (see Figures 4.1-5, 4.1-6, and 4.1-7) is due the reduction in the ^{237}Np dose rate. For this secondary phase analysis, the major dose rate contributors in 100,000 years are ^{99}Tc, ^{129}I, ^{239}Pu, ^{227}Ac, and ^{231}Pa,and most of the contribution to the ^{239}Pu dose is from the irreversibly sorbed fraction of ^{239}Pu.

5.2.5 Engineered Barrier System Transport

5.2.5.1 Sensitivity to Invert Diffusion

For nominal performance, the dose rate at early times is sensitive to the form of the diffusion model (and therefore the diffusion rate) chosen for diffusion of radionuclides in the invert. Changes among diffusion models result in differences of several thousand years. At times greater than 30,000 years, the differences are small, and the peak dose rate at 100,000 years is relatively insensitive to the diffusion model (i.e., diffusion rate). Those conclusions are illustrated in Figure 5.2-13. The differences in the three cases shown in the figure are described in the following paragraphs.

For the base case, the mean value of the diffusion coefficient as a function of liquid saturation and porosity is given by:

$$D_{mean} = D_{fw} s^{1.849} \phi^{1.3} \qquad \text{(Eq. 5.2-1)}$$

where D is the diffusivity (cm^2/s), D_{fw} is the free-water diffusion coefficient (cm^2/s), s is the liquid saturation, and ϕ is the porosity. The value for D_{fw} ($= 2.299 \times 10^{-5}$ cm^2/s at 25°C) is a bounding value for all radionuclides of interest for the TSPA. The exponent on the saturation, s, is based on a statistical analysis of data from Conca and Wright (CRWMS M&O 2000 [150418]; CRWMS M&O 2000 [150792]). This value is slightly less than 2, which is the typical value for Archie's law in a fine sand. The exponent on the porosity is 1.3, the typical value for Archie's law. In fact, the statistical fit to moisture content justifies using an exponent of 1.849 for the porosity; however, it has conservatively been left at the typical value for Archie's law of 1.3.

For the high-diffusion case, the mean response of the diffusion coefficient is given by:

$$D = D_{fw} \phi^{1.0} s^{1.0} \qquad \text{(Eq. 5.2-2)}$$

For the low-diffusion case, the diffusion coefficient is constant at $D = 10^{-11}$ cm^2/s.

5.2.6 Unsaturated Zone Transport

5.2.6.1 Sensitivity to Matrix Diffusion

Figure 5.2-14 shows the mean dose rate from the base case compared to a case with no matrix diffusion in the UZ and also compared to a case where the UZ anion and cation matrix diffusion coefficients were set at 100 times the matrix diffusion coefficients in the base case. It should be noted that these parameter values are outside the range of base-case probability distributions, in contradistinction to most of the other analyses in Section 5.2.

The results show that UZ matrix diffusion has a moderate effect on the dose history, especially between 20,000 and 30,000 years. This "bump" in the dose curve for the no matrix diffusion case is caused by ^{243}Am, which has a half life of ~7,000 years. With matrix diffusion, the travel time of ^{243}Am through the UZ is long enough for ^{243}Am to decay, thereby attenuating the dose. Without matrix diffusion, the ^{243}Am can transport through the UZ without significant retardation

or decay, causing the "bump" in the dose curve. The case with 100 times the base case matrix diffusion also implies that the base case probability distributions for matrix diffusion coefficients maximize the impact of matrix diffusion in the UZ, i.e., the best estimate ranges for matrix diffusion, based on available data, imply that matrix diffusion is an important phenomenon for transport in the UZ.

5.2.7 Saturated Zone Flow and Transport

The SZ flow and transport component of TSPA-SR is modeled independently of the TSPA calculations (Section 3.8). The modeling is incorporated in the TSPA calculations through a library of breakthrough curves. This structure would require a new library for every sensitivity case, and is therefore incompatible with one-off sensitivity analyses. Analyses examining a degraded SZ barrier, for which new breakthrough-curve libraries were created, are described in Section 5.3.7.

5.2.8 Biosphere

Two sensitivity analyses have been conducted to examine the range in nominal-scenario dose results due to the biosphere component of TSPA-SR. The sensitivity analyses address how the TSPA dose calculation is influenced by uncertainties in the BDCFs and uncertainties in the estimate of the water volume used by the proposed farming community. An analysis of uncertainties and sensitivities internal to the biosphere model is presented in Section 3.9.2.5.

5.2.8.1 Sensitivity to Biosphere Dose Conversion Factors

This sensitivity study addresses how the dose calculation is affected by the spread in the distributions used to define the BDCFs. BDCFs are the radionuclide-dependent factors used to convert radionuclide concentrations in groundwater into the annual dose incurred by a receptor within the critical group living 20 km from Yucca Mountain. Sensitivity to volcanic BDCFs are not considered here.

Figure 5.2-15 shows the mean value of the base-case nominal doses compared with curves labeled as 5th and 95th. These curves depict the mean-value results of the probabilistic TSPA base case (100 realizations) calculated with the values of the BDCFs held constant. In one case, the BDCFs for all the radionuclides are fixed at the 5th percentile value of their distributions and, for the other curve, at the 95th percentile value of their distributions. For any given radionuclide, the dose is proportional to the BDCF and for all the radionuclides the sum of the doses is proportional to a weighted sum of the BDCFs (weighted by radionuclide release rate). The curves have the same shape because the radionuclide release rates are the same in all three cases.

As shown in the figure, the BDCFs have little effect on the dose calculation. The 5th percentile curve reduces the mean dose by about half; the 95th percentile BDCFs increase the mean dose by approximately a quarter. As discussed in Section 3.9, most of the biosphere is prescribed by regulation. Using the average member of the critical group implies that the receptor has the average food consumption rates; using constant values for the consumption rates greatly reduces the spread in the BDCF distributions; little spread in the BDCF distributions implies little impact on the variance in the calculated doses. Because of the prescribed elements of the biosphere, the major sources of uncertainty in the BDCFs involve soil and dust pathways. The most important

pathway in the nominal biosphere model is the drinking water pathway, and the drinking water rate is set to a constant.

5.2.8.2 Sensitivity to Water-Usage Volume

This sensitivity study addresses how the dose calculation is affected by the spread in the distributions used to define the water-usage volume. The water-usage volume is the estimated amount of water used in one year by a hypothetical farming community living 20 km from Yucca Mountain. The water-usage volume is the calculational basis for determining the radionuclide concentration in groundwater; i.e., it is the amount of water that contains all radionuclides released from a potential repository at Yucca Mountain and that cross the 20 km distance to the hypothetical farming community each year.

Figure 5.2-16 shows the mean value of the base-case doses compared with curves labeled as 5th and 95th. The 5th and 95th curves depict the mean-value results of the probabilistic TSPA base case (100 realizations) calculated with the values of the water-usage volume held constant; in one case, the water-usage volume is fixed at the 5th percentile value of the distribution and, for the other curve, at the 95th percentile value of the distribution. For any given radionuclide, the dose is inversely proportional to the water-usage volume; therefore, the curves have the same shape.

As shown in the figure, the water-usage volume has little effect on the dose calculation. The 5th percentile of the water-usage volume is 1.404×10^6 m^3/yr; the 95th percentile is 3.589×10^6 m^3/yr; the mean is 2.394×10^6 m^3/yr. The 5th percentile curve reduces the mean dose by about half; the 95th percentile BDCFs increase the mean dose by approximately half. The implication is that the dose calculation is relatively insensitive to the range of water-usage volume assumed in TSPA-SR.

5.2.9 Disruptive Events

As Section 3.10 describes, igneous disruption is the only disruptive scenario that has been identified as requiring explicit analysis in the TSPA. Section 4.2 describes the TSPA-SR results for the igneous disruption scenario, and Section 5.1.2 describes uncertainty importance analyses associated with the TSPA-SR results. This section presents the results of additional analyses that examine specific cases designed to test the robustness of the TSPA-SR results to alternative modeling assumptions. Results are presented in the context of one-off sensitivity analyses, in which selected parameter values are fixed and sampled values are used for all other parameters, or as comparisons of performance using alternative conceptual models. For analyses that compare results using fixed values for selected parameters, values are chosen representing the 5th and 95th percentiles of the distributions used in the TSPA-SR. Analyses of alternative assumptions about parameter values that only affect the eruptive release (e.g., changes in wind speed) have been done using only the eruptive pathway portion of the GoldSim model, to allow a clearer display of the changes in performance. All analyses in which the eruptive probability-weighted mean annual dose rate from the TSPA-SR are based on 100 realizations of 100,000 year performance using the same sampled values for all other parameters. All analyses that include calculation of dose rates from igneous intrusion groundwater release scenario are based on 1,000 realizations of 20,000-year performance, using the same set of sampled

parameter values. As described in Section 4.2.3, the choice of 1000 realizations of 20,000-year performance provides adequate statistical coverage of during the period of greatest interest within reasonable computational constraints. The alternative modeling assumptions represented by these analyses are not considered to be realistic or appropriate for comparison to the proposed regulatory standards, and the probability-weighted mean 50,000-year dose rate described in Section 4.2.2 should be interpreted as the best estimate of future performance for the igneous disruption scenario class. Where shown, the 5th and 95th percentile dose rates represent extreme favorable and unfavorable deviations from expected performance that are equally likely (or unlikely) to occur.

5.2.9.1 Sensitivity to Alternative Models for the Probability of Igneous Activity

Figure 5.2-17 shows a comparison of the probability-weighted 20,000-year mean annual igneous intrusion dose rates, as described in Section 4.2.3, with the same dose rate calculated using a fixed annual probability of igneous intrusion equal to 10^{-7}, rather than a value sampled from a distribution with a mean of 1.6×10^{-8}. The conditional probability that an eruptive conduit intersects waste if an intrusion occurs within the repository footprint is set to 1, yielding an annual probability of 10^{-7} for both intrusive and eruptive events. This higher probability falls within the range of values sampled in the TSPA-SR (near the upper limit, at approximately the 99.5 percentile of the distribution sampled for igneous intrusion probability), and is the value used by the U.S. Nuclear Regulatory Commission (NRC) in analyses reported in the "Issue Resolution Status Report (Key Technical Issue: Igneous Activity, Revision 2)" (Reamer 1999 [119693], p. 10). The DOE recognizes that the value of 10^{-7} provides a useful upper bound to values that should be reasonably considered in the site recommendation. Because the event probability is used directly in the weighting of probabilistic doses, changes in event probability should result in a linear scaling of the mean annual dose. Figure 5.2-17 confirms this observation. The mean dose calculated using the fixed higher probability is about 17 times higher during the first 2,000 years than the mean dose calculated using the full distribution of probabilities for igneous intrusion and a conditional eruption probability of 0.36, as described in Section 3.10.1. At later times, the scaling between the curves varies slightly with time, reflecting both the sampling of the time of intrusion and the influence of individual realizations with varying probabilities on the location of the mean at different times. The highest peak mean dose is increased by approximately a factor of 10, to about 0.9 mrem/yr, and occurs at the end of the simulation, 20,000 years after closure.

5.2.9.2 Sensitivity to Assumption that the Wind Direction is Fixed toward the Location of the Critical Group

As described in Section 4.2, the TSPA-SR analysis of eruptive releases from igneous disruption includes an assumption that the wind direction is fixed in all realizations toward the critical group. This assumption is unrealistic given the wind data for the area, but it provides a conservative bound to uncertainty regarding wind direction. As discussed in Section 3.10.4, this assumption also compensates for uncertainty regarding the possibility that contaminated ash deposited by winds blowing in directions other than south might later be redistributed by wind or water to the location of the reasonably maximally exposed individual and could therefore contribute to the total probability-weighted dose from volcanic eruption.

Figure 5.2-18 shows a comparison of the probability-weighted mean annual igneous dose rate calculated using a fixed wind direction toward the critical group with the same dose rate calculated with the wind direction sampled from a wind rose based on available information, as described in Section 3.10. When the wind direction is sampled, dose is reduced by a factor of about 5 during the first approximately 2,000 years of the simulations, during the period when the annual dose rate is dominated by the eruptive release. This reduced dose rate is not presented here as a preferred alternative to the dose rate calculated assuming a fixed wind direction. The fixed-wind-direction analysis remains the preferred performance measure for the TSPA-SR because it conservatively bounds uncertainty related to future wind direction and compensates for uncertainty regarding surficial redistribution of contaminated ash and soil. Results of the comparison provide insight into the limits to potential reductions in the calculated dose rate that might be achieved by the development of realistic models for soil and ash redistribution. The extent to which such models might result in reduced annual dose rates during the first several thousand years after closure is unknown, but it will be no greater than the factor of approximately 5 shown here.

5.2.9.3 Sensitivity to Wind Speed

Figure 5.2-19 shows a comparison of the probability-weighted mean annual eruptive dose rate, as described in Section 4.2, with the same dose rate calculated using the 5th and 95th percentile value for the wind speed. The annual eruptive dose rate increases by a factor of 2 for the 95th percentile wind speed. The 95th percentile wind speed corresponds to a wind speed of 13.9 meters/second, and exceeds the value of 12 meters/second suggested by the NRC in the "Igneous Activity Issue Resolution Status Report" (Reamer 1999 [119693], p. 88) as a "reasonably-conservative basis to model aerial tephra dispersal." Dose rates increase by roughly a factor of 2 when wind speed is increased to the 95th percentile, and decrease by more than an order of magnitude at the 5th percentile.

5.2.9.4 Sensitivity to the Removal of Contaminated Soil by Erosion

As described in Section 3.10.3.2, the TSPA-SR model for the behavior of volcanic ash layers in the biosphere includes a characterization of soil removal processes. Soil is assumed to be eroded at a rate of 0.06 to 0.08 cm/yr, which corresponds to a mean erosion time for a 15 cm soil layer of 250 to 188 years. As discussed in Section 3.10, these values are appropriate for agricultural land that is consistent with the high air mass loading values assumed in the construction of the volcanic biosphere dose conversion factors. The analysis reported here uses an erosion rate that is set to 0.015 cm/yr, which corresponds to a mean erosion time for a 15 cm soil layer of 1,000 years. This assumption is unrealistic, but provides a conservative upper bound to doses that would result from alternative assumptions about soil removal rates. Note, for example, that the soil removal rates used by the NRC in analyses reported in their "Igneous Activity Issue Resolution Status Report" correspond to mean ash-layer erosion times ranging from 100 to 1,000 years (Reamer 1999 [119693], p. 14), with a preferred value of 1,000 years (Reamer 1999 [119693], p. 11).

Figure 5.2-20 shows that a 1,000-year mean soil erosion time results in probability-weighted annual eruptive doses that are a factor of 5 higher than the base case at 10,000 years. The probability-weighted annual eruptive doses for both cases reach a maximum level in the first

1,000 years and then decrease steadily. Eruptive doses for this assumption remain well below levels of concern, reaching a peak of about 0.01 mrem/yr.

5.2.9.5 Sensitivity to the Volume of Material Erupted

As described in Section 3.10, the ASHPLUME version 1.4LV code (CRWMS M&O 1999 [150744]) used in the TSPA-SR to simulate effects of volcanic eruptions uses the total volume of erupted material as the independent variable that defines the energy of the eruption. For example, the duration of the eruption and the height of the erupted column are derived parameters that are calculated within each realization based on the sampled value for erupted volume.

Figure 5.2-21 shows a comparison of the probability-weighted mean annual eruptive dose rate, as described in Section 4.2, with the same dose rate calculated using the 5th and 95th percentile value for the volume of material erupted. These percentiles correspond to erupted volumes of 0.0026 km^3 and 0.336 km^3, respectively, and correspond approximately to calculated column heights of 2 and 5 km above the ground surface. The total annual igneous dose rate is shown to be insensitive to range of values selected for erupted volume in this analysis, and is therefore insensitive to uncertainty regarding the energy of the eruptive event and the height of the eruptive column, both of which are derived from volume in ASHPLUME version 1.4LV (CRWMS M&O 1999 [150744]).

5.2.9.6 Sensitivity to the Number of Waste Packages Damaged by Volcanic Eruption

Figure 5.2-22 shows a comparison of the probability-weighted mean annual eruptive dose rate, as described in Section 4.2, with the same dose rate calculated using the 5th and 95th percentile values from the TSPA-SR distributions for the number of waste packages damaged during a volcanic eruption. These percentiles correspond to 6 and 16 waste packages, respectively. This comparison provides insight into the sensitivity of overall performance to uncertainty about diameter of eruptive conduits, their location, and the number of eruptive conduits within the potential repository associated with each igneous event. Results of this comparison show that performance is moderately sensitive to the total number of packages that are damaged during the eruptive event, and that peak dose may be increased by a factor of 1.5. However, overall peak mean dose from the eruptive event remains below 0.01 mrem/yr.

5.2.9.7 Sensitivity to the Number of Waste Packages Damaged by Intrusion

Figure 5.2-23 shows a comparison of the probability-weighted 20,000-year mean annual total igneous dose rate, as described in Section 4.2.3, with the same dose rate calculated using the 5th and 95th percentile values from the TSPA-SR distributions for the number of waste packages damaged by igneous intrusion. As described in Section 3.10.2.3.2, damage to three packages on either side of the intrusive dike and one package intersected by the dike is assumed to be sufficient that the packages provide no further protection to the waste package. This region is referred to as "Zone 1." In the remaining portion of all drifts intersected by a dike, damage is limited to failure of lid welds due to high temperature and pressure. This region is referred to as "Zone 2." As described in the following section, damage in Zone 2 is limited to the formation of an aperture of uncertain (and sampled) cross-sectional area in each damaged package. The 5th

and 95th percentile values for the number of packages damaged in Zone 1 are 108 and 219, respectively. The same numbers for Zones 1 and 2 combined are 132 and 6,516, respectively. For the purposes of this comparison, sampled values from the base case are used for the cross-sectional area of the aperture in Zone 2 packages.

This comparison provides insight into the sensitivity of overall performance to uncertainty about the potential repository's response to igneous intrusion. Results of this comparison show that performance is only moderately sensitive to the total number of packages that are damaged by intrusion, with peak dose increasing by less than a factor of 2. Overall peak mean dose from igneous activity rises only slightly above 0.1 mrem/yr for the 95th percentile case.

5.2.9.8 Sensitivity to the Magnitude of Damage to Packages in Zone 2

Figure 5.2-24 shows the probability-weighted 20,000-year mean annual total igneous dose rate, as described in Section 4.2.3, using the 5th and 95th percentile values from the TSPA-SR distributions for the diameter of apertures in waste package lids damaged by intrusion and the number of waste packages damaged by igneous intrusion. Values for the 5th and 95th percentile apertures are 3.5 cm^2 and 30 cm^2, respectively. This result compared with the mean curve from Figure 5.2-23 shows that performance is insensitive to the range of diameters considered in the analysis for the apertures in Zone 2 waste packages damaged by intrusion.

5.2.9.9 Sensitivity to Potential Doses during the Eruptive Event

This section examines the potential radiation dose received by an average member of the critical group who does not leave the region during the eruptive event. Doses are calculated using the eruptive-phase BDCFs described in Section 3.10.3.1 (DTN: MO0006SPAPVE03.001 [151768]) and the radionuclide inventory at year one. The analysis assumes PM_{10} (particles less than 10 microns) air mass loading of 1000 $\mu g/m^3$, as described in Section 3.10.1, and a uses a median eruptive duration of 8.2 days (CRWMS M&O 2000 [142657], Table 5). As described below, results indicate that the probability-weighted annual dose from this pathway will be on the order of 10^{-3} to 10^{-4} mrem/yr, significantly below the probability-weighted eruptive dose calculated for long-term exposure to the contaminated ash layer.

The dose for each radionuclide is calculated from the following equation (DTN: MO0006SPAPVE03.001 [151768]):

$$\text{Dose} = PM_{10} \times C_{ash} \times \text{BDCF} \qquad \text{(Eq. 5.2-3)}$$

where

- Dose = the dose from each individual radionuclide
- PM_{10} = the mass concentration of PM_{10} fraction of suspended particulates (g/m^3)
- C_{ash} = the activity concentration of radionuclide in ash (pCi/g ash)
- BDCF = the biosphere dose conversion factor for each individual radionuclide (rem/day/pCi/m^3).

This equation requires calculating the dose from each radionuclide separately and then summing the resulting individual doses to obtain the total dose to the average member of the critical group during the eruptive phase of the volcanic event. This summation of total dose is:

Total Dose = summation (dose from each radionuclide) (Eq. 5.2-4)

The 17 radionuclides for which eruptive phase BDCFs were provided are shown in Table 3.10-6, and are repeated here in Table 5.2-2 for convenience.

Table 5.2-2. BDCFs for the 17 Radionuclides Relevant to the Volcanic Event

Radionuclide	BDCF (rem/day/pCi/m^3)
^{227}Ac	6.92e-02
^{241}Am	4.64e-03
^{243}Am	4.60e-03
^{137}Cs	1.36e-06
^{231}Pa	1.34e-02
^{210}Pb	2.07e-04
^{238}Pu	4.10e-03
^{239}Pu	4.49e-03
^{240}Pu	4.49e-03
^{242}Pu	4.29e-03
^{226}Ra	1.16e-04
^{90}Sr	5.39e-06
^{229}Th	2.22e-02
^{230}Th	3.36e-03
^{232}U	6.80e-03
^{233}U	1.40e-03
^{234}U	1.37e-03

Source: DTN: MO0006SPAPVE03.001 [151768]

The activity concentration (C_{ash}) of radionuclides in ash is calculated separately for each radionuclide. This is done by first determining the mean value of the grams of fuel per gram of ash for all radionuclides combined together. This value was determined by extracting the average g/cm^2 of fuel and average g/cm^2 of ash that fell on the critical group 20 km downwind (assuming the wind always blew towards the critical group) from 100 simulations of the base case ASHPLUME version 1.4LV model (CRWMS M&O 1999 [150744]). The resulting means for fuel and ash concentrations were 2.77×10^{-6} g/ cm^2 and 2.30 g/cm^2, respectively. This results in a mean grams of fuel per gram of ash at the critical group of 1.20×10^{-6}. Put another way, each gram of ash that is deposited at the critical group contains 1.20×10^{-6} grams of the 17 radionuclides combined. These radionuclides are not present in equal quantities, and thus it is necessary to calculate the grams of each radionuclide per gram of ash and to then normalize these results so that the 17 radionuclides being tracked sum up to 1.20×10^{-6} grams for each gram of ash. This will ensure consistency with the ASHPLUME model results (CRWMS M&O 1999 [150744]).

The mass of each radionuclide in both CSNF and DSNF waste packages is listed in Table 5.2-3. The grouping of these into a hypothetical combined waste package is also shown assuming that 70 percent of the packages are CSNF and 30 percent are DSNF.

Table 5.2-3. Mass of Radionuclides in Waste Packages

Radionuclide	CSNF Mass	DSNF Mass	Combined Weighted Mass
^{227}Ac	3.09e-06	1.05e-04	3.37e-05
^{241}Am	8.76e+03	7.87e+01	6.16e+03
^{243}Am	1.29e+03	1.68e+00	9.04e+02
^{137}Cs	5.34e+03	5.52e+02	3.90e+03
^{231}Pa	9.87e-03	3.02e-01	9.75e-02
^{210}Pb	0	1.38e-08	4.14e-09
^{238}Pu	1.51e+03	8.79e+01	1.08e+03
^{239}Pu	4.38e+04	2.13e+03	3.13e+04
^{240}Pu	2.09e+04	4.55e+02	1.48e+04
^{242}Pu	5.41e+03	1.15e+01	3.79e+03
^{226}Ra	0	2.21e-06	6.63e-07
^{90}Sr	2.24e+03	3.01e+02	1.66e+03
^{229}Th	0	2.46e-02	7.38e-03
^{230}Th	1.84e-01	1.75e-02	1.34e-01
^{232}U	1.01e-02	1.37e-01	4.82e-02
^{233}U	7.00e-02	1.98e+02	5.94e+01
^{234}U	1.83e+03	2.77e+02	1.36e+03

Source: DTN: SN0003T0810599.010 [151021]

The total mass of these 17 radionuclides in this combined package is 6.50×10^4 g. This is well below the actual mass of a waste package because it does not include the mass of radionuclides (primarily ^{238}U) that are not significant contributors to dose.

The next step in the calculation is to take the mean grams of fuel per gram of ash for the combined radionuclides (1.20×10^{-6}) and multiply the percentage of the total package mass attributable to each radionuclide by this value. This results in the grams of each radionuclide per gram of ash and all 17 of these values sum to 1.20×10^{-6}. These results are shown in Table 5.2-4 below along with the specific activity for each radionuclide in Ci/g needed in the next step.

Table 5.2-4. Radionuclide Activities and Grams of Each Radionuclide per Gram of Ash

Radionuclide	Combined Weighted Mass	Percent of Total Mass	Grams Radionuclide per gram Ash	Specific Activity (Ci/gram-radionuclide)
^{227}Ac	3.37e-05	5.19e-08 %	6.22e-16	72.341
^{241}Am	6.16e+03	9.48 %	1.14e-07	3.4322
^{243}Am	9.04e+02	1.39 %	1.67e-08	0.19962
^{137}Cs	3.90e+03	6.00 %	7.21e-08	86.121

^{231}Pa	9.75e-02	1.50e-4 %	1.80e-12	0.047618
^{210}Pb	4.14e-09	6.37e-12 %	7.64e-20	75.326
^{238}Pu	1.08e+03	1.66 %	2.00e-08	17.12
^{239}Pu	3.13e+04	48.15 %	5.78e-07	0.062041
^{240}Pu	1.48e+04	22.77 %	2.73e-07	0.22787
^{242}Pu	3.79e+03	5.83 %	7.00e-07	0.003929
^{226}Ra	6.63e-07	1.02e-9 %	1.22e-17	0.98927
^{90}Sr	1.66e+03	2.55 %	3.06e-08	136.5
^{229}Th	7.38e-03	1.14e-5 %	1.36e-13	0.19761
^{230}Th	1.34e-01	2.06e-4 %	2.48e-12	0.020614
^{232}U	4.82e-02	7.42e-5 %	8.90e-13	22.365
^{233}U	5.94e+01	0.09 %	1.10e-09	0.010169
^{234}U	1.36e+03	2.09 %	2.52e-08	0.006236

The next step is to calculate the pCi of each radionuclide per gram of ash (C_{ash} in Eq. 5.2-3). This is done by multiplying the grams of radionuclides per gram of ash in the table above for each radionuclide separately by the activity for that radionuclide and then converting the result into pCi from Ci. The resulting values for C_{ash} are shown in Table 5.2-5 below along with the BDCFs for each radionuclide (Table 5.2-2).

Table 5.2-5. pCi of Each Radionuclide per Gram of Ash and BDCFs

Radionuclide	pCi Radionuclide per gram Ash (C_{ash})	BDCF (rem/day/pCi/m^3)
^{227}Ac	4.50e-02	6.92e-02
^{241}Am	3.90e+05	4.64e-03
^{243}Am	3.33e+03	4.60e-03
^{137}Cs	6.21e+06	1.36e-06
^{231}Pa	8.57e-02	1.34e-02
^{210}Pb	5.76e-06	2.07e-04
^{238}Pu	3.42e+05	4.10e-03
^{239}Pu	3.59e+04	4.49e-03
^{240}Pu	6.21e+04	4.49e-03
^{242}Pu	2.75e+02	4.29e-03
^{226}Ra	1.21e-05	1.16e-04

Table 5.2-5. pCi of Each Radionuclide per Gram of Ash and BDCFs (Continued)

Radionuclide	pCi Radionuclide per gram Ash (C_{ash})	BDCF (rem/day/pCi/m^3)
^{90}Sr	4.18e+06	5.39e-06
^{229}Th	2.69e-02	2.22e-02
^{230}Th	5.10e-02	3.36e-03
^{232}U	1.99e+01	6.80e-03
^{233}U	1.12e+01	1.40e-03
^{234}U	1.57e+02	1.37e-03

The final step is to calculate the dose for each radionuclide separately, using Eq. 5.2-3, and then sum the doses (Eq. 5.2-4) to get a total dose per day for the eruptive phase of the volcanic eruption. The doses are shown in the Table 5.2-6.

Table 5.2-6. Doses for Each Radionuclide During the Eruptive Phase of the Volcanic Event

Radionuclide	Dose (rem/day)
^{227}Ac	3.11e-06
^{241}Am	1.81
^{243}Am	0.015
^{137}Cs	0.008
^{231}Pa	1.15e-06
^{210}Pb	1.19e-12
^{238}Pu	1.40
^{239}Pu	0.161
^{240}Pu	0.279
^{242}Pu	0.001
^{226}Ra	1.40e-12
^{90}Sr	0.023
^{229}Th	5.98e-07
^{230}Th	1.71e-07
^{232}U	1.35e-04
^{233}U	1.56e-05
^{234}U	2.15e-04
Total Summed	**3.70**

The total dose to the average member of the critical group during the eruptive phase of a volcanic event that occurs in year one is 3.70 rem/day. Assuming this event lasts 8.2 days yields a total dose of 30.3 rem. The resulting probability weighted dose would be 4.8×10^{-4} mrem/yr, which is well below the peak mean annual dose for the base igneous case. Doses from eruptive events occurring at all times later than year one would be lower due to radioactive decay.

5.2.9.10 Sensitivity to Alternative Models for BDCFs

As discussed in Section 3.10.3.3, BDCFs have been developed (DTN: MO0006SPAPVE03.001 [151768]) for several different conditions that might exist following an eruptive event (Table 5.2-7).

Table 5.2-7. BDCFs for the Volcanic Igneous Event and the Effect on Dose (Normalized to the Results for Transition Phase [≤1cm] Average Member of the Critical Group BCDFs)

BDCF Description	Applicable Time Frame	Source Group Modeled	Relative Mean BDCF Effect on Dose
Transition Phase for Thin Ash Deposits (≤1cm)	For Several Years Immediately After Eruptive Phase Ends	Average Member of the Critical Group (AMCG)	100 percent (Set by Normalization)
Transition Phase for Thick Ash Deposits (15cm)	For Several Years Immediately After Eruptive Phase Ends	AMCG	63percent of Transition Phase (≤1cm) for AMCG
Steady State Phase for Thin Ash Deposits (≤1cm)	After Transition Phase Ends	AMCG	43percent of Transition Phase (≤1cm) for AMCG
Steady State Phase for Thick Ash Deposits (15cm)	After Transition Phase Ends	AMCG	60percent of Transition Phase (≤1cm) for AMCG
Transition Phase for Thin Ash Deposits (≤1cm)	For Several Years Immediately After Eruptive Phase Ends	RMEI	79percent of Transition Phase (≤1cm) for AMCG
Transition Phase for Thick Ash Deposits (15cm)	For Several Years Immediately After Eruptive Phase Ends	RMEI	43percent of Transition Phase (≤1cm) for AMCG
Steady State Phase for Thin Ash Deposits (≤1cm)	After Transition Phase Ends	RMEI	29percent of Transition Phase (≤1cm) for AMCG
Steady State Phase for Thick Ash Deposits (15cm)	After Transition Phase Ends	RMEI	40percent of Transition Phase (≤1cm) for AMCG

Table 5.2-7 shows that the most conservative BDCFs of the 8 possible sets are the transition phase BDCFs for thin ash deposits (≤1cm) applied to the average member of the critical group. The remaining 7 sets of BDCFs yield doses that are only 29 percent to 79 percent of this set of BDCFs. The transition phase BDCFs for thin ash deposits for the average member of the critical group are the BDCFs that are used within the TSPA-SR. This is a conservative choice for BDCFs because these BDCFs are applicable for the time frame immediately following the eruptive phase of a volcanic eruption. They are used for the full 10,000 years of the model which implies the mass loading of particulates in air remains elevated for the full 10,000 years instead of the expected tens of years. By using the thin ash layer BDCFs, the radionuclides are assumed to be concentrated near the surface. A more realistic assumption for agricultural land in which air mass loading might remain high would be to assume that the radionuclides are plowed into the soil and well mixed, reducing the concentration in the surface layer. Thus, the TSPA-SR use of the thin-layer transition phase eruptive BDCFs is conservative.

Figure 5.2-25 provides insight into the sensitivity of the eruptive dose rate to uncertainty in the values used for the thin-layer transition phase BDCFs by comparing the mean eruptive dose rate to the dose rate calculated with the BDCFs fixed at their 5th and 95th percentile values. The dose rate calculated using the 95th percentile values is approximately a factor of 2 higher than the mean dose rate, reaching a peak of approximately 0.02 mrem/yr.

5.2.9.11 Sensitivity to Incorporation Ratio

Figure 5.2-26 shows a comparison of the probability-weighted mean annual eruptive dose rate, as described in Section 4.2, with the same dose rate calculated using an incorporation ratio of 0.1 and 1.0. As described in Section 3.10.2, the incorporation ratio is used in ASHPLUME 1.4lv (CRWMS M&O 1999 [150744]) to characterize the entrainment of waste particles in the eruption. The base case analysis uses an incorporation ratio of 0.3, which causes waste particles with diameters that are up to 50 percent of the mean diameter of the ash particles to be incorporated in the eruption. The annual eruptive dose rate increases by a negligible factor for an incorporation ratio of 0.1, which increases the diameter of waste particles that are incorporated in the eruption to those that are 80 percent of the ash particle diameter. An incorporation ratio of 1.0, which results in incorporation of particles of up to 10 percent of the ash particle diameter, causes a reduction of less than a factor of 2 in the probability-weighted mean annual dose rate. The relative lack of sensitivity to uncertainty in this parameter suggests that most waste particles are being incorporated in the eruption with the base case value, and that even with the smaller value only the largest waste particles are too small to be incorporated.

5.2.10 Human Intrusion Sensitivity

Section 4.4 describes the TSPA-SR results for the human intrusion scenario. Included in Section 4.4 was a comparison of human intrusion analyses for intrusions occurring at 100 years and 10,000 years after potential repository closure. This section presents the results of an additional one-off sensitivity analysis, in which a selected parameter value (infiltration rate) was fixed and all other parameters were treated as in the human intrusion base case (the case with an intrusion at 100 years). The sensitivity simulation was run for 100 realizations.

For this analysis the infiltration rate was fixed at its 95th percentile value, representative of an extreme unfavorable deviation from expected (base case) performance. Figure 5.2-27 shows a comparison of the mean annual human intrusion dose rate for an intrusion at 100 years (as described in Section 4.4), with the same dose rate calculated using the 95th percentile value for the infiltration rate. The mean annual dose rate increased by a factor of about 5 for the 95th percentile infiltration rate. However, the peak mean annual dose rate for the 95th percentile infiltration rate did not exceed approximately 0.05 mrem/yr in the first 10,000 years after potential repository closure or over the entire 100,000 years.

5.3 ROBUSTNESS ANALYSES

The focus in this section is on the various natural and engineered barriers that make up the potential repository system, and on analyses that examine the robustness of the system by simulating potential repository performance with barriers assumed to be degraded, one at a time or in combination. The objective of such analyses is to evaluate the effectiveness and diversity

of the barriers to determine the overall resiliency of the potential repository system to extreme conditions that are unlikely, but within the range of those believed physically possible. These analyses address nominal performance of the system without the occurrence of unlikely disruptive events such as igneous activity.

The robustness analyses were conducted by fixing key parameters affecting the performance of each barrier near the extreme of their uncertainty distributions (either the 5th or 95th percentile, whichever leads to maximizing the dose rate over the time period of interest). By comparing the nominal performance results with the degraded performance results, one can examine the relative contribution of each of the barriers. Although the parameter values used in the degraded barrier analyses are within the range of values considered reasonably possible, the results should not be interpreted as representing the expected behavior of the system. In many of the analyses, several parameters are simultaneously set to unlikely values. The mean nominal performance results (Section 4.1) are the best approximation of the expected behavior of the system in the absence of igneous disruption, but even they contain many conservative assumptions or parameter values, so the base-case dose results are intended to be on the high side of the expected range of behaviors. The degraded barrier analyses are presented only to provide insight into the resilience of the potential repository system to extreme conditions. To ensure a balanced interpretation of the degraded barrier analysis, results are shown paired with comparable analyses using the 5th or 95th percentile values (as appropriate) of the same parameters, which results in more favorable performance. The mean result from the full nominal analysis should be interpreted as the best estimate of future performance, and the degraded- and enhanced-performance analyses should be interpreted as being equally likely (or unlikely) to occur.

The following barriers are considered in the robustness analyses:

- UZ. This barrier represents the function of the UZ above the potential repository in limiting the amount of water that reaches the potential repository. This barrier includes the climatic conditions at Yucca Mountain, the processes at and near the surface that lead to infiltration, and flow through the UZ above the potential repository.

- Seepage into emplacement drifts. This barrier represents the function of the drifts themselves as a capillary barrier that limits the amount of water that enters the drifts.

- Drip shield. The first of the engineered barriers, the drip shield limits the amount of water that reaches the waste package.

- Waste package. The primary engineered barrier, the waste package limits the amount of water that reaches the waste form and limits radionuclide transport out of the EBS.

- CSNF cladding. The Zircaloy cladding is an engineered barrier that is part of the waste form. It limits the amount of water that reaches the CSNF portion of the waste and limits radionuclide transport out of the CSNF waste form. (CSNF is planned to be approximately 90 percent of the mass of waste in the potential repository.)

- Concentration limits. This barrier represents the function of environmental conditions and radionuclide solubility limits in limiting radionuclide transport out of the EBS.

- EBS transport. This barrier represents the function of environmental conditions and diffusion in the drift invert in limiting radionuclide transport out of the EBS.

- UZ transport. This barrier represents the function of the UZ below the potential repository in delaying radionuclide transport to the biosphere.

- SZ. This barrier represents the function of the SZ in delaying radionuclide transport to the biosphere.

Of the nine "barriers" listed above, only two were found to be important in the uncertainty importance analyses described in Section 5.1: the waste package and the SZ. The importance ranking of parameters in the analyses of Section 5.1 is strongly dependent on two factors: the change in variance of dose rate with the variance of the parameter and the change in the dose rate itself with changes in the parameter. Thus a barrier may not appear as important in Section 5.1 if either of these two derivatives is small. For many of the above "barriers", it is the case that the variance derivative is small because the postulated range of uncertainty in the input parameter or model is either small or nonexistent. This is the case for EBS transport, concentration limits (particularly neptunium), and cladding. For others, such as UZ transport and UZ flow, the derivative of dose rate with the key model parameters is small, i.e., changes in dose rate with changes in those model parameters over reasonably expected ranges are small, so those barriers are less important than other barriers such as the waste package.[2] The remaining barriers listed above, i.e., drip shield and seepage, show up as unimportant because their performance is either masked by other processes or they act as redundant barriers. For example, the drip shield is redundant to the waste package and generally has a shorter lifetime, so its effect is masked by waste package performance. Similarly, the effect of seepage is masked by diffusive transport, which is quite high compared to advection in the first 50,000 years or so.

Another important point is that the uncertainty importance analyses in Section 5.1 are based on linear regression, whereas the TSPA-SR model is often nonlinear in its response. Thus, the overall fit of the regression model is not high enough to evaluate the importance of some of the lesser tier parameters, such as those related to UZ performance.

This section on robustness is another method to evaluate the importance of the various barriers, in order to help bolster or negate the case made in Section 5.1. Robustness of the system with respect to a given barrier will be demonstrated by "small" or negligible changes in the dose rate. Conversely, large changes in dose rate for a given change in a barrier parameter tend to indicate that the system is not as robust with respect to that barrier, i.e., adequate performance of that barrier is more critical to overall system performance than other less important barriers. As will be confirmed below with respect to each of the nine listed barriers, the robustness analyses of this section tend to confirm the results of Section 5.1. However, since all of the robustness analyses in this section necessarily stay within the base-case uncertainty ranges of the individual

[2] There is some disagreement on this point and one could argue that because of the nature of the underlying conceptual model used to model the UZ, it is not possible to show a great impact on dose rate. Perhaps an alternative conceptual model, e.g., one with less conservative assumptions, would reveal a greater influence. Also, as described in the next paragraph, linear regression may not be the most appropriate method for analyzing a highly nonlinear model.

parameters, they cannot elevate in importance any parameter or barrier which has a very restricted range of uncertainty.

The robustness analyses in this section were performed using probabilistic TSPA simulations with 100 realizations. One hundred realizations were used rather than the 300 used for the base-case simulations (see Sections 4.1 and 4.2) because 100 realizations are sufficient to see the relative effects when comparison is made to the base case (see Section 4.1.4).

5.3.1 Unsaturated Zone Flow

5.3.1.1 Degradation of Unsaturated Zone Flow

For purposes of these robustness analyses, UZ flow is degraded by considering the high-infiltration case and it is enhanced by considering the low-infiltration case. Changing the amount of infiltration affects the whole UZ system: the amount of seepage that enters emplacement drifts, the thermal hydrologic environment in the drifts, and the radionuclide transport time through the UZ. The degraded and enhanced UZ flow analyses are the same as the one-off analyses of infiltration discussed in Section 5.2.1.1. There, it was shown that there is only a small increase in doses for the degraded UZ flow case, but a significant decrease in doses for the enhanced UZ flow case.

5.3.1.2 Degradation of Seepage into Drifts

Degraded seepage conditions were defined as

- The seepage-uncertainty factor at its 95th percentile value
- The seepage flow-focusing factor at its 95th percentile value.

while enhanced seepage was defined as

- The seepage-uncertainty factor at its 5th percentile value
- The seepage flow-focusing factor at its 5th percentile value.

The seepage uncertainty factor is a uniform random variable that is used to correlate the sampling of seepage fraction, mean seep flow rate, and the standard deviation of seep flow rate from their respective distributions (see Section 3.2.4.3 for discussion of these parameters). When the seepage-uncertainty factor is at its 95th percentile value, all three of those seepage parameters are at their 95th percentile values, and similarly for the 5th percentile values. Thus, the amount of seepage flow and the number of waste packages affected are both high when the seepage-uncertainty factor is high, and both are low when it is low.

The effect of the flow-focusing factor is less straightforward. As discussed in Section 3.2.4.3, a higher flow-focusing factor causes higher seep flow rates for the waste packages that have seepage, but at the same time reduces the number of waste packages affected by seeps. The combined effect, as discussed in Section 5.2.1.2, is an increase in the total amount of seepage and an increase in radionuclide releases. Similarly, seepage and radionuclide releases decrease when the flow-focusing factor is decreased. Thus, an increased flow-focusing factor was

included in the degraded seepage case and a decreased flow-focusing factor was included in the enhanced seepage case.

Figure 5.3-1 shows a comparison of the mean annual nominal dose rate to the mean dose rates calculated under degraded and enhanced seepage conditions. The impact of degraded and enhanced seepage conditions starts to be seen at about 40,000 years. This is due to the waste packages not having failed "patches" (i.e., advection release pathways) until about 36,000 years, plus a travel time of approximately 4,000 years from the EBS to the critical-group location. Higher percolation fluxes due to the 95th percentile flow-focusing factor, along with higher seepage flows from the 95th percentile seepage-uncertainty factor result in higher mean dose rates in comparison to the nominal case. Conversely, the low percolation fluxes associated with the 5th percentile flow-focusing factor, along with lower seepage flows due to the 5th percentile seepage-uncertainty factor result in lower doses rates in comparison to the nominal case. The calculated increases and decreases in dose are only moderate, amounting to increases or decreases by a factor of at most 5 from the base case, and less than that most of the time.

5.3.1.3 Degradation of Unsaturated Zone Flow and Seepage

This sensitivity case is a combination of degraded UZ flow (Section 5.3.1.1) and degraded seepage (Section 5.3.1.2). That is, the seepage parameters are set to the pessimistic end of their uncertainty ranges and in addition infiltration is set to its high case. The corresponding enhanced UZ flow and seepage case has seepage parameters set to the optimistic end of their uncertainty ranges and infiltration set to its low case.

The results of these cases are presented in Figure 5.3-2. Shown in the plot are the mean nominal-scenario dose curves for the degraded and enhanced UZ flow and seepage cases, along with the mean dose curve for the nominal-scenario base case, for comparison. The results are seen to be a combination of the results of the individual cases (see Figures 5.2-1 and 5.3-1). The largest effect comes from the reduced infiltration, which greatly increases the transport time through the UZ (see Figure 3.7-10). The mean doses from the enhanced UZ flow and seepage case are significantly lower than the base case. However, the combination of high infiltration and degraded seepage still results in doses that are only moderately higher than the base case: increases by a factor of up to about 5 or so.

5.3.2 Engineered Barrier System Environments

No barrier degradation analyses were performed for the EBS environments alone; however, some aspects of the environments are modified along with other parameters for the analyses described in Sections 5.3.4.2 and 5.3.5.

5.3.3 Waste Package and Drip Shield Degradation

5.3.3.1 Degradation of Drip Shield

In the current EBS transport model, the titanium drip shield must be failed before any advective (flowing) water can contact the waste packages and carry away radionuclides from the failed waste packages. Analyses were conducted to evaluate the impact of drip shield performance on potential repository performance. The analyses were conducted by fixing the drip shield

degradation parameters at the 95th and 5th percentile values of their respective uncertainty distributions. The cases are referred to as the degraded drip shield case (95th percentile case) and the enhanced drip shield case (5th percentile case). Only the drip shield general corrosion is considered because it is the only active degradation mode in the base-case analysis (see Sections 3.4.1.3 and 3.4.1.5 for an explanation of why other modes are unimportant). The degraded case uses the 5th percentile uncertainty-variability partitioning ratio from the parent distribution of the titanium general corrosion rate (i.e., the spread in the parent distribution from the experimental measurements is considered to represent mostly variability, rather than uncertainty). It also sets the median general corrosion rate to the 95th percentile of the resulting uncertainty variance (i.e., the variance in shield-to-shield corrosion rates that results from setting the uncertainty-variability partitioning ratio to its 5th percentile). The enhanced case uses the 95th percentile uncertainty-variability partitioning ratio and the median general corrosion rate at the 5th percentile of the resulting uncertainty variance.

The analysis results for the predicted mean dose rate profile and mean drip shield failure profile are shown in Figures 5.3-3 and 5.3-4 respectively. Although the analyses show that the drip shield performance is affected significantly (Figure 5.3-4), there is almost no effect on the predicted mean dose rate (Figure 5.3-3). This is due primarily to the fact that waste package degradation is independent of drip shield performance in the WAPDEG model, (i.e., none of the individual corrosion models or parameters is affected by drips). As discussed above, the intact drip shields prevent dripping water from directly contacting the underlying waste packages, and this should affect the EBS transport process. However, this benefit appears not to be significant to the mean dose rate (Figure 5.3-3).

5.3.3.2 Degradation of Waste Package

This section analyzes the sensitivity of the potential repository and waste package performance to several major waste package degradation process parameters. Analyses were conducted by fixing the degradation parameters at the 95th and 5th percentile values of their respective uncertainty distributions. The cases are referred to as the degraded waste package case (95th percentile case) and the enhanced waste package case (5th percentile case). The degradation parameters considered are:

- Residual hoop stress state and stress intensity factor at the closure-lid welds
- Number of manufacturing defects at the closure-lid welds per waste package
- Alloy-22 general corrosion rate
- Enhancement factor to Alloy-22 general corrosion due to MIC
- Enhancement factor to Alloy-22 general corrosion due to aging and phase stability.

Note that individual variations of several of these parameters are presented in Section 5.2.3. In this section all of them are varied together to represent significantly degraded waste package performance. The degraded case uses:

- The 5th percentile uncertainty-variability partitioning ratio from the parent distribution of the Alloy-22 general corrosion rate (i.e., the spread in the parent distribution from the experimental measurements is considered to represent mostly variability, rather than uncertainty)

- The median general corrosion rate at the 95th percentile of the resulting uncertainty variance (i.e., the variance in package-to-package corrosion rates that results from setting the uncertainty-variability partitioning ratio to its 5th percentile)

- The uncertainty indices for the residual hoop stress and stress intensity factor in both the outer and middle lids at their 95th percentile values, implying earlier SCC failure than the base case

- The manufacturing defect parameters at their 95th percentile value, which maximizes the defects

- The MIC enhancement factor at its 95th percentile value

- The aging and phase stability enhancement factor at its 95th percentile value.

The enhanced case uses:

- The 95th percentile uncertainty-variability partitioning ratio

- The median general corrosion rate at the 5th percentile of the resulting uncertainty variance

- The uncertainty indices for the residual hoop stress and stress intensity factor in both the outer and middle lids at their 5th percentile values, implying later SCC failure than the base case

- The manufacturing defect parameters at their 5th percentile value, which minimizes the defects

- The MIC enhancement factor at its 5th percentile value

- The aging and phase stability enhancement factor at its 5th percentile value.

See Section 3.4 for the discussions on the enhancement factors due to microbiologically influenced corrosion and aging and phase stability. Also, it should be noted that in each of the above two cases there are a total of 9 parameters that are fixed, so the probability of this case ever being sampled is extremely small, on the order of 0.05^9 or about 10^{-12}.

The analysis results for the predicted mean dose rate profile and mean waste package failure profile are shown in figures 5.3-5 and 5.3-6, respectively. The enhanced case yielded no waste package failure, thus no dose, during the first 100,000 years. On the other hand, by fixing the major degradation parameters at their "degraded" values, the waste package degradation rate increases significantly, and the failure rates are significantly higher (Figure 5.3-6). The first failure time of the mean failure profile is about 7,000 years, compared to about 12,000 years for the base case. For the degraded case, there is 50 percent probability that 1 percent of waste packages fail at about 10,000 years and 10 percent of waste packages fail at about 12,000 years. For the base case it is about 25,000 years for the 1 percent failure and about 50,000 years for the

10 percent failure. Accordingly, the predicted mean dose starts earlier (about 8,200 years versus about 15,000 for the base case), and the predicted mean dose rates are much higher. These results are consistent with the individual sensitivity analyses presented in Section 5.2.3.

5.3.4 Waste Form Degradation and Mobilization

5.3.4.1 Degradation of CSNF Cladding

For the two most important radionuclides to nominal-scenario dose, ^{99}Tc and ^{237}Np, the CSNF represents over 86 and 95 percent of the total inventory, respectively. Hence, the CSNF cladding can directly influence the dose by reducing the release rate of these radionuclides.

The cladding model has five parameters that were sampled for TSPA-SR: (1) the number of rods initially perforated in a CSNF waste package (f_{rod}) (Initial_Rod_Failures), (2) the fraction of cladding perforated because of creep rupture and SCC (Creep_Used), (3) the uncertainty in localized corrosion rate (LC_uncert), (4) the uncertainty of the CSNF degradation rate (Uncert_a0), and (5) the uncertainty in the unzipping velocity of the cladding (Unzip_uncert) (Table 5.3-1). An estimate of the uncertainty that the cladding model causes in the dose was evaluated by setting all sampled parameters except the fraction of cladding perforated by creep rupture and SCC at the 5 percent and 95 percent values and observing the change in the mean dose (Figure 5.3-7). The mean dose only increases slightly (about a factor of 1.5) when the four parameter values are set at the 95th percentiles of their distributions. When the four parameters are set at their 5th percentiles, the mean dose decreases by about a factor of 4 in the first 100,000 years.

Table 5.3-1. Sampled Parameters in CSNF Cladding Degradation Model

Parameter	Description	Parameter Distribution
Initial_Rod_Failures	Percentage of cladding with initial perforation	Triangular (0.0155, 0.0948, 1.29)
Creep_Used	Fraction of cladding perforated due to creep rupture and SCC	Triangular (limits are a function of maximum temperature calculated in waste package for each simulation)
LC_uncert	Uncertainty in the localized corrosion rate	Loguniform (0.1, 10)
Uncert_a0	Uncertainty in the CSNF degradation rate (10^{x})	Uniform (–1, 1)
Unzip_uncert	Uncertainty in unzipping velocity	Triangular (1, 40, 240)

Until several tens of thousands of years after the waste package begins to fail, the only cladding perforated is CSNF cladding that arrives at the site perforated or perforates because of creep rupture during the first few hundred years. For example, the mean perforation fractions are respectively 0.0045 and 0.0765 for initial perforation and creep rupture for the 20 to 60 mm/yr infiltration bin. Only after 50,000 years does the perforated fraction of cladding change due to localized corrosion in those waste packages that have seepage (Figure 4.1-10). As described in Section 3.5, the localized corrosion is a direct function of the seepage volume into the waste

package. The sometimes-dripping case has the greater mean seepage volume; thus, the sometimes-dripping case has the most localized corrosion and greater perforation.

Overall, parameters related to the waste form degradation model or the cladding component, in particular, are not important to determining uncertainty in the dose in the first 100,000 years (see Section 5.1). However, between 100,000 years and 1,000,000 years, uncertainty in two parameters of the cladding component show up as important to determining uncertainty in the dose. During this period, more cladding begins perforating from localized corrosion. Of the five parameters varied in the cladding component, the order-of-magnitude uncertainty in the CSNF degradation rate was found to be the most influential (Figure 5.1-18). In addition, the two-order-of-magnitude uncertainty in the unzipping rate was found to be important at some times.

5.3.4.2 Degradation of Concentration Limits

The dose rate out to 100,000 years is relatively insensitive to the concentrations of dissolved and colloidal radionuclides in the waste package and invert. That conclusion is illustrated in Figure 5.3-8. For the degraded concentration case, parameters affecting concentrations were set to values at the pessimistic end of their uncertainty ranges. Radionuclide concentrations were set to their 95th percentile values, colloid stability was maximized, and the 95th percentile values were used for sorption coefficients of radionuclides onto colloids. In addition, the waste package chemistry was used in the invert, because the chemistry in the waste package generally favors higher concentrations in the TSPA model. The lack of importance of solubility is explained as follows.

The two most important radionuclides to dose in the first 100,000 years are ^{99}Tc and ^{237}Np. In the TSPA model, the solubility of technetium is set to a constant bounding value of 1 M; thus, although ^{99}Tc is still the most important radionuclide for determining the dose in the first ~30,000 years after waste package failure (see Section 4.1), uncertainty in technetium solubility does not influence the uncertainty in the total dose because it is a constant.

^{237}Npis the most important radionuclide for determining the dose after ~30,000 years, but its solubility does not influence the uncertainty in the dose either; however, the reason for its low importance is different. In the TSPA model, the solubility of neptunium is a function of the pH. Inside the waste packages, the pH varies substantially; consequently, the solubility of neptunium also varies (Figure 3.5-21). Yet, outside the waste package in the invert, the pH does not vary much. The TSPA model reevaluates the neptunium solubility at the invert using the invert pH (any excess ^{237}Np diffuses out of the invert or is held in the invert until the concentration drops at later times). A situation similar to ^{237}Np also occurs for uranium and americium since they are a function of pH as well. However, they are lesser contributors to the total dose for nominal performance.

Because the invert pH does not vary much, neither does the neptunium solubility in the invert. Thus, the calculated variability of the neptunium solubility is not large enough to substantially influence the variability in the dose (Figure 5.3-8); therefore, neptunium solubility does not show up as an important parameter in sensitivity analysis for TSPA-SR. As discussed in Section 5.2.4.2, the neptunium solubility used in TSPA-SR is probably somewhat conservative and does not account for the formation of secondary mineral phases. Section 5.2.4.2 also

presents a sensitivity analysis showing how potentially important neptunium solubility could be if it had a wide range of variation.

In the first 100,000 years, all three waste forms (i.e., HLW glass, DSNF waste matrix, and CSNF waste matrix exposed from unzipping of initially perforated cladding) liberate radionuclides faster than radionuclides are released from the waste package through either diffusion or advection. Thus, large amounts of various radionuclides are retained in the package prior to release (see, e.g., Figure 4.1-11). Hence, the waste-matrix degradation rate is unimportant to determining the dose and its uncertainty. As just discussed, the release is not regulated by the solubility of the radionuclides to a great extent, either. Rather, since most of the release of radionuclides is from diffusive rather than advective release (Figure 4.1-13), it is limited flux rate of material through the limited available surface area of the package that controls the release. Consequently, even the highly soluble ^{99}Tc is retained in the waste package for long periods of time as described in Section 4.1.

5.3.5 Engineered Barrier System Transport

This section analyzes the sensitivity of the potential repository to several important EBS transport and EBS environment parameters. The degraded EBS transport case is a combination of the degraded concentration limits case (Section 5.3.4.2) and the high-diffusion case (Section 5.2.5), while the enhanced EBS transport case is a combination of the enhanced concentration limits case (Section 5.3.4.2) and the low-diffusion case (Section 5.2.5). As defined in those earlier sections, "degraded concentration limits case" means high solubilities and "enhanced concentration limits case" means low solubilities.

The combined effects of EBS transport and related chemical environments on the early-arrival dose rate (time to a dose rate of 10^{-3} mrem/yr) are differences of several thousand years. Furthermore, the peak dose rate at 100,000 years is moderately sensitive to the diffusion model and to the effects of chemical environments on the concentrations of dissolved and colloidal radionuclides in the EBS. This is illustrated in Figure 5.3-9 by the factor of 5 increase in peak dose rate for the degraded EBS transport case.

5.3.6 Unsaturated Zone Transport

The following three subsections present robustness analyses related to UZ transport. Section 5.3.6.1 presents a degraded UZ transport analysis in which several UZ transport parameters are set at pessimistic values (i.e., values that put radionuclide transport time in the fast end of its uncertainty range). Section 5.3.6.2 combines the degraded UZ transport parameters with degraded UZ flow (i.e., high infiltration). Lastly, Section 5.3.6.3 combines the degraded UZ transport and UZ flow with degradation of seepage into drifts as well (seepage parameters set at pessimistic values). Each of these sections also presents the converse: the result if the same parameters are set to optimistic values. In this way, the effect on the calculated dose of a range of behaviors, from pessimistic to optimistic, can be evaluated.

5.3.6.1 Degradation of Unsaturated Zone Transport

To examine the effects of degraded UZ transport, the following parameters were set to values at the pessimistic end of their uncertainty ranges:

- All radionuclide sorption coefficients (K_ds) were set to their 5th percentile values (low sorption implies faster transport).
- All colloid partitioning factors (K_cs) were set to their 95th percentile values (high K_c implies faster transport of the reversible colloids).
- All diffusion coefficients were set to their 5th percentile values (low matrix diffusion implies faster transport).
- All fracture apertures were set to their 95th percentile values (large fracture apertures lead to less matrix diffusion, which implies faster transport).

In the corresponding enhanced UZ transport case, the above parameters were set to the optimistic end of their uncertainty ranges (that is, the 5th and 95th designations above were switched: K_ds at 95th percentile values, etc.). All other parameters were given the same (sampled) values as in the nominal-scenario base case.

The results of these cases are presented in Figure 5.3-10. Shown in the plot are the mean dose curves for the degraded and enhanced UZ transport cases, along with the mean dose curve for the nominal-scenario base case, for comparison. The effect of the degraded or enhanced UZ transport is small to moderate except for a large pulse in the degraded case between 20,000 and 30,000 years. That pulse is a result of a large release of ^{243}Am when waste packages start failing, which is then able to transport through the UZ relatively quickly and reach the biosphere before it decays (^{243}Am has a half-life of only about 7,000 years, so the longer transport times in the enhanced and base cases are enough to reduce its dose effect substantially). Comparison of the degraded case in Figure 5.3-10 with Figure 5.2-14 indicates that among the four degraded parameter distributions considered (i.e., apertures, sorption coefficients, K_cs, and matrix diffusion coefficient), matrix diffusion is apparently the most important parameter contributing to the attenuation of dose.

5.3.6.2 Degradation of Unsaturated Zone Flow and Transport

This sensitivity case is a combination of degraded UZ transport (Section 5.3.6.1) and degraded UZ flow (Section 5.3.1.1), i.e., transport parameters are set to the pessimistic end of their uncertainty ranges and in addition infiltration is set to its high case. As with the other degradation cases, a corresponding enhanced case is presented as well.

The results of these cases are presented in Figure 5.3-11. Shown in the plot are the mean nominal-scenario dose curves for the degraded and enhanced UZ flow and transport cases, along with the mean dose curve for the nominal-scenario base case, for comparison. The biggest change from Figure 5.3-10 (degraded UZ transport) is in the enhanced case: the low infiltration significantly increases the transport time through the UZ (see Figure 3.7-10). The mean doses from the enhanced UZ flow and transport case are significantly lower than the base case. The

combination of high infiltration and degraded UZ transport results in a large pulse at 20,000 to 30,000 years, as in Figure 5.3-10 and in addition gives doses about a factor of five higher than the base case at late times.

5.3.6.3 Degradation of Unsaturated Zone Flow and Transport and Seepage

This sensitivity case is a combination of degraded UZ transport (Section 5.3.6.1), degraded UZ flow (Section 5.3.1.1), and degraded seepage (Section 5.3.1.2), i.e., transport and seepage parameters are set to the pessimistic end of their uncertainty ranges and in addition infiltration is set to its high case. This case represents the degradation of all aspects of the UZ model. A corresponding enhanced case is presented as well.

The results of these cases are presented in Figure 5.3-12. Shown in the plot are the mean dose curves for the degraded and enhanced UZ flow, transport, and seepage cases, along with the mean dose curve for the nominal-scenario base case, for comparison. The curve for the enhanced case is essentially identical to the corresponding curve in Figure 5.3-11 (degraded UZ flow and transport), indicating that the enhancement of seepage had no additional effect beyond the enhancement of UZ flow and transport. The doses in the degraded case are somewhat higher than the corresponding doses for degraded UZ flow and transport: more than a factor of ten higher than the base case at some times.

5.3.7 Saturated Zone Flow and Transport

5.3.7.1 Degradation of Saturated Zone Flow and Transport

To evaluate the robustness of the SZ as a barrier to radionuclide release from a potential repository at Yucca Mountain, the SZ flow and transport model was parameterized for two cases: one case would give degraded behavior when compared with the base case; the other would give enhanced behavior.

To achieve degraded behavior, the 5th percentile value was taken from distributions of parameters known to positively affect radionuclide travel time, and the 95th percentile value was taken from distributions of parameters known to negatively affect radionuclide travel time. For example, sorption is known to positively affect travel time, because an increase sorption causes an increase in travel time, so, for the degraded SZ, the 5th percentile value for sorption coefficients (K_d) used. Similarly, groundwater flux is known to negatively affect travel time, because an increase groundwater flux causes a decrease in travel time; thus, for the degraded SZ, the 95th percentile value for groundwater flux was used. Conversely, to achieve enhanced behavior, the 95th percentile value was taken from distributions of parameters known to positively affect radionuclide travel time, and the 5th percentile value was taken from distributions of parameters known to negatively affect radionuclide travel time.

Figure 5.3-13 presents the mean nominal-scenario dose calculated from 100 realizations for the base case, the base case with a degraded SZ, and the base case with an enhanced SZ. The difference in dose between the degraded and the enhanced cases is between one and two orders of magnitude (between a factor of 10 and a factor of 100). Two other features are immediately noticeable in the plot: the degraded SZ is very similar to the base case, and the performance from the degraded and the enhanced cases is diverging at late time.

The performance of the degraded SZ is similar to the base case because the realizations that contribute to the largest doses, the doses that have the largest influence on the mean, are realizations that sample an SZ with characteristics similar to the degraded SZ. For example, the realizations with the largest doses in the base case are those using an SZ with a large groundwater flux. The degraded SZ has a high groundwater flux. Groundwater flux is singled out here because it is a parameter that is identified in the regression analyses as influencing dose (Section 5.1). The correspondence of the means of the degraded case and the base case implies that the SZ results are skewed by the least favorable realizations.

The dose from the enhanced SZ is leveling off at 100,000 years, while the dose from the degraded SZ and the base case is continuing to increase. The implication is that the performance of the two cases tends to diverge farther over longer periods of time. The reason for this divergence is that the enhanced SZ effectively reduces the impact of adsorbing radionuclides, such as neptunium, as well as radionuclides that undergo colloid-facilitated transport, such as plutonium, but not the unreactive radionuclides, such as technetium. Technetium is beginning to wane by 100,000 years, explaining the leveling of the enhanced SZ curve.

5.3.8 Biosphere

The biosphere is the endpoint for the TSPA simulation of radionuclide release and transport, and as such is not treated as a barrier to radionuclide contamination. An evaluation of the sensitivity of the TSPA dose calculation to uncertainty in modeling the biosphere is presented in Section 5.2.8. In addition, an evaluation of uncertainty internal to the biosphere model (for groundwater releases only), separate from the TSPA model, is presented in Section 3.9.2.5.

INTENTIONALLY LEFT BLANK

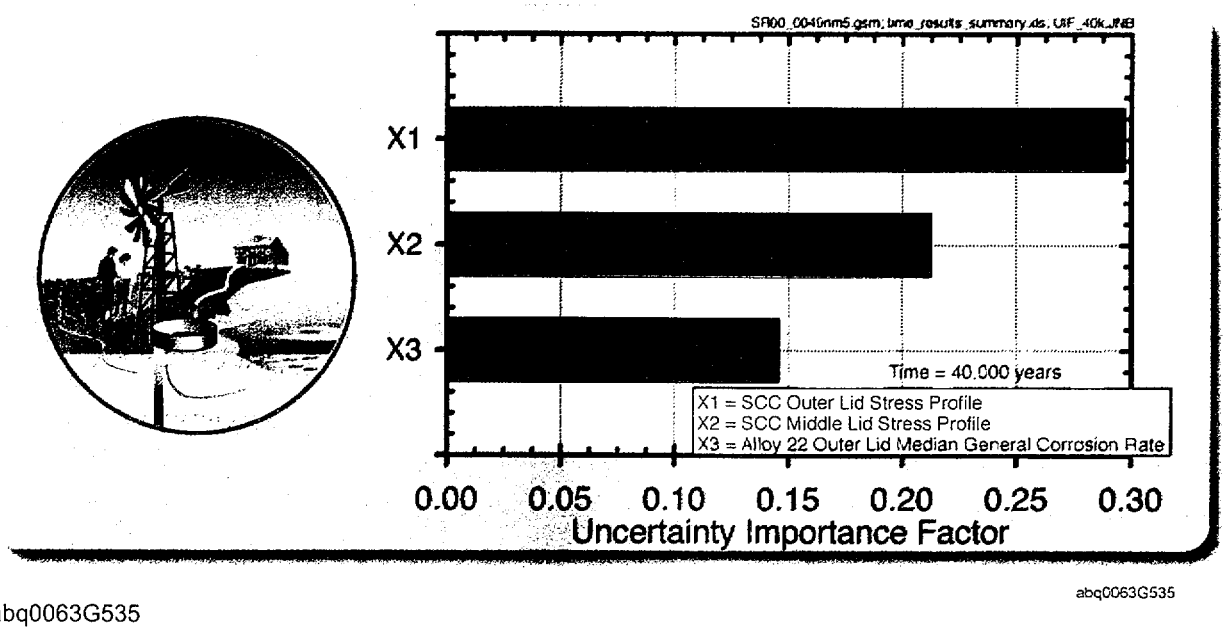

abq0063G535

Figure 5.1-1. Bar Chart Showing Uncertainty Importance Factors for the Most Important Variables at 40,000 Years for Total Dose, Nominal Scenario

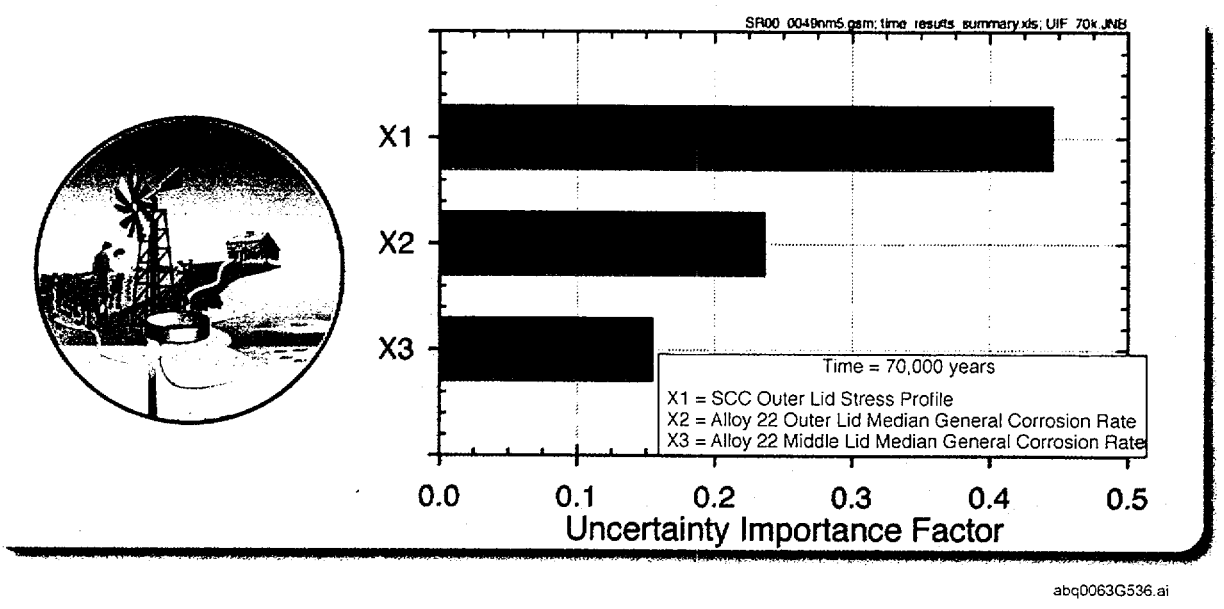

abq0063G536

Figure 5.1-2. Bar Chart Showing Uncertainty Importance Factors for the Most Important Variables at 70,000 Years for Total Dose, Nominal Scenario

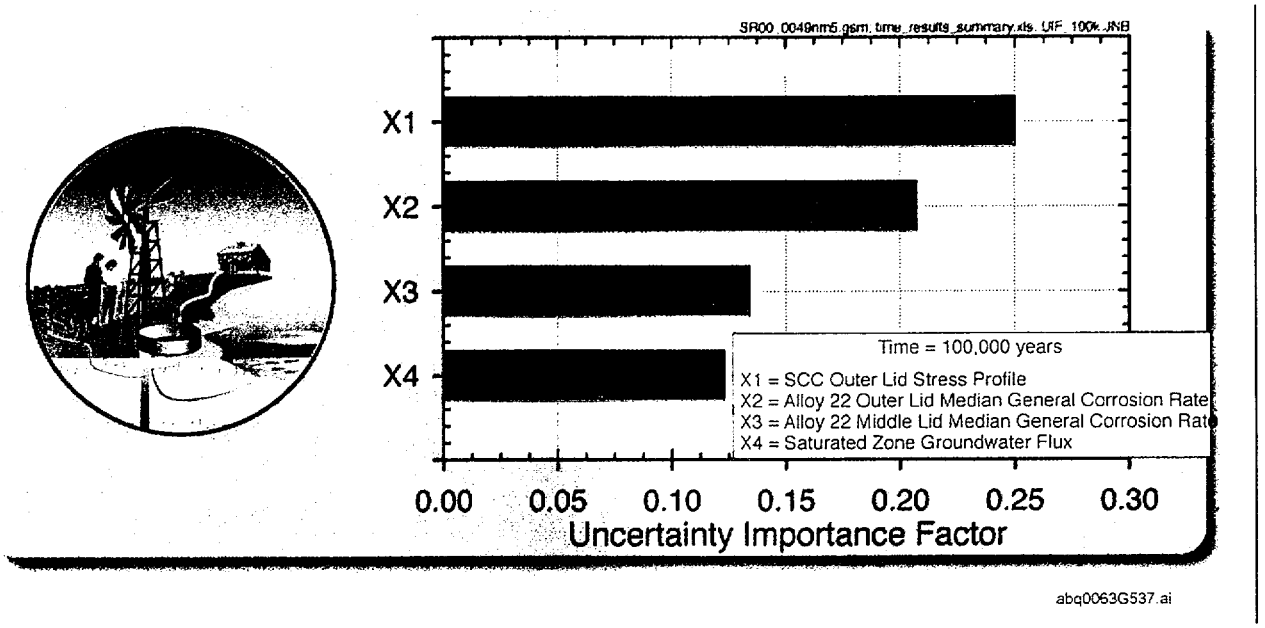

abq0063G537

Figure 5.1-3. Bar Chart Showing Uncertainty Importance Factors for the Most Important Variables at 100,000 Years for Total Dose, Nominal Scenario

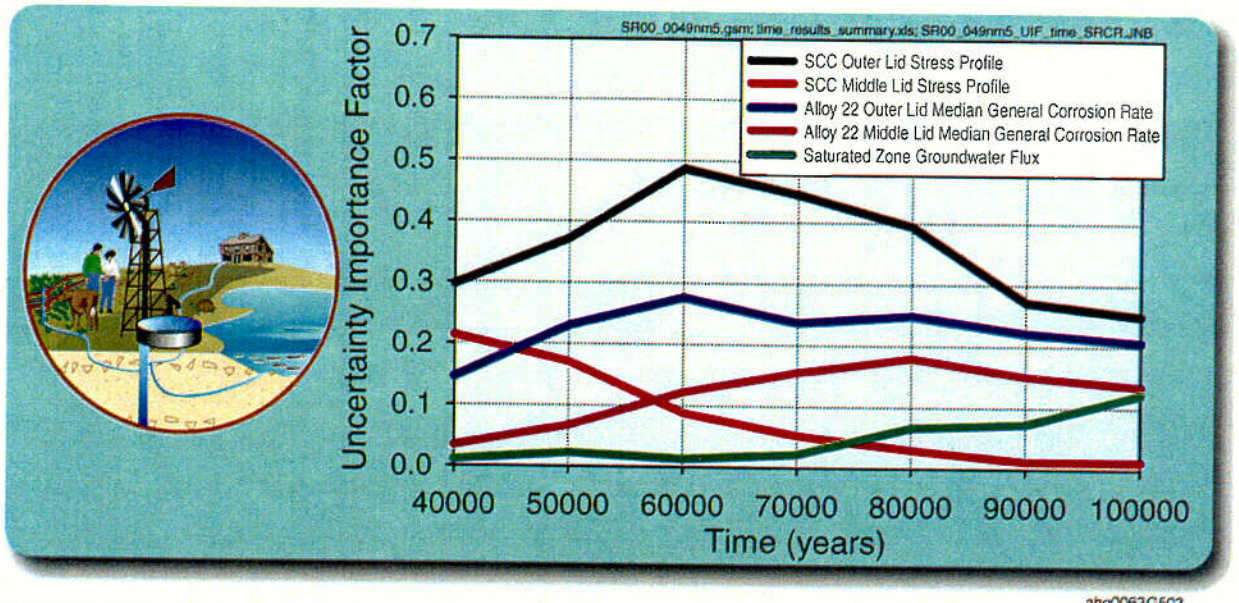

abq0063G503

Figure 5.1-4. Uncertainty Importance Factors at Multiple Time Slices for Total Dose, Nominal Scenario

L-43

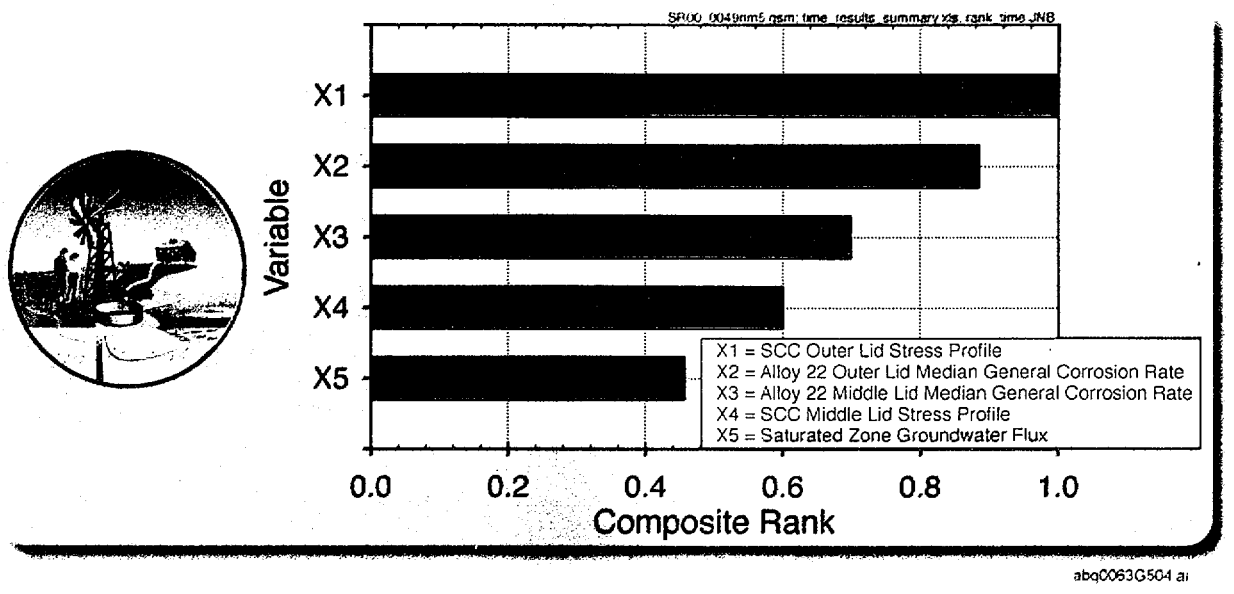

abq0063G504

Figure 5.1-5. Bar Chart Showing Time-Averaged Composite Uncertainty Importance Ranking for Total Dose, Nominal Scenario

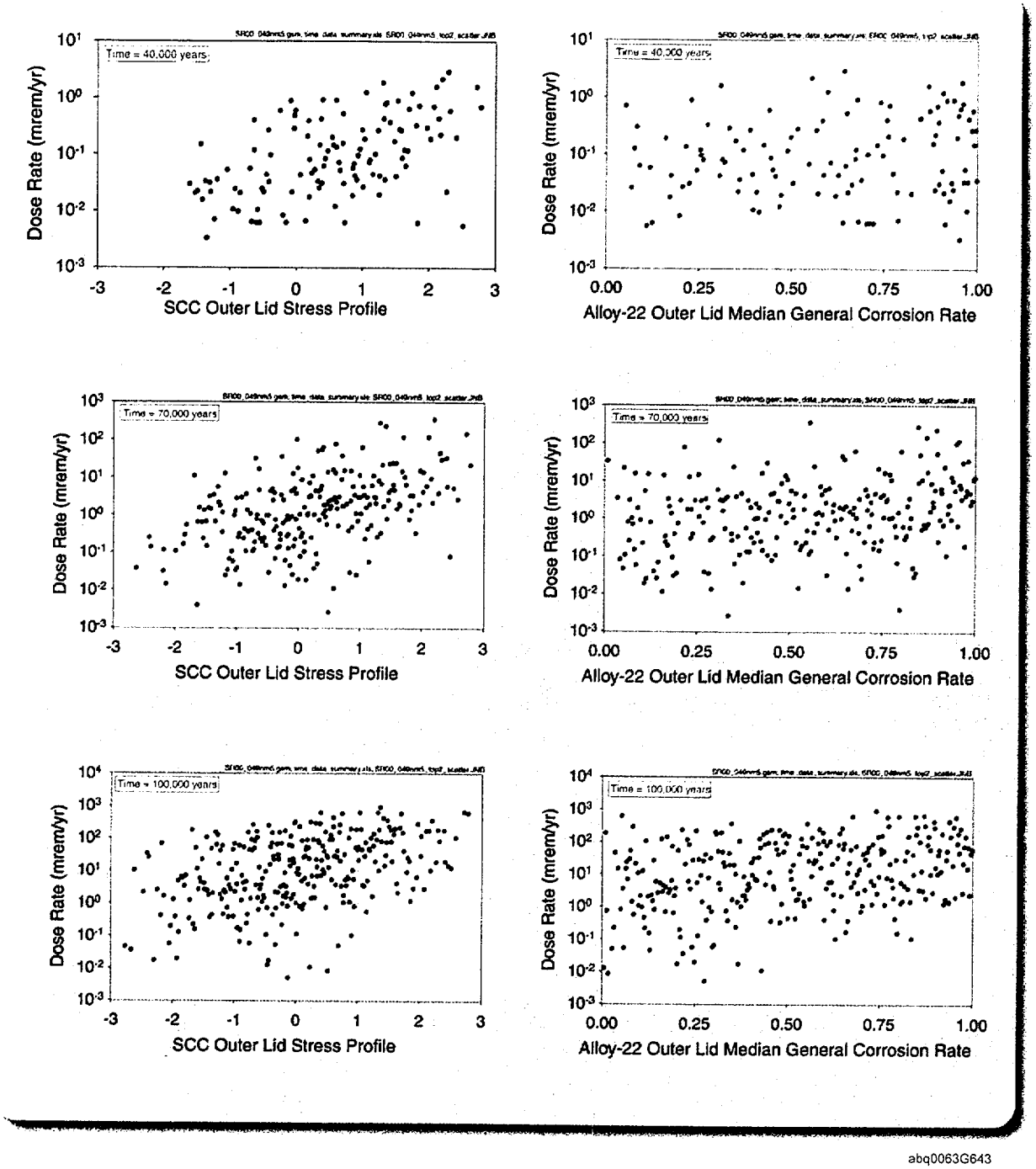

abq0063G643

Figure 5.1-6. Scatter Plots of Total Dose and the Two Most Important Uncertain Variables at Multiple Time Slices, Nominal Scenario

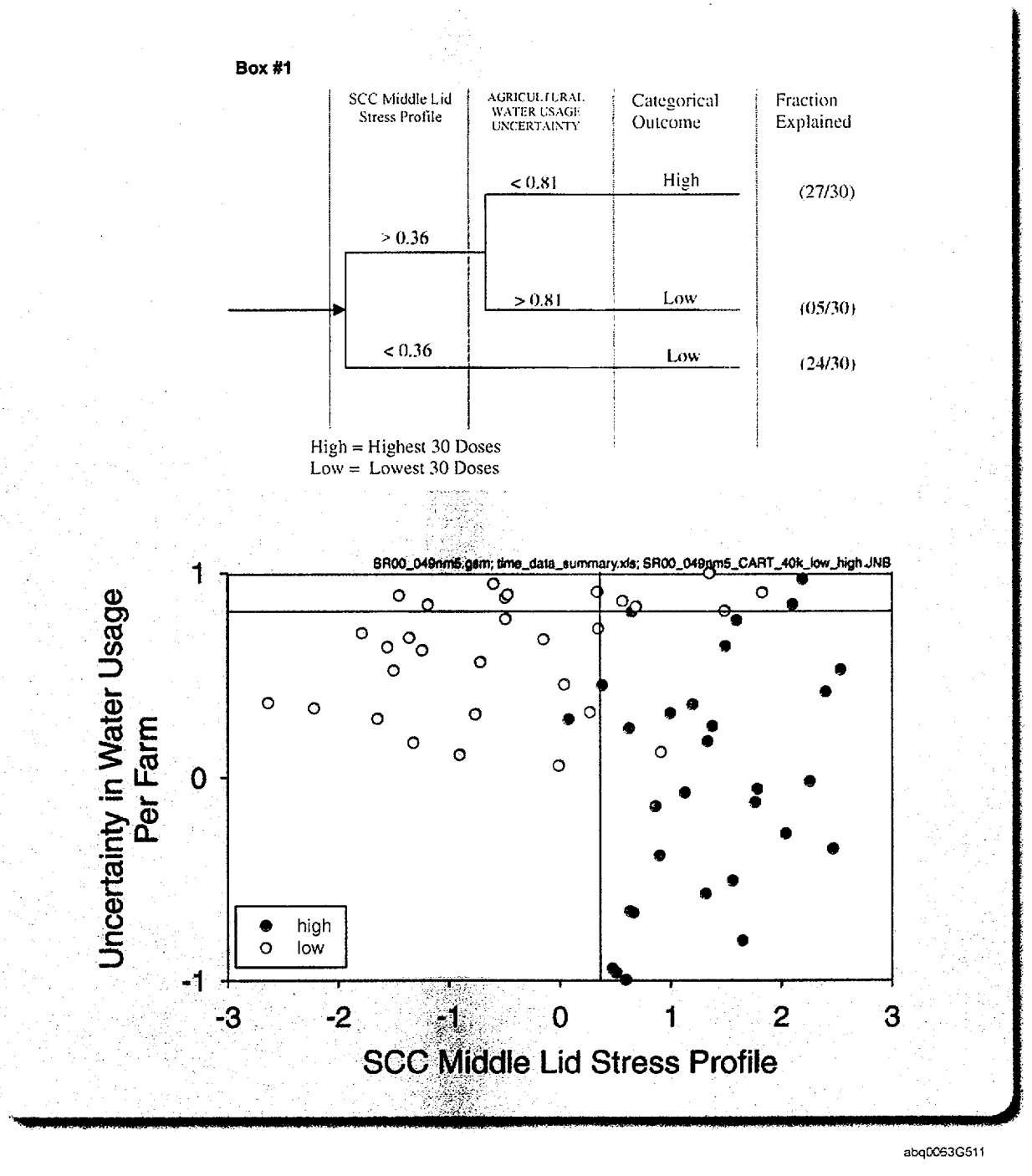

abq0063G511

Figure 5.1-7. Decision Tree Summarizing Classification Tree Analysis (Top) and Partition Plot Showing Clusters of Low-Dose (10th-Percentile and Lower) and High-Dose (90th-Percentile and Higher) Outcomes (Bottom) for the Two Most Important Variables at 40,000 Years, Nominal Scenario

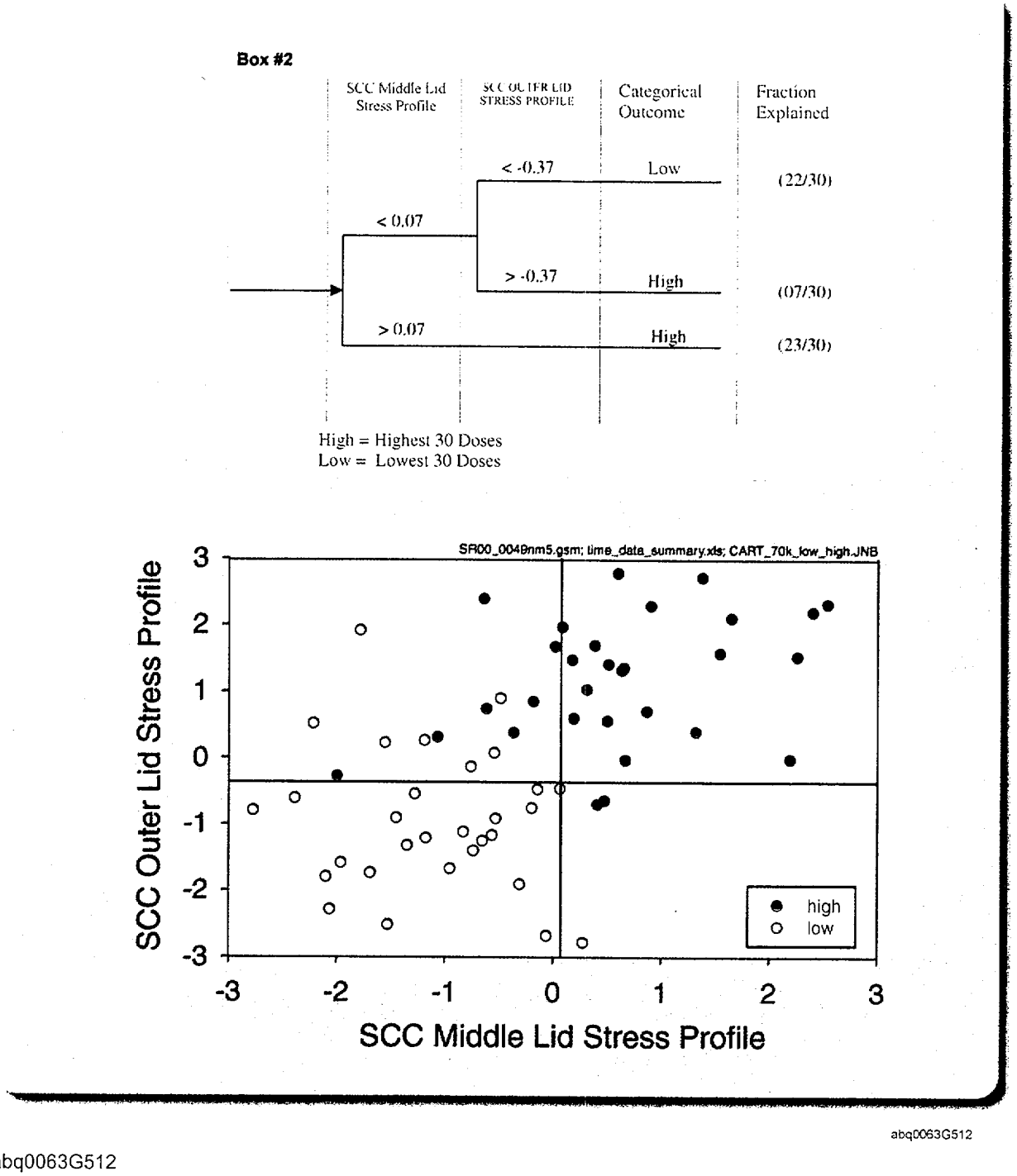

abq0063G512

Figure 5.1-8. Decision Tree Summarizing Classification Tree Analysis (Top) and Partition Plot Showing Clusters of Low-Dose (10th-Percentile and Lower) and High-Dose (90th-Percentile and Higher) Outcomes (Bottom) for the Two Most Important Variables at 70,000 Years, Nominal Scenario

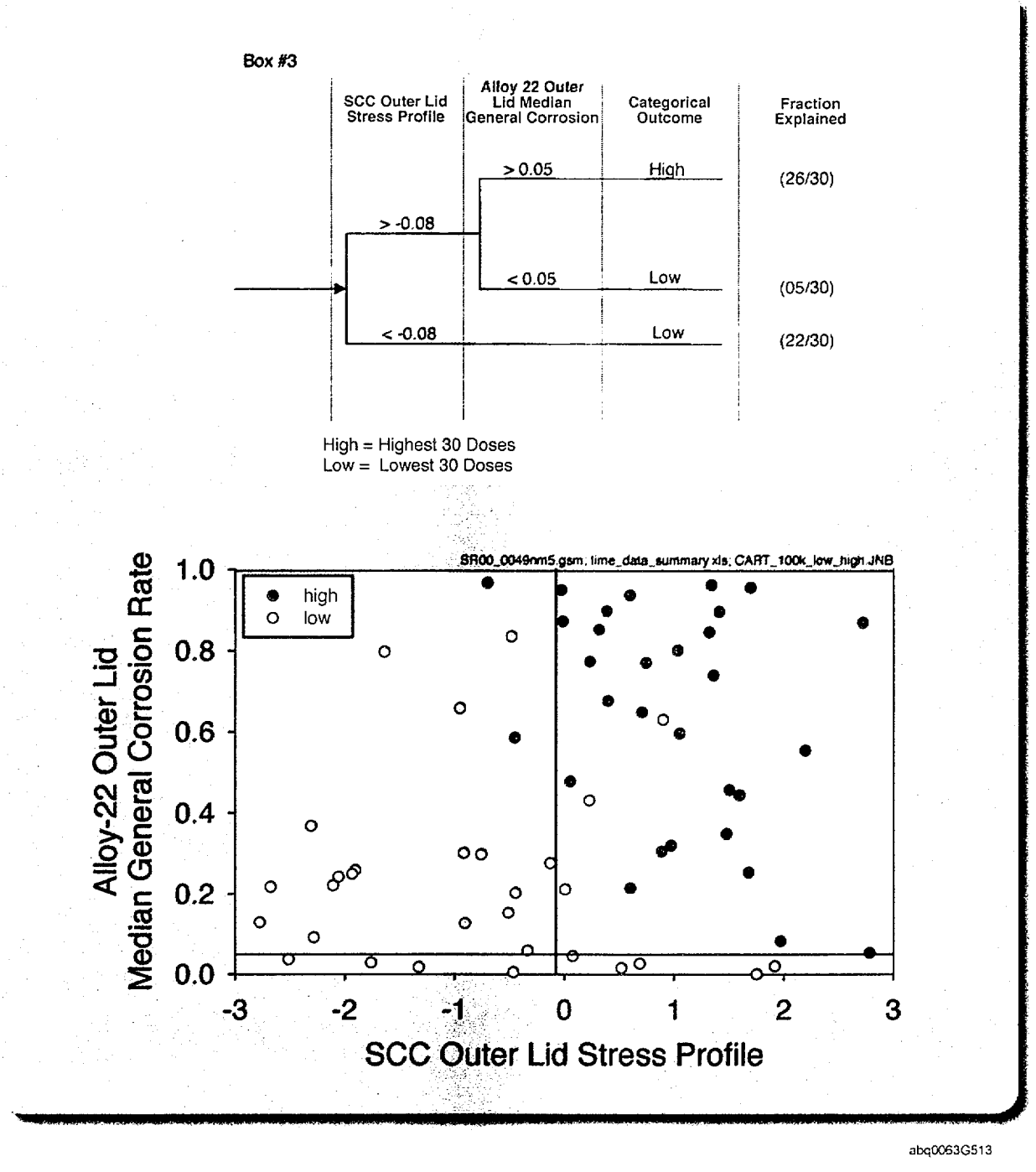

abq0063G513

Figure 5.1-9. Decision Tree Summarizing Classification Tree Analysis (Top) and Partition Plot Showing Clusters of Low-Dose (10th-Percentile and Lower) and High-Dose (90th-Percentile and Higher) Outcomes (Bottom) for the Two Most Important Variables at 100,000 Years, Nominal Scenario

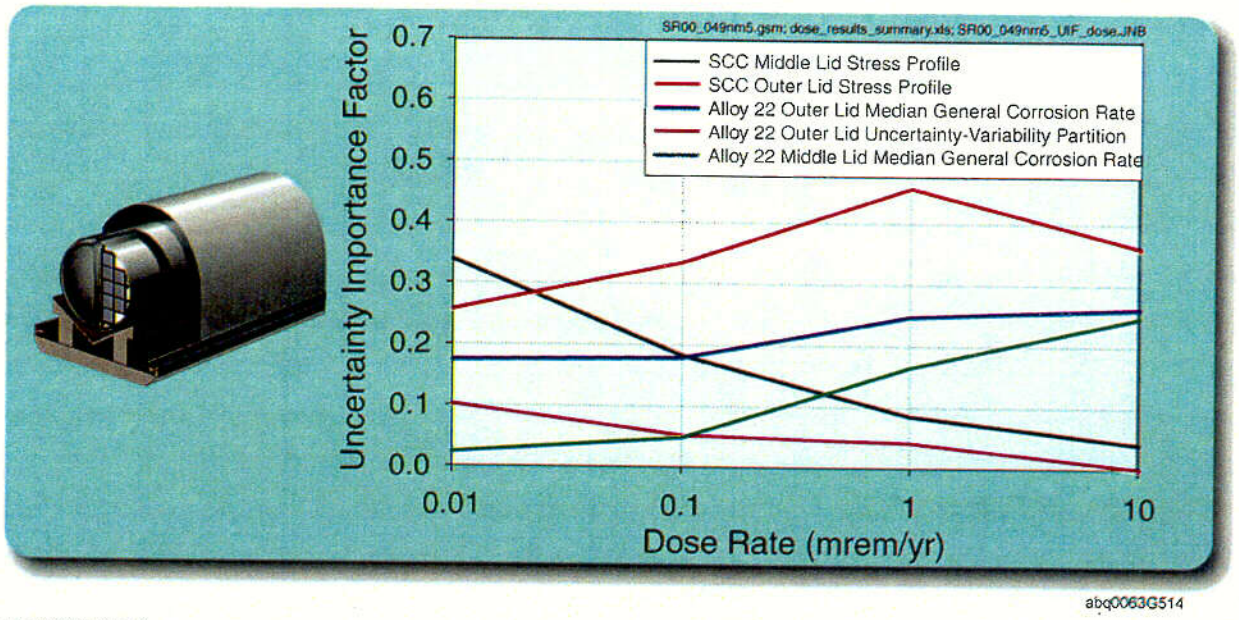

abq0063G514

Figure 5.1-10. Uncertainty Importance Factors at Multiple Dose Values for Time to Reach a Specified Dose, Nominal Scenario

C-44

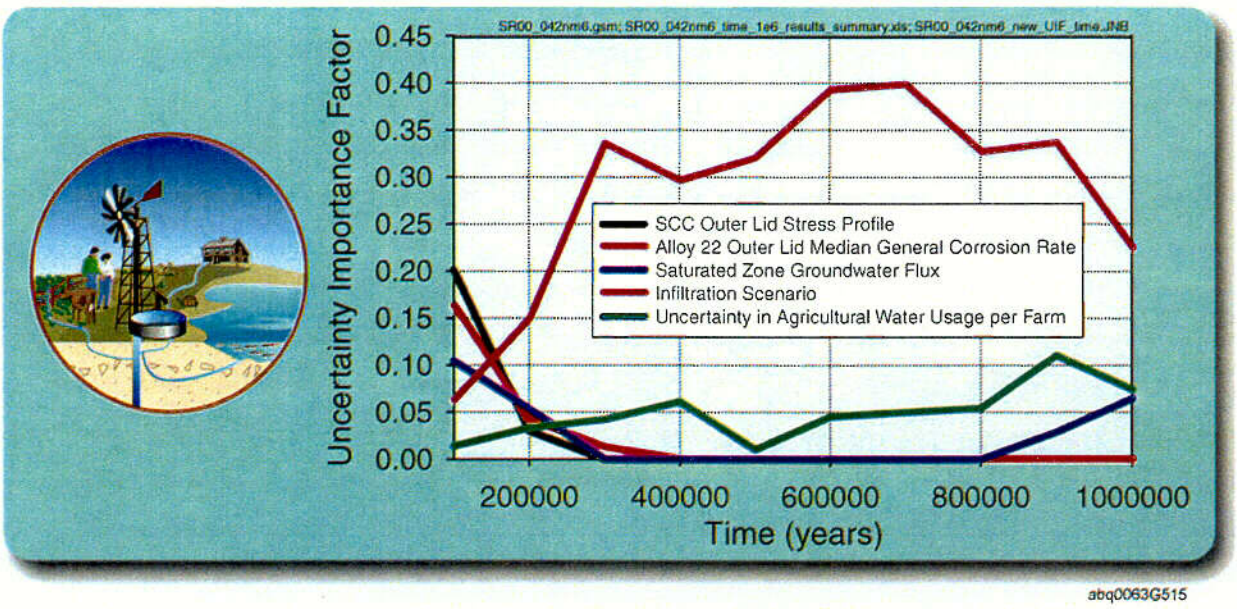

abq0063G515

Figure 5.1-11. Uncertainty Importance Factors at Multiple Time Slices Between 100,000 and 1,000,000 Years for Total Dose, Nominal Scenario

L-45

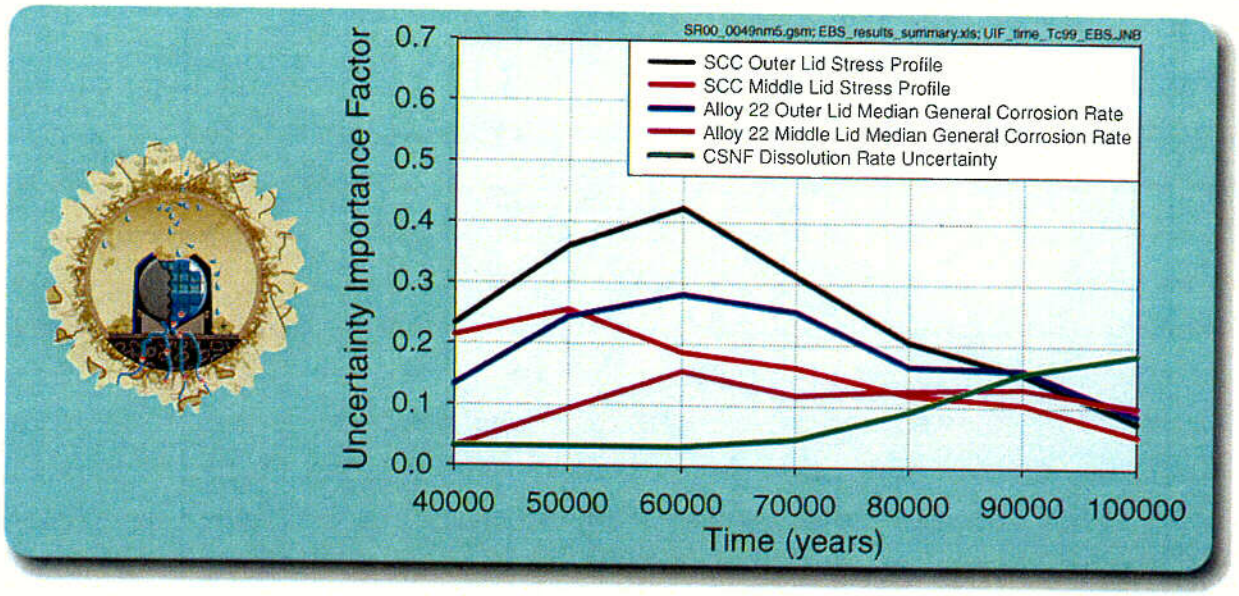

abq0063G538

Figure 5.1-12. Uncertainty Importance Factors at Multiple Time Slices for Mass Release of ^{99}Tc from Engineered Barrier System, Nominal Scenario

C-46

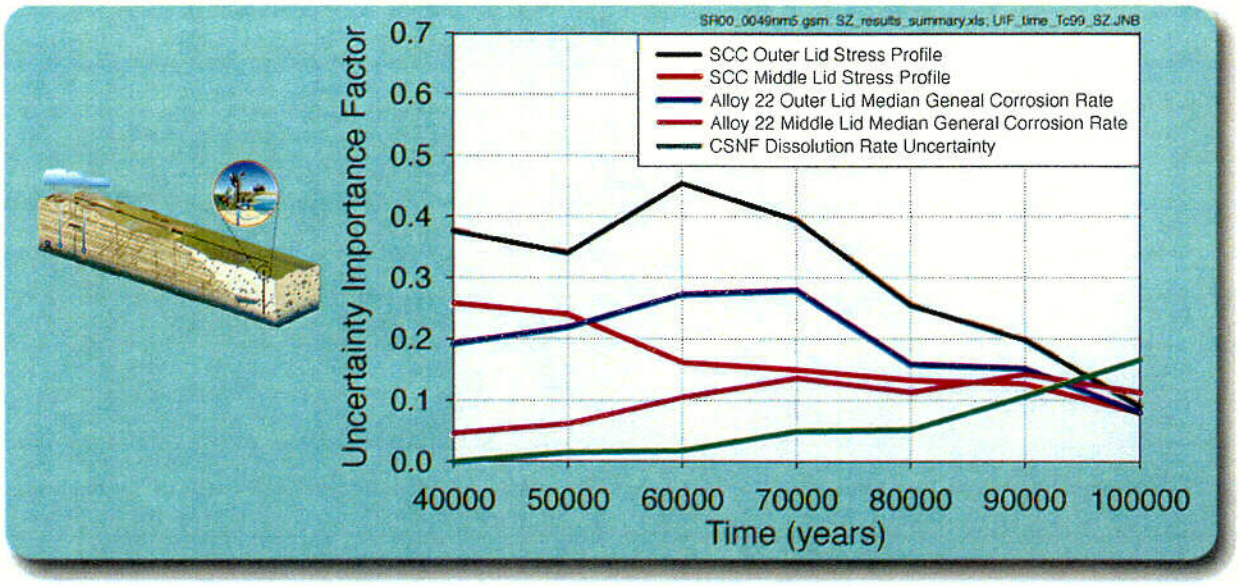

abq0063G539

Figure 5.1-13. Uncertainty Importance Factors at Multiple Time Slices for Mass Release of ^{99}Tc from Saturated Zone, Nominal Scenario

L-47

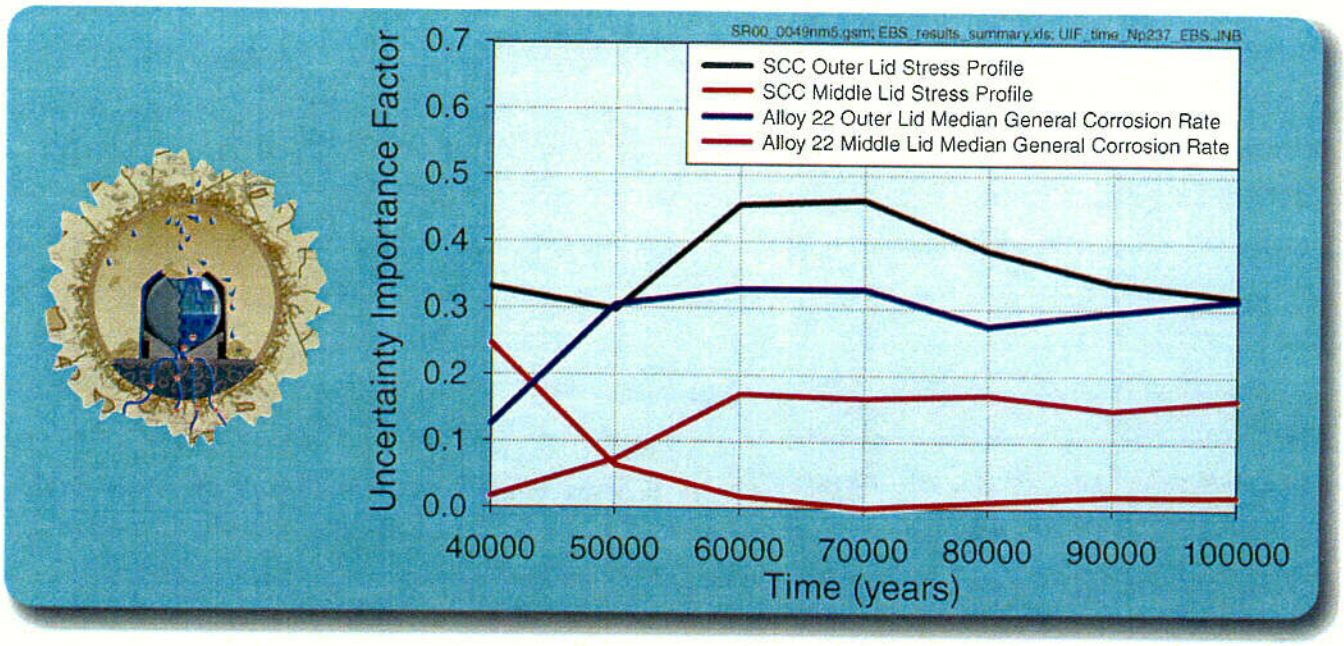

abq0063G540.ai

abq0063G540

Figure 5.1-14. Uncertainty Importance Factors at Multiple Time Slices for Mass Release of ^{237}Np from Engineered Barrier System, Nominal Scenario

C-48

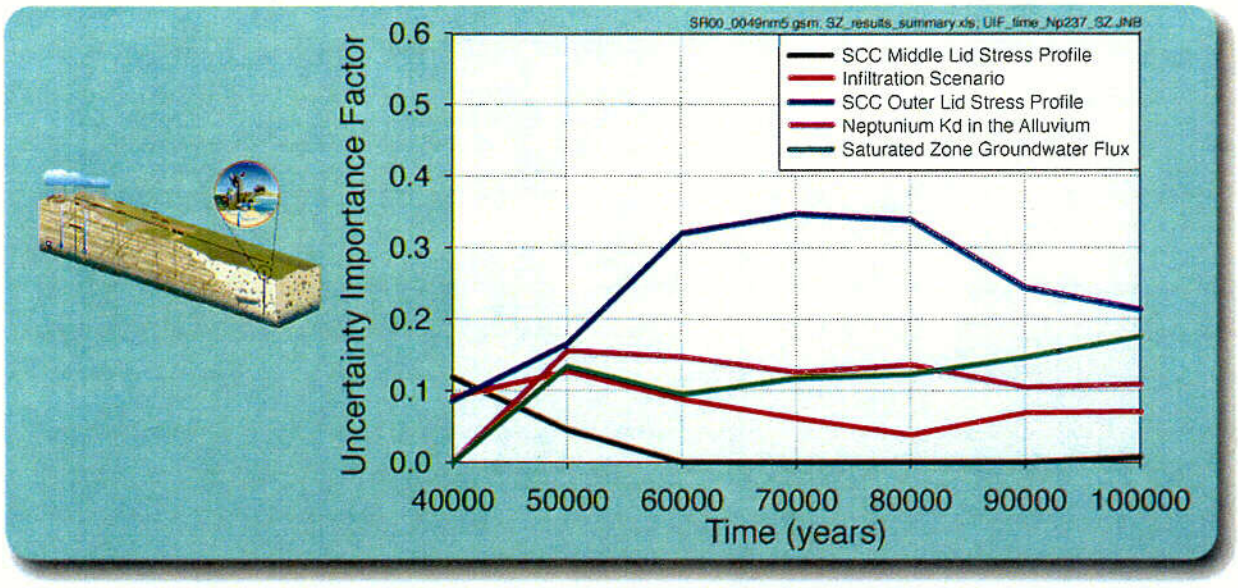

abq0063G541

Figure 5.1-15. Uncertainty Importance Factors at Multiple Time Slices for Mass Release of ^{237}Np from Saturated Zone, Nominal Scenario

L-49

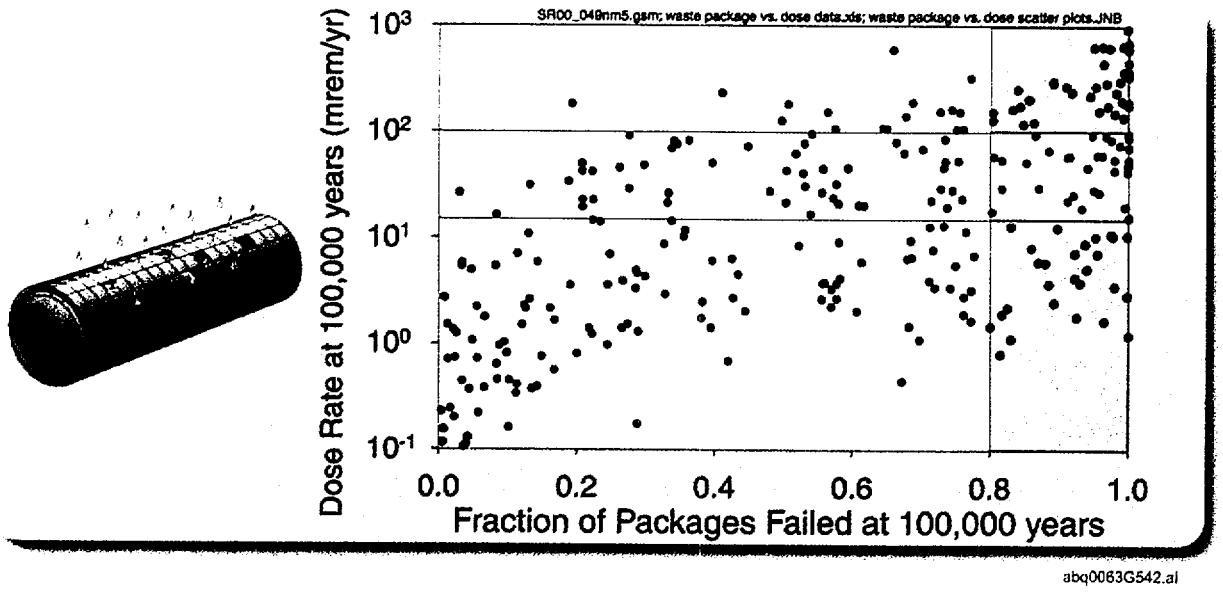

abq0063G542

Figure 5.1-16. Scatter Plot of Total Dose and Fraction Waste Packages Failed at 100,000 Years, Nominal Scenario

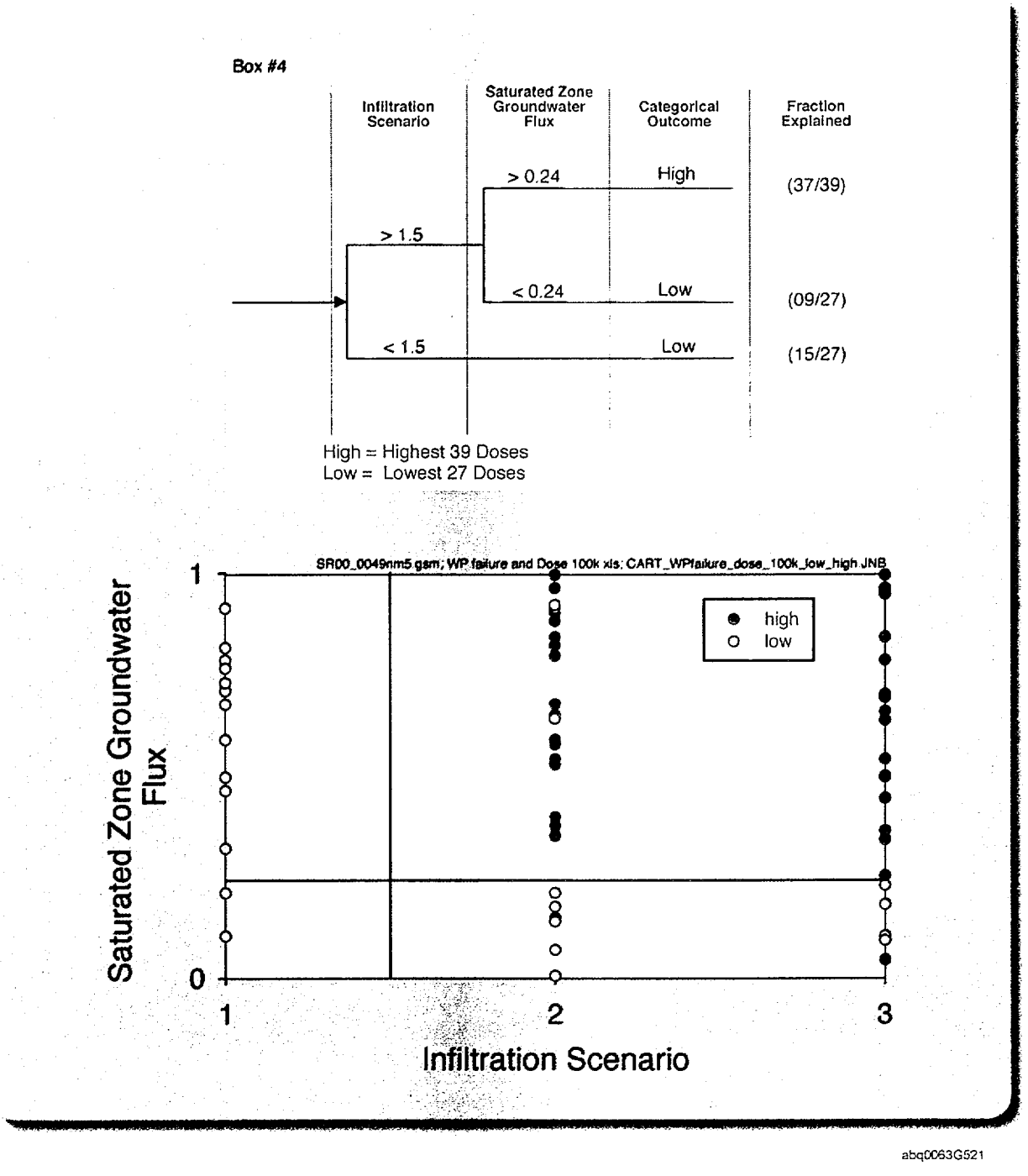

abq0063G521

Figure 5.1-17. Decision Tree Summarizing Classification Tree Analysis (Top) and Partition Plot Showing Clusters of Low-Dose (15 mrem/yr and Lower) and High-Dose (100 mrem/yr and Higher) Outcomes for Realizations with at Least 80 Percent Failed Packages (Bottom) for the Two Most Important Variables at 100,000 Years, Nominal Scenario

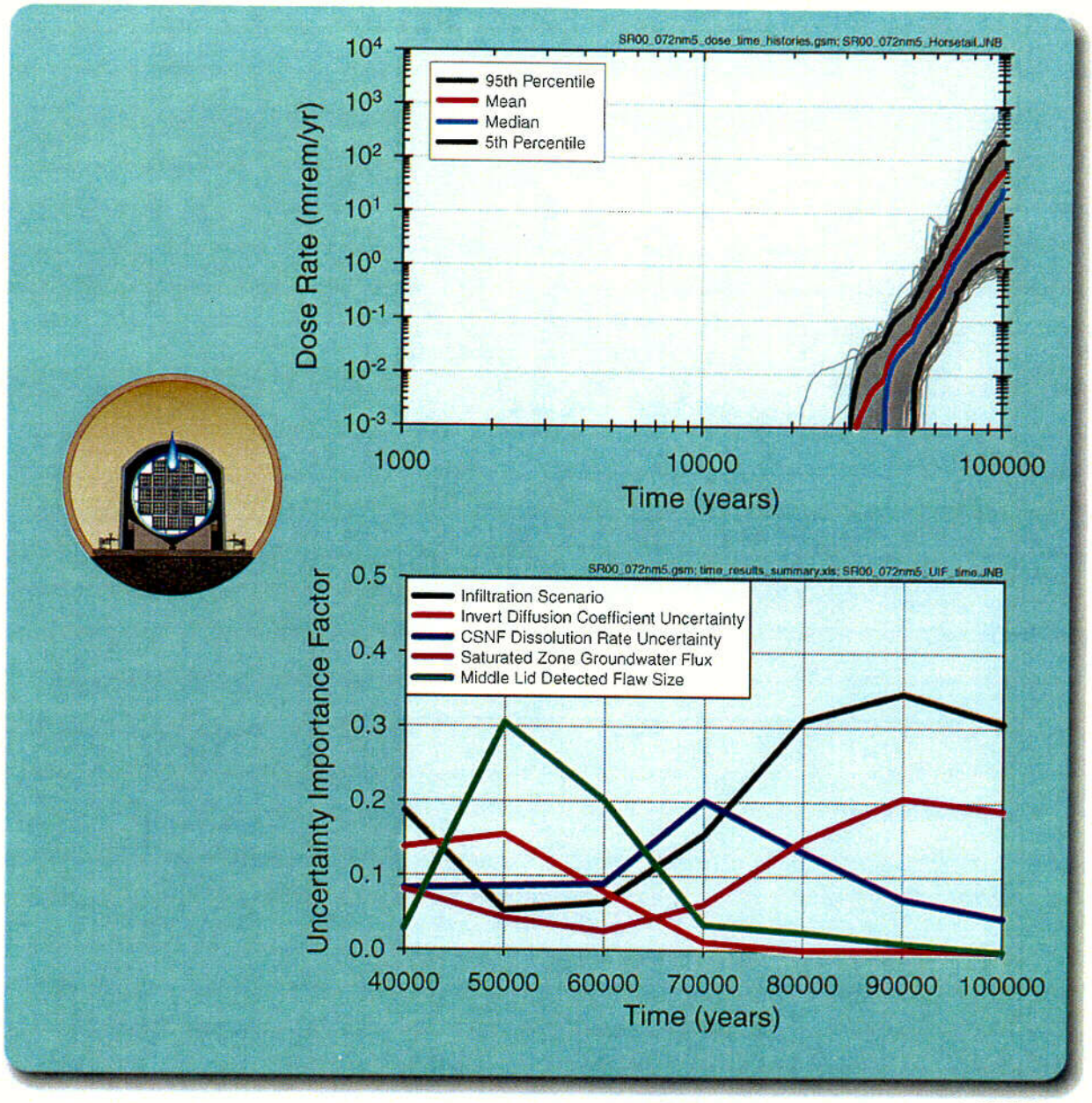

abq0063G522

Figure 5.1-18. Probabilistic Results (Top) and Uncertainty Importance Factors at Multiple Time Slices (Bottom), Nominal Scenario with Key Waste Package Parameters Fixed at Median Values

L-50

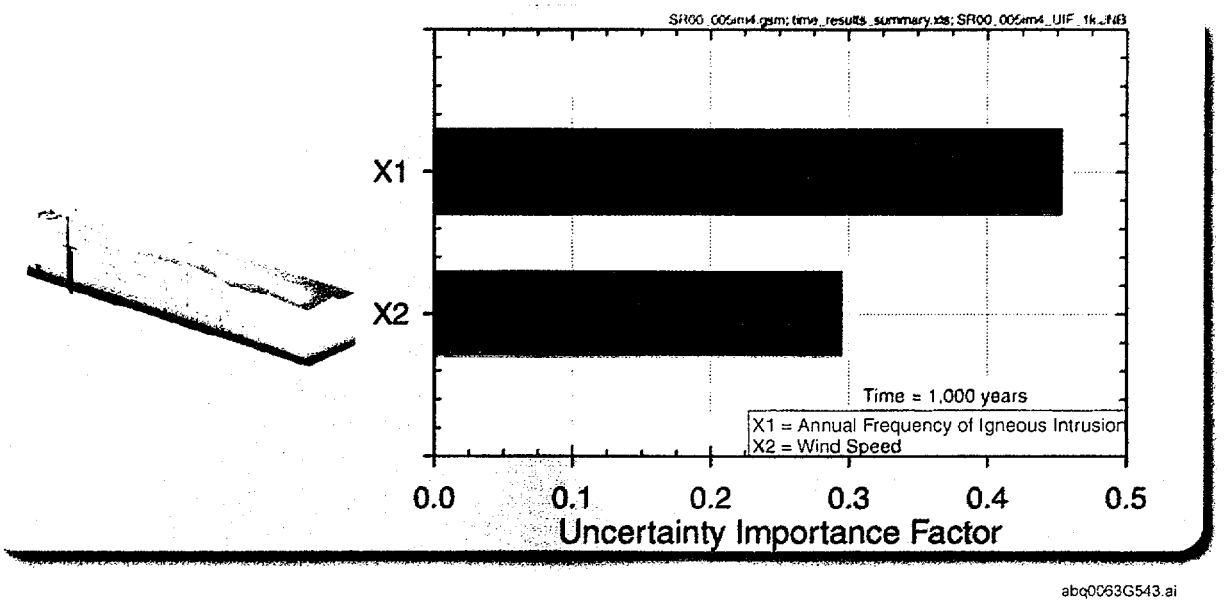

abq0063G543

Figure 5.1-19. Bar Chart Showing Uncertainty Importance Factors for the Most Important Variables at 1,000 Years for Total Dose, Igneous Scenario

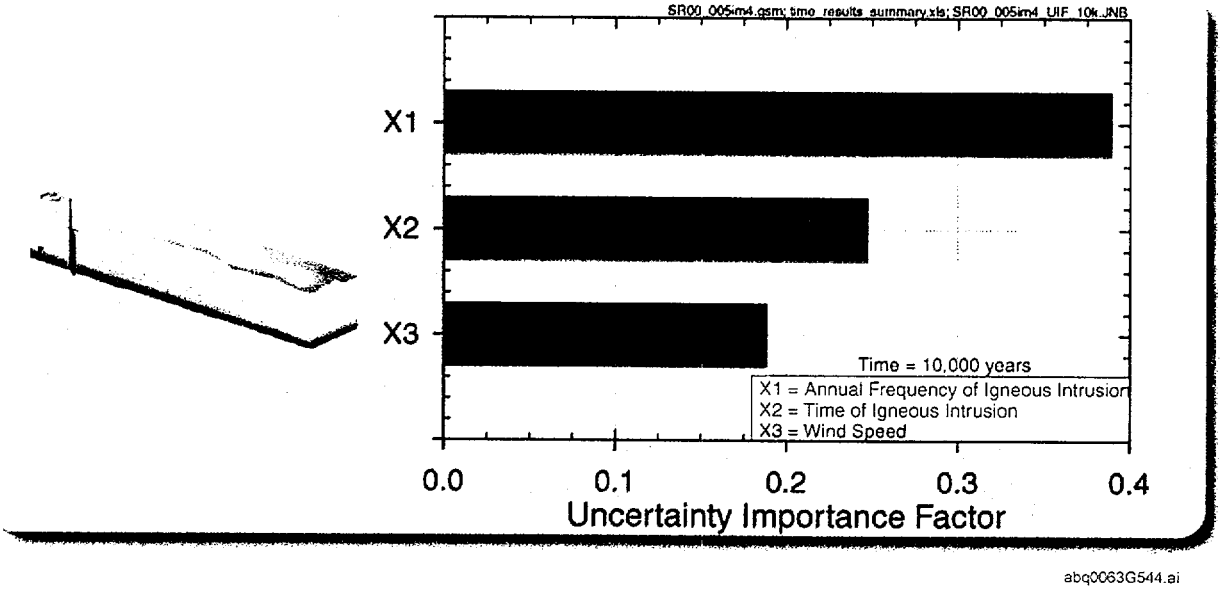

abq0063G544

Figure 5.1-20. Bar Chart Showing Uncertainty Importance Factors for the Most Important Variables at 10,000 Years for Total Dose, Igneous Scenario

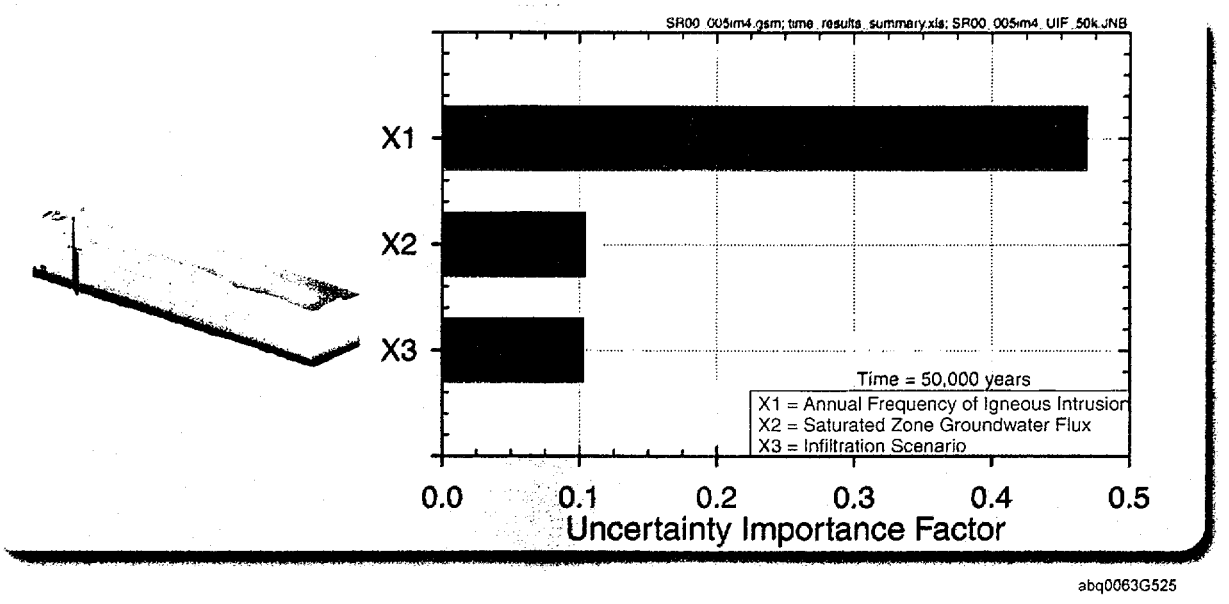

abq0063G525

Figure 5.1-21. Bar Chart Showing Uncertainty Importance Factors for the Most Important Variables at 50,000 Years for Total Dose, Igneous Scenario

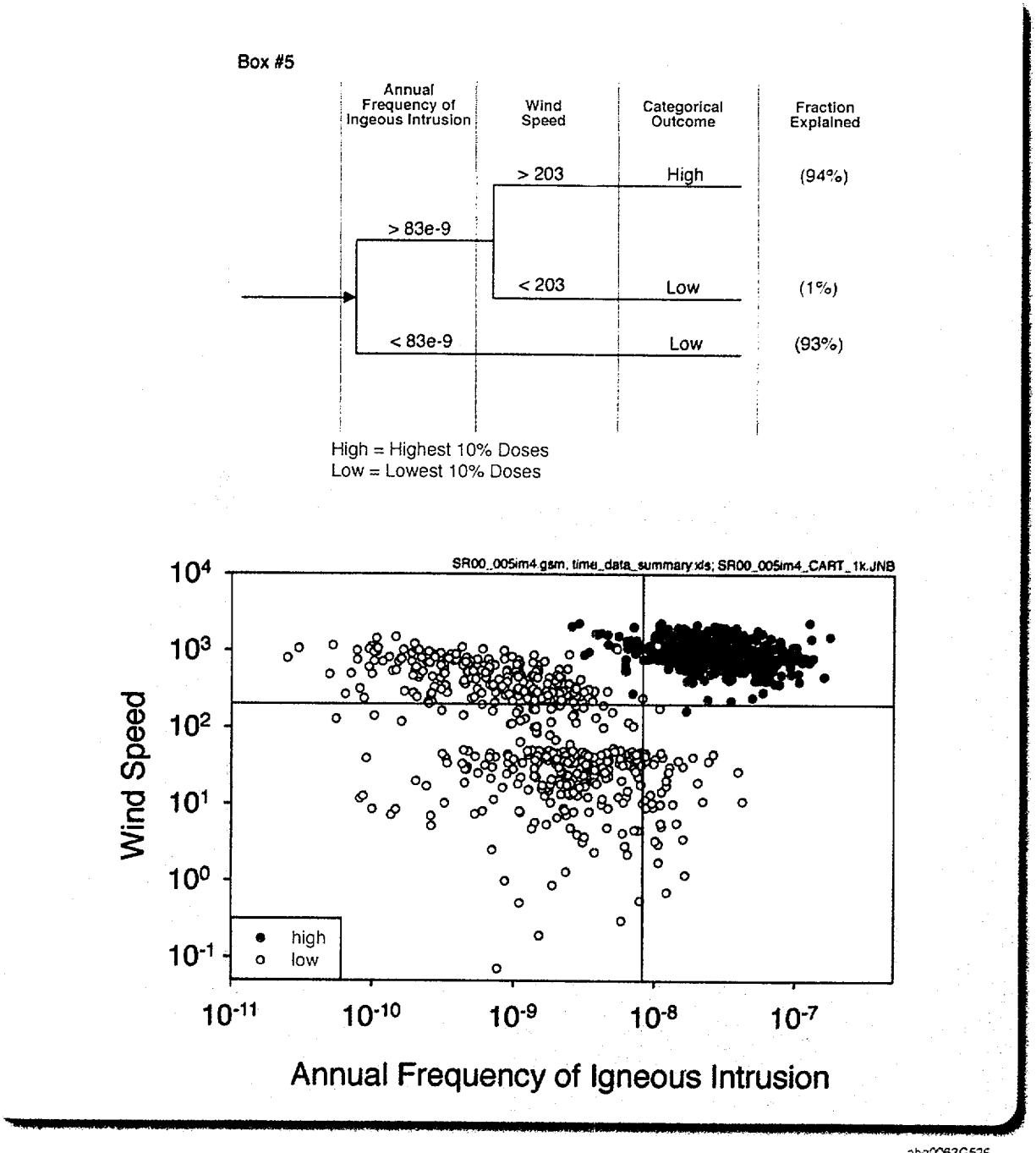

abq0063G526

Figure 5.1-22. Decision Tree Summarizing Classification Tree Analysis (Top) and Partition Plot Showing Clusters of Low-Dose (10th-Percentile and Lower) and High-Dose (90th-Percentile and Higher) Outcomes (Bottom) for the Two Most Important Variables at 1,000 Years, Igneous Scenario

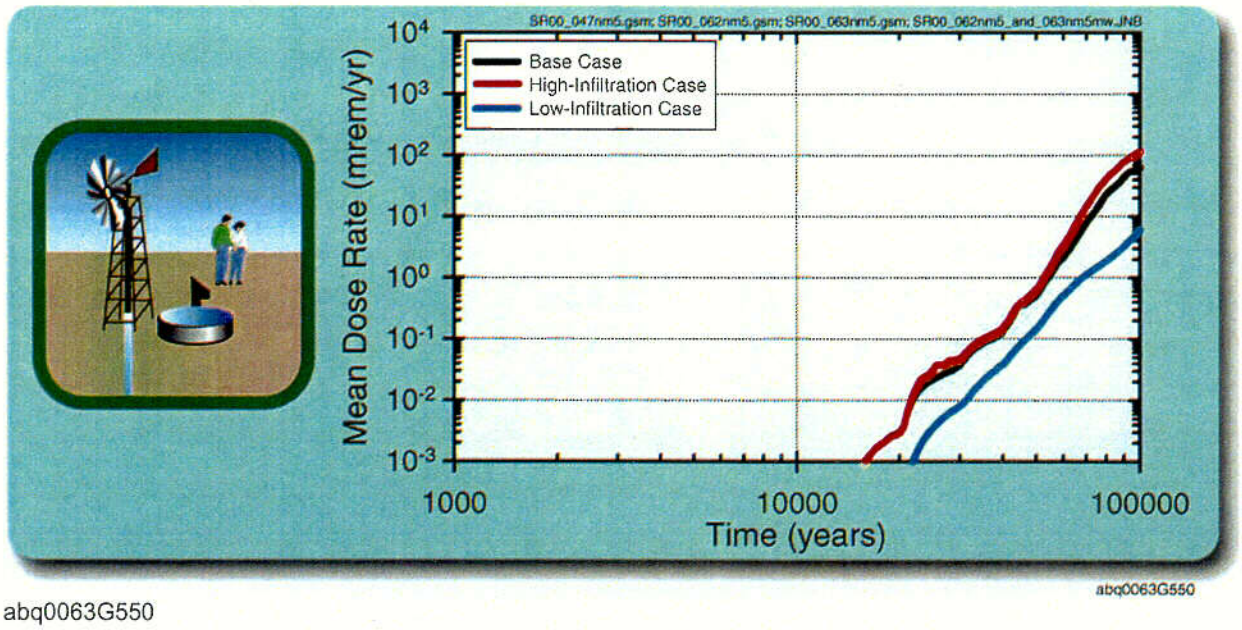

abq0063G550

Figure 5.2-1. Comparison of Mean Dose Rate for High- and Low-Infiltration Cases and Base Case

L-51

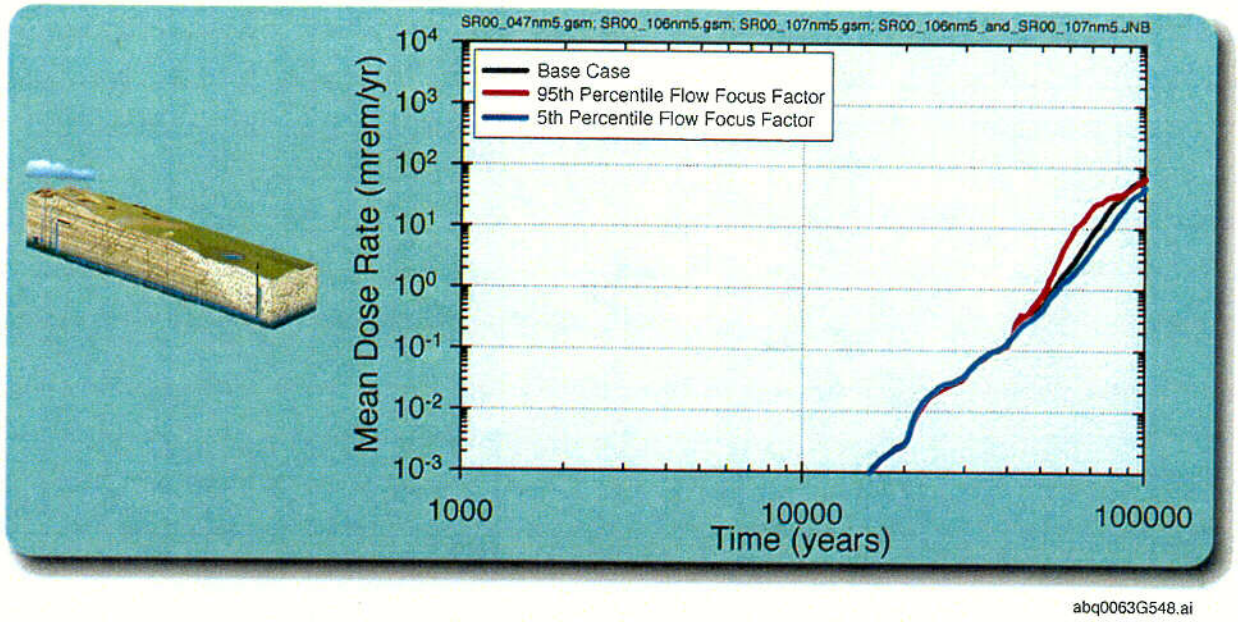

abq0063G548

Figure 5.2-2a. Comparison of Mean Dose Rate for Flow-Focusing Sensitivity Cases and Base Case

C-52

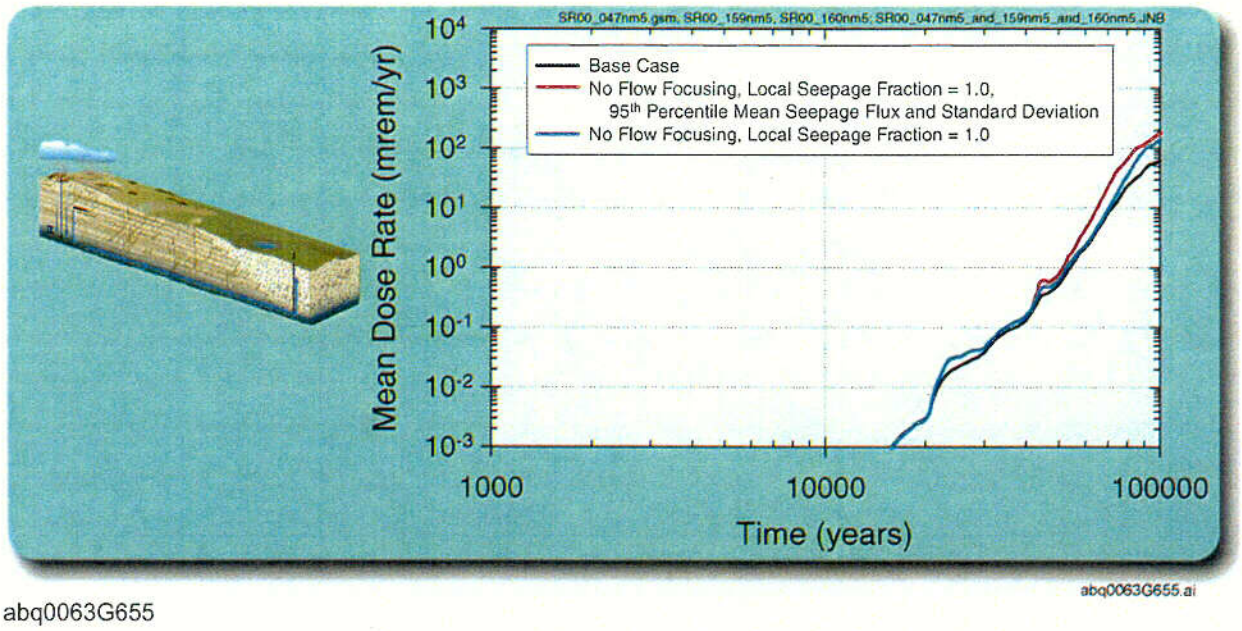

abq0063G655

Figure 5.2-2b. Comparison of Mean Dose Rate for Base Case with Sensitivity Cases having no Flow Focusing and no Local Spatial Variability of the Seepage Fraction

C-53

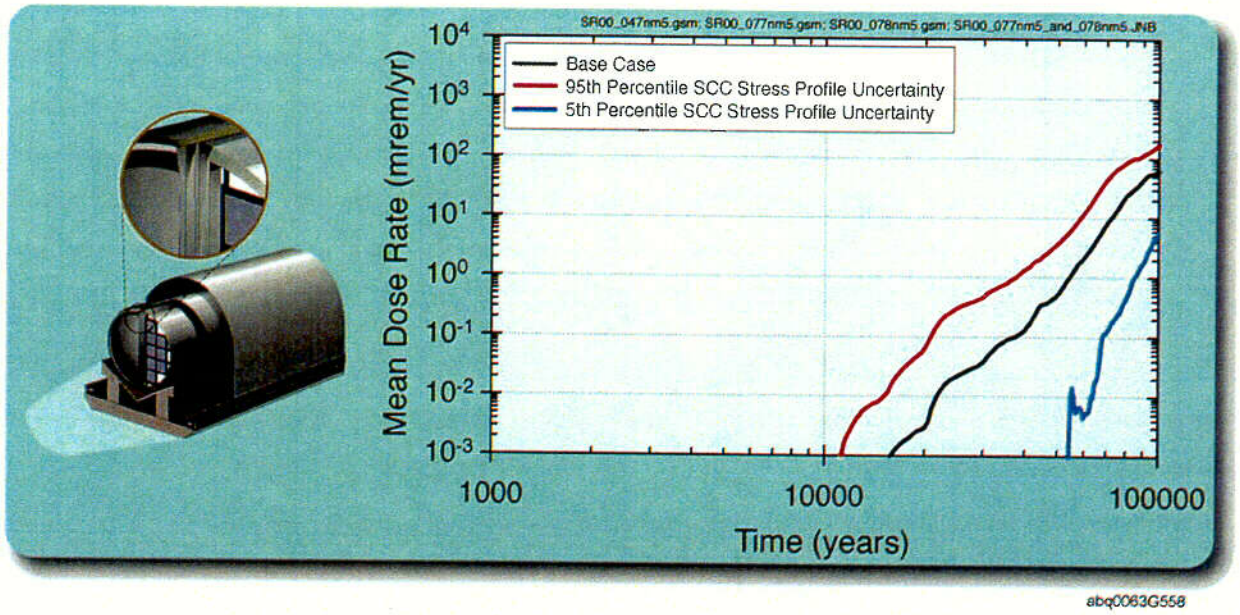

abq0063G558

Figure 5.2-3. Sensitivity of the Mean Dose Rate Profile to the Uncertainty of the Residual Hoop Stress and Stress Intensity Factor in the Outer Lid and Inner Lid Closure Welds

L-54

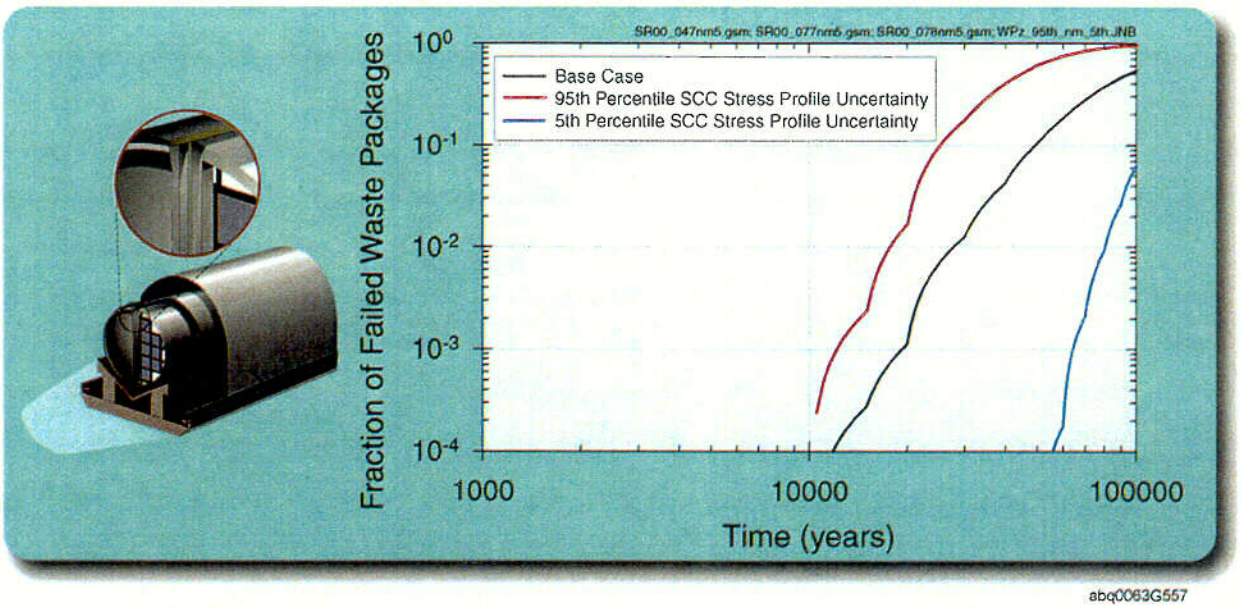

abq0063G557

Figure 5.2-4. Sensitivity of the Mean Waste Package Failure Profile to the Uncertainty of the Residual Hoop Stress and Stress Intensity Factor in the Outer Lid and Inner Lid Closure Welds

L-55

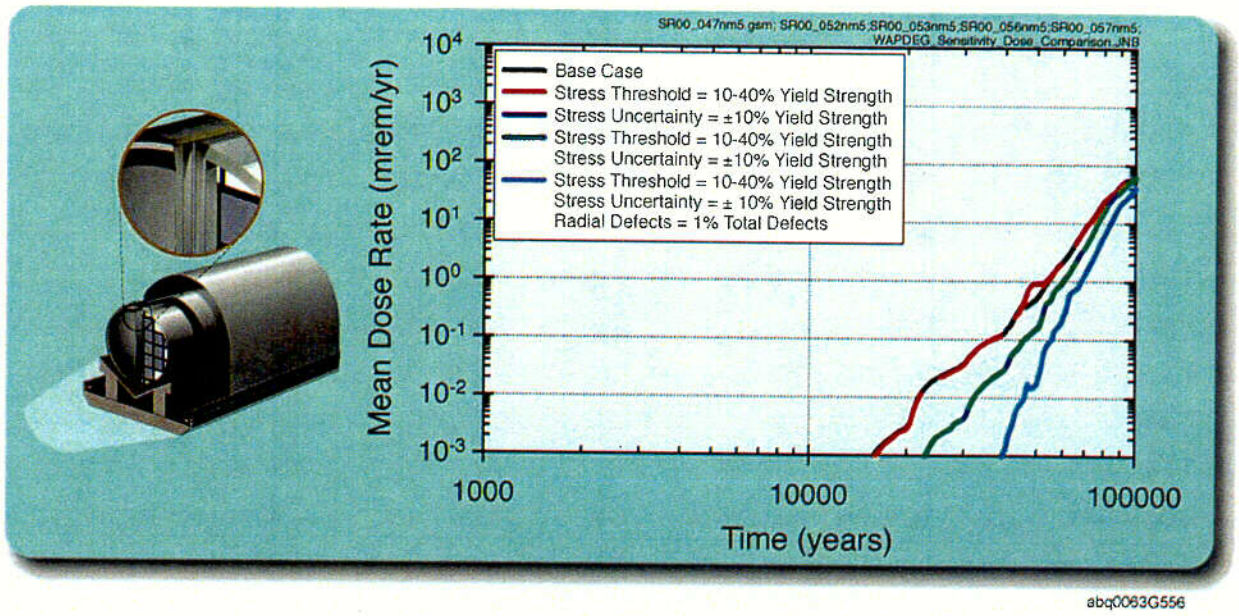

abq0063G556

Figure 5.2-5. Sensitivity of the Mean Dose Rate Profile to Alternative Uncertainty Ranges of the Stress Corrosion Cracking Model Parameters for the Waste Package Closure-Lid Welds

C-56

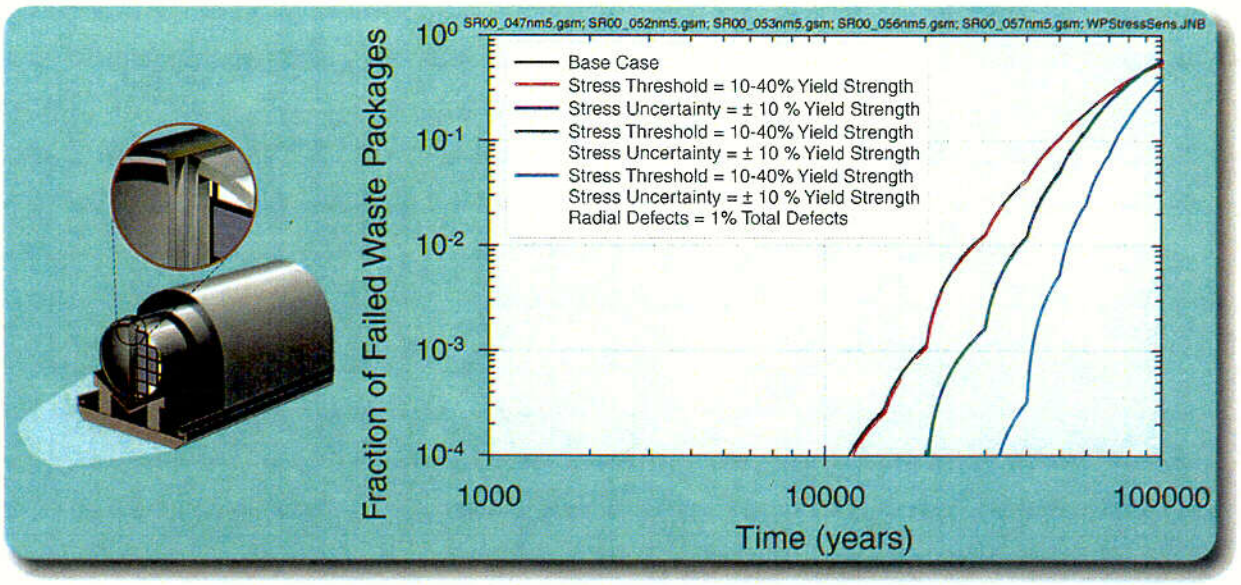

abq0063G555

abq0063G555

Figure 5.2-6. Sensitivity of the Mean Waste Package Failure Profile to Alternative Uncertainty Ranges of the Stress Corrosion Cracking Model Parameters for the Waste Package Closure-Lid Welds

C-57

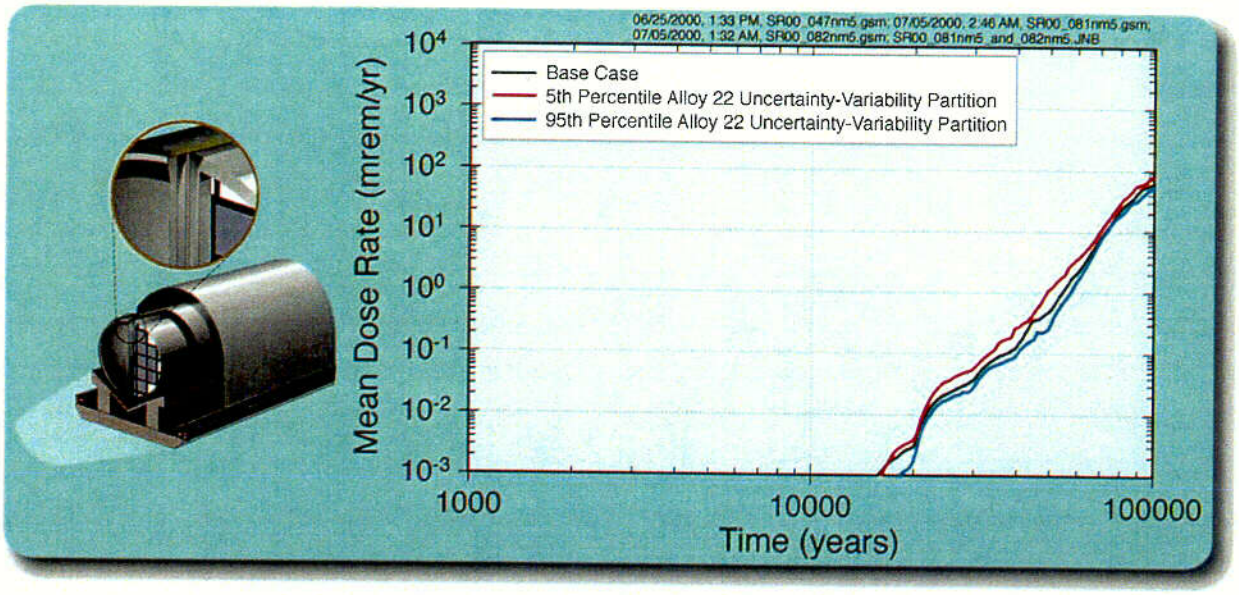

abq0063G554.ai

abq0063G554

Figure 5.2-7. Sensitivity of the Mean Dose Rate Profile to the Uncertainty and Variability Partitioning Ratio for Alloy-22 General Corrosion Rate

C-58

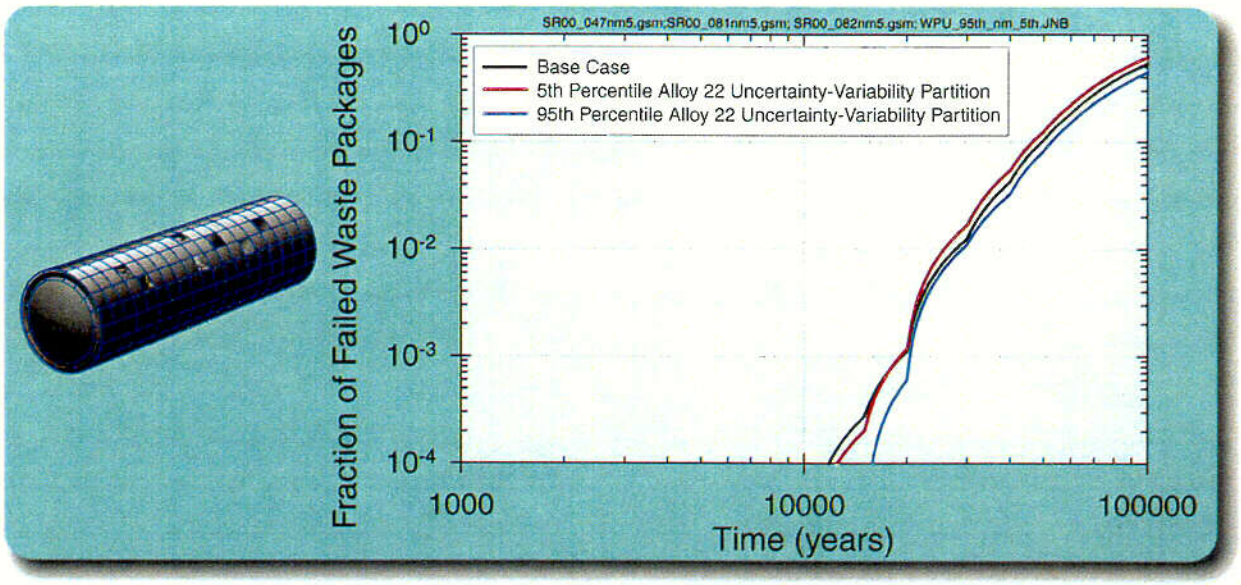

abq0063G553

Figure 5.2-8. Sensitivity of the Mean Waste Package Failure Profile to the Uncertainty and Variability Partitioning Ratio for Alloy-22 General Corrosion Rate

C-59

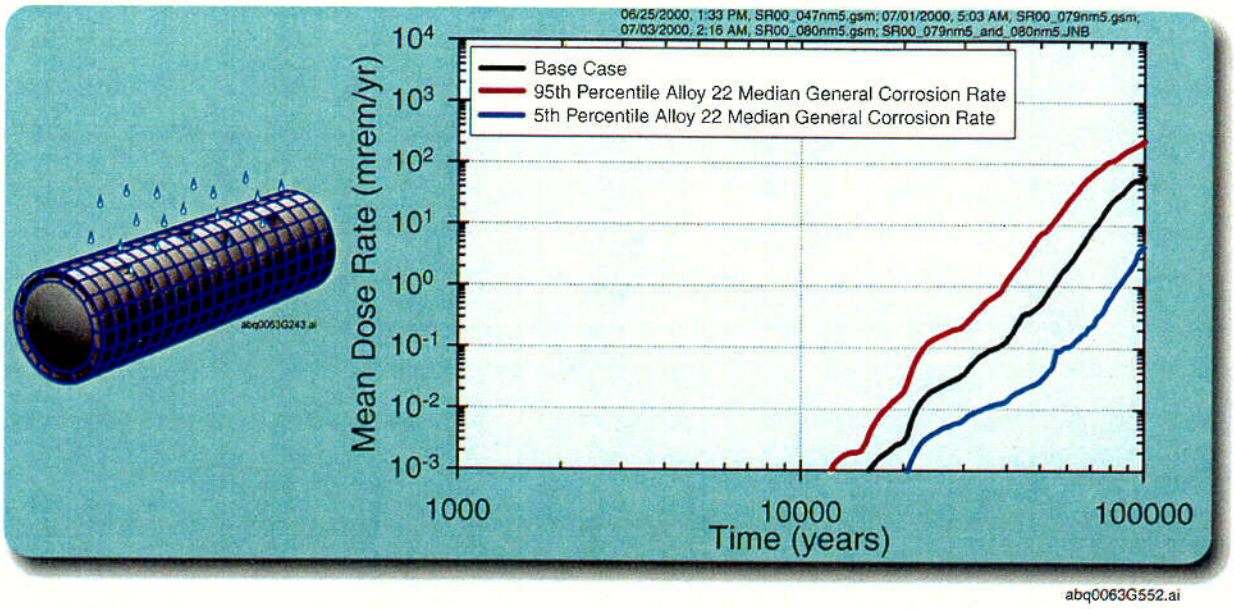

abq0063G552

Figure 5.2-9. Sensitivity of the Mean Dose Rate Profile to the Median General Corrosion Rate of Alloy-22

C-60

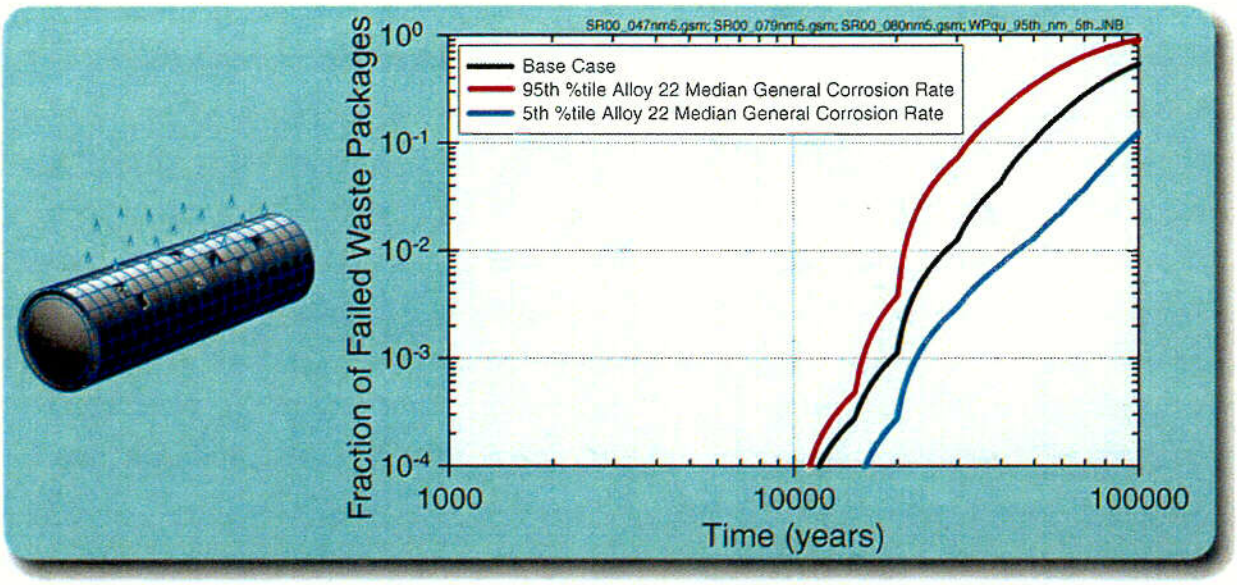

abq0063G551

Figure 5.2-10. Sensitivity of the Mean Waste Package Failure Profile to the Median General Corrosion Rate of Alloy-22

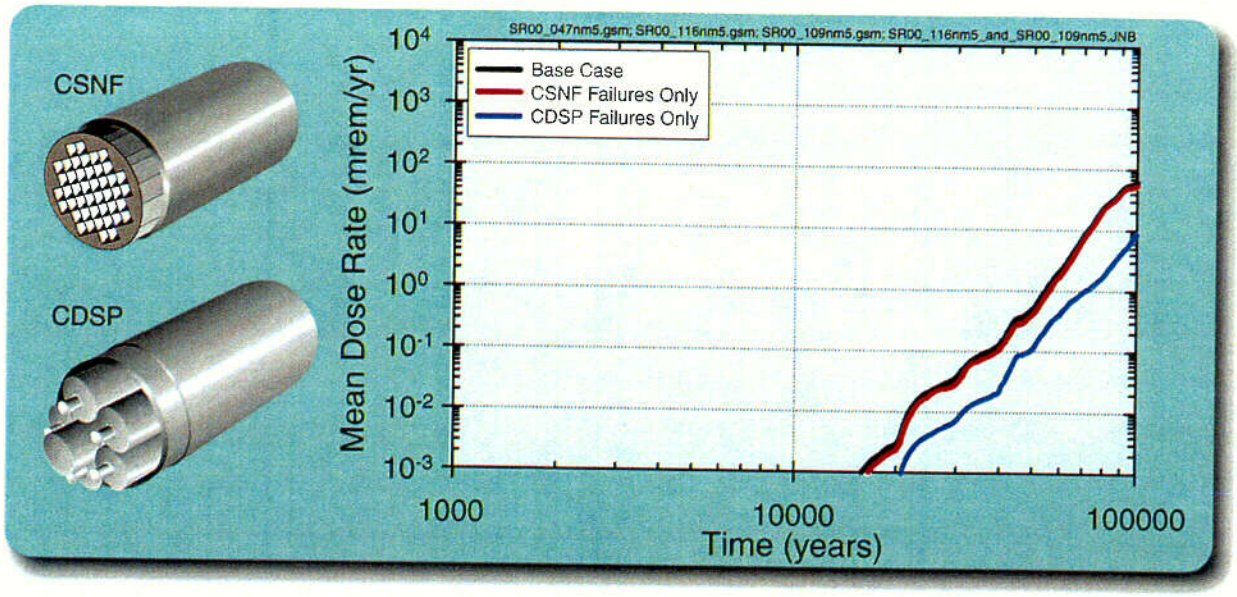

abq0063G559

abq0063G559.eps

Figure 5.2-11. Mean Base Case Dose Rate Compared to Cases with Commercial Spent Nuclear Fuel Package Failures only and Co-Disposal Package Failures only

C-62

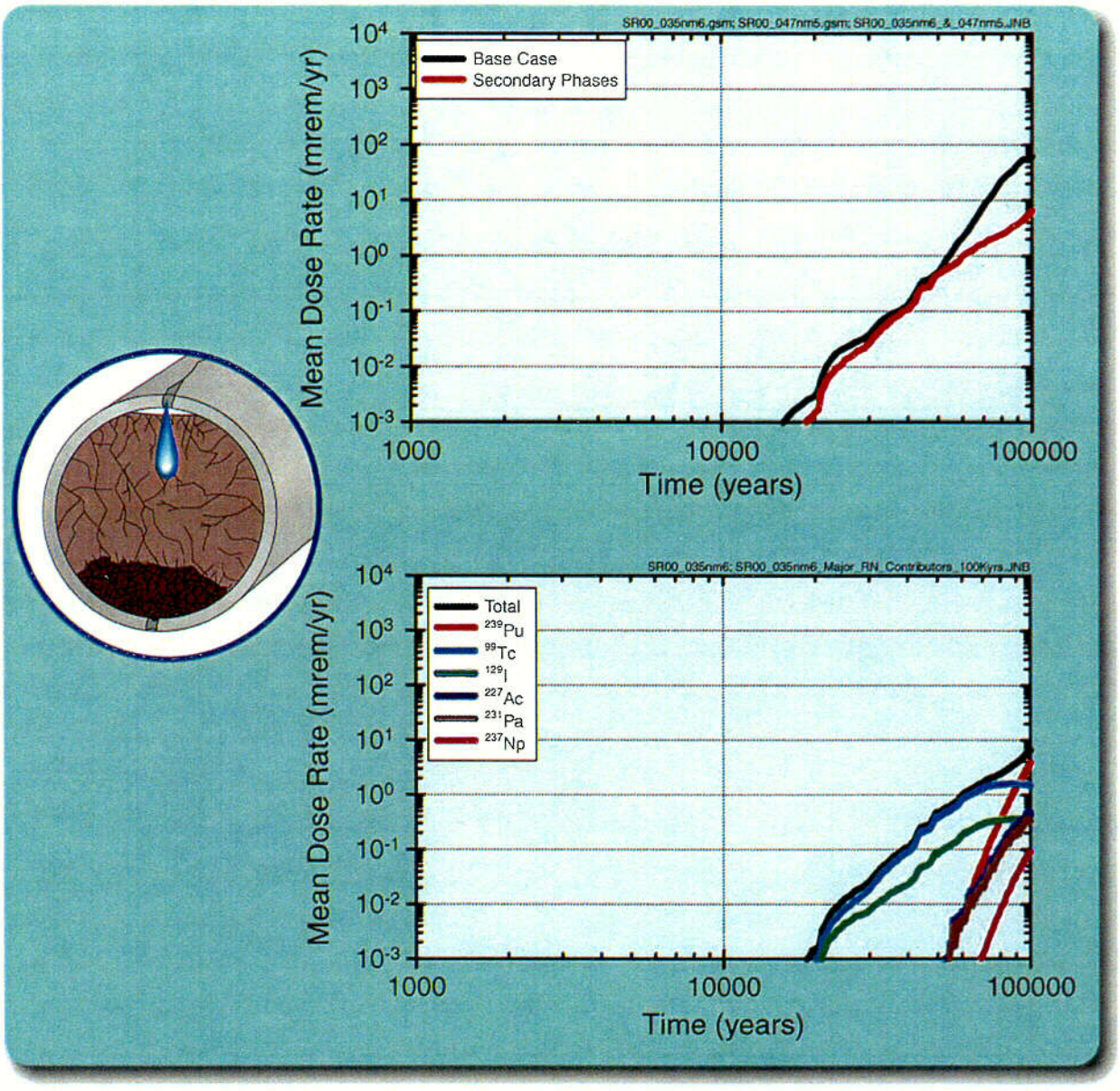

abq0063G664

Figure 5.2-12. Mean Dose Rate of Major Radionuclide Contributors for the Secondary Mineral Phase Sensitivity Case

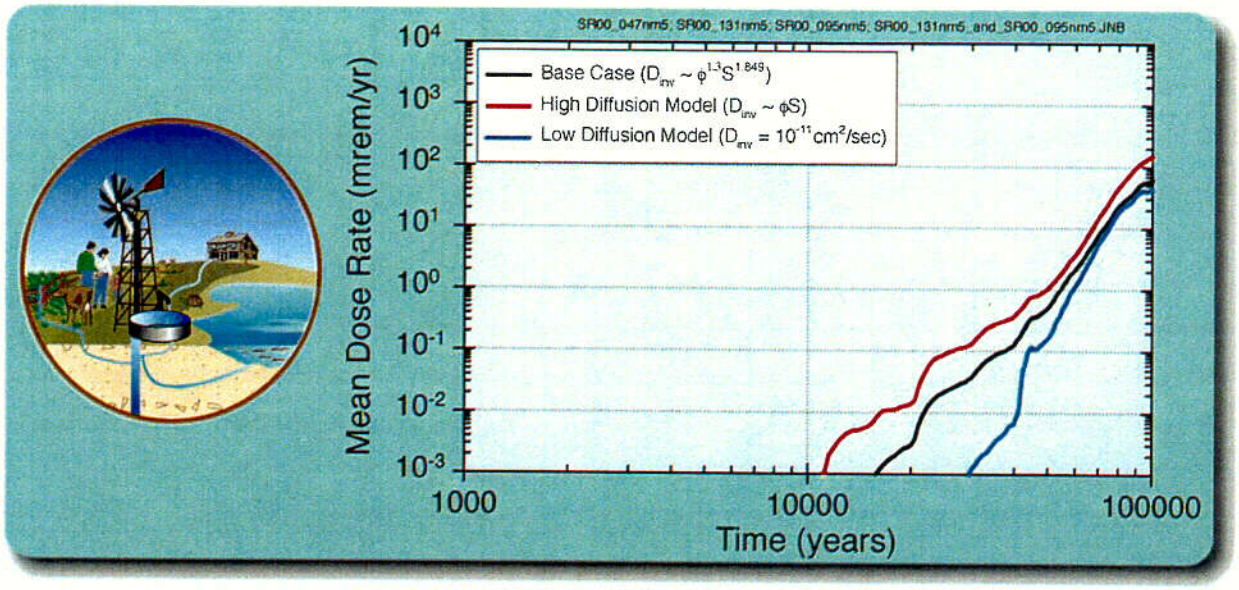

abq0063G560.ai

abq0063G560

Figure 5.2-13. Comparison of Mean Dose Rates for Three Invert Diffusion Models

C-64

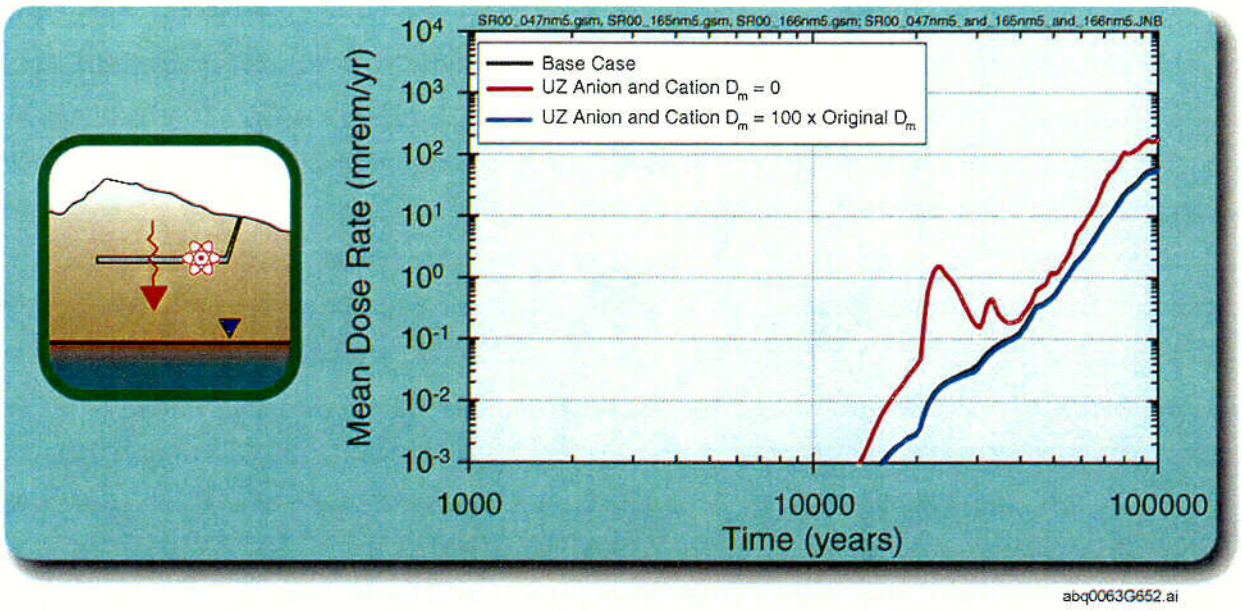

abq0063G652

Figure 5.2-14. Sensitivity to Matrix Diffusion in the Unsaturated Zone

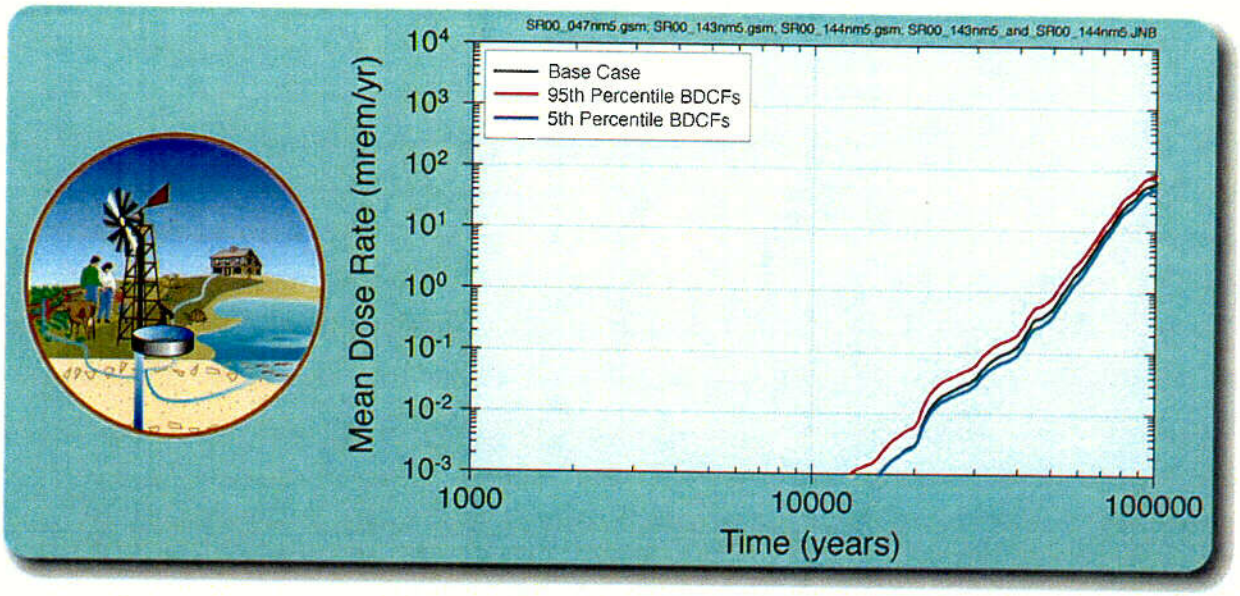

abq0063G562

Figure 5.2-15. Sensitivity to Biosphere Dose Conversion Factors

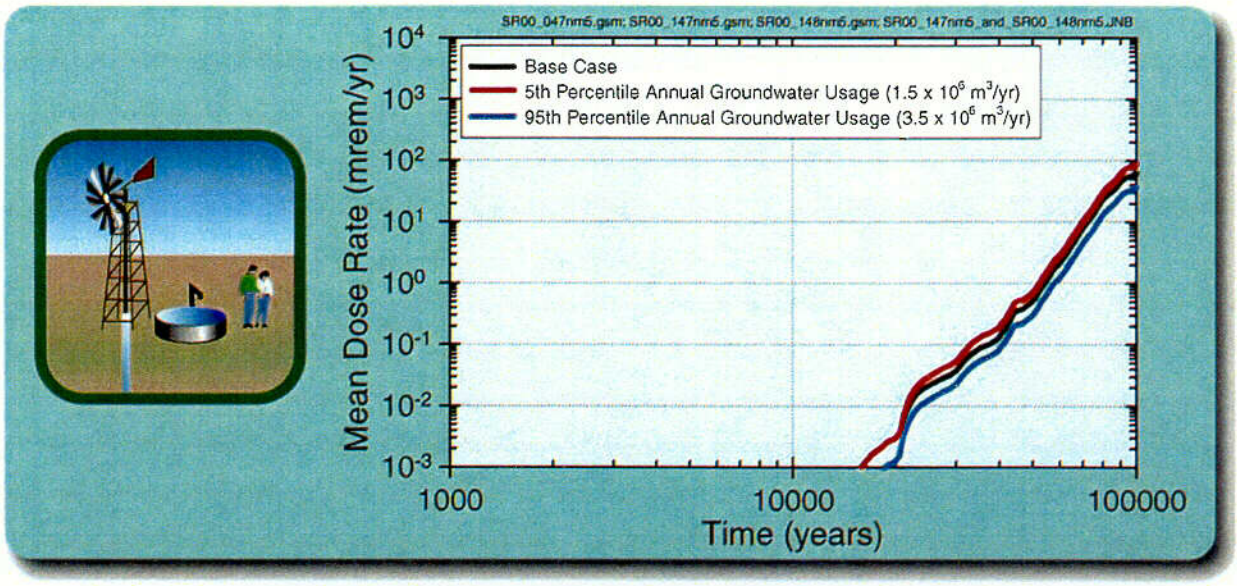

abq0063G561

Figure 5.2-16. Sensitivity to Groundwater Usage Volume

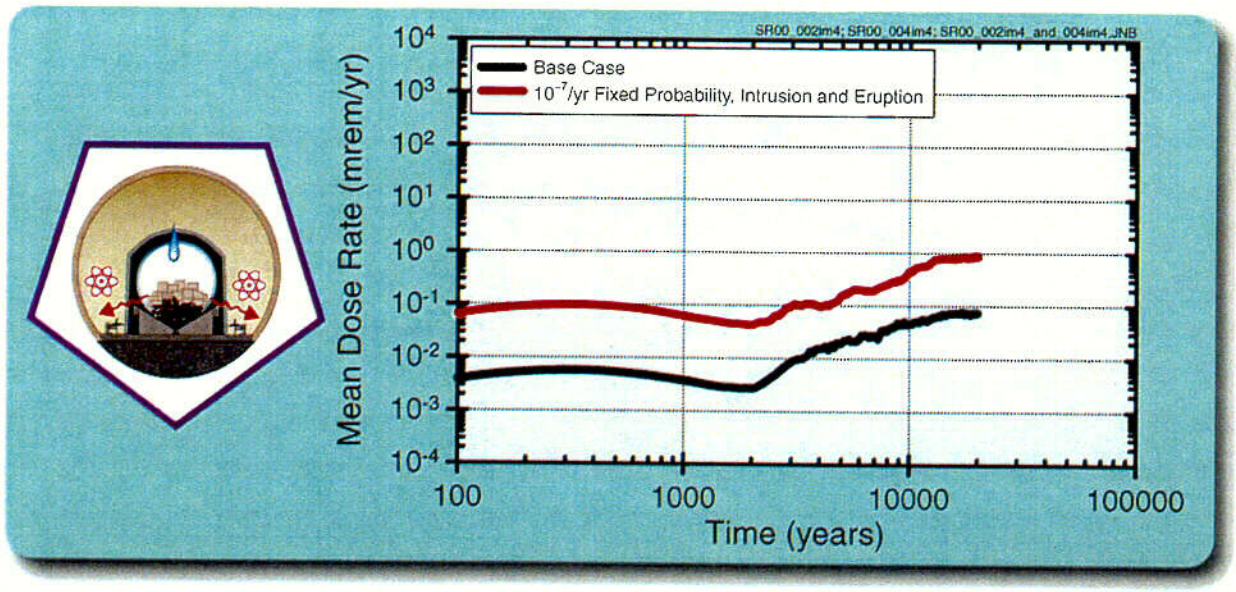

abq0063G598

Figure 5.2-17. Comparison of Total System Performance Assessment-Site Recommendation Probability-Weighted Mean Annual Igneous Dose Rate with the Dose Rate Calculated using a Fixed Annual Probability of Igneous Intrusion and Eruption Equal to 10^{-7}

C-68

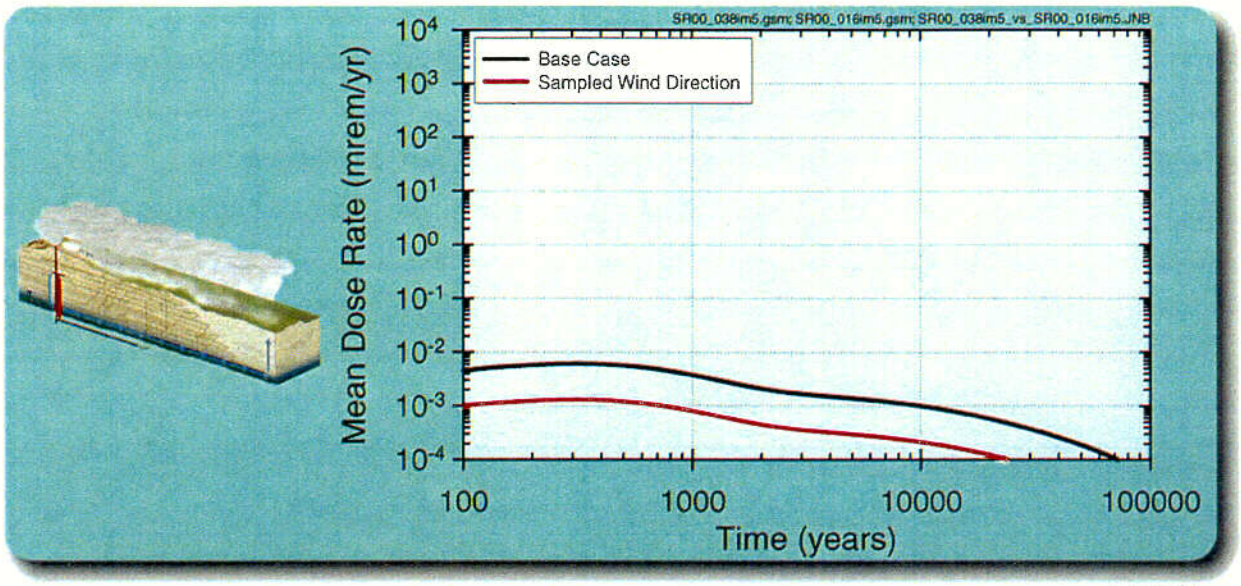

abq0063G603

Figure 5.2-18. Comparison of Total System Performance Assessment-Site Recommendation Probability-Weighted Mean Annual Eruptive Dose Rate with the Dose Rate Calculated using a Sampled Wind Direction, Rather than Assuming that the Wind always Blows Toward the Location of the Critical Group

L-69

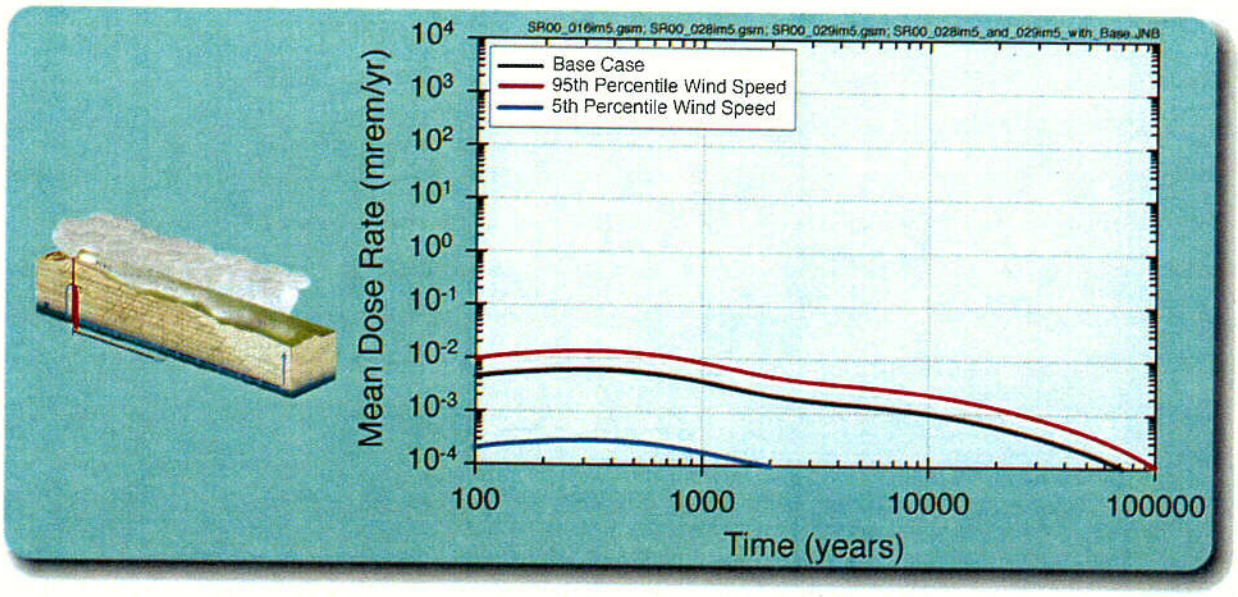

abq0063G602

Figure 5.2-19. Comparison of Total System Performance Assessment-Site Recommendation Probability-Weighted Mean Annual Eruptive Dose Rate with the Dose Rate Calculated using Wind Speed Fixed at the 5th and 95th-Percentile Values from the Distribution

L-70

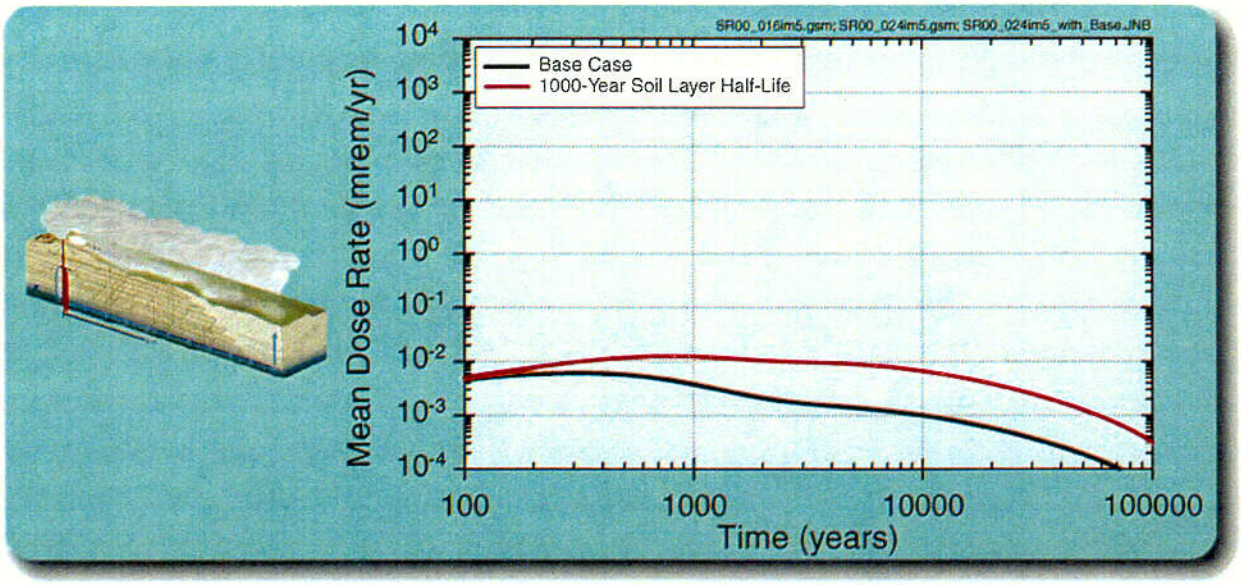

abq0063G605

Figure 5.2-20. Comparison of Total System Performance Assessment-Site Recommendation Probability-Weighted Mean Annual Eruptive Dose Rate with the Dose Rate Calculated using a 1,000-Year Mean Soil Removal Time Following Deposition of the Ash Layer

C-71-

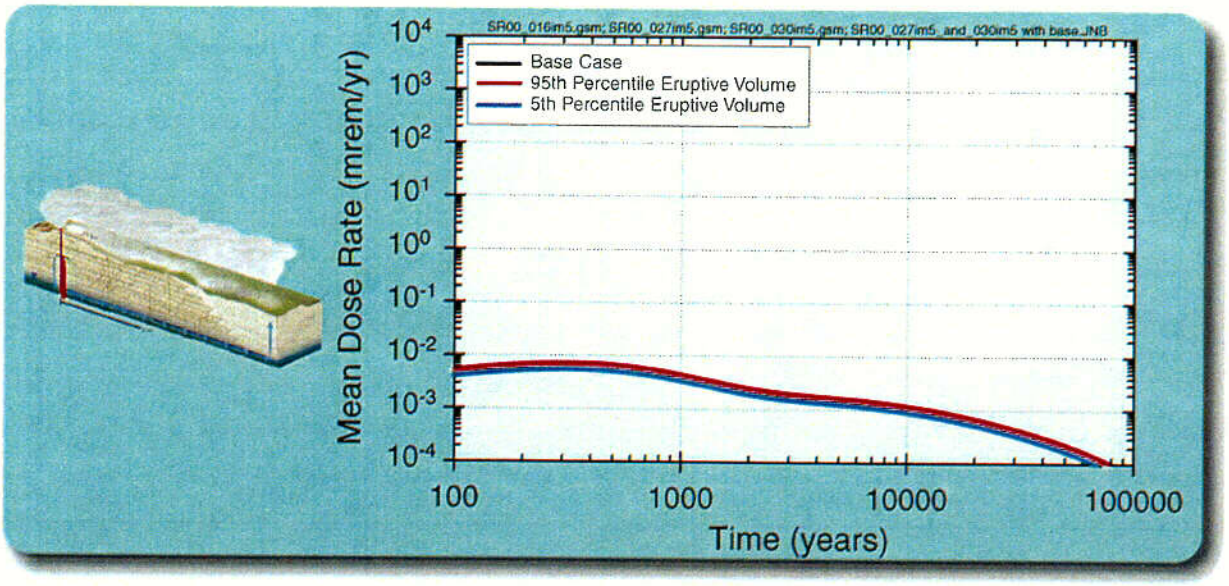

abq0063G597

Figure 5.2-21. Comparison of Total System Performance Assessment-Site Recommendation Probability-Weighted Mean Annual Igneous Dose Rate with the Dose Rate Calculated using the Volume of Erupted Material (which Characterizes the Power of the Eruptive Event) is Fixed at the 5th and 95th-Percentiles of the Distribution used in the TSPA-SR

L-72

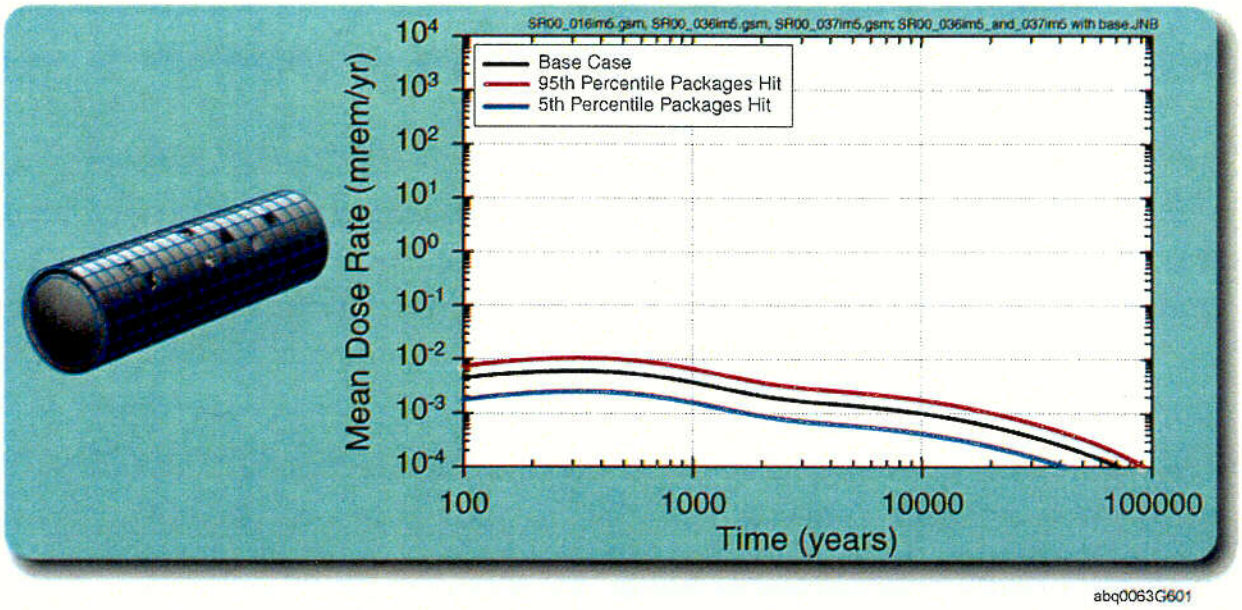

abq0063G601

Figure 5.2-22. Comparison of Total System Performance Assessment-Site Recommendation Probability-Weighted Mean Annual Eruptive Dose Rate with the Dose Rate Calculated Assuming that the Number of Packages Damaged for the Direct Release Event is Fixed at the 5th and 95th-Percentiles of the Distribution used in the TSPA-SR

L-73

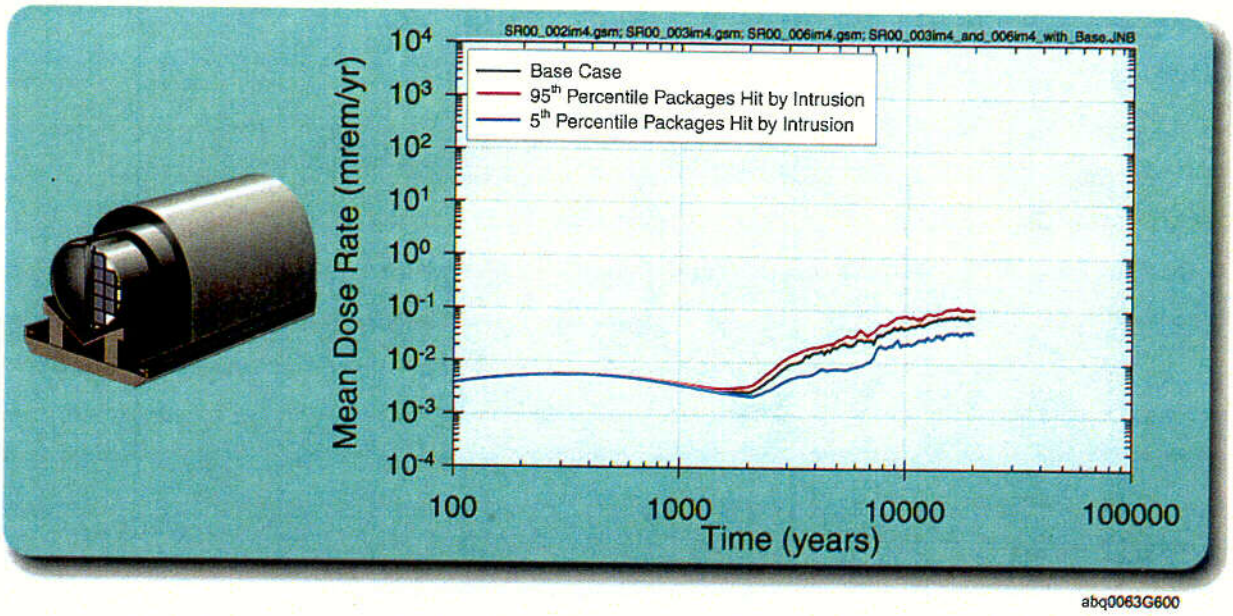

abq0063G600

Figure 5.2-23. Comparison of Total System Performance Assessment-Site Recommendation Probability-Weighted Mean Annual Igneous Dose Rate with the Dose Rate Calculated Assuming that the Number of Waste Packages Damaged by Intrusion is Fixed at the 5th and 95th-Percentiles of the Distribution used in the TSPA-SR

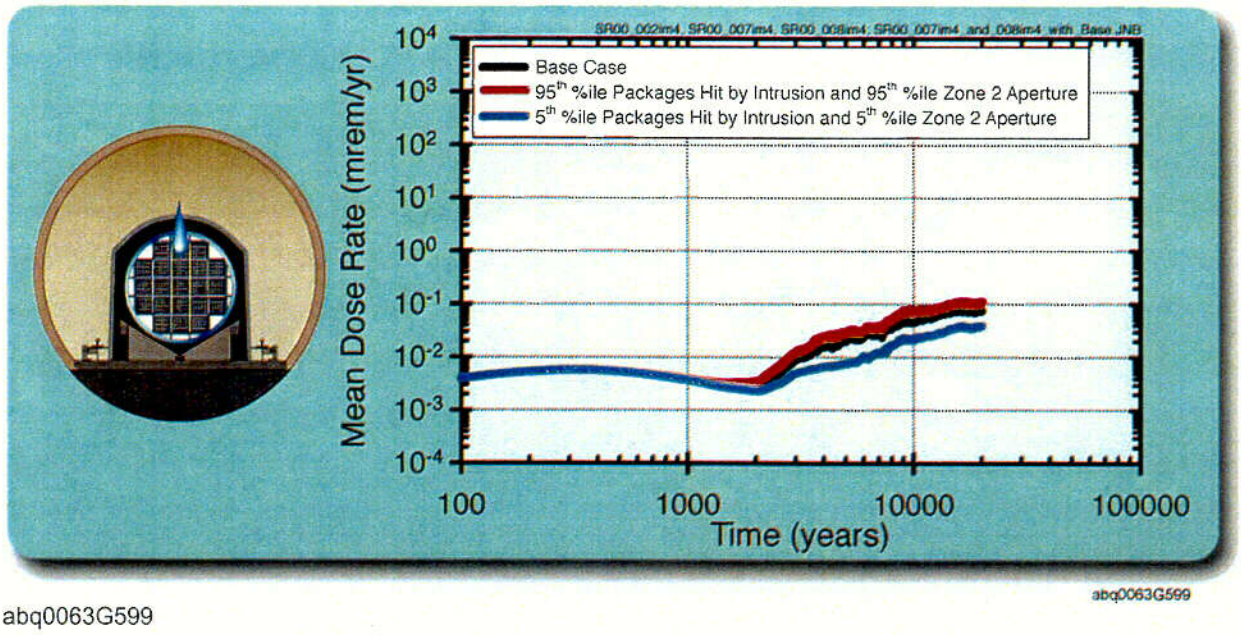

abq0063G599

Figure 5.2-24. Comparison of Total System Performance Assessment-Site Recommendation Probability-Weighted Mean Annual Igneous Dose Rate with the Dose Rate Calculated Assuming that the Diameter of the Aperture in Waste Packages Damaged by Intrusion and the Number of Waste Packages Damaged in Zones 1 and 2 by Intrusion are Fixed at the 5th and 95th-Percentiles of the Distributions used in the TSPA-SR

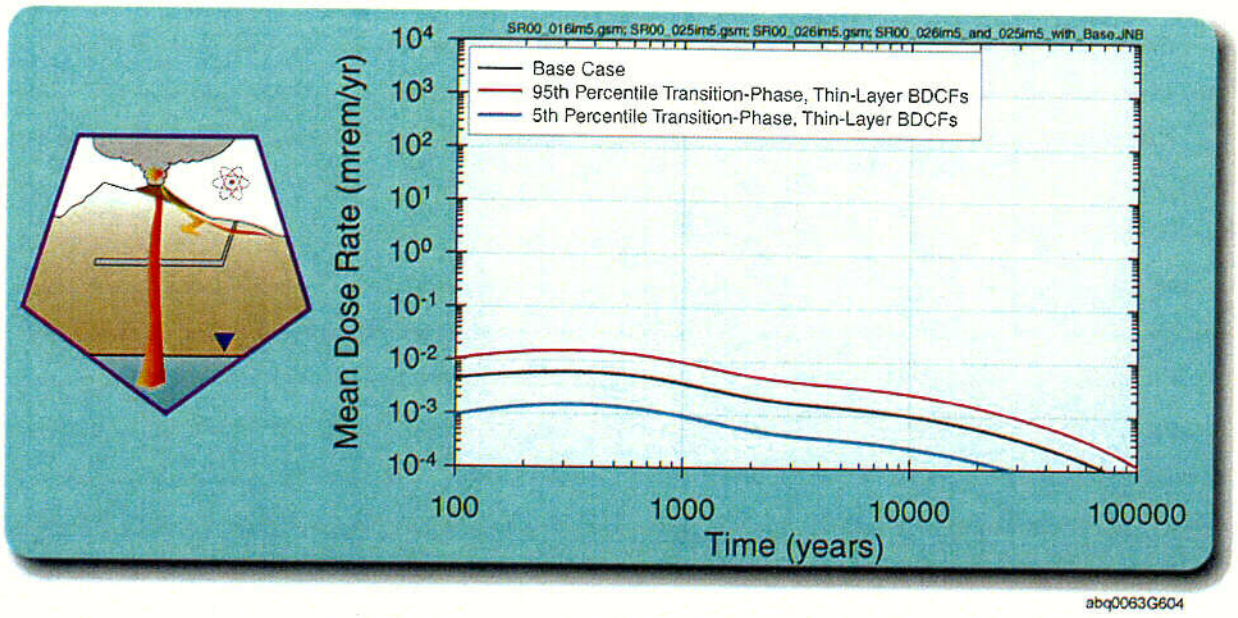

abq0063G604

Figure 5.2-25. Comparison of Total System Performance Assessment-Site Recommendation Probability-Weighted Mean Annual Eruptive Dose Rate with the Dose Rate Calculated Assuming that the Transition-Phase Thin-Layer BDCF's are Fixed at the 5th and 95th-Percentiles of the Distributions used in the TSPA-SR

C-76

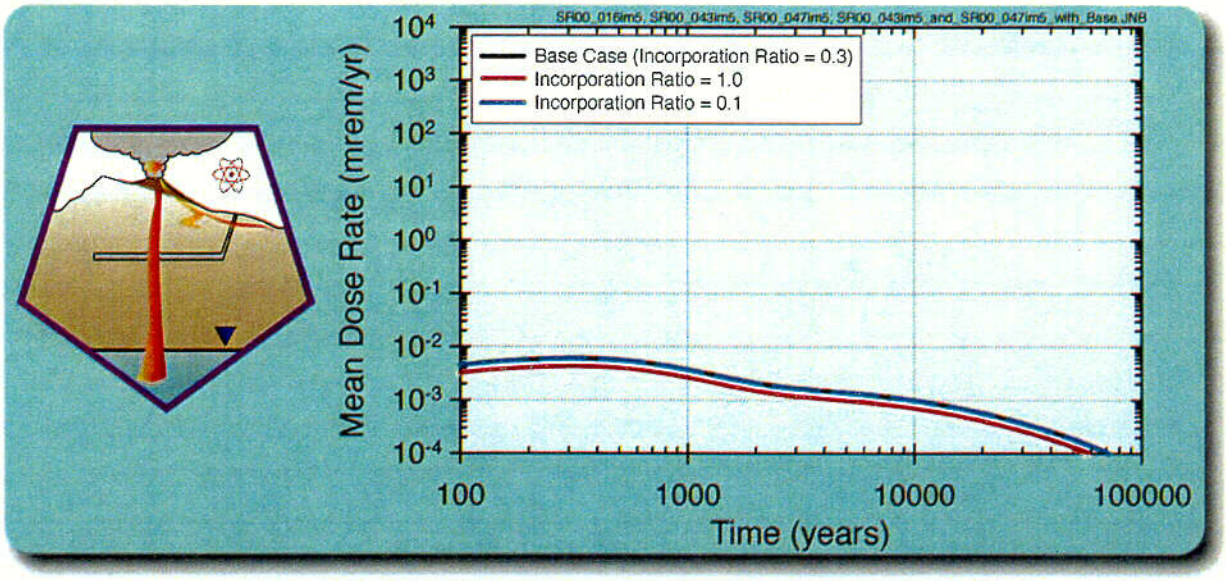

abq0063G653

Figure 5.2-26. Comparison of Total System Performance Assessment-Site Recommendation Probability-Weighted Mean Annual Eruptive Dose Rate with Dose Rates Calculated Using Incorporation Ratios of 0.3 (Base Case), 0.1, and 1.0.

L-77

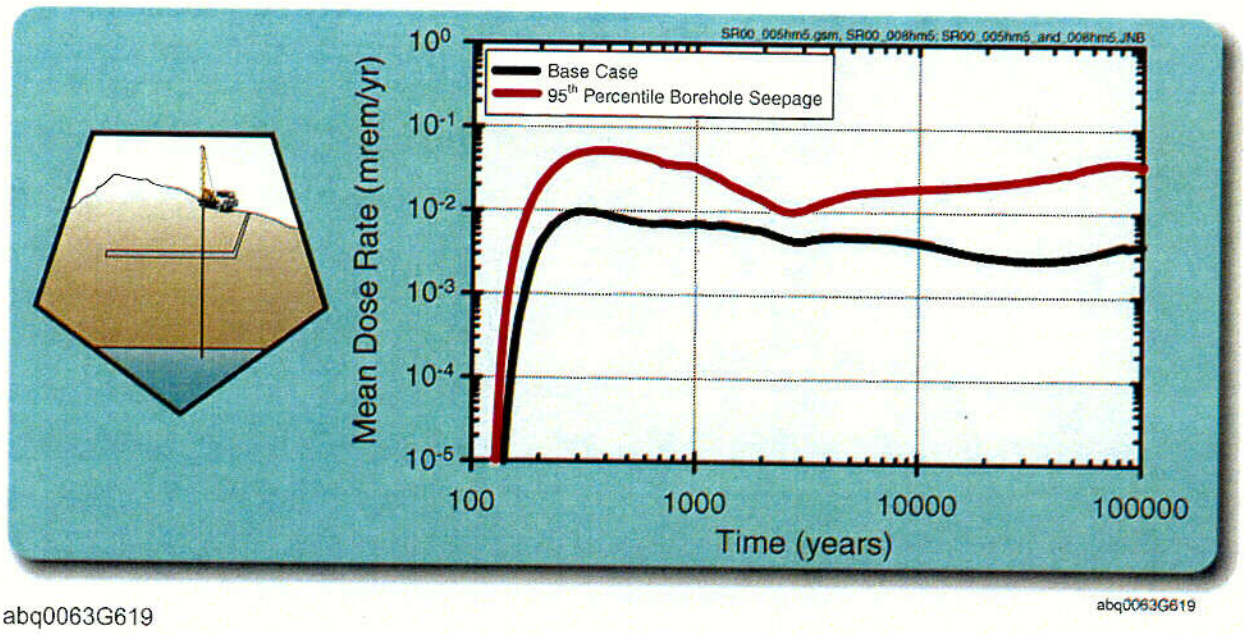

abq0063G619

Figure 5.2-27 Sensitivity Analysis of Mean Annual Dose for the Human Intrusion Base Case (an Intrusion Occurs at 100 Years after Potential Repository Closure) with the Infiltration Rate Fixed at the 95th-Percentile Value

C-78

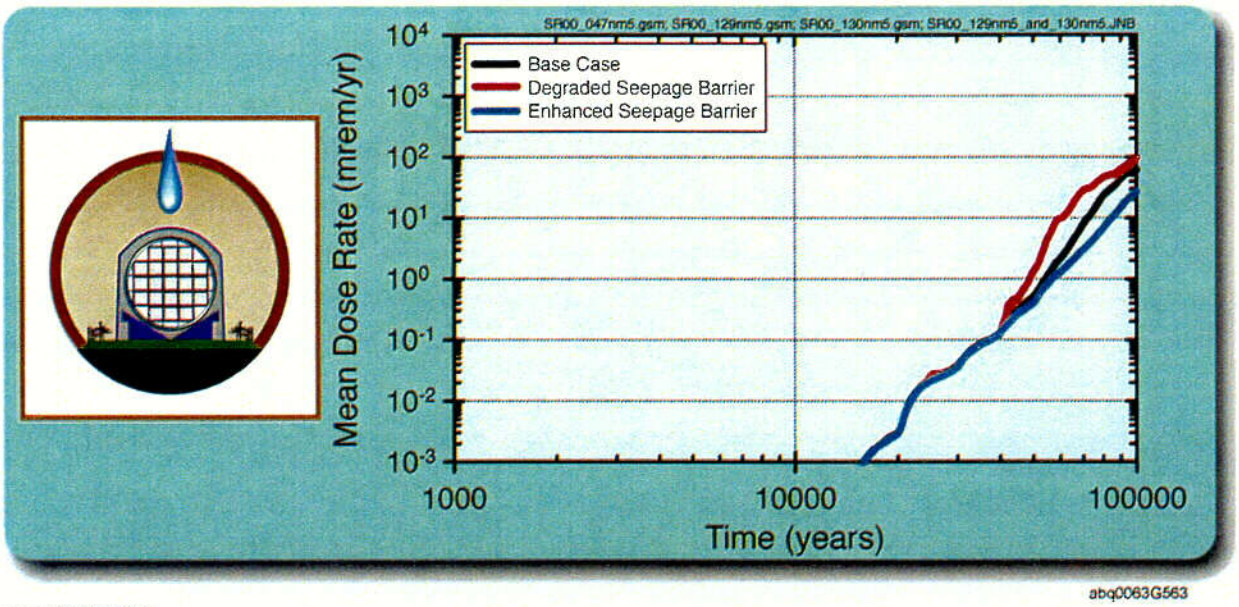

abq0063G563

Figure 5.3-1. Comparison of Mean Dose for Degraded and Enhanced Seepage Cases with the Base Case

L-79

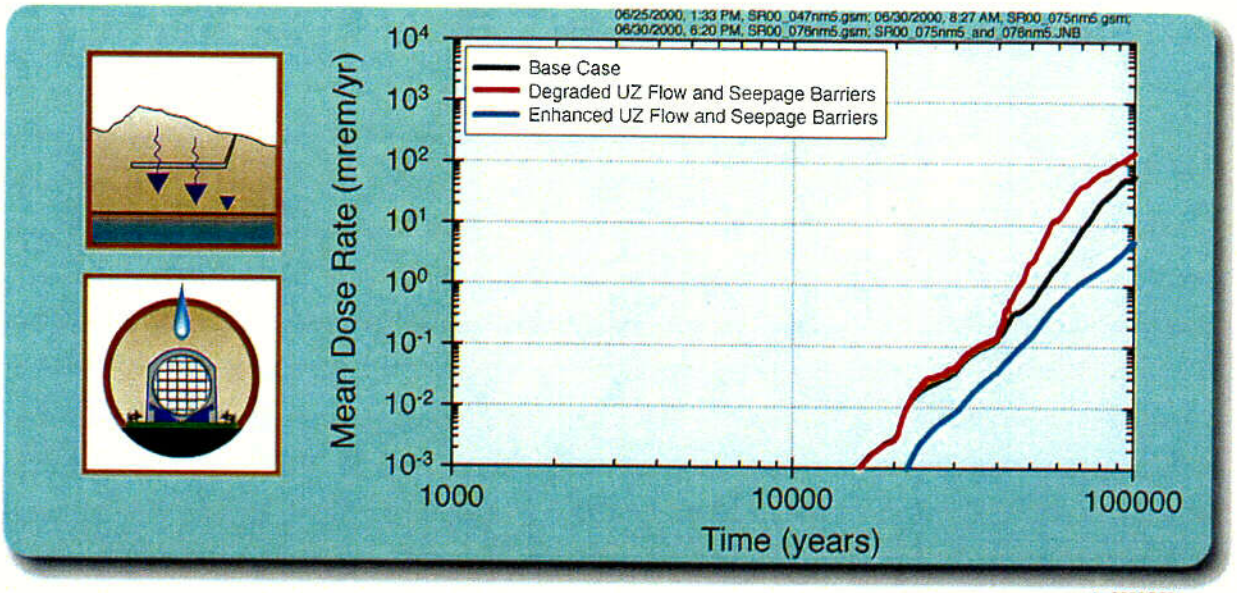

abq0063G564

Figure 5.3-2. Comparison of Mean Dose for Degraded and Enhanced Unsaturated Zone Flow and Seepage Cases with the Base Case

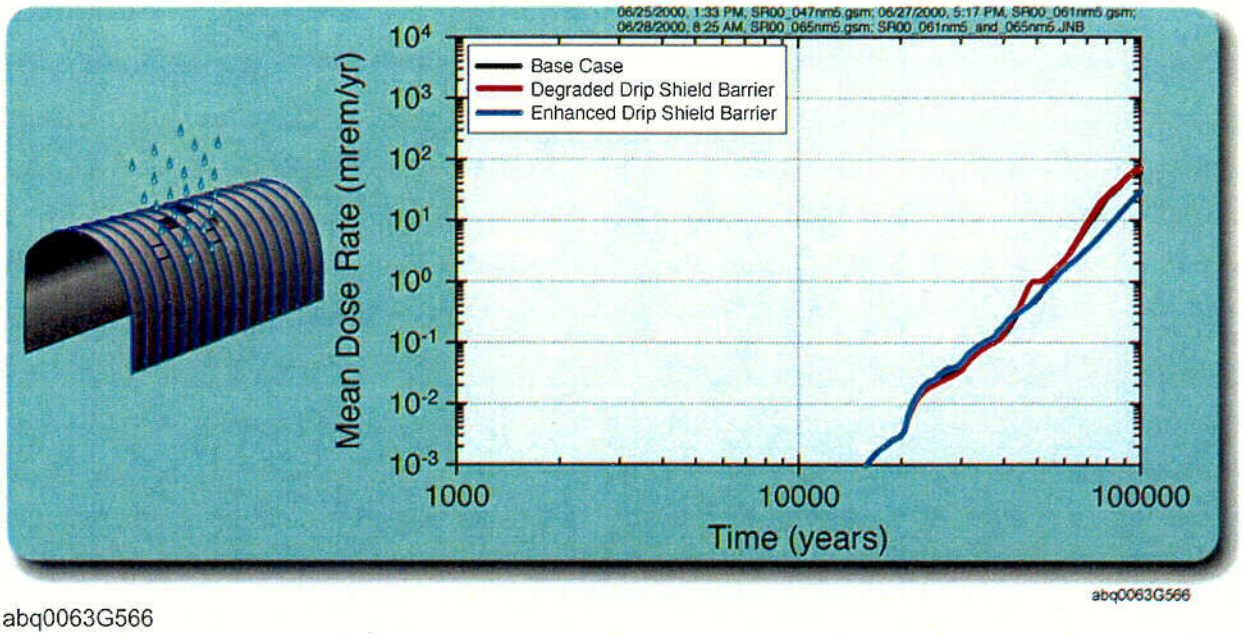

abq0063G566

Figure 5.3-3. Sensitivity of the Predicted Mean Dose Rate Profile to the Degraded and Enhanced Drip Shield Cases

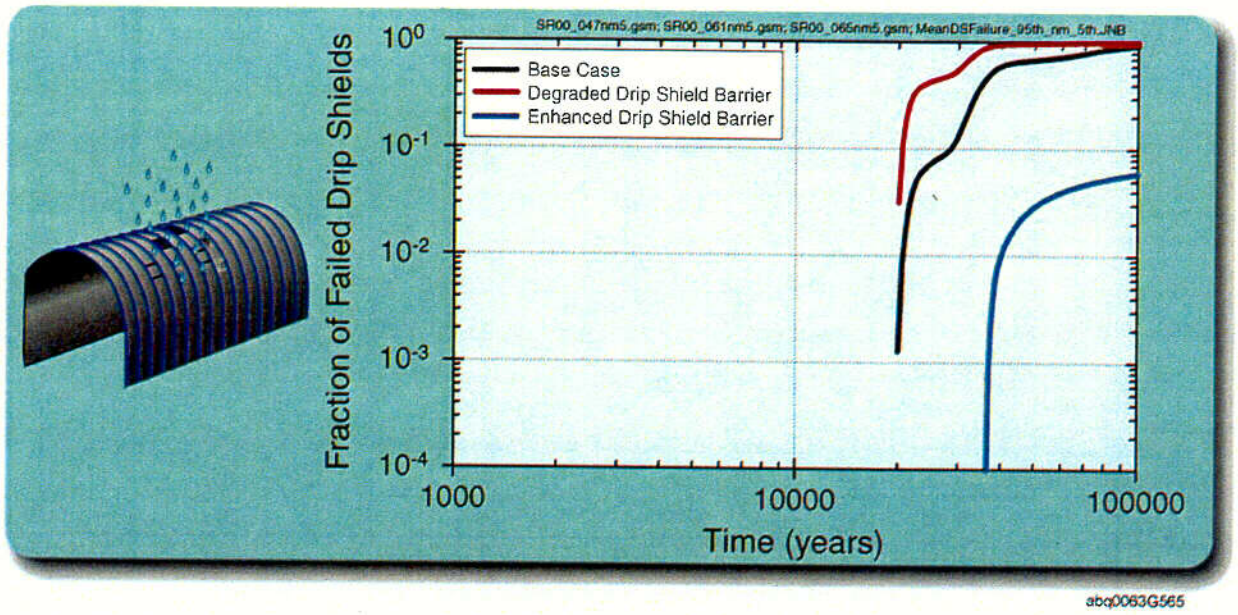

abq0063G565

Figure 5.3-4. Sensitivity of the Predicted Mean Drip Shield Failure Profile to the Degraded and Enhanced Drip Shield Cases

C-82

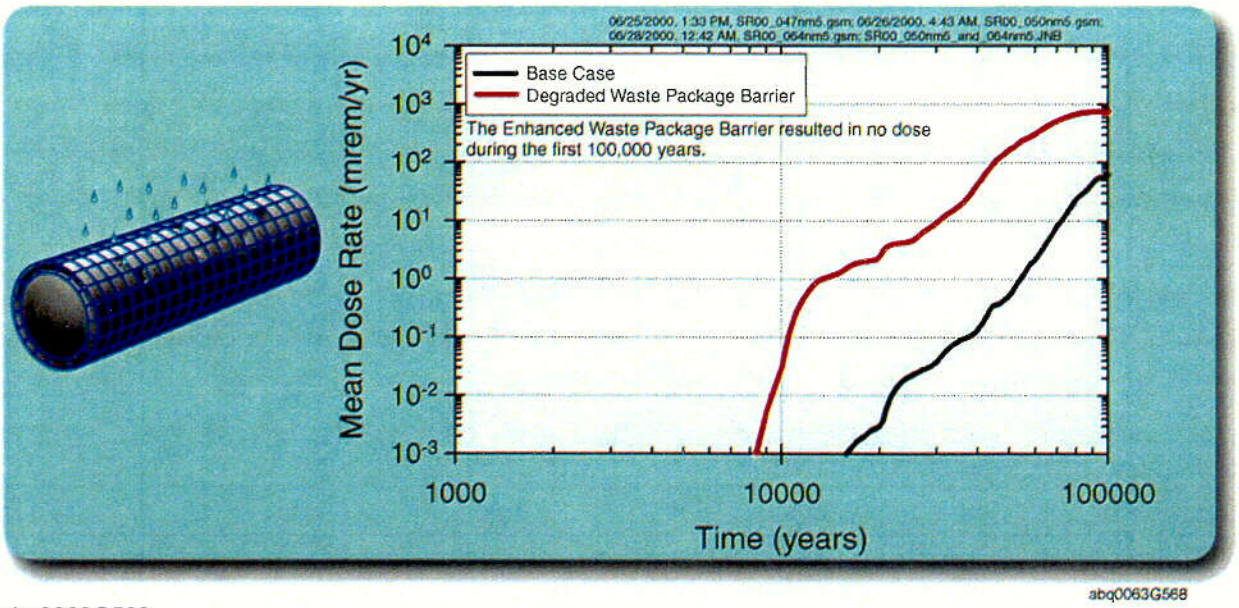

abq0063G568

Figure 5.3-5. Sensitivity of the Predicted Mean Dose Rate Profile to the Degraded and Enhanced Waste Package Cases

L-93

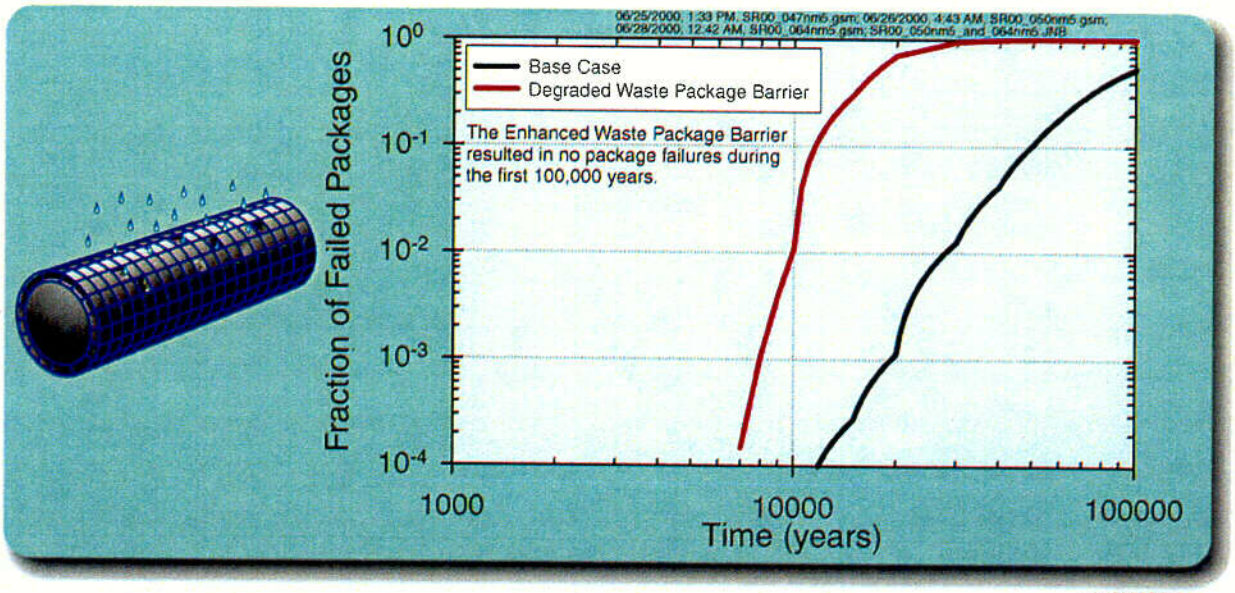

abq0063G567

Figure 5.3-6. Sensitivity of the Predicted Mean Waste Package Failure Profile to the Degraded and Enhanced Waste Package Cases

L-84

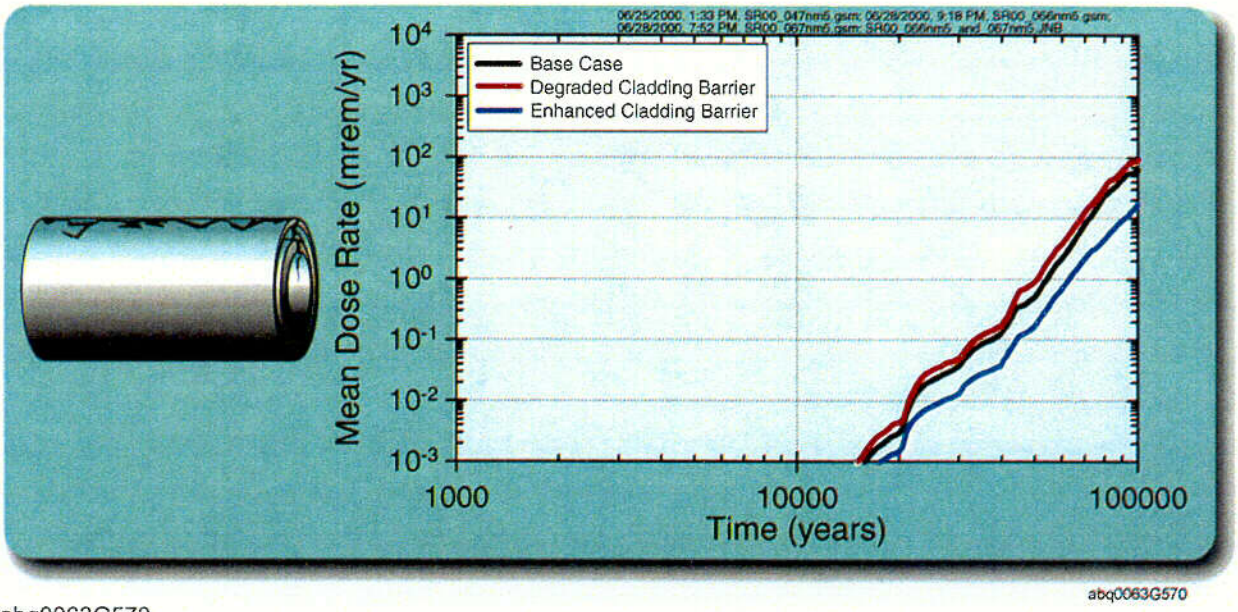

abq0063G570

Figure 5.3-7. Sensitivity of the Predicted Mean Dose Rate Profile to the Degraded and Enhanced Commercial Spent Nuclear Fuel Cladding Cases

C-45

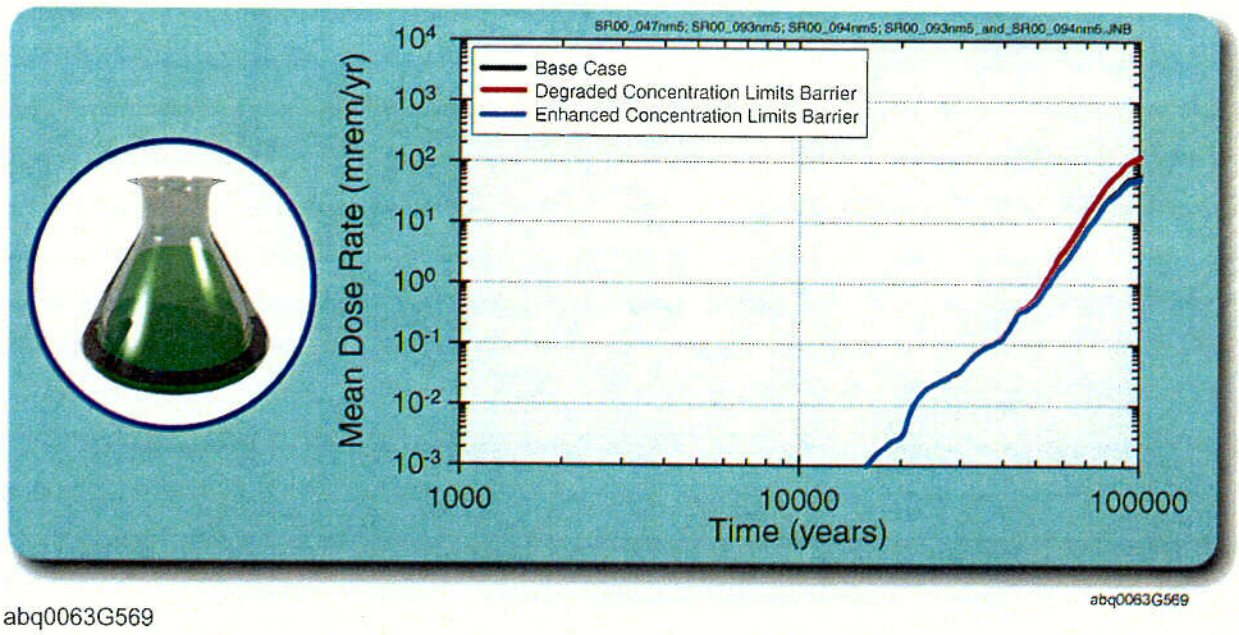

abq0063G569

Figure 5.3-8. Comparison of Mean Dose for Degraded and Enhanced Concentration Limits with the Base Case

C-86

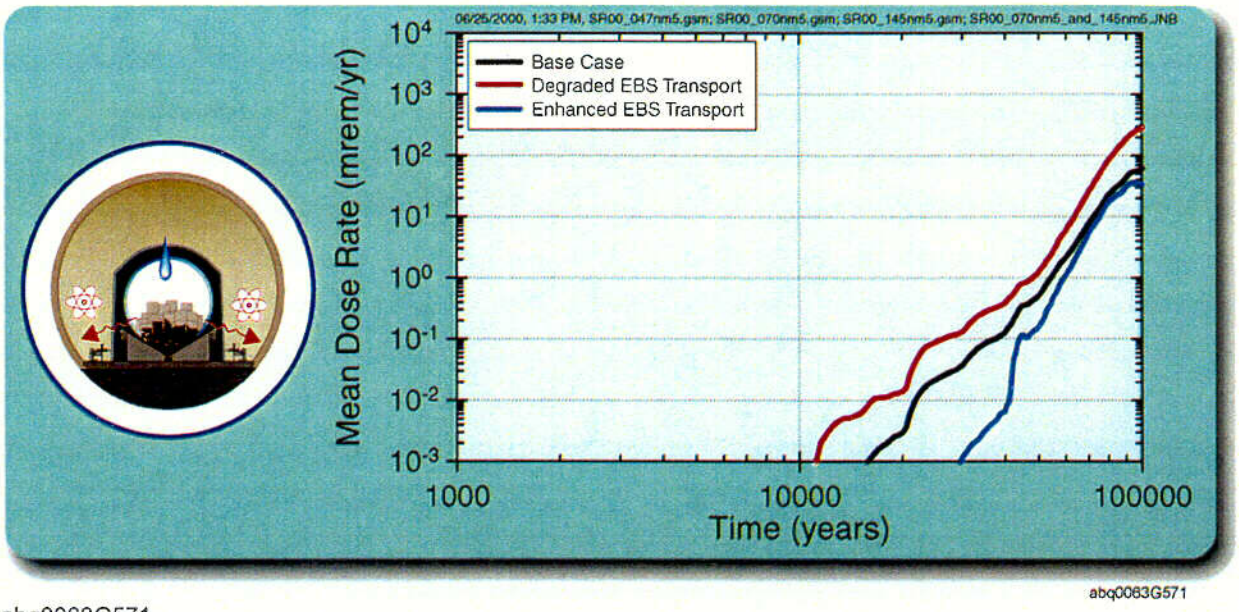

abq0063G571

Figure 5.3-9. Comparison of Mean Dose for Degraded and Enhanced Engineered Barrier System Transport Cases with the Base Case

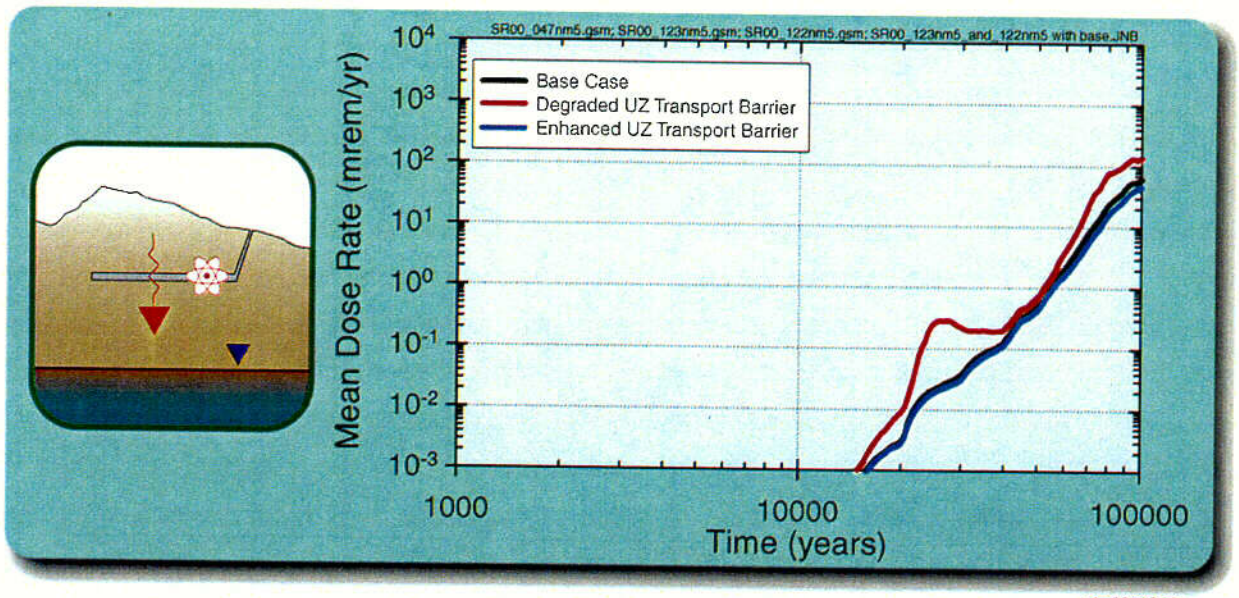

abq0063G574

Figure 5.3-10. Comparison of Mean Dose for Degraded and Enhanced Unsaturated Zone Transport Cases with the Base Case

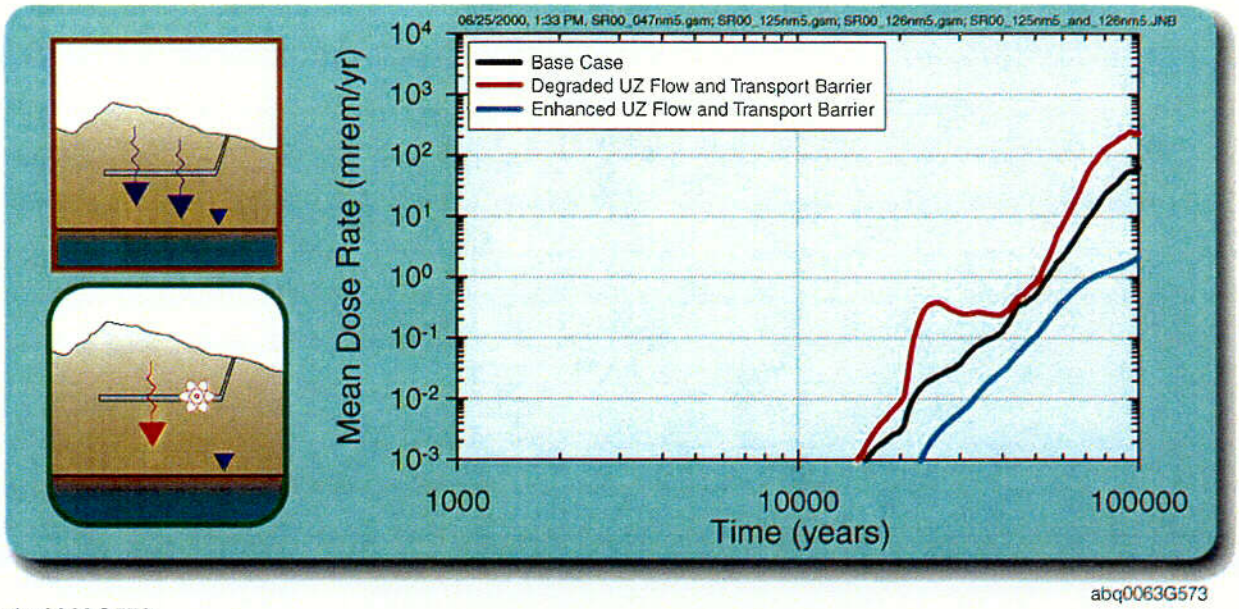

abq0063G573

Figure 5.3-11. Comparison of Mean Dose for Degraded and Enhanced Unsaturated Zone Flow and Transport Cases with the Base Case

L-89

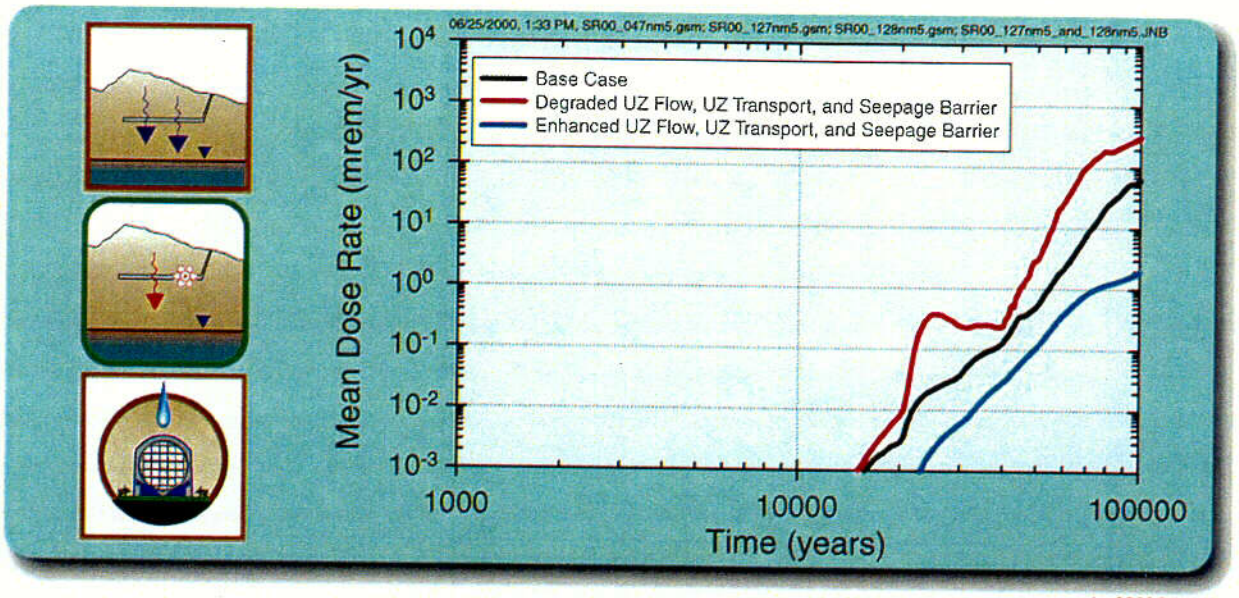

abq0063G572

Figure 5.3-12. Comparison of Mean Dose for Degraded and Enhanced Unsaturated Zone Flow, Transport, and Seepage Cases with the Base Case

C-90

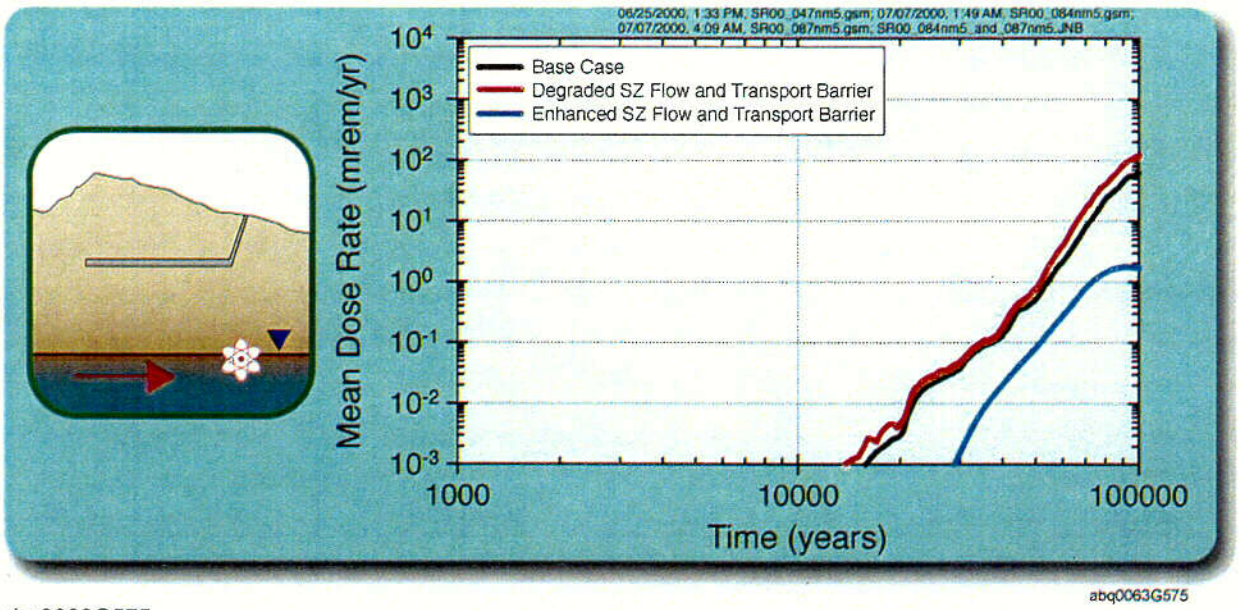

abq0063G575

Figure 5.3-13. Comparison of Mean Dose for Degraded and Enhanced Saturated Zone Flow and Transport Cases with the Base Case

C-91

INTENTIONALLY LEFT BLANK

6. SUMMARY AND CONCLUSIONS

The TSPA-SR is the culmination of a body of scientific work that aims to evaluate the adequacy of the Yucca Mountain natural and engineered barriers in meeting postclosure public health and safety goals specified in applicable proposed regulations promulgated by the EPA, the NRC, and the DOE. The present document has presented how this scientific information has been integrated into a consistent picture of the overall repository system and has projected the future evolution of the potential repository system using each of the integrated component models.

This summary and conclusions section synthesizes the information presented in each of the preceding sections and attempts to provide another integration thread through the entire document. The aim of this presentation is not to repeat the details presented in the earlier sections of this document. Rather, it is to describe how the overall objectives have been addressed and to provide a roadmap for where particular issues have been addressed within the body of this document or in the Appendixes.

The discussion of summary and conclusions is broken into a summary of the overall system performance results (Section 6.1) which is followed by a discussion of the basis for these results (Section 6.2). The document concludes with a discussion of the intended use of these TSPA-SR results and conclusions in Section 6.3.

6.1 SUMMARY OF OVERALL SYSTEM PERFORMANCE RESULTS

There are three applicable proposed regulations that describe the requirements for performance assessments of the Yucca Mountain site: proposed 40 CFR Part 197 (64 FR 46976 [105065]), proposed 10 CFR Part 63 (64 FR 8640 [101680]), and proposed 10 CFR Part 963 (64 FR 67054 [124754]). These proposed regulations also describe the standards or performance objectives that the potential repository must meet to be of acceptable risk.

The requirements for a performance assessment specified in proposed 40 CFR Part 197 (64 FR 46976 [105065]) are:

> 197.20 Individual Protection Standard
> *The DOE must demonstrate, using performance assessment,* that there is a reasonable expectation that for 10,000 years following disposal the reasonably maximally exposed individual receives no more than an annual committed effective dose equivalent of 150 microSv (15 mrem) from releases from the undisturbed Yucca Mountain disposal system. The DOE's analysis must include all potential pathways of radionuclide transport and exposure.

The requirements for a performance assessment specified in proposed 10 CFR Part 63 (64 FR 8640 [101680]) are:

> 63.113 Performance Objective For The Geologic Repository After Permanent Closure.

(c) The ability of the geologic repository to limit radiological exposures to those specified in 63.113(b) shall be demonstrated through a performance assessment that meets the requirements specified at 63.114, uses the reference biosphere and critical group specified at 63.115, and excludes the effects of human intrusion.

The requirements for a total system performance assessment specified in proposed 10 CFR Part 963 (64 FR 67054 [124754]) are:

963.15 Postclosure Suitability Determination.
DOE will apply the method and criteria described in Secs. 963.16 and 963.17 to evaluate the suitability of the Yucca Mountain site for the postclosure period. If DOE finds that the results of the total system performance assessments conducted under 963.16(a)(1) show that the Yucca Mountain site is likely to meet the applicable radiation protection standard, DOE may determine the site suitable for the postclosure period.

963.16 Postclosure Suitability Evaluation Method.
(a) DOE will evaluate postclosure suitability using the total system performance assessment method. DOE will conduct a total system performance assessment to evaluate the ability of the geologic repository to meet the applicable radiation protection standard.

Given these requirements for a performance assessment, it useful to define this term in the context used in each of the above regulations.

The definition of performance assessment as used in proposed 40 CFR Part 197 (64 FR 46976 [105065]) is:

Performance assessment means an analysis that:
(1) Identifies the processes, events, and sequences of processes and events (except human intrusion), and their probabilities of occurring over 10,000 years after disposal, that might, affect the Yucca Mountain disposal system;
(2) Examines the effects of those processes, events, and sequences of processes and events upon the performance of the disposal system; and
(3) Estimates the annual committed effective dose equivalent received by the reasonably maximally exposed individual, including the associated uncertainties, as a result of releases caused by all significant processes, events, and sequences of processes and events.

The definition of performance assessment as used in proposed 10 CFR Part 63 (64 FR 8640 [101680]) is:

Performance assessment means a probabilistic analysis that:
(1) Identifies the features, events and processes that might affect the performance of the geologic repository; and
(2) Examines the effects of such features, events and processes on the performance of the geologic repository; and

(3) Estimates the expected annual dose to the average member of the critical group as a result of releases from the geologic repository.

The definition of total system performance assessment as used in proposed 10 CFR Part 963 (64 FR 67054 [124754]) is:

> *Total System performance assessment* means a probabilistic analysis that is used to:
> (1) Identify the features, events and processes that might affect the performance of the geologic repository;
> (2) Examines the effects of such features, events and processes on the performance of the geologic repository; and
> (3) Estimates the expected annual dose to the receptor as a result of releases from the geologic repository.

This document, along with the supporting references cited in this document, contains all of the elements of the performance assessment outlined in the above requirements. Specifically, the relevant FEPs that might affect the performance have been presented in the appropriate subsections of Section 3. The details of the FEPs screening process and results are contained in Appendix B which cites the various FEPs screening AMRs which contain the technical basis for the screening arguments. The models developed to analyze the effects of the FEPs are presented in summary form in the various subsections of Section 3, while the effects of these FEPs are presented in the results described in Sections 4 and 5. Finally, the expected annual dose, as well as the uncertainty in the expected annual dose and the significance of the individual FEPs to the expected annual dose are presented in Sections 4 and 5.

Four post-closure performance objectives have been specified in the above proposed regulatory requirements. These four objectives are:

- Individual protection standard
- Human intrusion standard
- Groundwater protection standard
- Peak dose (required in proposed 40 CFR 197.30 [64 FR 46976 [105065]]).

The following sections summarize the TSPA-SR results with respect to these four post-closure performance objectives. Additional details of how these results have been generated are contained in Sections 4.1 through 4.3 (for individual protection), Section 4.4 (for human intrusion), Section 4.1.5 (for groundwater protection), and Section 4.1.3 (for peak dose). It bears noting that although the individual protection standard is the only post-closure performance objective that explicitly requires a performance assessment, the analyses to evaluate the other performance objectives have used the same methodology and models as used in the individual protection analysis. The differences are noted in the appropriate section of Chapter 4.

6.1.1 Summary of Individual Protection Performance Results

The requirements for individual protection performance as specified in proposed 40 CFR Part 197 (64 FR 46976 [105065]) are:

> 197.20 Individual-Protection Standard.
> The DOE must demonstrate, using performance assessment, that there is a reasonable expectation that for 10,000 years following disposal the reasonably maximally exposed individual receives no more than an annual committed effective dose equivalent of 150 microSv (15 mrem) from releases from the undisturbed Yucca Mountain disposal system. The DOE's analysis must include all potential pathways of radionuclide transport and exposure.

The requirements for individual protection performance as specified in proposed 10 CFR Part 63 (64 FR 8640 [101680]) are:

> 63.113 Performance Objective For The Geologic Repository After Permanent Closure.
> (b) The EBS shall be designed so that, working in combination with natural barriers, the expected annual dose to the average member of the critical group shall not exceed 0.25 mSv (25 mrem) TEDE at any time during the first 10,000 years after permanent closure, as a result of radioactive materials released from the geologic repository.

The requirements for individual protection performance as specified in proposed 10 CFR Part 963 (64 FR 67054 [124754]) are:

> 963.16 Postclosure Suitability Evaluation Method.
> (1)DOE will conduct a [TSPA] to evaluate the ability of the geologic repository to limit radiological exposures in the case where there is no human intrusion into the repository. DOE will model the performance of the geologic repository at the Yucca Mountain site using the method described in 963.16(b) and the criteria in Sec 963.17, excluding the criterion in 963.17(b)(4). DOE will consider the performance of the system in terms of the criteria to evaluate whether the geologic repository is likely to comply with the applicable radiation protection standard.

For the purpose of presenting the individual protection performance results, the analyses have been subdivided into a nominal performance scenario class and a volcanic event scenario class. Projections of the individual dose for the nominal scenario class are presented in Figure 6.1-1. Projections of the individual dose for the volcanic event scenario class are presented in Figure 6.1-2. Figure 6.1-3 combines these results to yield the projected total system dose to the individual.

Several points are worth summarizing on these projections:

- These projections have included the uncertainty in the dose attributed to the quantified uncertainty discussed in the process models, abstraction models and their included

parameters presented in Section 3. As a result, a distribution of potential doses has been developed reflecting this uncertainty.

- Additional unquantified uncertainty exists, the impacts of which have not been captured in the results presented. These unquantified uncertainties reflect in large part the conservative assumptions included in the analyses to increase the defensibility in particularly complex processes. Appendix F summarizes the most significance of these conservative assumptions included in the analyses. The result of this conservatism is to over-predict the possible performance.

- Projections are made beyond the 10,000-year regulatory time period specified in proposed 40 CFR Part 197 (64 FR 46976 [105065]) and proposed 10 CFR Part 63 (64 FR 8640 [101680]). These projections are important to evaluate the robustness of the system response and the contribution of both natural and engineered barriers to the overall system performance during the time period when the containment of the engineered barrier is being degraded. In addition to these post-10,000 year projections being performed to assure that no dramatic degradation of the performance occurs after the compliance period, they will also be used in the EIS to consider the effects of the peak dose.

- Projections are made for the dose to the individual residing 20 kilometers downgradient from the potential repository, in the vicinity of Lathrop Wells.

- These projections are applicable to both the average member of the critical group (using the definition of proposed 10 CFR Part 63 [64 FR 8640 [101680]]) and the reasonably maximally exposed individual (using the definition of proposed 40 CFR Part 197 [64 FR 46976 [105065]]). It is important to recognize that both of these individuals reside within a group of individuals likely to be most exposed to the risks associated with the long-term performance of the potential repository (given that the group of individuals is assumed to reside over the plume of contaminated groundwater). The exact characteristics of this individual (whether s/he is the "average member" or the "reasonably maximally exposed individual") are similar. In both instances the individual: (a) has a fraction of their diet based on the consumption of locally grown produce, milk, and meat; (b) lives in the vicinity of Lathrop Wells; (c) has a lifestyle consistent with the existing population of Amargosa Valley; and (d) drinks 2 liters of water per day derived from the contaminated groundwater.

- The projected doses for the volcanic event scenario class reflect probability-weighted doses as required in proposed 10 CFR Part 63 (64 FR 8640 [101680]); that is the probability of the event is multiplied by the dose consequence to yield the dose risk. This allows combining the nominal and volcanic event scenario classes to yield the total system dose response of Figure 6.1-3.

Based on the above, it is reasonable to conclude that the potential Yucca Mountain repository system is likely to meet the individual protection requirements of both proposed 10 CFR Part 63 (64 FR 8640 [101680]) and proposed 40 CFR Part 197 (64 FR 46976 [105065]).

6.1.2 Summary of Human Intrusion Performance Results

The requirements for human intrusion performance as specified in proposed 40 CFR Part 197 (64 FR 46976 [105065]) are:

> 197.25 Human Intrusion Standard.
> Alternative 1:
> The DOE must demonstrate that there is a reasonable expectation that for 10,000 years following disposal the reasonably maximally exposed individual receives no more than an annual committed effective dose equivalent of 150 microSv (15 mrem) as a result of a human intrusion. The DOE analysis of human intrusion must include all potential environmental pathways of radionuclide transport and exposure.
>
> Alternative 2:
> The DOE must determine the earliest time after disposal that the waste package would degrade sufficiently that a human intrusion (see 197.26) could occur without recognition by the drillers. The DOE must:
> (a) Demonstrate that there is a reasonable expectation that the reasonably maximally exposed individual receives no more than an annual committed effective dose equivalent of 150 microSv (15 mrem) as a result of a human intrusion, if complete waste package penetration can occur at or before 10,000 years after disposal. The analysis must include all potential environmental pathways of radionuclide transport and exposure; and
> (b) Include the results of the analysis and its bases in the environmental impact statement for Yucca Mountain as an indicator of long-term disposal system performance, if the intrusion cannot occur before 10,000 years after disposal.

The requirements for human intrusion performance as specified in proposed 10 CFR Part 63 (64 FR 8640 [101680]) are:

> 63.113 Performance Objective for the Geologic Repository After Permanent Closure.
> (d) The ability of the geologic repository to limit radiological exposures to those specified in §63.113(b), in the event of limited human intrusion into the EBS, shall be demonstrated through a separate performance assessment that meets the requirements specified at 63.114 and uses the reference biosphere and critical group specified at 63.115. For the assessment required by this paragraph, it shall be assumed that the human intrusion occurs 100 years after permanent closure and takes the form of a drilling event that results in a single, nearly vertical borehole that penetrates a waste package, extends to the SZ, and is not adequately sealed.

The requirements for human intrusion performance as specified in proposed 10 CFR Part 963 (64 FR 67054 [124754]) are:

> 963.16 Postclosure Suitability Evaluation Method.
> (a)(2) Consistent with applicable NRC regulations regarding a stylized human intrusion case, DOE will conduct a [TSPA] to evaluate the ability of the geologic

repository to limit radiological exposures in a stylized limited human intrusion case. DOE will model the performance of the geologic repository at the Yucca Mountain site using the method described in 963.16(b) and the criteria in Sec 963.17. DOE will consider the performance of the system in terms of the criteria to evaluate whether the geologic repository is likely to comply with the applicable radiation protection standard. The human intrusion evaluation under this paragraph will be separate from the evaluation conducted under 963.16(a)(1).

Human intrusion analyses have been conducted by assuming a borehole penetrates the engineered barriers (the drip shield, waste package, cladding, and invert) and provides a pathway from the surface to the repository and from the repository to the water table. Analyses have been conducted assuming the human intrusion occurs at 100 years (per proposed 10 CFR Part 63 [64 FR 8640 [101680]]) or 10,000 years (which would be required in the EIS even if the final EPA rule uses Alternative 2 of the proposed 40 CFR Part 197.25 (64 FR 46976 [105065]) and the DOE is able to demonstrate that the intrusion could not occur before 10,000 years). The results for these analyses are presented in Figures 6.1-4 and 6.1-5, respectively.

Several points are worth summarizing regarding the projections of the potential consequences associated with the stylized human intrusion scenario:

- It is highly unlikely that a borehole would be drilled from the surface of Yucca Mountain and that the driller would not detect the presence of the drift (due to loss of drilling fluid), or the drip shield, or the waste package (due to the difficulty in drilling through these metals). However, for the purposes of the analyses performed for the 100-year intrusion event, all of these considerations have been ignored.

- Should the final regulation appear more like alternative 2 of the proposed EPA standard, credit for the robustness of the engineered barriers during the intrusion event may be considered. In this case, the 10,000-year intrusion event would still be germane and included in the environmental impact statement.

- The uncertainty in the projected dose from the event is controlled by the uncertainty in the flow rates through the borehole, the concentration of the radionuclides in the intruded waste package, and the uncertainty in the SZ flow and transport characteristics.

Based on the above, it is reasonable to conclude that the potential Yucca Mountain repository system is likely to meet the human intrusion requirements of both proposed 10 CFR Part 63 (64 FR 8640 [101680]) and proposed 40 CFR Part 197 (64 FR 46976 [105065]).

6.1.3 Summary of Groundwater Protection Performance Results

The requirements for groundwater protection performance as specified in proposed 40 CFR Part 197 (64 FR 46976 [105065]) are:

197.35 What Standards Must DOE Meet?
In its license application to NRC, DOE must provide a reasonable expectation that, for 10,000 years of undisturbed performance after disposal, release of radionuclides from radioactive material in the Yucca Mountain disposal system

will not cause the level of radioactivity in the representative volume of groundwater at the point of compliance to exceed the limits in [the table] as follows:

Radionuclide or type of radiation emitted	**Limit**	**Is natural background included?**
Combined ^{226}Ra and ^{228}Ra	5 picocuries per liter	Yes
Gross alpha activity (including ^{226}Ra, but excluding radon and uranium)	15 picocuries per liter	Yes
Combined beta and photon emitting radionuclides	40 microsieverts (4mrem) per year to the whole body or any organ	No

The results of the groundwater protection analyses are illustrated in Figure 6.1-6 and 6.1-7 for the concentration and dose performance measures, respectively. Figure 6.1-6 illustrates the combined ^{226}Ra and ^{228}Ra concentrations in the representative volume of groundwater, as well as the gross alpha activity concentration (including ^{226}Ra, but excluding radon and uranium). Figure 6.1-7 shows the dose associated with the beta and photon emitting radionuclides (^{129}I, ^{99}Tc, and ^{14}C). The critical organ for each of these three radionuclides is the thyroid (for ^{129}I), the gastrointestinal tract (for ^{99}Tc), and fat (for ^{14}C). Several summary observations are possible from these analyses:

- Although the regulatory time period for groundwater protection is 10,000 years, the analyses have been extended to 100,000 years to illustrate the long-term behavior of the system. As noted in the individual protection analyses, these longer term projections are useful to assure that no significant degradation of the performance occurs after the 10,000 year time period of regulatory concern and to provide input to longer term assessments required in the EIS.

- The groundwater protection analyses assumed a representative water volume of 1,285 acre-ft/yr. centered on the highest concentration in the plume of contamination within the freshwater aquifer. In this analysis, all radionuclides that reach a distance of 20 km (12 miles) from the potential repository in any given annual period are contained in 1,285 acre-ft of water to determine the concentration. Taking all radionuclides in this manner produces the highest estimate of concentration that is possible for the specified volume of water. It is not necessary to specify an exact location or dimensions for the representative volume, which could be different in each Monte Carlo realization with this method.

- This projection considers undisturbed performance (i.e., performance not disturbed by the potential consequences associated with low-probability disruptive events) such as volcanism.

- The natural background concentrations are not illustrated on these plots. As noted in *Radioactivity in FY 1998 Groundwater Samples from Wells and Springs Near Yucca*

Mountain (CRWMS M&O 1999 [150420], pp. 8 to 9), the gross alpha activity background concentration ranges from –0.2 ± 0.5 to 2.7 ± 3.0 pCi/L, with the well closest to the 20-kilometer compliance location having a concentration of 0.4 ± 0.7 pCi/L. Concentrations of ^{226}Ra and ^{228}Ra were not reported because the gross alpha activity was below 5 pCi/L. However, another source reports ^{226}Ra concentrations in the well closest to the compliance point of 0.04 pCi/L and ^{228}Ra concentrations less than 1 pCi/L (DTN: GS971000012847.004 [149980]). The measurement errors are not reported in this reference. Measurements in the same reference at other wells and springs in the vicinity of Yucca Mountain and Amargosa Valley range from 0.03 to 0.5 pCi/L for ^{226}Ra and from less than 1 to 1.1 pCi/L for ^{228}Ra.

Based on the above, it is reasonable to conclude that the potential Yucca Mountain repository system is likely to meet the groundwater protection requirements of proposed 40 CFR Part 197 (64 FR 46976 [105065]).

6.1.4 Summary of Peak Dose Performance Results

The requirements for peak dose performance as specified in proposed 40 CFR Part 197 (64 FR 46976 [105065]) are:

> 197.30 What Other Projections Must Be Made by DOE?
> To complement the results of 197.20, DOE must calculate the peak dose of the reasonably maximally exposed individual that would occur after 10,000 years following disposal but within the period of geologic stability. While no regulatory standard applies to the results of this analysis, DOE must include the results and their bases in the environmental impact statement for Yucca Mountain as an indicator of long-term disposal system performance.

The results of the peak dose performance assessments are illustrated in Figure 6.1-8 for three different representations of the models used to project the peak dose. Several summary observations are possible from the following results:

- The time period of geologic stability is considered to be 1,000,000 years as suggested by the National Academy of Sciences.

- The peak dose occurs after the engineered barriers have been degraded sufficiently to allow advective flux of groundwater into all of the waste packages that are contacted by seepage.

- The expected value of the peak dose is a function of the degree of conservatism incorporated in the models and analyses used to produce the peak dose estimate. Because the base case models used in the development of the nominal performance projections were designed to be reasonably conservative to maximize their defensibility during the 10,000-year compliance period, they are less appropriate for projections of the peak dose. More appropriate representations would include considerations of the long-term (post-10,000-year) climate states and the long term effects of secondary phases.

- Depending on the representation considered, the peak dose varies from 460 mrem/yr for the case of extending the conservative models developed for the 10,000-year compliance analyses to the time of the peak dose, to 120 mrem/yr for the case of extending all the conservative models except the post-10,000 year climate model (described in Section 3.2.5) and the long-term secondary phase solubility limit model (described in Section 3.5.), to 30 mrem/yr for the case of extending all the conservative models except the long-term secondary phase solubility model.

- The variance in the peak dose magnitude is relatively small (a few orders of magnitude), because at that time all of the uncertainty associated with engineered barrier performance and the travel time in the natural barrier are insignificant to the magnitude of the peak dose.

As noted in proposed 40 CFR 197.30 (64 FR 46976 [105065]), no regulatory standard applies to the results of the peak dose analyses. They are provided to support the development of the environmental impact statement. Although these results do provide insights into the possible long term performance of a repository at Yucca Mountain, they should not be interpreted as accurate predictions of the likely performance over these time periods due to the large uncertainties and conservative approximations included in the models that were designed for assessing the 10,000-year compliance performance.

6.2 SUMMARY OF TECHNICAL BASIS OF OVERALL SYSTEM PERFORMANCE RESULTS

The projections of total system performance summarized in the previous section must be interpreted in light of their technical foundation. The technical basis for the TSPA analyses are contained within a family of AMRs that have been summarized in nine PMRs. The integration of the analyses and models in the context of the TSPA-SR model is presented in detail in the TSPA-SR Model Document (CRWMS M&O 2000 [148384]). The purpose of this section is to provide the reader with a series of roadmaps that depict where the technical basis is presented. Additional roadmaps are presented in the appendices to this document, in particular Appendix E which present the information flow used to develop the TSPA-SR model and Appendix F which summarizes the major assumptions and conservatisms used in the TSPA-SR model.

The summary of the technical basis for a complex system, such as the postclosure performance model of the potential Yucca Mountain repository system, is a daunting task. In order to provide some rational logic to the presentation, the discussion is broken into the following major topics:

- How the TSPA-SR has provided an integrated and traceable analysis using the family of over one hundred AMRs which have been summarized in the nine PMRs.

- How the TSPA-SR has addressed the uncertainty and variability in the component models and evaluated the significance of this uncertainty in the projection of overall performance.

- How the TSPA-SR has addressed both technical and process recommendations made during the generation of earlier TSPAs and by reviewers of earlier TSPA analyses, most notably the TSPA-VA completed in 1998.

- How the TSPA-SR has addressed the goals and objectives outlined in proposed regulatory requirements (notably proposed 40 CFR Part 197 [64 FR 46976 [105065]], proposed 10 CFR Part 63 [64 FR 8640 [101680]], and proposed 10 CFR Part 963 [64 FR 67054 [124754]]) along with the NRC's Acceptance Criteria noted in their Issue Resolution Status Report on Total System Performance Assessment and Integration (NRC 2000 [149372]).

- How the TSPA-SR may be used to address the regulatory requirements and other supporting information that may be required of decision makers.

The first three of these items are addressed in this section. The last two items are addressed in Section 6.3. With this information, combined with the information presented in the technical discussions in the previous chapters, the interested reader, whether a policy maker, decision maker, regulatory reviewer, or member of the public, can make an informed decision on the adequacy of the analysis for the intended purpose of evaluating the suitability of the potential Yucca Mountain repository system.

6.2.1 Summary of Traceability and Transparency of the Integrated TSPA-SR Analyses

An overall objective of any integrated performance assessment, but in particular total system performance assessments of potential nuclear waste repositories, is to provide a "transparent and traceable" analysis that allows the reader the opportunity to understand the basic assumptions and their scientific basis in such a way that he/she may understand and test the accuracy and reproducibility of the conclusions. Although no common definitions of these terms exist, the Nuclear Energy Agency has defined transparency as a document written in such a way that the reader can gain a clear understanding of what has been done, what the results are, and why the results are as they are (Nuclear Energy Agency 1998 [111738]). The Nuclear Energy Agency has defined traceability as an assessment that provides a complete record of the decisions and assumptions made and the models and data used to arrive at a given result.

Throughout this report, the underlying data, assumptions, models, and analyses have been discussed with appropriate conceptual drawings and integration graphics to illustrate the role of the component model, the technical basis of the component model, and the information flow from or to each component model. In addition, interim results have been presented both at the component level in Chapter 3 and the subsystem level in Chapter 4 to illustrate how information (in terms of mass, water, energy, activity) flows from one component of the system to the next in the integrated total system model. Finally, Appendix E presents the hierarchy of all analysis model reports that support the final information feed to the TSPA-SR model.

In the presentation of the individual component models that form the technical foundation of the TSPA-SR model, we have lumped the processes into "process model factors." This subdivision allows a convenient way of illustrating not only how and where that component fits into the total system representation, but also provides a traceable roadmap for summarizing the inclusion or

exclusion of relevant features, events, and processes (as documented in Appendix B). In addition, these process model factors allow for a convenient means of lumping the key input parameters for the TSPA-SR model and the supporting documentation where these parameters are discussed in more detail.

Table 6.2-1 summarizes the source (i.e., the relevant AMR) of the technical basis for each of the process model factors or model components used in the TSPA-SR model. The process model report which summarizes and synthesizes the technical defensibility of the analysis model reports is also indicated. In addition, this table provides a roadmap to figures in Section 3 and 4 where the intermediate performance results and key parameters affecting system performance are presented.

The defensibility of the analyses and models which support the TSPA-SR model is contained in the relevant AMRs and PMRs. It is the analysis model reports and process model reports which provide the fundamental scientific underpinning, and the associated assumptions and conservatisms necessary for a defensible, yet reasonably cautious analysis of expected performance.

It is beyond the scope of this document to summarize the depth and breadth of the information contained in the analysis model reports and process model reports that form the basis for the TSPA-SR. Suffice it to say that the individual models are based on appropriate site-specific information, analog data, and relevant literature data sources that have been integrated by the principal scientific investigators to provide a reasonable and defensible characterization of each individual process relevant to postclosure performance. As discussed in the following section, quantifiable uncertainty in the individual component model was included as appropriate. Where the individual process model was subject to significance complexity or the available information did not allow a definitive conclusion regarding the most reasonable representation, the analyst or modeler chose to apply some conservatism to the individual model. Areas where conservative representations were employed and the basis for that conservatism are enumerated in Appendix F.

It is these AMRs which provide the fundamental scientific underpinning, associated assumptions, and conservatisms necessary for a defensible, yet reasonably cautious analysis of expected performance.

In addition to the analysis model reports providing a traceable chain of references for the defensibility of the scientific bases for the TSPA-SR, they also provide a hierarchy of data tracking numbers. Appendix E summarizes the sources and hierarchy of data sets used as input to the TSPA-SR model. Additional details of the data sets used as input are contained in the TSPA-SR Model Report (CRWMS M&O 2000 [148384]). The quality status of each data set used as input to the TSPA-SR model can be ascertained by tracing the data set and all its predecessors using the Document Input Reference System database. This capability allows the DOE and NRC to track the status of all data sets used in the development of the postclosure safety case.

Table 6.2-1. Summary of Analysis Model Reports, Process Model Reports, and Figures Illustrating Key Input Parameters to Total System Performance Assessment-Site Recommendation

Key Attributes of System	Factor	Analysis Model Report	Process Model Report	Figure Illustrating Key Input Parameters or Intermediate Performance Results
Limiting Water Contacting Waste Package	Climate	*Future Climate Analysis* (USGS 2000 [136368])	UZ[a]	
	Net Infiltration	*Analysis of Infiltration Uncertainty* (CRWMS M&O 2000 [143244])	UZ[a]	3.2-7
	UZ Flow	*Abstraction of Flow Fields for RIP* (CRWMS M&O 2000 [123913])	UZ[a]	3.2-8
	Coupled Effects on UZ Flow	*Drift Scale Coupled Processes (DST and THC Seepage) Models* (CRWMS M&O 2000 [141389])	UZ[a]	
	Seepage into Emplacement Drifts	*Abstraction of Drift Seepage* (CRWMS M&O 2000 [142004])	UZ[a]	3.2-15
		Draft of AMR Abstraction of NFE Drift Thermodynamic Environment and Percolation Flux (CRWMS M&O 2000 [152204])	NFE[b] EBS[c]	
	Coupled Effects on Seepage	*Abstraction of Drift Seepage* (CRWMS M&O 2000 [142004])	UZ[a]	3.2-15
Long Waste Package Lifetime	In-Drift Physical and Chemical Environments	*Draft of AMR Abstraction of NFE Drift Thermodynamic Environment and Percolation Flux* (CRWMS M&O 2000 [152204])	NFE[b] EBS[c]	3.3-9 3.3-10
		In-Drift Precipitates/Salts Analysis. (CRWMS M&O 2000 [127818])	EBS[c]	
	In-Drift Moisture Distribution	*EBS Radionuclide Transport Abstraction Model* (CRWMS M&O 2000 [129284])	EBS[c]	
	Drip Shield Degradation and Performance	*Analysis of Mechanisms for Early Waste Package Failure* (CRWMS M&O 2000 [147359])	WP[d]	
		Calculation of General Corrosion Rate of Drip Shield and Waste Package Outer Barrier to Support WAPDEG Analysis (CRWMS M&O 2000 [147641]) *WAPDEG Analysis of Waste Package and Drip Shield Degradation* (CRWMS M&O 2000 [146427])	WP[d]	3.4-11 3.4-16 3.4-17 4.1-7

Table 6.2-1. Summary of Analysis Model Reports, Process Model Reports, and Figures Illustrating Key Input Parameters to Total System Performance Assessment-Site Recommendation (Continued)

Key Attributes of System	Factor	Analysis Model Report	Process Model Report	Figure Illustrating Key Input Parameters or Intermediate Performance Results
Long Waste Package Lifetime (Continued)	Waste Package Degradation and Performance	Environment on the Surfaces of the Drip Shield and Waste Package Outer Barrier. (CRWMS M&O 2000 [146460])	WP[d]	
		Calculation of General Corrosion Rate of Drip Shield and Waste Package Outer Barrier to Support WAPDEG Analysis. (CRWMS M&O 2000 [147641])	WP[d]	3.4-10 3.4-12 3.4-13
		WAPDEG Analysis of Waste Package and Drip Shield Degradation (CRWMS M&O 2000 [146427])	WP[d]	3.4-16 4.1-8
		Aging and Phase Stability of Waste Package Outer Barrier (CRWMS M&O 2000 [147639])	WP[d]	
		Environment on the Surfaces of the Drip Shield and Waste Package Outer Barrier (CRWMS M&O 2000 [146460])	WP[d]	
		Abstraction of Models for Pitting and Crevice Corrosion of Drip Shield and Waste Package Outer Barrier (CRWMS M&O 2000 [147648])	WP[d]	
		Abstraction of Models for Stress Corrosion Cracking of Drip Shield and Waste Package Outer Barrier and Hydrogen Induced Corrosion of Drip Shield (CRWMS M&O 2000 [135773])	WP[d]	3.4-5 3.4-6 3.4-7 3.4-8
		Calculation of Probability and Size of Defect Flaws in Waste Package Closure Welds to Support WAPDEG Analysis (CRWMS M&O 2000 [144551])	WP[d]	3.4-9
Slow Rate of Radionuclide Mobilization and Release from the EBS	Radionuclide Inventory and Distribution in Repository	*Inventory Abstraction* (CRWMS M&O 2000 [136383])	WF[e]	3.5-8 3.5-9
	In-Package Environments	*In-Package Chemistry Abstraction* (CRWMS M&O 2000 [129287])	WF[e]	3.5-11
	Cladding Degradation and Performance	*Clad Degradation - Summary and Abstraction* (CRWMS M&O 2000 [147210])	WF[e]	3.5-18 3.5-19 4.1-9

Table 6.2-1. Summary of Analysis Model Reports, Process Model Reports, and Figures Illustrating Key Input Parameters to Total System Performance Assessment-Site Recommendation (Continued)

Key Attributes of System	Factor	Analysis Model Report	Process Model Report	Figure Illustrating Key Input Parameters or Intermediate Performance Results
Slow Rate of Radionuclide Mobilization and Release from the EBS (Continued)	CSNF Degradation and Performance	*CSNF Waste Form Degradation: Summary Abstraction* (CRWMS M&O 2000 [136060])	WF[e]	3.5-12
	DSNF Degradation and Performance	*DSNF and Other Waste Form Degradation Abstraction* (CRWMS M&O 2000 [144164])	WF[e]	3.5-13
	Defense HLW Degradation and Performance	*Defense High Level Waste Glass Degradation* (CRWMS M&O 2000 [143420])	WF[e]	3.5-14 3.5-15
	Dissolved Radionuclide Concentrations	*Summary of Dissolved Concentration Limits* (CRWMS M&O 2000 [143569])	WF[e]	3.5-21
	Colloid-Associated Radionuclide Concentrations	*Waste Form Colloid-Associated Concentrations Limits: Abstraction and Summary* (CRWMS M&O 2000 [125156])	WF[e]	3.5-24
	In-Package Radionuclide Transport	*EBS Radionuclide Transport Abstraction* (CRWMS M&O 2000 [129284])	EBS[c]	
	EBS (Invert) Degradation and Performance	*EBS Radionuclide Transport Abstraction* (CRWMS M&O 2000 [129284])	EBS[c]	4.1-10 4.1-12 4.1-14 4.1-15
		Draft of AMR Abstraction of NFE Drift Thermodynamic Environment and Percolation Flux (CRWMS M&O 2000 [152204])	NFE[b]	
Long Transport away from the EBS	UZ Radionuclide Transport (Advective Pathways; Retardation; Dispersion)	*Unsaturated and Saturated Transport Properties* (CRWMS M&O 2000 [141440])	UZ[a]	
		Abstraction of Flow Fields for RIP (ID: U0125) (CRWMS M&O 2000 [123913])	UZ[a]	
		Particle Tracking Model and Abstraction of Transport Processes (CRWMS M&O 2000 [141418])	UZ[a]	3.7-9 3.7-10 3.7-11 4.1-18 4.1-19
		UZ Colloid Transport Model (CRWMS M&O 2000 [122799])	UZ[a]	

Table 6.2-1. Summary of Analysis Model Reports, Process Model Reports, and Figures Illustrating Key Input Parameters to Total System Performance Assessment-Site Recommendation (Continued)

Key Attributes of System	Factor	Analysis Model Report	Process Model Report	Figure Illustrating Key Input Parameters or Intermediate Performance Results
Long Transport away from the EBS (Continued)	Coupled Effects on UZ Radionuclide Transport	*Unsaturated Zone and Saturated Zone Transport Properties* (CRWMS M&O 2000 [141440])	UZ[a]	
	SZ Radionuclide Transport (Advective Pathways; Retardation; Dispersion)	*Uncertainty Distribution for Stochastic Parameters* (CRWMS M&O 2000 [147972])	SZ[f]	
		Input and Results of the Base Case Saturated Flow and Transport Model for TSPA (CRWMS M&O 2000 [139440])	SZ[f]	3.8-18 3.8-19 4.1-20
	Wellhead Dilution	*Groundwater Usage by the Proposed Farming Community* (CRWMS M&O 2000 [144056])	BIO[g]	3.9-9
	Biosphere Dose Conversion Factors	*Distribution Fitting to the Stochastic BDCF Data* (CRWMS M&O 2000 [144055])	BIO[g]	
		Abstraction of BDCF Distributions for Irrigation Period (CRWMS M&O 2000 [144054])	BIO[g]	3.9-11
Minimal Effects of Potentially Disruptive Processes and Events	Probability of Volcanic Eruption	*Characterize Framework for Igneous Activity at Yucca Mountain, Nevada (T0015)* (CRWMS M&O 2000 [141044])	DE[h]	
	Characteristics of Volcanic Eruption	*Igneous Consequence Modeling for TSPA-SR* (CRWMS M&O 2000 [139563])	DE[h]	
	Effects of Volcanic Eruption	*Igneous Consequence Modeling for TSPA-SR* (CRWMS M&O 2000 [139563])	DE[h]	
	Atmospheric Transport of Volcanic Eruption	*Igneous Consequence Modeling for TSPA-SR* (CRWMS M&O 2000 [139563])	DE[h]	
	Biosphere Dose Conversion for Volcanic Eruption	*Disruptive Event Biosphere Dose Conversion Factor Analysis* (CRWMS M&O 2000 [143378])	BIO[g]	
	Probability of Igneous Intrusion	*Characterize Framework for Igneous Activity at Yucca Mountain, Nevada (T0015)* (CRWMS M&O 2000 [141044])	DE[h]	
	Characteristics of Igneous Intrusion	*Igneous Consequence Modeling for TSPA-SR* (CRWMS M&O 2000 [139563])	DE[h]	

Table 6.2-1. Summary of Analysis Model Reports, Process Model Reports, and Figures Illustrating Key Input Parameters to Total System Performance Assessment-Site Recommendation (Continued)

Key Attributes of System	Factor	Analysis Model Report	Process Model Report	Figure Illustrating Key Input Parameters or Intermediate Performance Results
	Effects of Igneous Intrusion	*Igneous Consequence Modeling for TSPA-SR* (CRWMS M&O 2000 [139563])	DE[h]	

NOTES: [a] UZ = *Unsaturated Zone Flow and Transport Model Process Model Report* (CRWMS M&O 2000 [145774])
[b] NFE = *Near-Field Environment Process Model Report* (CRWMS M&O 2000 [146589])
[c] EBS = *Engineered Barrier System Degradation, Flow, and Transport Process Model Report* (CRWMS M&O 2000 [145796])
[d] WP = *Waste Package Degradation Process Model Report* (CRWMS M&O 2000 [138396])
[e] WF = *Waste Form Degradation Process Model Report* (CRWMS M&O 2000 [138332])
[f] SZ = *Saturated Zone Flow and Transport Process Model Report* (CRWMS M&O 2000 [145738])
[g] BIO = *Biosphere Process Model Report* (CRWMS M&O 2000 [151615])
[h] DE = *Disruptive Events Process Model Report* (CRWMS M&O 2000 [141733])
N/A = not applicable

In conclusion, the data, analyses, and models used as the technical basis for the TSPA-SR, as well as the assumptions, uncertainty, variability, and conservatism that go along with these data, analyses, and models are all traceable back to their source documents and data sets. This traceability allows all interested reviewers to examine the defensibility of the individual component models and reach their own conclusions regarding their scientific adequacy.

6.2.2 Summary of Uncertainty Treatment in TSPA-SR Analyses

Total system performance assessments are by their very nature uncertain projections of the possible behavior of the individual component models describing the relevant processes affecting the containment and isolation of radioactive wastes from the biosphere. This uncertainty is explicitly included in the models and resulting analyses in the form of discrete probability distributions that encompass the range of possible outcomes.

As noted throughout this document and within the individual analysis model reports and process model reports that provide the technical basis for the TSPA-SR model, there remains uncertainty in the individual process models and their abstraction into the TSPA-SR model. Much of this uncertainty has been quantified and is included in the TSPA-SR model. The TSPA-SR results reflect this quantified uncertainty. For example, the full distribution of individual dose rates illustrated on Figure 6.1-1 indicate a range of possible dose rates that extends over about 6 orders of magnitude between the 5th and 95th percentile. This range is a direct indication of the degree of uncertainty incorporated in the individual models used as input to the TSPA-SR model.

In addition to the quantified uncertainty in the TSPA-SR model, there is also unquantified uncertainty that has been generally represented by using a more bounded or conservative representation of a particular process model. These conservatisms result when there is insufficient information available or significant complexity exists that is not amenable to quantified uncertainty (although elicitation approaches could be used if one desired to quantify the uncertainty in these conservative judgments). These conservatisms are summarized in Appendix F.

Simply acknowledging the nature and magnitude of uncertainty is one aspect of a performance assessment. However, more important is the assessment of the significance of that uncertainty in the ability of the site and engineered barriers to meet performance objectives. Chapter 5 of this document focused on the significance of the quantified uncertainty on the total system performance. (Note: The principal means for investigating the significance of unquantified uncertainties is through the use of alternative representations in "what-if" analyses. The content of this document has focussed on the quantified uncertainties. Unquantified uncertainties have been investigated as part of the barrier importance analyses conducted in support of the Repository Safety Strategy Rev 04, which are documented in *Repository Safety Strategy Revision 4* [CRWMS M&O 2000 [151001]]). In addition, continuing efforts are ongoing to evaluate the significance of conservatisms and other unquantified uncertainties. The objective of these analyses is to quantify the degree of conservatism in the total system performance results represented by the "base-case" models.

The quantitative uncertainty analyses have statistical evaluations of significance (such as regression analyses and classification analyses) documented in Section 5.1 and sensitivity and barrier importance analyses documented in Section 5.2 and 5.3, respectively. The distinction between sensitivity and barrier importance analyses is slight. In the former, only one model component (and in most cases only one parameter within one model component) is fixed at either the optimistic or pessimistic end of the uncertainty distribution to see the effect of that parameter or model on the total system performance. In barrier importance analyses, several model components (or parameters of several model components) are fixed at extreme values of their uncertainty distributions to see their effect on the system response.

Table 6.2-2 summarizes the sensitivity and barrier importance analyses conducted for the TSPA-SR. (Note: Additional barrier importance analyses conducted in support of the Repository Safety Strategy Rev 04 are documented in *Repository Safety Strategy Revision 4* [CRWMS M&O 2000 [151001]]). This table depicts the figure number in Section 5.2 or 5.3 which illustrates the significance of the quantified uncertainty on the overall system response. These figures generally illustrate the robustness of the overall repository response even when some components or barriers are fixed at their most pessimistic values within the uncertainty distribution that is believed most defensible in the corresponding analysis model report.

Table 6.2-2. Summary of Sensitivity and Barrier Importance Analyses in TSPA-SR

Key Attributes of System	Process Model Factor	Figure Illustrating Sensitivity Analysis	Figure Illustrating Barrier Importance Analysis
Water Contacting Waste Package	Climate		
	Net Infiltration	5.2-1	
	UZ Flow		5.3-1 5.3-2
	Coupled Effects on UZ Flow		
	Seepage into Emplacement Drifts	5.2-2	
	Coupled Effects on Seepage		
Waste Package Lifetime	In-Drift Physical and Chemical Environments		5.3-3
	In-Drift Moisture Distribution		
	Drip Shield Degradation and Performance	5.2-12 5.2-13	5.3-4 5.3-5
Waste Package Lifetime (Continued)	Waste Package Degradation and Performance	5.2-3 5.2-4 5.2-5 5.2-6 5.2-7 5.2-8 5.2-9 5.2-10 5.2-11	5.3-6 5.3-7
Radionuclide Mobilization and Release from the EBS	Radionuclide Inventory	5.2-14	
	In-Package Environments		
	Cladding Degradation and Performance		5.3-8
	Commercial Spent Nuclear Fuel Degradation and Performance		
	DOE-owned spent nuclear fuelDSNF Degradation and Performance		
	Defense high level radioactive waste Degradation and Performance		
	Dissolved Radionuclide Concentrations		5.3-9 5.3-10 5.3-11
	Colloid-Associated Radionuclide Concentrations		
	In-Package Radionuclide Transport		
	EBS (Invert) Degradation and Performance	5.2-22	

Table 6.2-2. Summary of Sensitivity and Barrier Importance Analyses in TSPA-SR (Continued)

Key Attributes of System	Process Model Factor	Figure Illustrating Sensitivity Analysis	Figure Illustrating Barrier Importance Analysis
Transport Away from the EBS	UZ Radionuclide Transport (Advective Pathways; Retardation; Dispersion; Dilution)		5.3-12 5.3-13 5.3-14
	SZ Radionuclide Transport		5.3-15
	Wellhead Dilution		
	Biosphere Dose Conversion Factors	5.2-23 5.2-24	N/A
Effects of Potentially Disruptive Processes and Events	Probability of Volcanic Eruption	5.2-25	N/A
	Characteristics of Volcanic Eruption	5.2-29 5.2-30	
	Effects of Volcanic Eruption	5.2-30	
	Atmospheric Transport of Volcanic Eruption	5.2-26 5.2-27	
	Biosphere Dose Conversion for Volcanic Eruption	5.2-28 5.2-33	
	Probability of Igneous Intrusion	5.2-25	
	Characteristics of Igneous Intrusion	5.2-31 5.2-32	
	Effects of Igneous Intrusion		

The figures cited on Table 6.2-2, along with the discussions in Chapter 5, also indicate the fact that when a particular uncertain parameter is fixed at an extreme value (i.e., either the 5th or 95th percentile of the distribution) the resulting variance of the projected dose is reduced. This variance reduction is a function of the degree the underlying parameter contributes to the overall variance in the base case analysis. For example, a significance fraction of the total variance of the dose at 100,000 years is the result of the wide distribution of waste package failures. Fixing the failures over a much narrower distribution reduces the variance of the projected dose.

Inherent uncertainties exist in any projection of the future performance of a deep geologic repository. These uncertainties must be considered in a demonstration of compliance with radiation protection standards that require waste containment for thousands of years. Many, but not all, of those uncertainties have been quantified and addressed in the TSPA; examples include:

- Potential changes in climate, seismicity, and other processes over the long compliance period for geologic disposal (i.e., 10,000 years)
- Variability and lack of knowledge of the properties of geologic media (e.g., heterogeneous permeability and porosity) over large spatial scales of the hydrogeologic setting (e.g., 20-km [12.5-mi] flow path from the repository to the point of compliance)

- Incomplete knowledge about the long-term material behavior of engineered components (e.g., corrosion of metals over many thousands of years).

Both the EPA and the NRC have recognized that uncertainty about the future performance of the repository will remain even after site characterization is complete. The NRC perspective is articulated in proposed 10 CFR Part 63, which states, "Proof that the geologic repository will be in conformance with the objective for postclosure performance is not to be had in the ordinary sense of the word" (64 FR 8640 [101680], Section IX, p. 8650). In place of such proof, the NRC regulation makes the determination of compliance with the standards contingent upon a regulatory finding of "reasonable assurance," which would be made on the basis of the record before it. Similarly, the EPA explicitly states that "unequivocal numerical proof of compliance is neither necessary nor likely to be obtainable" (64 FR 46976 [105065], p. 46997). The EPA prescribes a "reasonable expectation" approach for demonstrating compliance with its standard.

As the National Research Council (1990 [100061], p. 13) and others have noted, there are residual uncertainties with deep geologic disposal that cannot easily be quantified and incorporated into performance analyses. Nevertheless, their potential impact must be, to the extent practicable, addressed and, if important, mitigated to provide confidence in post-closure safety. Examples of residual uncertainties associated with geologic disposal that are difficult to quantify include:

- The potential for currently unknown processes to affect performance

- The possibility that incompletely characterized processes have been incorporated in the TSPA in a manner that results in the underestimation of radionuclide releases; examples of incompletely characterized processes include thermal, chemical, hydrologic, and mechanical processes that are coupled in complex ways that cannot be completely tested at the scale of a repository, and processes that are difficult to observe and test, such as colloidal transport of radionuclides

- Uncertainty associated with the projections of engineered barrier performance over geologic time periods (e.g., 10,000-years) based on data from short-term (e.g., several years) laboratory testing

- Uncertainty associated with the large spatial scale of the three-dimensional groundwater flow system, which makes it difficult to characterize flow paths and processes.

Substantial effort has been made to identify, characterize, and mitigate the potential impacts of residual uncertainties that could significantly affect long-term performance. Where possible, more tests have been conducted to collect additional information that would provide insight to analysts. Where additional testing was not feasible (e.g., it is not possible to run tests over the same time period as the repository must perform), or of limited benefit (e.g., no amount of excavation or drilling could completely characterize the natural system) modelers used conservative assumptions to "bound" their analyses of uncertain processes. To do this, they have incorporated assumptions in their models that represent the range of properties and processes that they believe are feasible. In addition, use has been made of empirical observations and qualitative lines of evidence from natural analogues to address uncertainties.

In conclusion, addressing the uncertainty inherent in the models used for post-closure performance assessment has been an integral ingredient in the development of the component models and parameters used in the TSPA-SR model. In addition, examining the significance of quantified uncertainty has been an important objective of the TSPA analyses themselves. Ongoing efforts to quantitatively evaluate the significance of unquantified uncertainties will add additional insights to support the determination of the degree of conservatisms included in the "base case" models described in Section 3.

6.2.3 Summary of Technical Issues Addressed in TSPA-SR Model and Analyses

The TSPA-SR is the fifth major iteration of TSPAs conducted by the DOE over the past decade in support of evaluating the suitability of the Yucca Mountain site and engineered barriers. The first three iterations of the TSPAs (Barnard, et al. 1992 [100309]; CRWMS M&O 1994 [100111]; CRWMS M&O 1995 [100198]) focussed on developing, implementing and testing the approach and methodology for performing a TSPA and on identifying the key information needs of those component models that were most significant contributors to system performance. The fourth iteration (DOE 1998 [100550], Volume 3) was conducted in support of the DOE Viability Assessment. Each of these previous iterations has benefited from insights, reviews, and criticisms developed from the predecessor analyses. As the scientific information available to evaluate the performance of the potential Yucca Mountain repository system has evolved over time, so too have the TSPA analyses.

The current TSPA-SR Rev 00 has benefited from reviews of the TSPA-VA completed by a Peer Review Panel (see Budnitz et al. 1999 [102726]), the NRC (Paperiello 1999 [146561]), Clark County, NV (Cohen 1999 [151783]), and the U.S. Geological Survey (Anderson et al. 1998 [101656]). It is anticipated that the TSPA-SR Rev 01 (to be completed following the completion of the Site Recommendation Consideration Report) will benefit from reviews conducted by similar review groups, including the Nuclear Waste Technical Review Board, as well as the public.

While it is difficult to enumerate every comment on the TSPA-VA, Appendix H presents a summary of many of the most significant comments and how they have been addressed. However, this comment resolution correlation matrix does not completely represent the breadth of comments received on all aspects of the VA. For example, numerous issues associated with the models included in the TSPA-VA have been identified in the NRC's Key Technical Issues Issue Resolution Status Reports (IRSRs) as Acceptance Criteria for evaluating the sufficiency of the DOE site recommendation. These issues are addressed in the individual PMRs that most closely correlate to the corresponding key technical issues.

While the models and analyses that support the TSPA-SR may not have addressed every issue or comment raised on the previous TSPA iterations, they have addressed the most significant issues. For example, a significant cross-cutting issue raised on the TSPA-VA was the reliance on expert elicitation in the absence of sufficient site or engineering data. In the present analysis, with the exception of volcanic and seismic hazards which are most amenable to elicitation methods and a use of TSPA-VA elicitations to confirm the uncertainty in some parameters used in the SZ flow and transport model, there have been no elicitations used in lieu of site data.

Another criticism on the TSPA-VA was related to the lack of traceability of the TSPA to the underlying data and analyses. In the present TSPA-SR, this traceability has been significantly enhanced by the tracking of specific AMRs and data tracking numbers generated under common process controls by all scientific investigators. An example of this traceability is the information flow presented in Appendix E. Another example is the listing of model runs included as Appendix G.

A cross-cutting comment on the TSPA-VA was the treatment of uncertainty in the models and analyses used to support the TSPA. In particular it was noted by the TSPA-VA Peer Review Panel (Budnitz et al. 1999 [102726]) that an analysis of the future "probable" behavior of the proposed repository may be beyond the analytical capability. They go on to acknowledge that various approaches can be used to evaluate the complex and difficult to analyze processes that comprise the total system model. These approaches include (Budnitz et al., 1999 [102726]): (1) updating the component models, (2) expanding the quality and quantity of data available as input to these analyses, (3) using bounding analyses (i.e., intentionally conservative assumptions, parameters and models), and (4) design changes.

All of these approaches have been embodied in the TSPA-SR. All models, analyses and data used to support the TSPA-SR have been substantially improved over those used in the development of the TSPA-VA. In addition, the same quality processes have been used in the development, testing, checking and review of the products (in particular the Analysis/Model Reports) used to support the TSPA-SR model. Also, intentionally conservative assumptions have been utilized in those areas of large conceptual uncertainty. Examples of areas with intentionally conservative assumptions include near-field coupled process effects, and in-drift and in-package thermal hydrology and radionuclide transport. Finally, the design analyzed in the TSPA-SR has several attributes that are included to mitigate the effects of some uncertainties; for example a drip shield that minimizes the effects of seepage, a wider drift spacing and closer waste package spacing to minimize localized effects of heat-induced water mobilization and a cooler operating mode to minimize some of the near-drift coupled process effects.

In conclusion, the comments and criticisms made on previous TSPA iterations have improved the methodology and approach and their implementation in this current analysis. The models used to support the TSPA have been significantly enhanced to reflect the most current understanding of the features, events and processes relevant to the post-closure performance. The family of models and analyses have been developed and controlled through a formal process to assure they are adequate for their use in projecting the long-term performance. Finally, the documentation of the models, their integration and the resulting post closure projections of performance have been enhanced to more clearly illustrate the behavior of the system.

6.3 SUMMARY OF HOW AND WHERE TSPA-SR HAS ADDRESSED THE PROPOSED REGULATORY OBJECTIVES

The requirements for a performance assessment (as defined in proposed 10 CFR Part 63 [64 FR 8640 [101680]]) or a total system performance assessment (as defined in proposed 10 CFR Part 963 [64 FR 67054 [124754]]) have been specified in the applicable proposed regulations and in Acceptance Criteria in the Total System Performance Assessment and Integration key technical issues in the Issue Resolution Status Report. This section reiterates

these requirements and enumerates where they have been addressed in this TSPA-SR report or the family of AMRs and PMRs that provide the technical foundation for the TSPA-SR. (Note: This section does not present the compliance argument with the requirements and criteria specified in proposed 10 CFR 963.16 and 963.17 [64 FR 67054 [124754]]). The compliance demonstration for these two sections of Part 963 is being presented in the *Site Recommendation Consideration Report,* which is currently being developed.

6.3.1 Regulatory Objectives of Proposed 10 CFR Part 63 (64 FR 8640 [101680])

The requirements for performance assessment are specified in proposed 10 CFR 63.114 (64 FR 8640 [101680]), as follows:

> Any performance assessment used to demonstrate compliance with 63.113(b) shall:
> (a) include data related to the geology, hydrology, and geochemistry (including disruptive processes and events) of the Yucca Mountain site, and the surrounding region to the extent necessary, and information on the design of the EBS, used to define parameters and conceptual models used in the assessment,

This requirement has been addressed in the analyses and models included in the TSPA-SR that are summarized in (1) Section 3; (2) the nine PMRs and (3) the over one hundred AMRs that provide the "family tree" for the TSPA-SR as indicated in Appendix E. This body of information is extensive and the interested reader is referred to the appropriate PMR or AMR that has been cited throughout this technical document.

> (b) Accounts for uncertainties and variabilities in parameter values and provide the technical basis for parameter ranges, probability distributions or bounding values used in the performance assessment,

This requirement has been addressed in the analyses and models summarized in Chapter 3 and the nine process model reports. Full parameter distributions are summarized in Chapter 3 and are presented in greater detail in the TSPA-SR Model document (CRWMS M&O 2000 [148384]). In some cases the uncertainty or variability has not been explicitly quantified but has been addressed by more bounding approximations. This is particularly true for complex coupled processes for which there is limited site-specific information over the spatial and temporal time scales of interest.

> (c) Consider alternative conceptual models of features and processes that are consistent with available data and current scientific understanding, and evaluate the effects that alternative conceptual models have on the performance of the geologic repository,

This requirement has been addressed in the over one hundred analysis model reports that support the TSPA-SR "family tree" as illustrated in Appendix E. In these documents, the effects of alternative conceptual models are addressed primarily by their effect on some component process model or abstraction rather than their effect on the performance of the repository system as a

whole. Additional analyses to quantify the effect of unquantified alternative conceptual models may still be required to fully address this requirement.

(d) Consider only events that have at least one chance in 10,000 of occurring over 10,000 years,

This requirement has been addressed through the features, events and process screening process, the results of which are summarized in Appendix B and the nine process model reports.

(e) Provide the technical basis for either inclusion or exclusion of specific features, events, and processes of the geologic setting in the performance assessment. Specific features, events, and processes of the geologic setting must be evaluated in detail if the magnitude and time of the resulting expected annual dose would be significantly changed by their omission.

This requirement has been addressed through the features, events and process screening process, the results of which are summarized in Appendix B and the nine process model reports.

(f) Provide the technical basis for either inclusion or exclusion of degradation, deterioration or alteration processes of engineered barriers in the performance assessment, including those processes that would adversely affect the performance of natural barriers. Degradation, deterioration, or alteration processes of engineered barriers must be evaluated in detail if the magnitude and time of the resulting expected annual dose would be significantly changed by their omission.

This requirement has been addressed in Sections 3.3 through 3.6 and the cited analysis model reports and process model reports that relate to engineered barrier degradation processes.

(g) Provide the technical basis for models used in the performance assessment such as comparisons made with outputs of detailed process-level models and/or empirical observations (e.g., laboratory testing, field investigations, and natural analogs).

This requirement has been addressed in Chapter 3 and the TSPA-SR Model document (CRWMS M&O 2000 [148384]) as well as the individual abstraction models referenced in Chapter 3.

(h) Identify those design features of the EBS, and the natural features of the geologic setting, that are considered barriers important to waste

(i) Describe the capability of the barriers identified as important to waste isolation to isolate waste, taking into account uncertainties in characterizing and modeling the barriers.

This requirement has been addressed by the identification of barriers included in Section 5.3. In addition, Table 6.3-1 below illustrates the correlations between the individual barriers and the process model factors presented in Section 3 and identifies the corresponding key attributes of

the repository safety strategy. As indicated in Table 6.3-1, not all component models in the TSPA-SR model are barriers in the strict definition of the term (e.g., limiting water flow or radionuclide migration); many are simply required in order to have a complete total system model.

Table 6.3-1. Correlation of Barrier and Barrier Functions to Key Attributes of Yucca Mountain Repository System and Process Model Factors

Key Attributes of System	Process Model Factor	Barrier	Barrier Function
Limiting Water Contacting Waste Package	Climate	Surficial soils and topography	Reduce the amount of water entering the unsaturated zone by surficial processes (e.g., precipitation lost to runoff, evaporation, and plant uptake
	Net Infiltration		
Limiting Water Contacting Waste Package (Continued)	Unsaturated Zone Flow	Unsaturated rock layers overlying the repository and host unit	Reduce the amount of water reaching the repository by subsurface processes (e.g., lateral diversion and flow around emplacement drifts)
	Coupled Effects on Unsaturated Zone Flow		
	Seepage into Emplacement Drifts		
	Coupled Effects on Seepage		
Prolonging Waste Package Lifetime	In-Drift Physical and Chemical Environments	N/A	These factors provide conditions that affect performance, but are not barriers per se in the TSPA-SR.
	In-Drift Moisture Distribution		
	Drip Shield Degradation and Performance	Drip shield around the waste packages	Prevent water contacting the waste package and waste form by diverting water flow around the waste package; therefore limiting advective transport through the invert
	Waste Package Degradation and Performance	Waste package	Prevent water from contacting the waste form
Limiting Radionuclide Mobilization and Release from the Engineered Barrier System	Radionuclide Inventory	N/A	These factors provide conditions that affect performance, but are not barriers per se in the TSPA-SR.
	In-Package Environments		
	Cladding Degradation and Performance	Spent fuel cladding	Delay and/or limit liquid water contacting spent nuclear fuel after waste packages have degraded
	CSNF Degradation and Performance	Waste form	Limit radionuclide release rates as a result of low solubilities or low diffusion through degraded engineered barriers
	DSNF Degradation and Performance		
	DHLW Degradation and Performance		
	Dissolved Radionuclide Concentrations		
	Colloid-Associated Radionuclide Concentrations		
	In-Package Radionuclide Transport		
	EBS (Invert) Degradation and Performance	Drift Invert	

Table 6.3-1. Correlation of Barrier and Barrier Functions to Key Attributes of Yucca Mountain Repository System and Process Model Factors (Continued)

Key Attributes of System	Process Model Factor	Barrier	Barrier Function
Slow Transport Away from the Engineered Barrier System	Unsaturated Zone Radionuclide Transport (Advective Pathways; Retardation; Dispersion; Dilution)	Unsaturated rock layers below the repository	Delay radionuclide movement to the groundwater aquifer because of water residence time, matrix diffusion, and/or sorption
	Saturated Zone Radionuclide Transport	Tuff and alluvial aquifers (flow path extending from below the repository to point of compliance)	Delay radionuclide movement to the receptor location by water residence time, matrix diffusion, and/or sorption
	Wellhead Dilution	N/A	These factors provide conditions that affect performance but are not barriers per se.
	Biosphere Dose Conversion Factors		
Addressing Effects of Potentially Disruptive Processes and Events	Probability of Volcanic Eruption	N/A	These factors provide conditions that affect performance but are not barriers.
	Characteristics of Volcanic Eruption		
	Effects of Volcanic Eruption		
	Atmospheric Transport of Volcanic Eruption		
	Biosphere Dose Conversion for Volcanic Eruption		
	Probability of Igneous Intrusion		
	Characteristics of Igneous Intrusion		
	Effects of Igneous Intrusion		

This requirement has been addressed in the barrier importance analyses presented in Section 5.3. Additional information on this topic may be found in the Repository Safety Strategy Rev 04 (CRWMS M&O 2000 [148713]).

(j) Provide the technical basis for the description of the capability of the barriers, identified as important to waste isolation, to isolate waste.

This requirement has been addressed in the barrier importance analyses presented in Section 5.3. Additional information on this topic may be found in the Repository Safety Strategy Rev 04 (CRWMS M&O 2000 [148713]).

In conclusion, the basic requirements for a performance assessment as specified in proposed 10 CFR Part 63 have been addressed with the suite of analyses and models that support the TSPA-SR, by the TSPA-SR model itself, and by the analyses described in the present technical document. This is not to imply that the potential Yucca Mountain repository is suitable for licensing. That is a decision that will only be made by the Secretary upon consideration of all information, including sufficiency reviews by NRC and comments from the public.

All of the above information and their integration in the context of this TSPA-SR provide a sound, traceable and transparent technical picture of the possible performance of a potential repository at Yucca Mountain. These projections have incorporated the best available science and technology developed over years of investigating the Yucca Mountain site and the associated waste forms and waste packages. Although significant uncertainty exists in some of the component models underlying the TSPA-SR (as identified in Section 3 and Appendix F), these uncertainties have either been reasonably quantified, or in some cases of great complexity, conservatively bounded. Therefore, it is reasonable to conclude that the expected performance, and the associated uncertainty in that performance, of a potential repository at Yucca Mountain has been captured in the suite of analyses presented in this document.

6.3.2 Regulatory Objectives in the Total System Performance Assessment and Integration Issue Resolution Status Report

The Issue Resolution Status Report on Total System Performance Assessment and Integration is the principal vehicle by which the NRC staff provides the DOE with feedback regarding Total System Performance Assessment and Integration issue resolution before the Site Recommendation and License Application. The Total System Performance Assessment and Integration Issue Resolution Status Report (NRC 2000 [151753], pp. 3 to 4) notes that:

> ... a critical aspect of an acceptable TSPA is the integration of information from many technical disciplines in the modeling and abstraction of the engineered system and natural features, events and processes (FEPs). The need to adequately address this integration of technical disciplines in the development of a TSPA is specifically addressed in this [Issue Resolution Status Report]. The incorporation of acceptance criteria addressing the integration issues in this [Issue Resolution Status Report] is designed to ensure that in issue resolution and the eventual [License Application], the transfer of information among the technical disciplines and to DOE's TSPA occurs, the analysis is focused on the integrated total system assessment, and the assessment is transparent, traceable, defensible and comprehensive.

NOTE: A more recent revision (Revision 3) of the Total System Performance Assessment and Integration Issue Resolution Status Report (IRSR) has become available in September 2000. As of this writing, this document has not been evaluated in the context of the applicable acceptance criteria revised in this version of the IRSR. Future analyses will consider the changes made in this and any subsequent revisions of this document or the risk-informed performance-based Yucca Mountain Review Plan currently in development by NRC staff.

The Issue Resolution Status Report is divided into four subissues and several related acceptance criteria. The four subissues are:

- System description and demonstration of multiple barriers
- Scenario analysis
- Model abstraction
- Demonstration of the overall performance objective.

The following discussion briefly describes the status of how and where the acceptance criteria have been addressed in the TSPA-SR family of documents.

Two programmatic acceptance criteria, quality assurance and expert elicitation, are applicable to all the TSPA subissues. These acceptance criteria are:

> Criterion P1: The collection, documentation, and development of data, models, and/or computer codes have been performed under acceptable quality assurance procedures, or if the data, models, and/or computer codes were not subject to an acceptable [Quality Assurance] procedure, they have been appropriately qualified.

This acceptance criterion was addressed through the process of controlling all the information supporting the TSPA-SR model and all the analyses conducted with the TSPA-SR model that have been documented in this report. For example, all data have been controlled per QA procedure AP-SIII.3Q [149901], all models and analyses have been controlled per AP-3.10Q [151293], all calculations controlled per AP-3.11Q [153200], all technical reports controlled per AP-3.12Q [153122], and all software have been controlled per AP-SI.1Q [146376].

> Criterion P2: Formal expert elicitations can be used to support data synthesis and model development for DOE TSPA, provided that the elicitations are conducted and documented under acceptable procedures.

This criterion was addressed because the two expert elicitations that support the TSPA-SR (namely the Probabilistic Volcanic Hazard Assessment and the Probabilistic Seismic Hazard Assessment) were both performed under the applicable procedures that were driven by guidance provided in NUREG. In addition, input from an expert elicitation conducted to support the TSPA-VA were used to support the determination of the uncertainty in some parameters of the SZ flow and transport model.

The Acceptance Criteria related to the System Description and Demonstration of Multiple Barriers subissue include those that relate to:

1. Transparency and traceability of the analysis, including
    a. TSPA documentation style, structure, and organization
    b. Features, events and processes identification and screening
    c. Abstraction methodology
    d. Data use and validity
    e. Assessment results
    f. Code design and data flow.
2. Demonstration of multiple barriers.

The Acceptance Criteria related to the TSPA Methodology of Scenario Analysis subissue include those that relate to:

1. Identification of an initial set of processes and events
2. Classification of processes and events

3. Screening of processes and events
4. Formation of scenarios
5. Screening of scenario classes.

The Acceptance Criteria related to the TSPA Methodology of Model Abstraction subissue apply to all component models included in the TSPA model. These criteria include those that relate to:

1. Data and model justification
2. Data uncertainty
3. Model uncertainty
4. Model support
5. Integration.

The Acceptance Criteria related to the Demonstration of the Overall Performance Objective subissue are not yet available. They will be established by NRC after proposed 10 CFR Part 63 (64 FR 8640 [101680]) is published in final form.

Each of the above acceptance criteria are addressed in Appendix D. For the current state of FEPs screening and scenario development; model abstraction development and documentation; TSPA model integration; and the treatment and documentation of the uncertainty associated with the TSPA analysis, these acceptance criteria have been adequately addressed. Again, that is not to imply that no remaining analysis or model development is required prior to licensing, if the Yucca Mountain site is found suitable and is recommended to the President.

In conclusion, the documentation of the TSPA-SR, including the analysis model reports, process model reports and the TSPA-SR model document, provide the technical basis to address the NRC acceptance criteria in the Total System Performance Assessment and Integration Issue Resolution Status Report, as well as the TSPA-related acceptance criteria in the other key technical issues Issue Resolution Status Reports. In addition, these same documents provide the scientific basis for evaluating the suitability of the Yucca Mountain site. This suitability evaluation, which uses proposed 10 CFR Part 963 (64 FR 67054 [124754]) evaluation criteria, is being presented in the *Site Recommendation Consideration Report* currently under development.

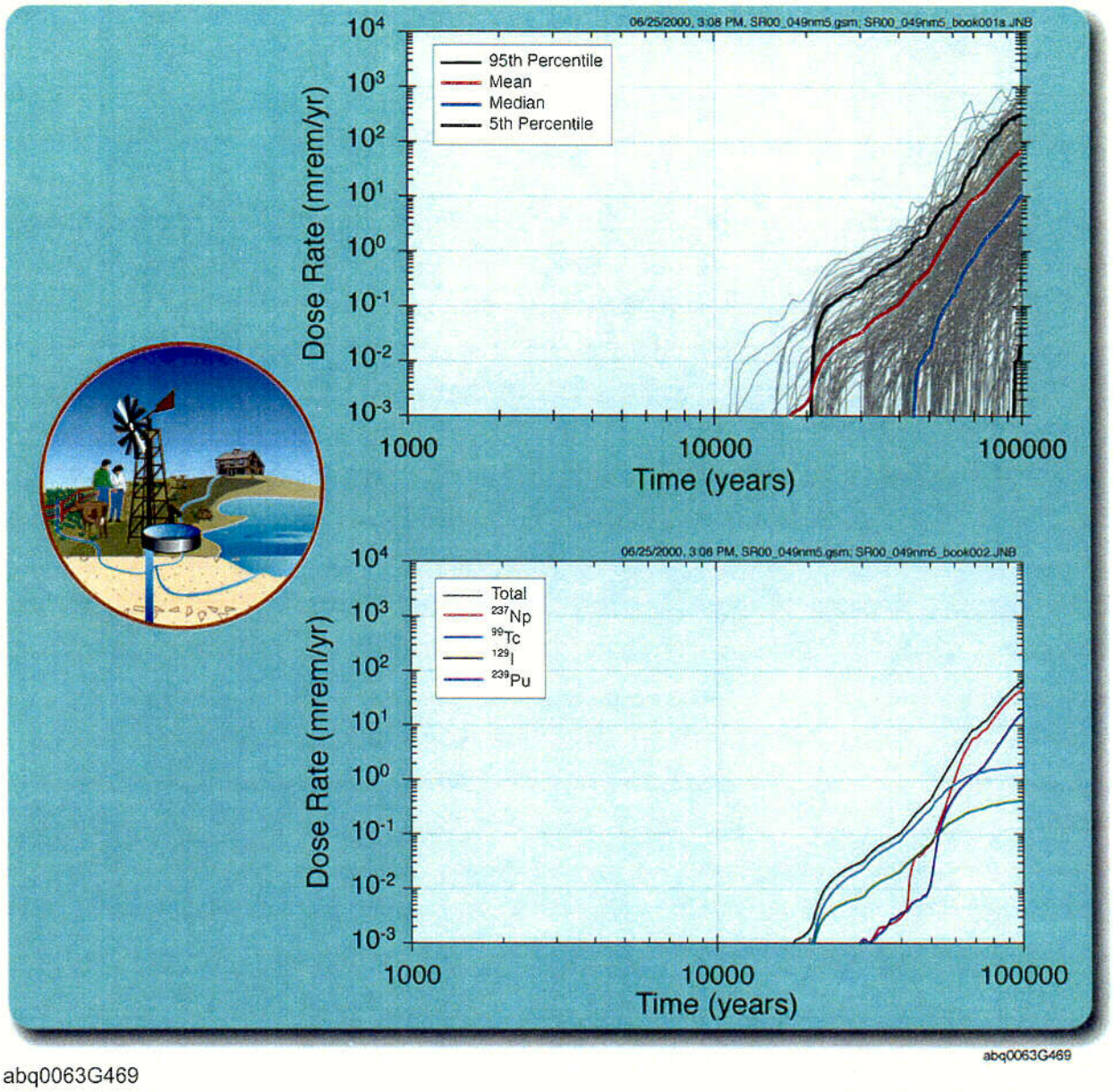

abq0063G469

Figure 6.1-1. Summary of Individual Protection Performance Results–Nominal Scenario Class

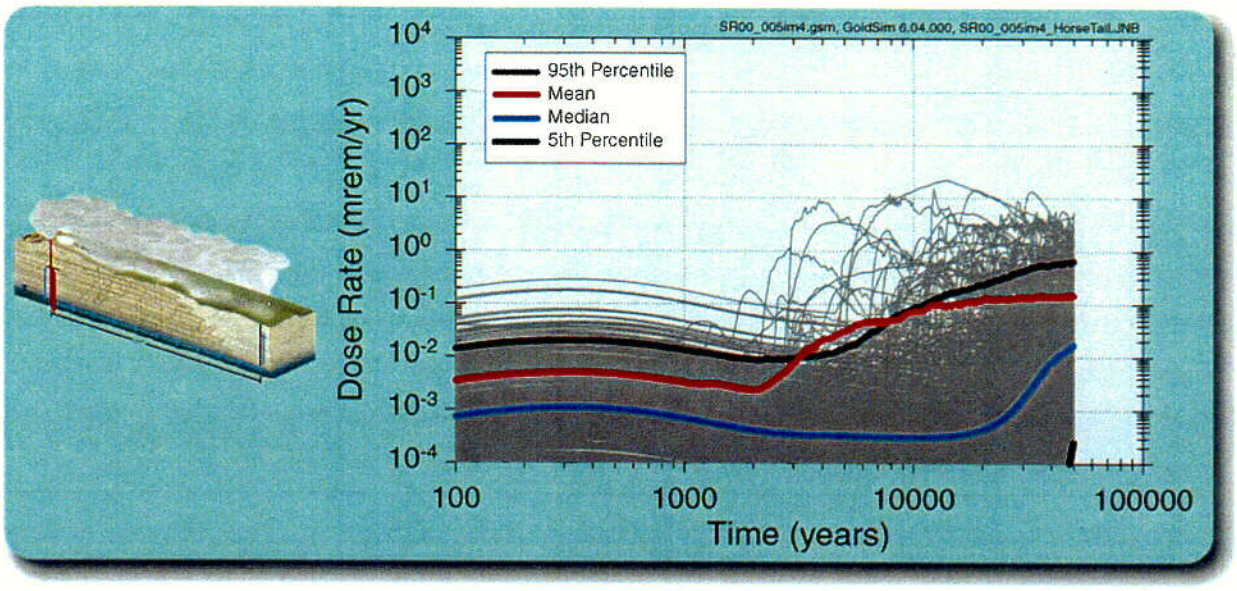

abq0063G531

Figure 6.1-2. Summary of Individual Protection Performance Results–Volcanic Scenario Class

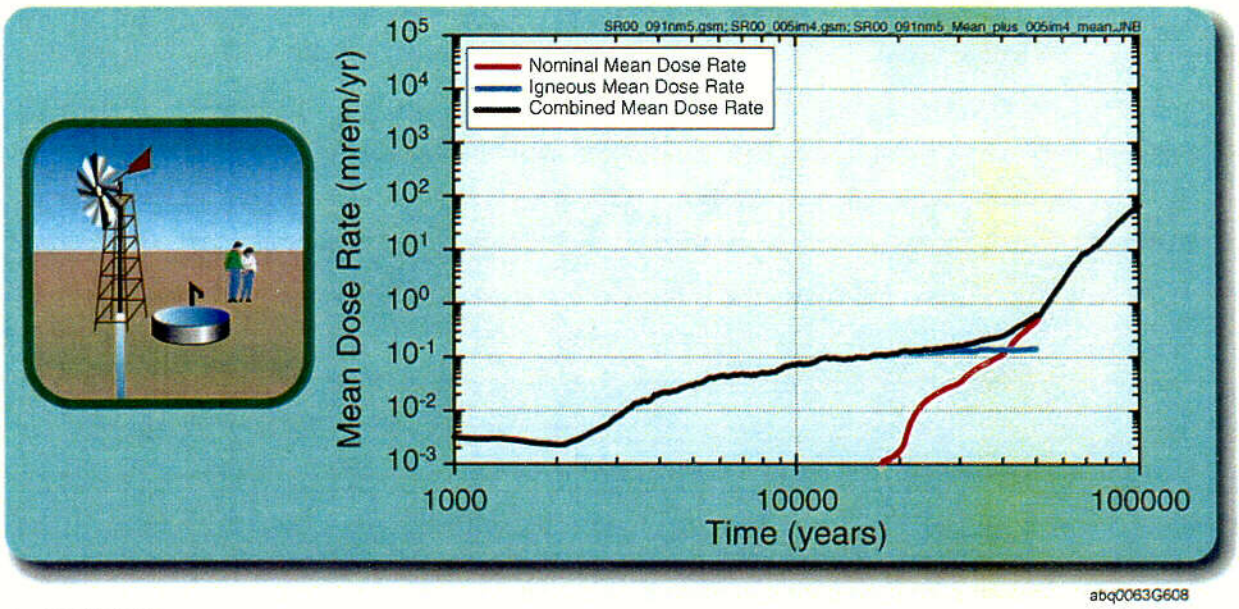

abq0063G608

Figure 6.1-3. Summary of Individual Protection Performance Results–Total System Combined Scenario Class

c.94

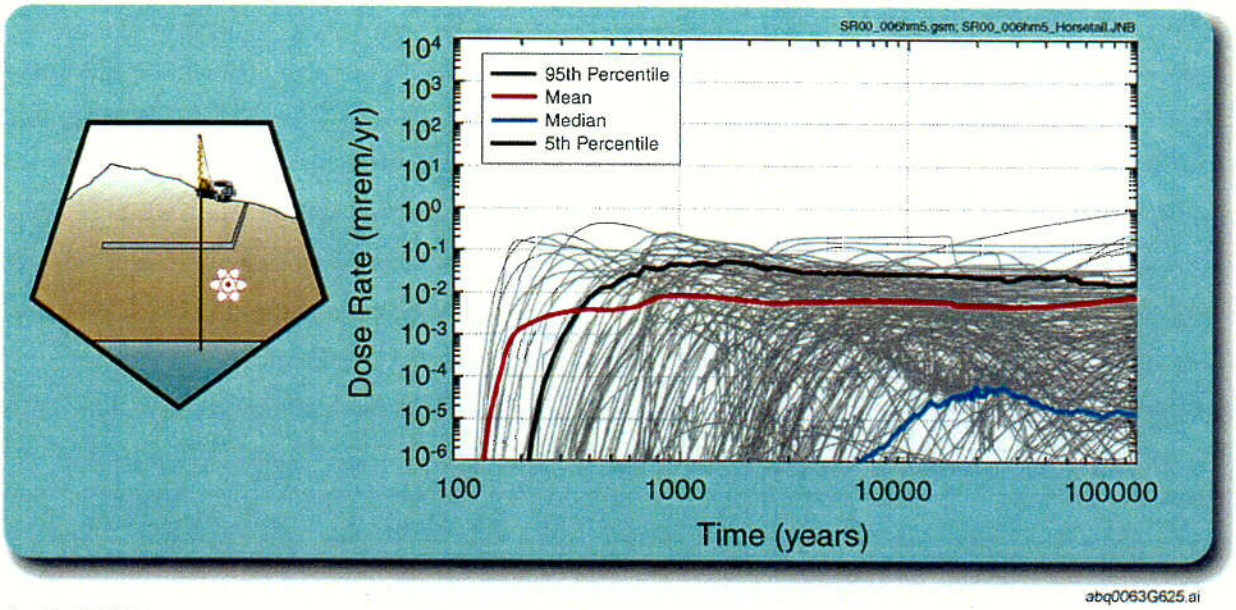

abq0063G625

Figure 6.1-4. Summary of Human Intrusion Performance Results–Assumed Human Intrusion Event Occurs at 100 Years

C-95

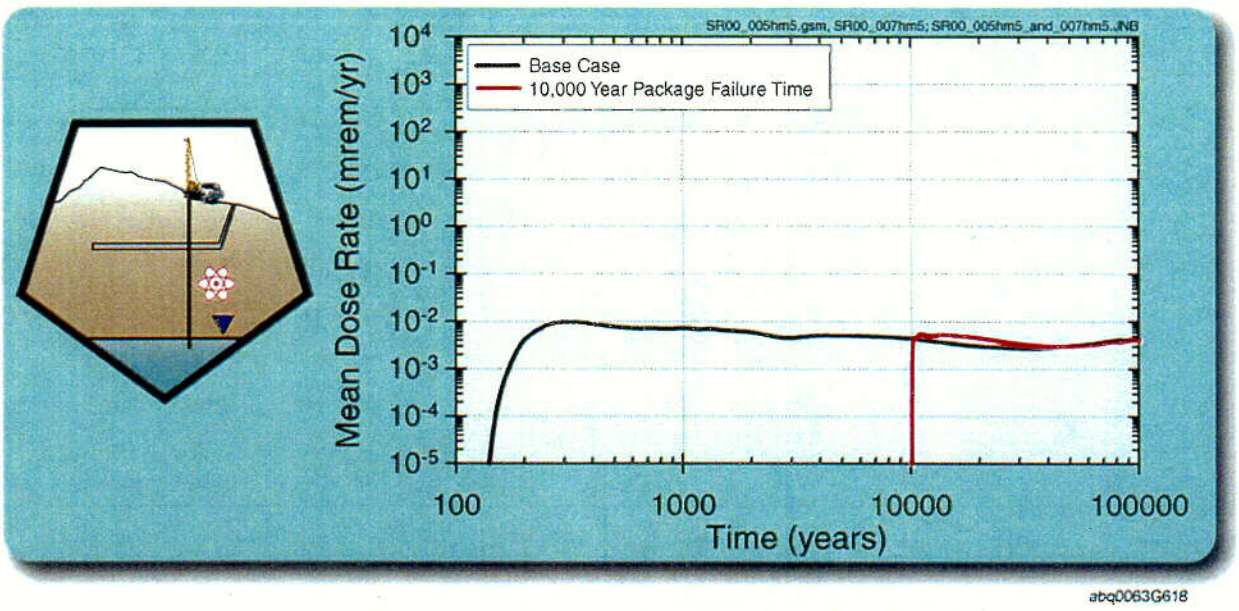

abq0063G618

Figure 6.1-5. Summary of Human Intrusion Performance Results–Assumed Human Intrusion Event Occurs at 10,000 Years

C-96

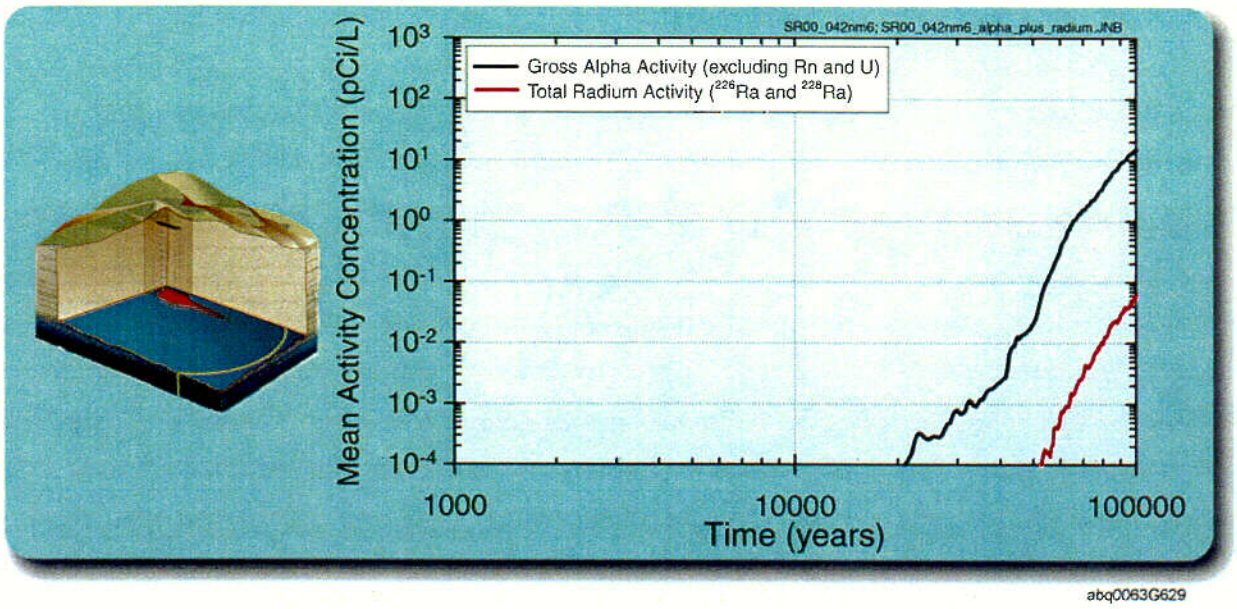

abq0063G629

Figure 6.1-6. Summary of Groundwater Protection Performance Results–Gross Alpha Activity

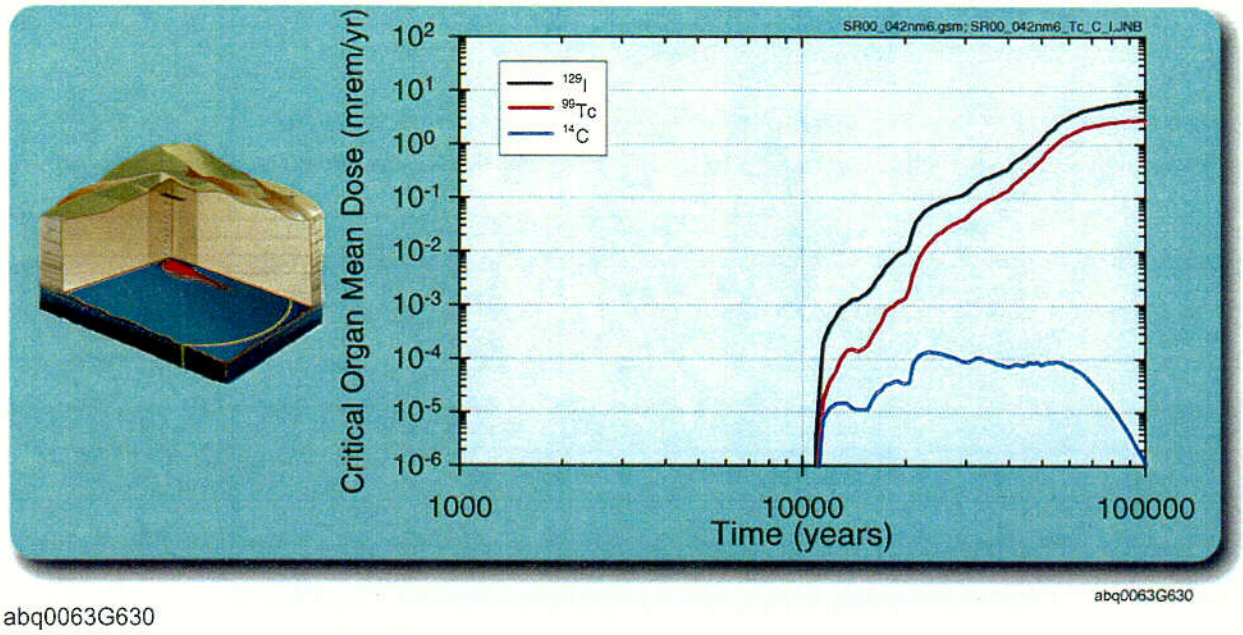

abq0063G630

Figure 6.1-7. Summary of Groundwater Protection Performance Results–Combined Beta and Photon Emitting Radionuclides

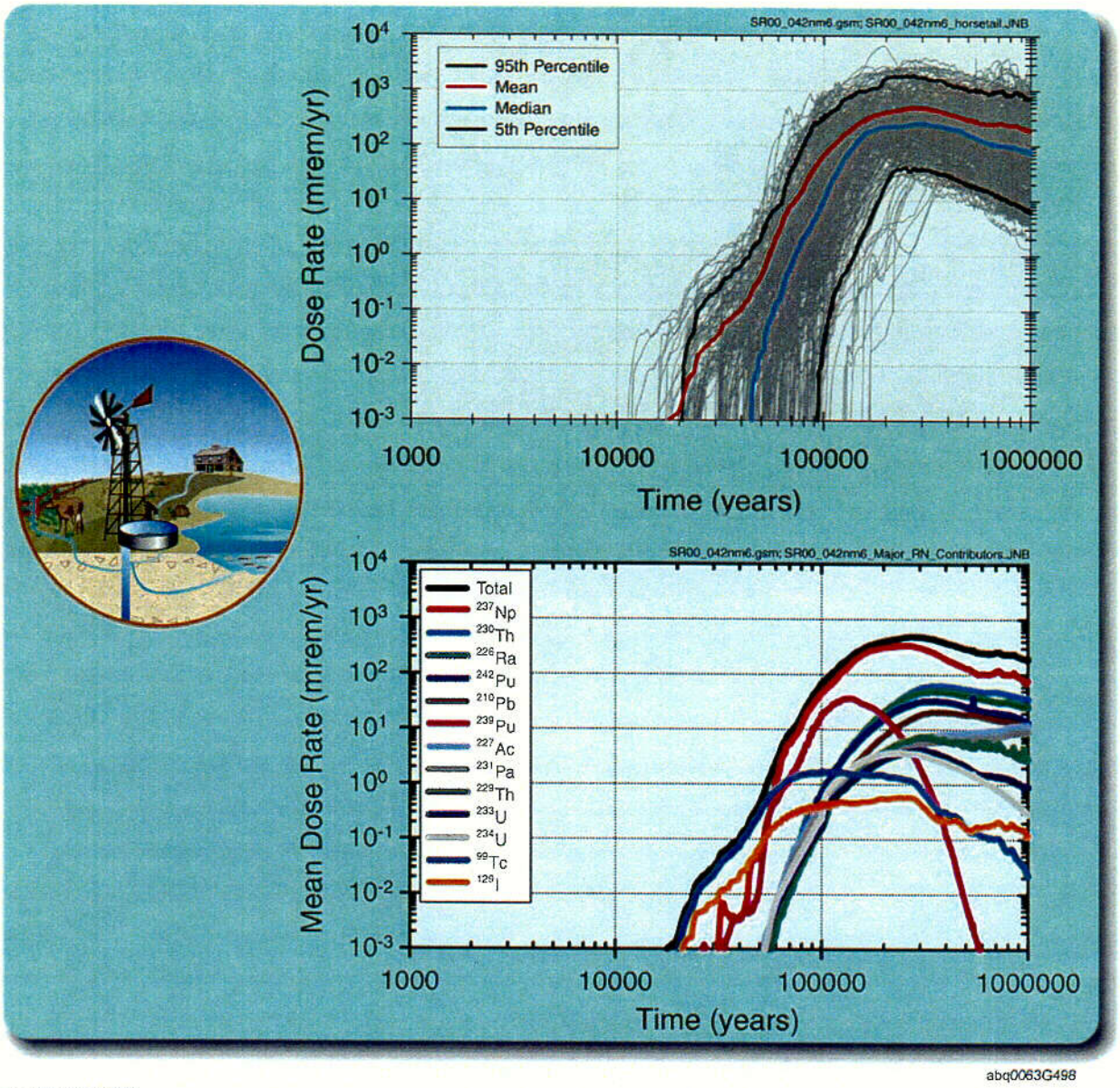

abq0063G498

Figure 6.1-8. Summary of Peak Dose Performance Results